UNIVERSIDADE DE LISBOA

INSTITUTO SUPERIOR TÉCNICO

Development of a novel purification platform for Fab antibody fragments based on affinity peptides and multimodal ligands

André Nunes dos Santos Nascimento

Supervisors: Doctor Ana Margarida Nunes da Mata Pires de Azevedo

Doctor Steven M. Cramer

Co-Supervisor: Doctor Pankaj Karande

Thesis approved in public session to obtain the PhD Degree in
Biotechnology and Biosciences

Jury final classification: Pass with Distinction

2020

Homologo, 17 Abril 2020

TÉCNICO LISBOA

UNIVERSIDADE DE LISBOA

INSTITUTO SUPERIOR TÉCNICO

Development of a novel purification platform for Fab antibody fragments based on affinity peptides and multimodal ligands

André Nunes dos Santos Nascimento

Supervisors: Doctor Ana Margarida Nunes da Mata Pires de Azevedo

Doctor Steven M. Cramer

Co-Supervisor: Doctor Pankaj Karande

Thesis approved in public session to obtain the PhD Degree in

Biotechnology and Biosciences

Jury final classification: Pass with Distinction

Jury

Chairperson: Doctor Duarte Miguel de França Teixeira dos Prazeres, Instituto Superior Técnico da Universidade de Lisboa

Members of the Committee:

Doctor Maria Raquel Múrias dos Santos Aires Barros, Instituto Superior Técnico da Universidade de Lisboa

Doctor Duarte Miguel de França Teixeira dos Prazeres, Instituto Superior Técnico da Universidade de Lisboa

Doctor Ana Cecília Afonso Roque, Faculdade de Ciências e Tecnologia da Universidade Nova de Lisboa

Doctor Ana Margarida Nunes da Mata Pires de Azevedo, Instituto Superior Técnico da Universidade de Lisboa

Doctor Cristina Maria da Costa Peixoto Lisboa, iBET- Instituto de Biologia Experimental e Tecnológica

Funding Institutions

FCT – Fundação para a Ciência e Tecnologia

CBIS – Center for Biotechnology & Interdisciplinary Studies, Rensselaer Polytechnic Institute

2020

Dedicated to my grandmother, mother and father

Acknowledgment

The PhD experience of the last four years was indubitable a long and winding road that would never be possible to trail without the constant support and motivation of Professor Ana Azevedo. All her help, mentorship and wisdom were fundamental for the completion of this thesis and in my growth as a PhD student and a scientist. I would also like to express my profound gratitude towards Professor Seven Cramer and Professor Pankaj Karande for the opportunity of developing my research on their laboratories and research groups. They have inspired me to always pursuit different challenges and create clear and sharp science. I want also to acknowledge Professor Raquel Aires Barros, her support and scientific inputs during this last four years were tremendously important.

One of the most exciting rewards of my PhD was the possibility of working in four different research groups. I thank to all the friends I've made at the different laboratories I've worked. Their knowledge and ideas were decisive in some of the paths I've chosen during my PhD. In particular, I consider myself lucky to have shared the lab-bench and several whiteboarding sessions with Inês Pinto. In addition to her availability to always answer my questions and clarify my doubts, I'm grate for all the silly and light conversations, paired with several laughs, that we had in these last years. The number of friends I've made during this time is not small, and despite knowing that I will be unfair to some, I would like to specially thank to Isabel Pinto, Ruben Soares, Ronak Gudhka, Ricardo Fradique and Rui Silva for all the lessons and information I was able to take from all of them.

An essential part of every PhD is to help other researchers and share knowledge. During my PhD I had the opportunity of mentoring two master students, Miguel Ambrósio and Rachid Santos. To both, I'm grateful for their help in my research project and for allowing me to grow as a mentor. This experience helped me to better communicate science and gave me the necessary tools for an efficient team-based experimental design and execution. To Miguel and Rachid wish all the best, and I'm sure they will have a brilliant future ahead. I am also thankful to Mariana São Pedro, those three months we worked together were both productive and joyful. Our discussions were always enlightening and I'm sure that her new PhD life will be full of great achievements.

My time in the USA was memorable, and in Troy (NY), I was tremendously fortunate. In addition to the opportunity of working at Rensselaer Polytechnic Institute, I had the fortune of meeting an academic collaborator that rapidly became a friend, Akshat Mullerpatan. It is difficult to express how thankful I'm for all his help, patient, guidance, wisdom and friendship. The fight we fought to find peptides was epic and will be remembered forever. Thanks man, without the late-night conversations and general foolishness this would be terrible boring. The other friend I've made, also part of the phage team, is Ronit Gosh. I'm really glad I had the opportunity of sharing all sort of conversations with him, all the laughs and craziness will always be remembered with a smile.

The Troy experience would not be the same without my friends (and housemates) Tânia Baltazar, Marta Carvalho and João Silva. Thanks so much for living Troy with me. Without our conversations, gossip, workout sessions (ones more than the others), beers, junk and healthy food, movies (completed and not so completed) Troy could have been a dull and depressing place. You made Troy a place that I will always remember and want to return.

The next two paragraphs are for my two families. Words will fall short to express how lucky I'm to have the friends (siblings) I have. To Nuno, Edgar, Daniela, Margarida and Inês, I'm profoundly thankful for always being present and for all the moments we share during the time of my PhD. I will always be in debt with you. Thank you.

Finally, I would like to thank to the two greatest and most resilient warriors I know, my mother and my father. Your support, patient, and endless trust in me deserved a chapter on this thesis. The strength and love you gave me in these last years were immeasurable. Thank you for all your guidance, help and constant presence. I cannot thank enough to my grandmother for everything she did and does for me. If I was able to complete this challenge was because I had her on my side all the time, supporting and helping me throughout this journey. Lastly, to my aunt and cousin, your constant presence and availability were (are) indispensable for me, thank you so much for always being there.

A final word to Fab fragments, we had a good run, buddy.

Resumo

Derivados de anticorpo são uma classe de proteínas idealizadas como alternativas a anticorpos monoclonais. A produção de fragmentos de anticorpo, uma das proteínas desta classe, não é eficiente, especialmente na fase a jusante do processamento. De modo a dissipar esta limitação, duas abordagens foram sugeridas como novas alternativas à purificação de Fragmentos de anticorpo. Cromatografia de afinidade, usando péptidos, e cromatografia multimodal foram as duas soluções escolhidas e avaliadas

Nesta tese, uma abordagem evolutiva, baseada na técnica de phage display, foi usada para rastear e descobrir péptidos de afinidade capazes de ligar a fragmentos de anticorpo. Três diferentes esquemas de selecção foram desenhados, onde a complexidade e foco na região constante do fragmento era aumentada. O resultado foram cinco péptidos com a capacidade de ligar a fragmentos de anticorpo. Apesar de nenhum péptido ser considerado um ligando universal, três dos cinco podem ser considerados ligandos específicos para três, ou mais, proteínas semelhantes. O uso de um dos péptidos como solução de cromatografia de afinidade foi desenvolvida, tendo a sua eficácia sido demonstrada através da purificação de fragmentos de anticorpo presente num sobrenadante complexo.

O potencial de cromatografia multimodal é tão grande quanto sua complexidade. De modo a fazer um varrimento rápido de diferentes condições de cromatografia, para purificar fragmentos de anticorpo usando ligandos multimodais, uma plataforma microfluídica de alto rendimento foi usada. Um estudo exaustivo, de onze resinas multimodais, visando fragmentos de anticorpo, outras proteínas e duas misturas complexas, a diferentes pHs e concentrações de sal, foi feito. Com esta abordagem, uma selecção sustentada nos melhores ligandos e condições cromatográficas foi feita, e o desenho de uma processo de purificação totalmente baseado em ligandos multimodais foi concebido.

Este trabalho lança bases para a descoberta de novas soluções de purificação para uma classe emergente de derivados de anticorpo. As duas abordagens adoptadas podem ser consideradas contribuições valiosas para um processo de purificação de fragmentos de anticorpo, ou outras biomoléculas, mais eficiente.

Palavras-chave: Fragmentos de anticorpo, cromatografia multimodal, cromatografia de afinidade baseada em péptidos, microfluídica, varrimentos de alto rendimento.

Abstract

Antibody derivatives are a class of engineered proteins idealized as alternatives to monoclonal antibodies. The production of Fab fragments, the oldest of this class, in comparison to mAbs is not as efficient, especially the downstream processing. To tackle this limitation, two different approaches were suggested as new solutions to purify Fab fragments. Peptide affinity chromatography and multimodal chromatography were the chosen and evaluated solutions.

In this thesis an evolutive approach, based on phage display, was taken to screen and discover peptide affinity ligands capable of binding to Fab fragments. Three different biopanning schemes were designed, with increase complexity and increased focus on the constant regions of Fabs. The outcome were five different peptides with the ability to bind Fab fragments. While a truly universal ligand was not identified, three of those obtained peptides can be considered ligands specific to three or more closely related biologics. The application of one of those peptides as a chromatographic affinity solution was developed, and its efficacy was demonstrated for Fab purification from a complex cell culture fluid mixture.

The potential of multimodal chromatography is as big as its complexity. To rapidly screen chromatographic conditions to purify Fab fragments using multimodal ligands, a high-throughput platform, based on chromatographic microfluidics was applied. An exhaustive study of eleven multimodal resins, targeting Fabs, other proteins and two complex mixtures, at different pH and salt conditions was executed. With this high-throughput approach a sustained selection of the best ligands and chromatographic conditions was taken, and the design of a full multimodal Fab downstream process was made.

This work lays the foundation for the discovery new purification solutions for a class of emergent antibody derives. The two different approaches adopted can be considered valuable contributions for a more efficient purification process of Fab fragments and other types of biomolecules.

Keywords: Fab fragments, multimodal chromatography, peptide affinity chromatography, microfluidics, high throughput screen.

Table of Contents

List of Figures

List of Tables

List of Abbreviations

A5 peptide – WHYNWQDVSDRQ

AOX1 – Alcohol oxidase I

B1 peptide – WIPNSEFEHERT

BDP – BODIPY

BSA – Bovine Serum Albumin

C7 peptide – HQNHHSTFWEIY

CCF – Cell Culture Fluid

CDR – Complementarity-determining regions

CEX – Cation Exchange

CFT – Complete Fab Target

C_H1 – Constant Heavy Chain

CHO – Chinese hamster ovary

CIP – Cleaning in place

CL – Constant Light chain

CM – Carboxymethyl

CV – Column volum

D2 peptide – Sequence information withheld

DF – Diafiltration

DNA – Deoxyribonucleic acid

DSP – Downstream process

EDTA – Ethylenediamine tetraacetic acid

ELISA – Enzyme-Linked Immunosorbent Assay

ESPript – Easy Sequencing in PostScript

F3 peptide – Sequence information withheld

Fab fragment – Antigen-binding fragment

Fc fragment – Fragment crystallizable

FP – Fluorescence polarization

GAP – Glyceraldehydes-3-phosphate dehydrogenase

GFP – Green fluorescent protein

Glu – Glutamic Acid

HCP – Host Cell Protein

HEK – Human Embryonic Kidney

His – Histidine

HT – High-throughput

IBs – Inclusion bodies

IEF – Isoelectric focusing

IEX – Ion exchange

IgG – Immunoglobulin G

KD – Dissociation constant

LB – Lysogeny broth

Leu – Leucine

Lys – Lysine

mAb – Monoclonal antibody

MFT – Multiple Fab target

$MgCl_2$ – Magnesium chloride

mRNA – Messenger RNA

MWCO – Molecular weight cut off

NHS – N-Hydroxysuccinimide

PBA – Phenylboronic acid

PBS – Phosphate buffered saline

PBST – PBS with 0.1% Tween 20

PBS2T – PBS with 0.5% Tween 20

PDMS – Polydimethylsiloxane

PEG – Polyethylene glycol

Pfu – Plaque-forming unit

pI – Isoelectric point

PpL – Protein L

QbD – Quality by design

RNA – Ribonucleic acid

RP-UPLC – Reverse-phase UPLC

RT – Room temperature

scFv – Single-chain variable fragment

SDS-PAGE – Sodium dodecyl sulphate-polyacrylamide gel electrophoresis

SEC – Size exclusion chromatography

SFT – Single Fab Target

SIP – Sterilization in place

Thr – Threonine

TNFα – Tumour necrosis factor alfa

Toyo – TOYOPEARL MX-Trp-650M

UF – Ultrafiltration

UPLC – Ultra pressure liquid chromatography

V_H – Variable heavy chain

V_HH – Single-domain antibody

V_L –Variable light chain

Chapter 1

Introduction

Monoclonal antibodies (mAbs) play a pivotal role in both biotechnology and pharmacology. MAbs are one of the pillars of the pharmaceutical industry, used as a therapeutic agent against several types of diseases, including auto-immune disorders, neurological and specially cancer [1]. The intrinsic structural nature of mAbs, their flexibility and vast know-how led to the idealization and creation of mAb derivatives including Fab fragments, single-chain variable fragment (scFvs), nanobodies and bispecific antibodies.

From all mAb derivatives, Fab fragments have already proven their potential, with four approved Fab-based therapeutics (ReoPro®, Lucentis®, Cimzia® and Praxbind®) and numerous of Fabs currently in clinical trials [2,3]. Additionally, Fabs, like mAbs, are a source of economical profit, with sales of over $3.5 billion US dollars reported in 2010 [4]. In comparison to intact antibodies, the lack of Fc region makes Fabs smaller and simpler. This structure allows Fabs to have different pharmacologic properties capable of offering some advantages including higher tissue penetration ratios, reduced nonspecific binding (caused by the lack of Fc) and higher sensitivity in antigen detection [5]. In terms of production, there are some differences between mAbs and Fabs. MAbs are mainly produced in mammalian cell lines (CHO or HEK) and their purification relies on the use of protein A, an affinity solution based on the interaction between the Fc region and the protein A ligand. To produce Fabs, two routes can be taken, enzymatic digestion of full antibodies or recombinant cell expression. Regardless the Fabs production process, its purification process is not as defined as it is for mAbs, since the lack of Fc region impedes the use of protein A to purify Fab biomolecules. Currently, protein L, from *Peptostreptococcus magnus,* is the most commonly used tool to purify Fab fragments, however, this affinity solution is only able to purify a certain isotype of this biomolecules – Fabs having a kappa light chain. Protein L lack of universality and the reduced efficiency and robustness, when compared to protein A, makes the search for a protein L alternative a fascinating challenge as there is still no stablished affinity solution capable of purifying all classes of Fab fragments (with kappa and lambda light chain). Other

frequently use techniques to purify Fabs, not based on affinity interactions, include ion exchange, hydrophobic interaction and size exclusion.

The increased importance and demand of Fabs in the current biotechnology and pharmaceutical scenario requires a universal affinity solution to purify all classes of Fab fragments, like protein A can purify most of antibodies. One hypothesis could be the use of peptides as affinity ligands. Their ease of engineering and structural characteristics allows them to be developed as ligands for downstream purposes. This hypothesis is enhanced by reported studies where peptides were successfully used in a chromatography format to purify whole antibodies. Other possibility, not based on affinity, is the use of multimodal ligands. Multimodal chromatography is a relative new concept in chromatography, that combines in one ligand different types of interactions. The complexity of multimodal ligands brings one limitation, the need for a thorough process development to find the best purification conditions. Nevertheless, when all the chromatographic conditions are determined, the higher specificity of multimodal ligands, compared to the traditional ion or hydrophobic, could make multimodal chromatography a valuable alternative in the purification of Fab fragments.

Objectives of this work

The application of biomolecules as biotech tools has one major limitation, their downstream processing. The slow process development and high prices, commonly associated with purification procedures, makes the search for faster and cheaper alternatives an attractive task. These limitations are demonstrated in the production of Fab fragments. The use of protein L affinity chromatography as the established procedure to purify these antibody-derivatives, despite its constrains (price, lack of universality, low robustness and efficiency), has motivate the development of better alternatives. The aim of this thesis is thus to tackle protein L limitations, by finding alternatives for the purification of Fab fragments.

One of the suggested alternatives is the use of peptide as affinity ligands. When compared to protein domain ligands (protein A, G or L) peptides are cheaper and more stable, making them good candidates for affinity purification solutions. The major limitation of the use of peptides is related with a laborious process of finding the best amino acid

combination to create a peptide responsible for the binding to the desired target. Phage display is a high-throughput technique that could be applied in the discovery of affinity peptides, being the success of this finding highly based on the correct design of the phage biopanning. In this thesis, different biopanning strategies where applied towards the finding of new peptide ligands that could be applied and developed as alternatives for protein L in the purification of Fab fragments.

The other suggested alternative is the use of multimodal chromatography to purify Fab fragments. When compared to traditional ion exchange, or hydrophobic interaction, multimodal chromatography offers an increased selectivity, higher pH and salt tolerance [6,7]. The application of this type of chromatography is appealing, however, the potential of the multimodal comes with a price: the complexity of this ligands demands a laborious process of finding the ideal chromatographic conditions. In this thesis several multimodal resins were selected, and a thorough study, based on microfluidic chromatography, was done with the purpose of developing a multimodal purification process for Fab fragments.

Specific objectives

In order to achieve this thesis goal, the following specific objectives were set-up:

1) To design a standard papain digestion protocol to generate Fab fragments from a mixture of Human antibodies;
2) To design a standard downstream process to purify Fab fragments generated from the digestion of whole antibodies;
3) To development of phage biopanning strategies to find peptide affinity ligands to purify Fab fragments;
4) To evaluate lead peptides for their ability to bind Fab fragments by measuring dissociation constants and to test them as chromatographic solutions;
5) To screen of chromatographic conditions, using high-throughput microfluidic chromatographic chips in order to develop a purification process, based on multimodal resins;
6) To validate and apply the results obtained with the microfluidic device at a lab-scale chromatographic setup.

Thesis outline

This thesis is divided into seven chapters, four of them containing the description of experimental work and the results obtained under the scope of the goals purposed for this thesis. The structure of each chapter is similar across all the chapters with experimental data. There is an initial introduction, where the techniques applied in the chapter are summarily described and the objectives are defined. This is followed by the description of the experimental work and respective results and discussion. In the end of each chapter, there is a conclusion section where the main achievements are summarized. In every chapter, if applicable, the collaborations which contributed for the development of the described work are indicated. Scientific publications resulted from the work developed, in the context of the chapter, will also be indicated.

Chapter 1 – introduces the main purpose and motivation of this thesis and depicts the objectives of the work. Also describes the organization of this document.

Chapter 2 – presents the state-of-the-art on Fab fragments, focusing on the main topics related with this antibody-derivate. A comparison between Fabs and mAbs is made, and the key characteristics of both are described and discussed. Moreover, structural features of Fabs are described and an amino acid sequence analysis in done, to compare both kappa and lambda Fabs. Additionally, the main aspects of Fab production are described. The use of enzymatic cleavage and different cell expressions systems, to generate Fab fragments, are summarized. Regarding downstream process, the most common purification procedures are discussed, with a special focus on protein L affinity chromatography and other affinity solutions. Furthermore, a complete description of the available therapeutics based on Fab fragments is made. Other applications where Fab fragments are employed are also described. In this chapter is possible to acknowledge that as a result of Fab structure and production route, Fab fragments is an extremely variable biomolecule.

Chapter 3 – presents an optimization of a cleavage protocol to generate Fab fragments using the proteolytic enzyme papain. A digestion protocol is tuned in order to efficiently digest a mixture containing different types Human IgG. After defining a standard digestion protocol, four different downstream processes, based on affinity chromatography (protein A and L) and centrifugal ultrafilters, are evaluated to access the

best method to purify digested Fab fragments. With the results obtained in this chapter was possible to create a digestion and purification protocol able to generate pure digested Fab fragments employed in subsequent studies of this thesis.

Chapter 4 – describes the development of biopanning strategies to discover peptide affinity ligands. Three phage biopanning strategies were developed to find lead peptide ligands with affinity towards Fab fragments. Five peptides were selected and their dissociation constants against different types of Fabs were determined. One of the discovered peptides was successfully immobilized in a chromatographic bead and used as a chromatographic solution.

Chapter 5 – reports the use of a microfluidic platform, as a high-throughput system, to evaluate the use of commercially available multimodal resins in the downstream process of Fab fragments. Binding studies of Fabs to the selected resins were executed, at different pHs and salt concentrations. Additionally, the same studies targeting other proteins (Human IgG, Fc fragment and BSA) and complex media (CHO supernantant and *Escherichia coli* lysate) were also accomplished. The results obtained with the microfluidic platform were confirmed at lab-scale, using an ÄKTA purifier system. Finally, the design of a two-step purification scheme, using multimodal resins, to purify Fab fragments was studied.

Chapter 6 – evaluates the potential of phenylboronate chromatography to purify Fab fragments. Microfluidic chromatography is applied to study phenylboronate ligand for its ability to bind digested Fab fragments. Binding and elution studies were developed targeting both kappa and lambda Fabs, Fc fragments, Human IgG and CHO supernatant. The results obtained with the microfluidic system were validated at normal lab-scale with an ÄKTA purifier system.

Chapter 7 – an overall evaluation of the achievements accomplished in this thesis are consummated. The main conclusions of the accomplishments are highlighted, and further future work is briefly discussed.

Chapter 2

Antibody Fragments: from their production to their application

2.1. Introduction

Therapeutic antibodies are currently the workhorse of the pharmaceutical industry and a source of success in clinical applications and drug discovery [8,9]. In addition, antibodies are already established analytical tools being routinely used in techniques such as: ELISAs, immunofluorescence, Western blotting, protein microarray, flow cytometry, and others [10,11]. Their extraordinary potential and flexibility led to the creation of the hypothesis that antibodies can be fragmented and customized for specific application [12]. The theory was rapidly applied and single chain variable fragments (scFv), antigen-binding fragment (Fab), multivalent scFv's, and others, rose as the next wave of antibody-based biomolecules [12]. The focus of this chapter is to highlight the importance of Fab fragments in the actual biotechnology and pharmaceutical scenario. A broad overview of their structure, production process and applications will be discussed, with emphasis on their extremely variability that could interfere with the implementation of a defined purification process.

Fab fragments are the "arms" of antibodies, each Fab contains one binding site that interacts with a single antigen epitope (see esquematic representation on **Table 2.1**) [13]. They are constituted of four chains: two constants – heavy (C_H1) and light (C_L) chain, and two variable – heavy (V_H) and light (V_L). Despite being already a valuable tool in both biotechnology and biomedical industry, a regular question is made every time Fab fragments applied or subjected to study. Why not to use a whole antibody instead of a fragment? To answer this, it is interesting to analyse the differences of antibodies and Fab fragments, and briefly summarized the current state of the art of the last.

2.2. mAbs vs Fabs: singularities of each ones, not pros and cons

It is common, when Fab fragments and monoclonal antibodies (mAbs) are discussed to mention the advantages or disadvantages of one over the other. Herein the comparison of these two classes of proteins will be made having in consideration their application. The key difference between these two biomolecules is their size, Fab fragments are three times smaller than mAbs. Being a ~50 kDa biomolecule, Fab fragments have better tissue penetration and are cleared from the blood or kidney, *in vivo*, faster than the 150 kDa whole mAb [14,15]. This feature makes Fabs better suited for a rapid and selective delivery of radioisotopes, toxic drugs and toxins to the antigen[16]. For imaging applications, when radiolabelled probes are used, a fast clearance from the system is essential, making Fabs a natural choice for this application. Moreover, the lack of Fc reduces the putative biological activity of Fab fragments, avoiding possible side effects that could perturb the imagining result[17]. On the other hand, if we use these antibodies derivatives for therapeutic application, mAbs are generally the best option. The presence of the Fc fragment ensures higher half-life *in vivo*, promoting a longer exposure of the drug to the desired site[18]. For Fabs, the absence of Fc, promotes a faster blood and kidney clearance, and so reducing their half-life, when compared to a whole mAb [19].In addition, the presence of Fc fragment will promote a stronger interaction with the receptors on the surface of the leukocytes creating a more effective biological response, such as, activation of complement or antibody-dependent cell-mediated cytotoxicity [20].

Fabs and mAbs production process is other significant difference between these biomolecules. The last has a complex glycosylation pattern, and so, the host of choice to produce them is generally mammalian cells: human embryonic kidney (HEK 293T) or Chinese hamster ovary (CHO) cells [21,22]. Fabs, having no glycosylation pattern, can be produced in a wider range of cell system, including mammalian [23], bacteria [24], yeast [25], insect [26,27] and plants [28]. This makes the production process mAbs less flexible, slower and more expensive than Fabs [29]. Nevertheless, the production of mAbs has no secrets, high titters - around 10 g/L, are easily obtained [30], and all the features of their production are well known and so implemented, in both biotechnology and pharmaceutical industry, that is relatively simple to make changes in any type mAb structure without risking the overall production process. An example of this is the

production of bispecific antibodies, capable of simultaneously binding two different targets [31].The know-how acquired during the last years, in terms of mAb production, is probably the reasons why some Fab fragments are produced using proteolytic enzymes, capable of cleaving a mAb and creating two Fab fragments. On the contrary, Fab production is not so straightforward. There is a lot of laborious process development that include: choice of production host, improvement of the host genetic machinery, and especially design of an efficient downstream process [32]. The lack of Fc does not allow the use of Protein A as a downstream solution for Fab fragments, and so, alternative purification routes must be taken to purify them. For the downstream processing of mAbs, the use of a Protein A affinity chromatography step is a guaranty of a process able to deliver a highly pure mAb without significant loses [33,34].

The main differences between Fabs and mAbs are summarized in **Table 2.1**. To compare both biomolecules and state advantages or disadvantages is a fairly simple way to analyze these. A structural advantage for a mAb molecules can be a disadvantage for a Fab and vice-versa. Nevertheless, an assumption can be made, Fabs fragments will never out-perform mAbs as their alternatives, however, if properly engineered and applied to a specific application, they have an incredible utility as drug therapies and biotechnological/biomedical tools.

Table 2.1 Comparison of the distinct features of antibody Fab fragments and whole antibodies

	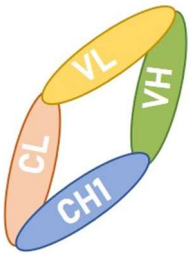	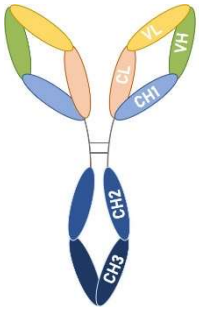
	Fabs	**mAbs**
Size (kDa)	~50	~150
Half-Life	Short	Long
Blood/Renal Clearance	Fast	Slow
Tissue Penetration	Fast	Slow
Avidity	Low	High
Production	(1) Mammalian, bacteria, yeast, insect and plant cell lines (2) Enzymatic Cleavage	Mammalian cell lines
Glycosylation	(1) Produced in mammalian cell systems (2) Produced by enzymatic cleavage	Always
Purification	Not defined for all classes of Fabs. Protein L only able to purify Kappa Light Chain Fabs	Defined for all mAbs. Protein A as key player
Manufacture Cost	Low	High
Best Suited Application	Imaging applications	Therapeutics

2.3. Fab fragments and their structure

Fab fragments are heterodimers, with high thermal stability and solubility, ideal for long-term plasma residency and so, ideal for therapeutic applications [35–37]. These four-domain protein have a molecular weight of approximately 50 kDa, with one heavy and a light chain bond together by several inter- and intrachain disulfide bonds [38]. Both heavy and light chain have one variable and one constant region (**Figure 2.1**). Each variable domain contains three hypervariable loops, known as complementarity-determining regions (CDRs), which are responsible for the binding of Fabs to the target epitope [39]. The great stability of Fab fragments is conferred by the inter-domain cooperativity, making Fabs more stable than other antibodies derivatives, for example scFv, which have their hydrophobic interface exposed, while in Fab this region is buried by the constant domains [40].

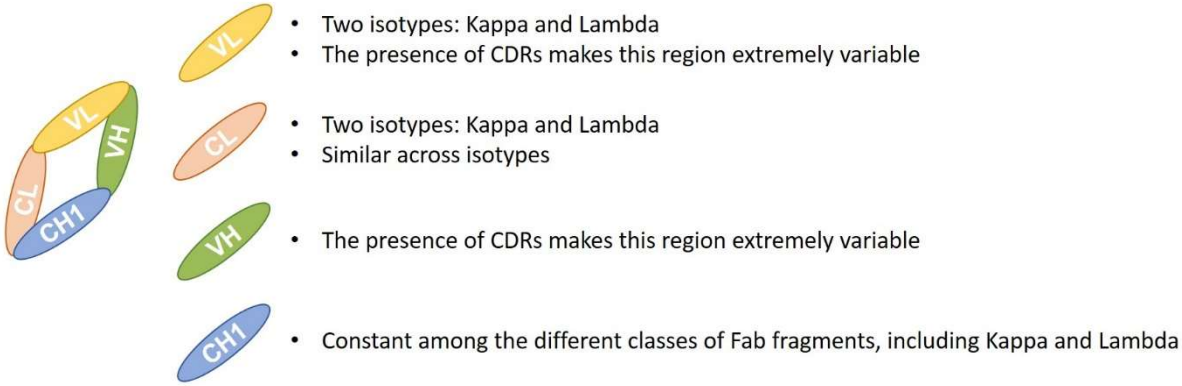

Figure 2.1 Schematic representation of a Fab fragments. A brief description of the differences that each domain can have is made.

The high specificity of an antibody is given by their region of epitope recognition, the CDR loops, presented at the Fab region, and the major source of Fab and mAb variability. Additionally, there are two possible light chain classes - kappa (κ) and lambda (λ), that further increases the variability of this biomolecules [41]. The isotypes ratio varies with Fab fragment origin, for example in human, the κ:λ ratio is 2:1, while in mice is 20:1[41–43]. The main difference between the two isotypes is related with the location of the genes that code for these two different light chains, located in different chromosomes. Other differences include: flexibility, half-life, solubility, size and propensity to alter antibody specificity [41,44–46]. In terms of structure, there is one structural difference between

lambda and kappa light chains Fabs, lambda Fabs have in general larger elbow angle than kappa [47]. The work of Toughiri *et al.* suggested other difference between kappa and lambda antibodies: the domain interaction is dependent on the Fab isotype [37]. In his work, the domain interaction within Fabs was studied by generating Fabs with both native and non-native V-gene and C-gene pairing, creating, among other combinations, the same Fab having the two different light chains. One of the observations obtained in this work was that the constant lambda domain when paired with the constant heavy domain is more stable then when the kappa constant domain is used. However, in terms of inter-subunit cooperativity, when kappa chains are used, it grants more cooperative within an intact Fab. An interesting result was the less aggregation of pertuzumab Fab with C_L/lambda than with the native kappa pertuzumab. Other conclusions obtained in this work corroborates what was previously known, Fab fragments with different chains have different stability, different solubility, and different biophysical properties [37].

Glycosylation is a predominant protein modification that increases the pharmacokinetic and biophysical properties of therapeutic proteins[48]. MAbs, are glycoproteins, and have N-glycans in both Fc and Fab region[49,50]. Fc have a glycan attached to Ans297, while Fabs, being such a variable region among antibody classes, can be glycosylated in both heavy and light chain, CDRs, and framework region[51,52]. In healthy individuals, 15% to 25% of the Fab portions are known to have N-glycans, involved in the affinity and avidity of antibodies for antigens [51]. When Fabs are produced, using a cell expression system, they can be glycosylated or not, depending on the cell used for their production. If Fabs are produced in mammalian cell system, they will be glycosylated, once these cells can perform post-translational modifications. However, if Fabs are produced using simpler cell system, such as *E. coli*, these are not able to do post-translational modifications, and so, Fab fragments will not be glycosylated [53]. There is another alternative to produce Fab fragments, cleaving a whole antibody using proteolytic enzymes, such as papain and pepsin. When this is the method of choice to produce Fabs, these will have the glycosylation pattern of the initial antibody. The digestion of Fabs with papain will not interfere with the glycosylated residues of this region, in fact, the presence of N-glycans makes antibody digestion, with papain or pepsin, more difficult, proving that glycosylation increases the stability of both antibody and Fab fragments [54,55].

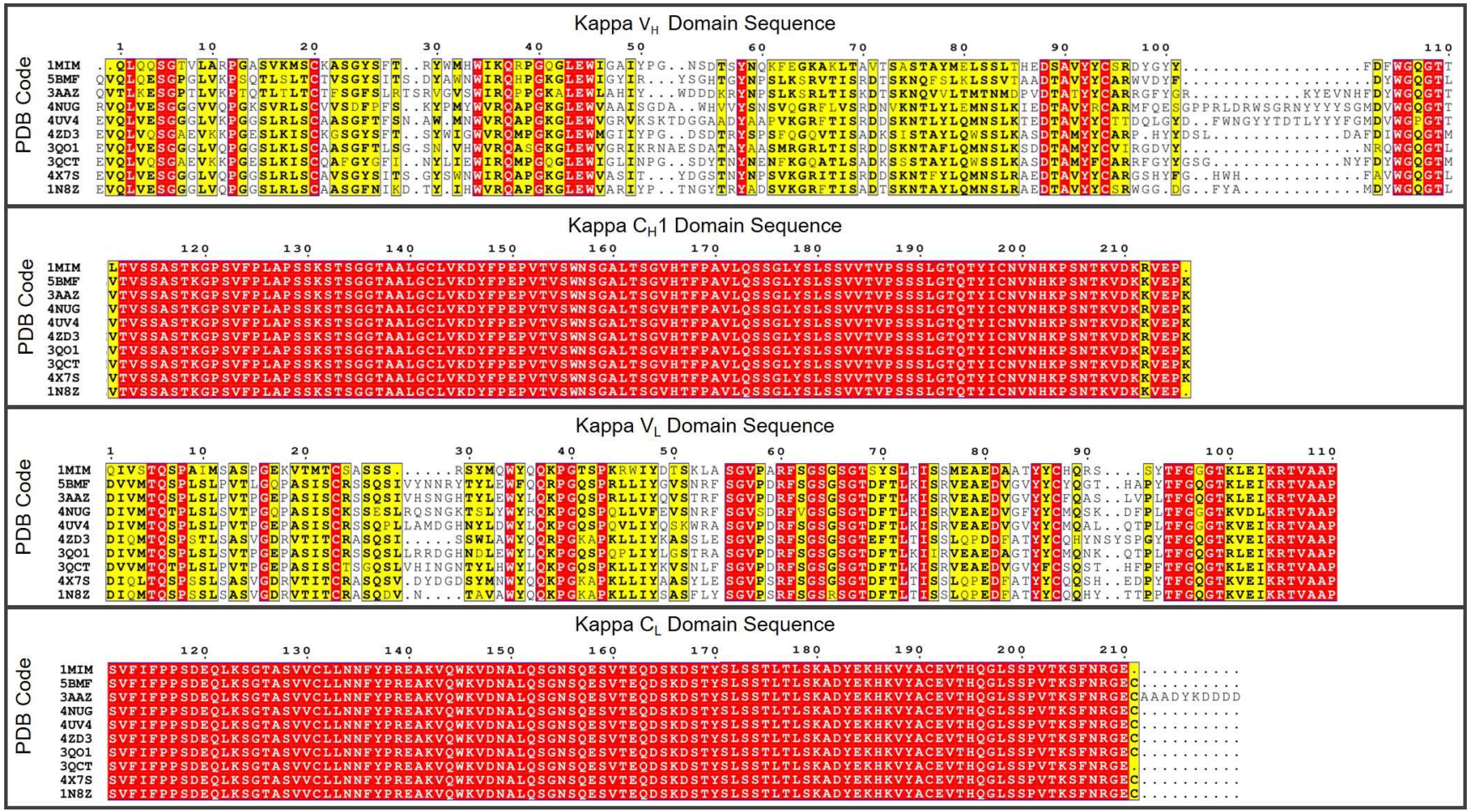

Figure 2.2 Multiple sequence analysis of ten kappa light chain Fab Fragments. All sequences were downloaded from PDB (identified by their four-character accession codes), aligned with Clustal Omega, and analysed with ESPript 3.0. Highlighted in white on red boxes are the conserved residues. With similar residues – identified by the ESPript default parameters (Risler, global score 0.7) are highlighted in yellow.

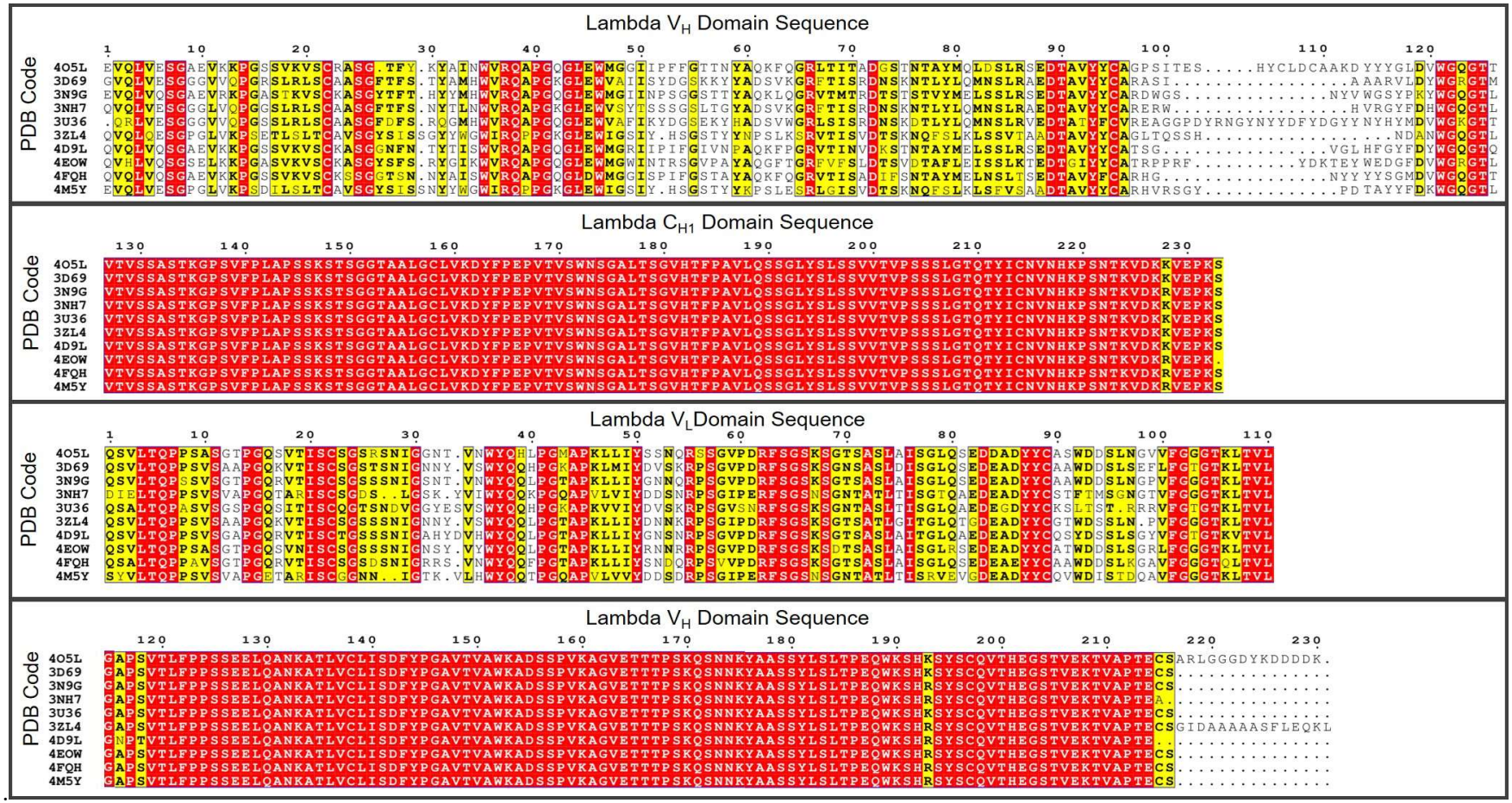

Figure 2.3 Multiple sequence analysis of ten lambda light chain Fab Fragments. All sequences were downloaded from PDB (identified by their four-character accession codes), aligned with Clustal Omega, and analysed with ESPript 3.0. Highlighted in white on red boxes are the conserved residues. With similar residues – identified by the ESPript default parameters (Risler, global score 0.7) are highlighted in yellow.

2.3.1. Sequence analysis of kappa and lambda light chain Fab fragments

Kappa and lambda Fabs have different light chains, with the main differences briefly described here and in studies elsewhere. However, it is interesting to take some time and evaluate differences between them based on their amino acid sequences. To accomplish this, a search on the Protein Data Bank (PDB - https://www.rcsb.org/) for Fab fragments was executed and arbitrarily downloaded 96 FASTA sequences of these, with either a kappa or lambda light chain. In this search, only the free Fab fragments were selected, i.e. not in complex with other molecules. Of the 96 selected sequences, 70 were identified as kappa Fabs, and remaining 26 were lambda Fabs. With this initial analysis, one can corroborate the general assumption that the majority of Fabs, for any application, possess a kappa light chain. Once the Fabs were divided into kappa and lambda, 20 sequences – 10 kappa and 10 lambda – were randomly selected and aligned using the Clustal Omega tool. The free online software ESPript (Easy Sequencing in PostScript) was used to access and visualize their sequence similarities [56,57]. Starting with the heavy chain, the V_H (position 1 to 110) is not significantly conserved across different Fabs (**Figure 2.2 and 2.3**). Despite the presence of some conserved motifs in both type of light chains, the amino acids in this region are highly variable. CDR loops, present in this region, are responsible for each Fab fragment's antigen specificity and therefore a great extent of variability is expected in this region of the Fab. In contrast to the V_H domain, C_H1 (position 110 to 220) is highly conserved in all the selected kappa and lambda Fabs. Regarding the light chains (**Figure 2.2 and 2.3**), the V_L domain (position 1 to 110), where the CDR loops are, makes this region unique to each Fab, and so the degree of homology is low. The C_L (position 110 to 220) of the light chain is similar for Fabs of the same class, with very low homology when the two are compared.

While this method was a simple way to emphasize the difference between Kappa and Lambda sequences, the number of Fabs here selected is small. For a deeper sequence analysis, the selection of Fabs must be broader, and must include: (1) Fabs from different antibody sub-classes (IgG1, IgG2, IgG3 or IgG4) and (2) Fabs having different subtypes of kappa and lambda light chains. In addition to this intrinsic variability among Fabs, numerous Fabs have been subjected to affinity maturation by sequence alteration, further increasing the variability within this class of proteins. Nevertheless, with the data here

presented, is interesting to note that most Fabs share a high degree of homology, even in the traditional denominated variable region.

2.4. Fab Fragments: production process

One of Fab fragments particularities, when compared to whole mAbs, is their production flexibility. Fabs can be produced in several and economical cell systems while keeping the same epitope specificity. The lack of the Fc and glycosylation makes the production of Fab fragments easier and possible to be directed towards the periplasm in prokaryotes, such as *E. coli* or in the endoplasmic reticulum of eukaryotes (yeasts, insect and mammalian), which facilitate proper translation towards the extracellular medium [58]. The ability to produce Fab fragments in simpler cell systems is a clear advantage against whole mAbs, generally produced only in mammalian cells due to their ability to perform human-like N-glycosylation and correct post-translation modification [59]. However, mAb upstream production is an extremely defined and stablished process, and so, a great number of Fabs, especially for research purposes, are produced by enzymatic digestion of whole mAbs, with proteolytic enzymes, such as papain. Here an overview of the most common Fab fragment production processes will be made, focusing on both enzymatic cleavage and recombinant production.

2.4.1. *Escherichia Coli* as a solution for Fab production

The preferred cell host choice to produce non-glycosylated proteins is the gram-negative bacterium *E. coli* [60]. The extensive knowledge and characterization of this organism simplifies the implementation of a trustworthy production platform for proteins. Their low-cost production, rapid growth rate, high cell density cultures, scalability and clear regulation for therapeutic protein production makes *E. coli* ideal to produce non-glycosylation recombinant proteins [61,62]. Moreover, being such a studied host, *E. coli* can be easily manipulated to promote better protein expressions and titers [63,64]. To produce Fab or other non-glycosylated antibody derivatives, *E. coli* is the most common cell host. The production of functional antibody fragments in this organism represents a

breakthrough in the antibody engineering field, promoting the production of high titers of these class of recombinant proteins[65]. It is possible to produce Fab fragments in two different compartments of *E. coli*: (1) cytoplasm [66] and (2) periplasm[67,68] (**Figure 2.4**). The strategy to produce these can vary accordingly to the chosen compartment.

When Fab fragments are produced in the cytoplasm, the lack of a proper oxidizing environment, for the formation of disulfide bonds, and consequent appropriate protein folding, will promote the formation inclusion bodies (IBs)[69]. The accumulation of these insoluble proteins aggregates in the cytoplasm of *E. coli* is one of the major problems of Fab production in *E.coli* [60]. Two strategies can be taken to avoid this: (1) disrupt the cell, and refold the inclusion bodies [70] (**Figure 2.4** – route 2 and 3) or (2) use a mutant *E. coli* strains capable to promote the correct disulfide bond formation or creating an oxidizing cellular environment (**Figure 2.4** – route 4 and 5)[71]. When the first strategy is chosen, the inclusion bodies are subjected to an *in vitro* refolding to make the protein functional and active. This process is generally tedious and expensive, with refolding and purification steps that could lead to high degree of protein loss[72]. The second strategy to produced Fab fragments in the cytoplasm of *E. coli* is based upon expression technology, where engineering strains are used to promote proper folding of the Fab fragments. Null mutations in the thioredoxin-reductase and glutathione reductase genes improves the formation of disulfide due to the promotion of a more oxidizing environment in the cytoplasm [73]. The expression of cytoplasmic chaperones such as GroEL/S and/or trigger factor, used singly or in combination, improve Fab fragments solubility and can enhance their yield of functional in *E. coli* [60,71].

Alternatively to the production in the cytoplasm, Fab fragments can be directed towards the periplasm and/or in the extracellular medium[74,75]. The presence of a leader peptide at the N-terminus of the recombinant polypeptide chains (V_H-C_H1 and V_L-C_L) will promote their translocation to the periplasmic space, where its naturally-oxidizing environment and the presence of *E. coli* disulphide bond chaperones (Dsc proteins) will create the necessary conditions for a proper Fab fragment folding (**Figure 2.4** – route 6 and 7) [74,76–78]. Once formed, Fabs can stay in the periplasm or if they have a signal sequence can be secreted to the extracellular space (**Figure 2.4** – route 8)[79]. To secrete Fab fragments to the periplasm/extracellular space is the preferred choice, once the generation of an oxidizing cytoplasm in *E. coli* is directly related with metabolic problems and poor growth [74]. Moreover, the presence of Fab fragments in the periplasm makes

their downstream process much simpler, consequence of the lower amount of proteins and endotoxins [32]. Additionally, protease activity in the periplasm is far lower than that in the cytoplasm [74]. The secretion of Fabs to the extracellular will simplify even more the downstream process. Disadvantages associated with the production of Fab fragments in the periplasm are its small size, in comparison with the cytoplasm, and the possible overload of the secretion apparatus that can reduced protein expression levels[61].

Presently there are two Fab fragments being commercialized that are produced using *E. coli* – Lucentis and Cimzia [60,80]. These two examples are just the tip of the iceberg of the work that is currently being done with the production of Fab fragments in this expression system. Currently, soluble Fab molecules can be produced up to 1-2 g/L [81], which makes it extremely attractive for a myriad of different studies, including: production of Fab-effector fusion protein [82]; development of Fabs after phage display

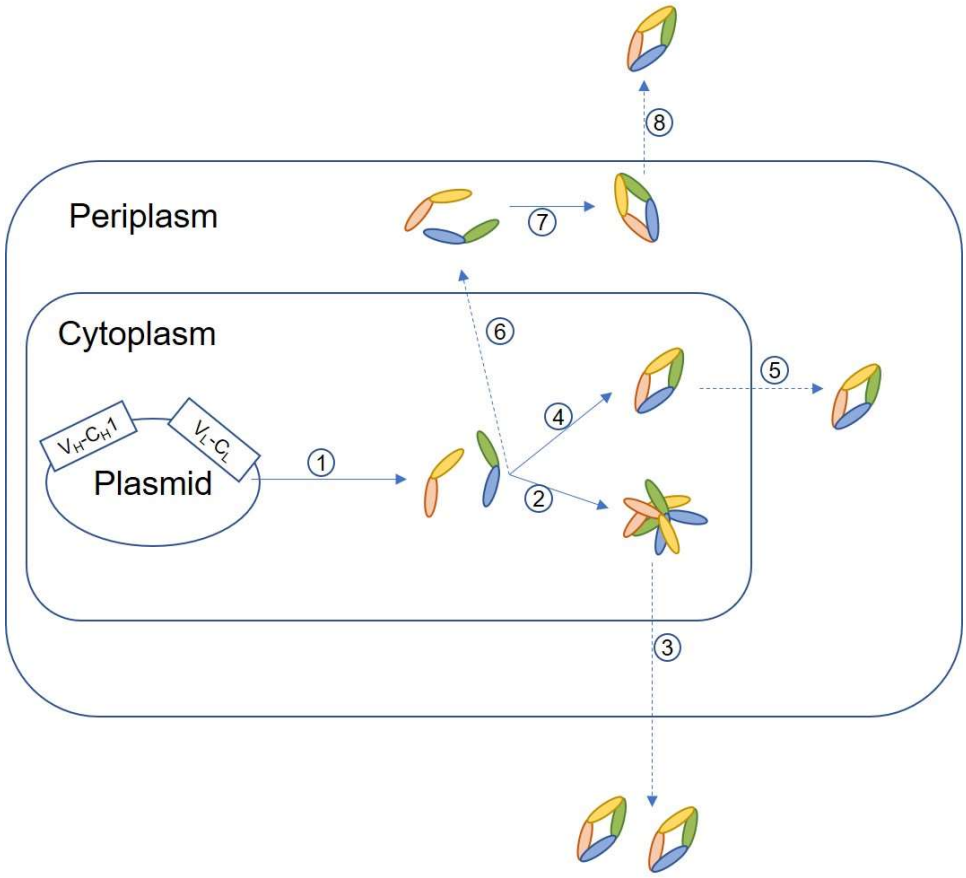

Figure 2.4 Schematic representation for the possible production routes of Fab Fragments in *E. coli*. (1) Gene expression of light and heavy chain, (2) Formation of inclusion bodies, (3) *In vitro* refolding of inclusion bodies after cell disruption, (4) Folding of Fab inside the cytoplasm, (5) Secretion of folded Fab to the periplasm, (6) Secretion of unfolded Fab to the periplasm (7) Folding of the Fabs in the periplasm, (8) Secretion of the Fab to the extracellular medium (leader sequence or by cell disruption) (adapted from [72]) .

technique [83]; optimization of recombinant protein expression in *E. coli* [77]; structural studies [84] and others [85].

2.4.2. Yeast as a solution for Fab Production

Other frequent host for biotechnology applications is the engineered yeasts *Saccharomyces cerevisiae* and *Pichia pastoris* [86]. To produce antibodies and derivatives, the last one has shown more success than the first. The intensive glycoengineering work done in *P. pastoris* led to the production of antibodies with human-type glycosylation[87] and Fab fragments [88,89]. Despite being less popular than *E. coli* and mammalian production hosts, the development of *P. pastoris* technology is creating the needs for a well stablished expression system to produce high levels of antibodies, Fabs and other derivatives [90]. When compared to other yeast strains, specially *S. cerevisiae*, *P. pastoris* shows better capacity for the production and secretion of heterologous proteins, without secreting large amounts of its own proteins, creating simpler downstream processes [21]. Moreover, *P. pastoris* can be cultivated in fed batch, with high cell density cultures, promoting a scalable and cost-effective process [91].

A crucial factor influencing the production of antibody derivatives in *P. Pastoris* is the choice of the promoter. Two options are commonly used: (1) methanol-inducible promoter (AOX1) or (2) glycolytic glyceraldehyde-3-phosphate dehydrogenase (GAP) [92]. AOX1 is a strong promotor, strictly regulated by methanol, preferred for high cell density cultures and high-level of protein expression in *P. pastoris* [93]. An example of AOX1 as an efficient promoter for high level production of recombinant Fab fragments is reported in the work of Ning *et al.* [94]. In this study the quantity of produced Fab fragment was up to 420~458 mg/L in 5 L bioreactor. The production of other antibody derivatives, with as the AOX1 promoter is vastly reported, and summarized in other publications [95]. GAP promoter is the most common alternative to AOX1 in *P. Pastoris*. This constitutive promoter is weaker, when compared to AOX1, and it is mainly used when there is a need for a time consuming Fab fragment folding [90]. In contrast to AOX1, GAP protein expression used glucose, glycerol and other carbon sources as substrate[96]. The expression level of soluble Fab fragments using GAP promotor is around 420 to 458 mg/L[94].

P. Pastoris have been extensively studied in the last years, especially in terms of molecular biology and gene functions. The use of Fab fragments as model proteins is a

common procedure to acquire more knowledge about this organism and explore its full potential. In his work, Pfeffer *et al.*, used the Fab3H6 - the anti-idiotype to the HIV neutralizing antibody 2F5 – to study the protein translation, translocation, folding, process and secretion in *P. Pastoris* [97]. Using Fab fragments as model proteins, they confirmed that intracellular retention of secreted protein is one of the major bottlenecks in recombinant protein production in *P. Pastoris*. Another conclusion was the importance of intracellular degradation, and the impact of proteasomal degradation in the production of the Fab 3H6, that may degrade more than just misfolded Fabs. To explore the key factors involved in to folding of recombinant proteins in *P. Pastoris*, Gasser *et al.* used Fab fragment as a model molecule. In this work, they identified that protein folding and heterodimer assembly in the ER are the limiting step in Fab secretion [90]. To solve this, overexpression of *S. cerevisiae* protein disulfide isomerase and unfolded protein response transcription factor was engineered in *P. pastoris*. The result was an increase of Fab secretion. Other studies using Fab fragments as model recombinant protein in *P. pastoris* include: vector design [88], carbon source [96], and growth temperature [98]. Expression of Fab fragments in the surface of *P. pastoris* to perform Fab-display technology is another application of this host [99,100].

The use of the yeast *P. Pastori*s as a recombinant Fab fragment production solution is clearly a very strong alternative to other microorganisms, such as *E. coli*. However, there is a need for a deeper understanding about all the aspects of protein production in *P. Pastoris,* especially to increase production titers in Fab fragments and other antibody derivatives. The other yeast, commonly used to produce recombinant proteins, is *S. cerevisiae*, however, for heterologous proteins, like mAbs and antibody fragments, inefficient trafficking and misfolding is a common problem when this host is chosen [101,102]. Another common problem is the tendency that *S. cerevisiae* to hyperglycosylate heterologous proteins, even at positions that are not generally glycosylated. However, because Fab fragments are not glycosylated, they can be produced in this yeast, without the characteristic hypermannosylation [21,103,104]. Nevertheless, and despite the extensive strain engineering work to increase the secretory capacity and productivity of *S. cerevisiae* [105], a long way must be trailed to make this host a valuable solution to produce antibodies and derivatives [106].

2.4.3. Mammalian cells as a solution for Fab Production

There are two options to produce Fab fragments in mammalian cell systems: (1) use of proteolytic enzymes to cleave whole antibody into Fab fragments or (2) clone Fab genes into a vector and express it in a mammalian cell lines.

2.4.3.1. Antibody cleavage with proteolytic enzymes

The traditional enzymes to generate Fab fragments from mAbs are papain [107] or pepsin [108], both can cleave immunoglobulins near the hinge region. When pepsin is used, the cleavage occurs bellow the disulfide bridges creating one divalent fragment, $F(ab)_2$ (100 kDa) [109], while papain cleaves in the two key hinge disulfide bridges, creating one Fc fragments and two Fab fragments [110] (**Figure 2.5**). For the purpose of this thesis, only the antibody digestion with papain will be described.

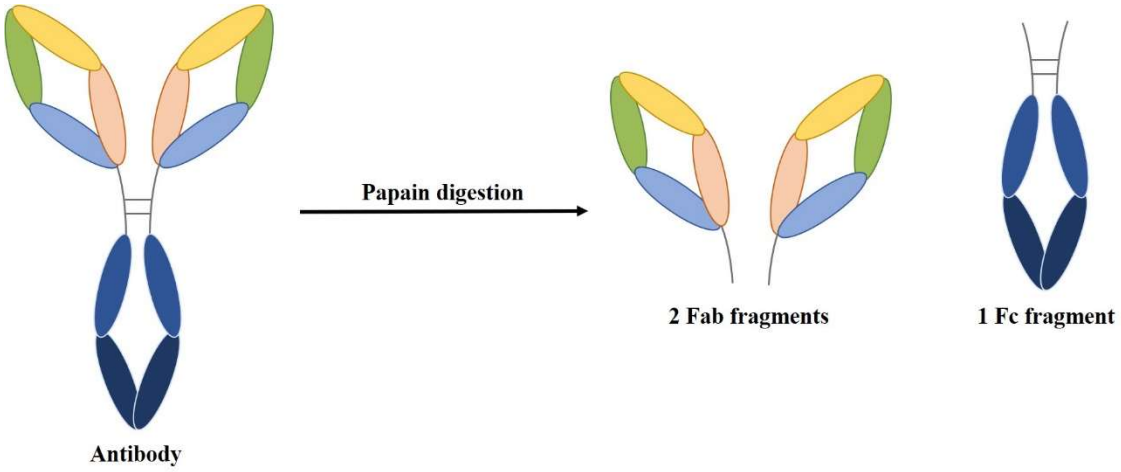

Figure 2.5 Schematic representation of the antibody digestion process with papain.

Papain is a proteolytic enzyme from the cysteine protease family, that cleaves IgG molecules in two different sites: His224/Thr225 and Glu233/Leu234[111]. The use of this enzyme is a very studied process, with the first report of this application made in the fifties [107]. The literature is vast, and different approaches have been used to study the best conditions to cleave antibodies [111–113]. Currently there are commercially

available kits that use agarose beads, complexed with papain, to digest whole antibodies into Fab fragments. However, to make the digestion process efficient, there is always the need to spend some time adjusting the variables of the papain digestion protocol. Several factors influence the digestion efficiency, including: digestion time, papain and cysteine concentration, and the class of antibody [110,111]. Papain needs to be active in the presence of cysteine to promote a more efficient digestion, and both cysteine and enzyme concentration must be correctly tuned to avoid low digestion yield or over digestion of the Fab fragments [110]. The major limitation of this enzymatic solution to generate Fab fragments is related with the digestion yield, it will never be 100%, there will always be undigested IgG in the end of a digestion process [114]. Other less popular process to cleave mAbs is the one that uses the endoproteinase Lys-C, that recognizes the C-terminal of a lysine in the hinge region, generating one Fc and two Fab fragments [115,116].

2.4.3.2. Fab produced as a recombinant protein in mammalian cell lines

The other mammalian source of Fabs is the transient expression of Fab fragments in mammalian cell lines [23,117]. Nowadays it is relatively simple to clone the antibody genes and express them in the format of Fab fragments, with the two polypeptide chains, the heavy ant the light [58]. Comparing with *E. coli* expression systems, these cell lines are more expensive, and the production rate is slower, however, they have all the machinery needed to achieve a correct folding and secretion of the fragments. Another advantage of using mammalian cell lines is the ability to use all the know-how acquired by the production of mAbs and apply it to produce the Fab fragments. The most common line of mammalian cells to produce these recombinant protein are HEK 293T [117] or CHO cells [118].

Unlike mAbs, the production of Fab fragments can be done in different expression systems or by proteolytic degradation of whole antibodies. As a consequence of all the genetic work developed in *E. coli* and *P. pastoris*, these are playing an important role in the production of Fab fragments, being a solution in the production of these recombinant proteins in small and large scale. There are other alternative systems to produce Fab fragments, including plants, insects and others, but not with the preponderance of the previously referred methods.

2.5. Fab Fragments: purification process

2.5.1. Protein L

An efficient mAbs purification platform is mandatory to answer the actual market needs for these biomolecules. The use of protein A, from *Staphylococcus aureus,* as affinity chromatography is the most applied solution to purify antibodies [119,120]. Protein A binds to the Fc region of mAbs, making it the universal purification solution for the majority of antibodies [121,122]. With the advent of Fab fragments, a purification platform similar to the one used for mAbs is essential. Though, the lack of Fc fragment makes the purification of these fragments a challenge. Protein A has some affinity towards certain Fab fragments [123], however, not enough to be used as a Fab purification chromatography step. Protein G, from group G *streptococci,* is another affinity solution to purify whole antibodies [124], and like protein A, it has affinity for Fab fragments, specifically C_H1 domain [125]. However the affinity for this Fab region, when compared to the Fc is lower [126], precluding the application of protein G, without any mutational changes, as a solution to purify Fab fragments. Bailey and colleagues have made key mutations on amino acids of protein G structure in order to increase its affinity towards a 4D5 scaffold Fab [127]. The final protein G variant, with 8-point mutations in the binding domain, showed an approximate 100-fold improvement affinity towards the tested IgG1 Fab molecule. The same did not happen with different Ig's isotypes, where the same protein G variant showed a decrease of ~20–50- fold for IgG2, IgG3 and IgG4. Nevertheless, the result obtained in this study showed that there is space for affinity maturation processes, where low binding affinities can be improved to create high affinity interactions. In this case, protein G was mutated to create a Fab-based affinity solution [127].

An alternative to protein A and protein G is protein L (PpL), a 76-106 kDa bacterial cell wall protein, present in the surface of the anaerobic bacterial species *Peptococcus magnus* [128–130], with high affinity towards the framework region of kappa light chains of Fab fragments [131]. Like protein A, PpL show a broad affinity across different classes of antibodies, including, IgG, IgM, IgA, IgE, and IgD [130,132]. Depending on the strain, PpL has four to five highly homologous binding domains [133,134]. The folding structure of B1 chain on protein L, previous solved by NMR spectroscopy, resembles the folding

structure and orientation of Protein G, with a β sheet composed of two pairs of anti-parallel β strands and a α helix in the top of the sheet (**Figure 2.6**) [135,136].

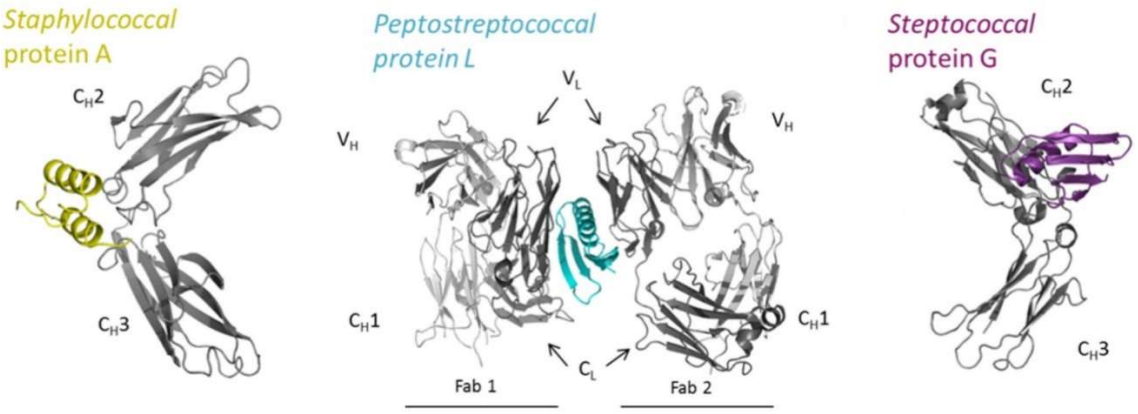

Figure 2.6 Molecular structures of the three antibody-binding domains – Protein A, L and G. Protein A (yellow) binds preferentially the Fc region of an antibody – between C_H2 and C_H3 region. Protein L (blue) binds two Fab fragments – close to the V_L region. Protein G (purple) preferentially the Fc region of an antibody – between C_H2 and C_H3 region (adapted from [137]).

The binding of PpL to the kappa light chain occurs mainly at the V_L domain. Two different interfaces on PpL can bind to the Fab [138]. In the first, the one where the binding has higher affinity, 13 residues are involved, being 10 presented at the Fab framework region, other in the segment connecting V_L with C_L, one in the C_L region and finally one in the CDR-L1 region. In the second interface, 15 residues are involved, with 10 of them being common to the first interface. None of the residues that contribute significantly to the second interface are involved in the first one. Despite interacting in very similar areas of the Fab, the two binding sites have different affinities towards the Fab, being the affinity between the first interface and the Fab one order of magnitude higher than the second [138].

2.5.2. Affinity alternatives to Protein L

For any biomolecule, to have an affinity purification step is a guarantee of a reliable downstream process. Protein A, G and L are proof of this. These natural immunoglobulin-binding ligands have been adopted as the capture step of choice for antibodies and derivatives in both industry and academia. However, the drawbacks of these ligands (high cost, limited life cycles, low scale-up potential, poor column stability [137]) are

encouraging the finding of alternatives that promote even more efficient purification methods [139,140]. For Fab fragments, PpL is a conservative purification solution, but it was one major limitation: it is not a universal solution to purify Fab fragments. The lack of affinity towards lambda light chain isotypes and some subclasses (VκII) of kappa light chain Fabs makes PpL unable to be implemented as an affinity chromatography solution for all classes of Fab fragments[132,141]. To make the downstream process of Fab molecules as efficient as the mAbs, it is mandatory to create a universal affinity chromatography step, able to bind all classes and subclasses of Fab fragments. One of those alternatives is reported on the work of Roque *et al*. A triazine-based ligand was synthesized (ligand 8/7) and despite having lower affinity than PpL, ligand 8/7 could compete, as a downstream solution, for the binding of IgG and Fab [142]. The versatility of ligand 8/7 was tested, and the ability to bind both human kappa and lambda IgG1, and polyclonal IgG from a wide range of different species was demonstrated. This low-molecular weight biomimetic ligand can be one of the alternatives to traditional Ig-binding proteins, with the advantage of being relatively cheap to produce, and resistant do SIP and CIP.

Another alternative that can be applied to purify Fab fragments is the use of one of the smallest antigen-binding domains, the nanobodies [143]. These recombinant camelid antibody fragments, consisting of a variable single domain (V_HH) [144], offer several advantages when comparing to traditional protein-based ligands, including high stability, low immunogenicity, easy cloning and high solubility [137,145]. Currently, Thermo Fischer Scientific has, under the name of CaptureSelect^{TM}, a range of affinity ligands based of V_HH able to bind antibodies and Fab fragments by interacting with different regions. CaptureSelect^{TM} IgG-CH1Affinity Matrix is a commercially available resin that can target the C_H1 domain of human IgGs. C_H1 is highly conserved across different antibodies and Fab fragments, hence this ligand offers the possibility of purifying a broad range of these class of biomolecules, including all IgG subclasses of both kappa and lambda isotypes.

The lack of a consistent universal answer to purify Fab fragments, especially those displaying a lambda light chain, was the key drive for the development of different affinity solutions able to perform a robust initial capture step. One of these solutions is LambdaFabSelect, commercialized by GE Healthcare Life Sciences, a camelid-based affinity ligand able to purify lambda light chain Fab fragments. In the work of Eifler *et*

al., the performance of this new affinity ligand was meticulously evaluated [146]. LambdaFabSelect displayed an ability to bind a broader range of human Fabs than both protein A and L. The results obtained for its binding capacity and scalability were comparable with protein A for mAbs purification. The main conclusion of this work was that the LambdaFabSelect can be seen as a robust and efficient capture step for the purification of antibodies or derivatives with a lambda light chain.

2.5.3. Purification of digested Fab fragments

It has been previous referred that one of the options to produce Fab fragments is by cleaving a whole antibody. Protein A in this process plays a central role, despite its inability to bind Fab fragments. After the digestion procedure, the final mixture contains undigested antibodies, Fc fragments and other digested fragments. Due to its high affinity towards Fc, protein A is frequently the first step (operated in flow-through mode or in batch) in the purification of Fab fragment after enzymatic digestion, once it can bind both Fc and undigested antibodies [147]. The following steps, where cysteine, papain, EDTA, and digested fragments are removed can be accomplish by membrane dialysis, size exclusion chromatography (SEC), ion exchange (IEX) and PpL affinity chromatography [113,148,149]. From all the polishing options, the use of membrane dialysis or membrane spin filters are the most common to separate the smaller impurities from digested Fab and performing buffer exchange at the same time.

2.5.4. Non-affinity chromatographic solutions

Ion exchange is a classical solution for the purification of recombinant proteins. For Fab fragments, cation exchange chromatography (CEX) is usually used after an initial affinity chromatography step (protein A, G or L, depending if Fabs are generated by enzymatic digestion or expressed) to remove trace amount of impurities. The use of CEX, in a pH gradient mode, combined with the more basic profile of Fab fragments, allows the implementation of a simple and robust chromatography step able to yield a product with the required purity and recovery [150]. Similarly, with the downstream process of mAb, the use of an IEX step, as part of Fab fragment purification, is a very straightforward process. It does not have the resolution of an affinity purification solution, but it is ideal to remove trace amount of impurities, specially DNA. CEX can be used also as an

analytical tool for Fab fragments, for example to profile their charge heterogeneity [115] or to separate Fab fragments, with a difference in pI as low as 0.1 [151]. Another traditional method for analytical studies of Fab fragments is the use of SEC [152,153].

The vast knowledge on mAbs and Fabs, makes them model proteins, thus, it is common to use them to evaluate new chromatographic supports or ligands, to investigate new downstream solutions, or to do process development by studying different chromatographic conditions, such as: salt, pH, conductivity and phase modifiers. Nevertheless, and after a thorough literature research, the number of references that focus on downstream process development of Fab fragments is not vast, and there are two main reasons for that. The first, is the use of an affinity chromatography solution to purify the most of Fab fragments produced in *E. coli* and/or mammalian cell lines. Ppl can purify those Fabs very efficiently, with high purities and recovery yields. This purification step is possible since the great majority of Fabs have a kappa light chain, especially the recombinantly produced ones. The steps that follow PpL are very similar to the ones executed for mAbs after protein A, being those very straightforward and routine. The second reason is related with the production of Fab fragments using papain to cleave antibodies. The purification of the digested Fab fragments is done with the vastly studied and perfected protein A affinity chromatography, which is followed by other polishing steps - IEX, SEC or membrane dialysis

An interesting work, where two routes of production and purification of Fab fragments were compared was done by Zhao and colleagues [154]. In the first route, Fabs produced by enzymatic cleavage were purified using the traditional method: protein A in flow-through mode, to separate Fab fragments from undigested IgG and Fc, followed by cation exchange to polish the Fab fragments. In the second route, Fabs produced using *E. coli*, having an a His-tag, were purified with a Ni–NTA Sepharose resin, being this followed by a SEC and an IEC steps. Both purification processes were comparable in terms of recovery yield and purity. In the end, the authors choose to produce and purify the Fab obtained using an expression system. For their application, crystallization experiments, the presence of the His-tag permits the production of higher quality X-ray crystals. Nevertheless, they pointed out that if mAbs are available, high-quality Fabs can be rapidly produced by papain digestion even for crystallization or other research applications.

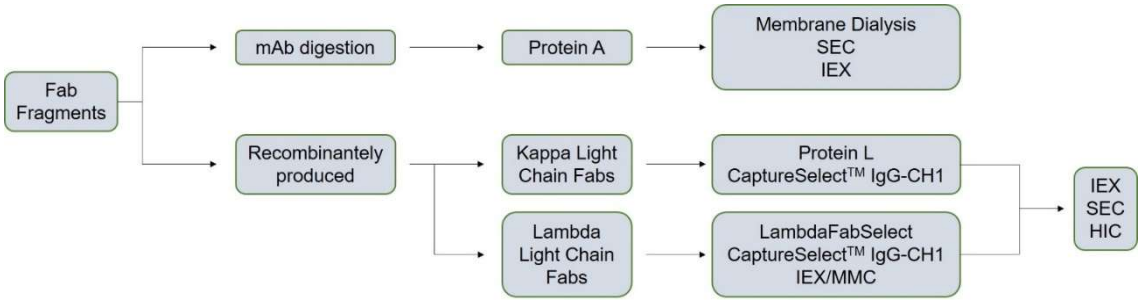

Figure 2.7 Traditional downstream scheme to purify Fab fragments. This scheme was design having one affinity step playing the central role in the downstream train.

A summary of the most applied processes to purify Fab fragments is schematized in **Figure 2.7**. Although the purification of these biomolecules is based upon the robustness of affinity downstream tools, there is still space for development of other purification solutions. Example of this is the lack of more alternatives to purify lambda light chain Fab fragments, that need a purification solution as efficient and straightforward as PpL is for the kappa light chain Fab fragments. Other hypothesis that is not very explored and could represent a valuable solution to purify Fab fragments is the use of multimodal ligands as a chromatography purification step[113,155,156]. In addition to chromatography, precipitation and other purification methods can be also developed to create alternatives purifaction processes for Fab fragments.

2.6. Fab fragments: current applications

Fab fragments inherent features make them valuable tools for a variety of applications, where they have a better performance than whole antibodies. The two main areas where Fabs are widely used are: for therapeutic applications and as imaging and diagnostic agents.

2.6.1. Fab fragments as therapeutics

The first Fab fragment approved as a therapeutic was abciximab (c7E3 Fab), trademark name ReoPro® (Centocor/Lilly), in 1994[12]. This platelet aggregation inhibitor is a chimeric Fab, with mouse variable and human constant domain [157]. It is expressed using mammalian cell lines, in continuous perfusion, and subsequently cleaved in the

upper hinge region between amino acids His224 and Thr225, using papain [158,159]. Abciximab binds the glycoprotein IIb/IIIa ($\alpha_{IIb}\beta_3$) receptor preventing the binding of fibrinogen and von Willebrand factor responsible for the activation of platelets [157]. It is administered in patients undergoing high-risk coronary artery angioplasty and atherectomy, being also used as a treatment for basilar artery thrombosis, and has been found to prevent rethrombosis[160].

Other Fab fragment available in the market for clinical applications, since 2006, is ranibizumab (Y0317 Fab), trademark name Lucentis® (Genentech/Novartis)[12]. This humanized Fab fragment is produced in the periplasmic space of *E. coli*, and it is used in patients that suffer from vision loss, to treat "wet" age-related macular degeneration [161,162]. Ranibizumab is a result of an affinity maturation process, using phage display and recombinant DNA selection steps, of an existing anti-VEGF variant. The final ranibizumab construct differs at five residues in the variable domain and one residue in the constant domain from the mAb bevacizumab (Avastin, Genentech) [163]. This maturation process led to an increase of 100-fold binding affinity towards VEGF [162]. The smaller size of ranibizumab (Fab), in comparison with bevacizumab (mAb), promotes a higher mobility and tissue penetration capability of this Fab, allowing an easier local administration through intraocular injection [5]. These anti-VEGF therapeutics are a good example of the advantages/limitations of using a mAb versus a Fab, and one should consider different aspects including, cost, administration periodicity, side-effects, among others. A deeper comparison between these two therapeutics will lead out of the focus of this thesis, plus, the literature concerning this matter is detailed [164,165].

In 2008, certolizumab pegol, trademark name Cimzia® (UCB), the third Fab fragment was approved for clinical applications [12]. This anti-inflammatory PEGylated Fab is used to treat Chron's disease and rheumatoid arthritis, by binding to the Tumor necrosis factor alpha (TNFα) [166]. Certolizumab is a humanized Fab, produced in the periplasm of *E. coli*, with two cross-linked chains of 20 kDa PEG in the near hinge region [167]. The presence of these two high-molecular molecules promotes an increase of hydrodynamic size, solubility, stability and extends the plasma half-life of this fragment[168,169].

The last approved Fab fragment for therapeutic purposes was idarucizumab, with the trademark name of Praxbind® (Boehringer Ingelheim), in 2015 [170,171]. Idarucizumab

is a humanized Fab fragment, produced in mammalian cell lines, used as a reversal agent of the anticoagulant dabigatran [172,173]. It binds to these nonpeptidic inhibitor of thrombin, the key serine protease in the coagulation cascade, reversing the anticoagulant effect without interfering with the blood coagulation pathway [173]. Idarucizumab was the last, of four, Fab fragment approved for clinical applications. The first referred three had a total sales of over $3.5 billion US dollars in 2010[12], proving that these antibody derivatives can, as mAbs, be a profitable solution for specific application where the properties of Fab fragments fits the needs of the pharmaceutical and medical scenario.

The four-approved therapeutic Fab fragments (summarized in **Table 2.2**), confirm the importance of these biomolecules in the pharmaceutical industry. Currently there are some examples of these biomolecules in clinical trials, among them citatuzumab bogatox (VB6-845) [174] and naptumomab estafenato (ABR-217620) [175]. Both represent an actual trend in the application of Fab fragments, the fusion of these with toxins or organic compounds. In the case of these two therapeutic candidates, they are fused with a toxin, attached to the framework of a Fab, that targets a specific antigen. The Fab and toxin construct promotes a more selective delivery of the toxin to the desired target, making its release and subsequent internalization more effective [176].

VB6-845 is a recombinant fusion protein used to treat epithelial tumors. It consist of a Fab fragment conjugated with bouganin, a plant-derived type I ribosome-inactivating protein, that can block protein synthesis via deadenylation of rRNA [174]. VB6-845 is specific for epithelial cell adhesion molecule (EpCam) and upon binding to EpCam-positive tumor cells it inhibits its growth [177]. Naptumomab Estafenato, a tumour target superantigen, currently being tested in a range of solid tumors, including, renal cell carcinoma [178]. This construct of a Fab (5T4FabV18) and a staphylococcal enterotoxin E (SEA/E-120) recognizes the tumor associated oncofetal trophoblast glycoprotein 5T4 [179]. The presence of SEA, a mutated variant of a superantigen (Sag), actives and induce multiplication of T-cells directing them to the tumour cells[175]. This fusion protein has been subject to a series of mutations and improvements, in both the Fab and SEA molecules, to decrease both toxicity and antigenicity and improve pharmacokinetics [179,180]. Naptumomab estafenato is an example of a fusion Fab fragment, with murine origin, that can be produced in *E. coli* [179].

Table 2.2 Approved therapeutic antibody Fab fragments

	Abciximab	**Ranibizumab**	**Certolizumab Pegol**	**Idarucizumab**
Year of approval	1994	2006	2008	2015
Tradename	ReoPro®	Lucentis®	Cimzia®	Praxbind®
Production	Digestion from a Chimeric mAb	Periplasmic space of *E.coli*	Periplasmic space of *E.coli*	Mammalian cell lines
Type of Fab	Chimeric Fab Fragment	Humanized Fab fragment	PEGylated Fab fragment	Humanized Fab fragment
Function	Platelet aggregation inhibitor	Binding to VEGF	Binding to the TNFα	Reversal agent of the anticoagulant dabigatran
Therapeutic Application	High-risk coronary artery angioplasty and atherectomy	"Wet" age-related macular degeneration	Chron's disease and rheumatoid arthritis	Rapid reversal of Pradaxa anticoagulant effects is required

2.6.2. Fab fragments as imaging tools

Tumor imaging is an expanding technique applied for cancer treatment and diagnosis. This technique allows the direct visualization of cellular processes in living subjects and by combining the knowledge of different fields, such as, cell biology, pharmacology and imaging, it allows the characterization, diagnosis and treatment optimization against different cancers cells [181,182]. Antibody and Fab fragment conjugated with a radionuclide can be a tool in both cancer therapy and in vivo molecular imaging [183]. However, the lack of the Fc portion makes Fab fragments more qualified in vivo diagnosis for several reasons, including, (1) their shorter half-life promotes a faster blood and kidney clearance of the tracer radiolabelled molecules from the system, avoiding an increase of background and overexposure of the radiolabelled probes that may affect healthy organs near the radiation[184]; (2) their small size allows for an higher tumor penetration and diffusion, promoting a faster accumulation in the targeted epitope [185];

(3) their homologous distribution makes them more indicated for high precision and contrast imaging results [17,186,187]. The disadvantages of using Fab fragments as imaging solution are the low avidity and the possibility of renal radiotoxicity as a consequence of high renal uptake [187].

Fab fragments as imaging tools is a stablished solution with several examples approved for radiotherapy and imaging, and others for *in vitro* studies. Arcitumomab, trademark name CEA-SCAN, is a murine Fab fragment, labelled with technetium 99m (^{99m}Tc) that targets carcinoembryonic antigen (CEA). It was approved in 1996 for radiotherapy and imaging of collateral cancer [186]. This Fab fragment have the particularity of initially being cleaved with pepsin followed by reduction, generating a Fab fragment with the hinge region [188]. Bectumomab, tradename LymphoScan, share the same structure and medical radioisotope (^{99m}Tc) with arcitumomab [189]. Bectumomab targets CD-22, a cell-surface molecule expressed on most B cell lymphomas to study non-Hodgkin's lymphoma[190]. Nofetumomab merpentan, trademark name Verluma, is another example of a murine Fab, conjugated with ^{99m}Tc and approved in 1996 for radiotherapy and imaging. This Fab fragment identifies advanced-stage small cell lung cancer [191].

2.6.3. Fab fragments: other applications

Fab fragments can be used to sequester and mitigate or obliterate the toxicity, in vivo, of low formula mass poisons, with high toxicity, such as digoxin, colchicine and tricyclic antidepressants [192,193]. The application of these antibody fragments for clinical toxicology, opposed to whole antibodies, results in a faster reversal of toxicity, which is particularly advantageous in case of life threatening poisoning [194]. The limitation of Fab fragments for anti-poisoning applications is their shorter plasma half-lives that may require more administration to completely prevent toxicity. DigiFab is a commercial available anti-digoxin Fab antibody, indicated for the treatment of digoxin toxicity or overdose [3]. Anti-digoxin Fab can be applied not only against digoxin but has already proved to be successfully used in the treatment of poisoning caused by parts of plants or animals such as coconut crab. Colchicine poisoning is rare but lethal, and is caused by overdose or by eating meadow saffron (*Colchicum autumnale*) leaves of flowers or glory

lily (*Gloriosa superba*) tubers [195]. Currently there is no approved Fab fragment against this compound, however, there are some studies where anti-colchicine Fab fragments shown to be effective in several toxicological models. Clinical studies in humans are needed to use Fab colchicine antidote in humans [195]. Overdose of tricyclic antidepressant is a common form of poisoning in developed countries, and Fab fragments are currently being tested as antidotes against this type of compound. In addition to the referred types of poisoning, others can be treated with Fab fragments, including: crotalid, snake venoms, paraquat and phencyclidine.

Finally, other area where Fab molecules are a valuable tool is X-Ray crystallography [196]. This technique uses Fab fragments as instruments for high-resolution protein structure determination, specially membrane proteins, that are generally very difficult determine without the help of Fab fragments [197]. The minor flexibility of these biomolecules, in comparison with whole antibodies, makes them perfect tools for resolving difficult protein structures, by increasing their stability and solubility. Moreover, Fab fragments can be used as affinity solution to purify membrane proteins, delivering highly purified material essential for crystallization purposes [198]. Other applications for Fab fragments are mundane, being these applied on a day-to-day basis in research for several techniques including: western blot, ELISA, flow cytometry, tag based affinity purification, among others.

Chapter 3

Designing of a universal papain-based digestion protocol to generate pure Fab fragments

3.1. Introduction

The production and purification of Fab fragments was summarized in **Chapter 2**. As described, there are two routes to produce Fab fragments: (1) by enzymatic digestion, where a whole antibody is cleaved, creating two Fab fragments, or (2) by recombinant production, where an expression system is chosen and Fabs are directly produced. Both of Fabs (digested and non-digested) where used in this thesis, however, in this chapter only digested Fabs were employed.

Papain is a proteolytic enzyme used to cleave whole antibodies, creating two Fab fragments and one Fc. Fragmentation of antibodies, with this enzyme, is a well-known procedure, and because every antibody is different, there is always a need to spend some time adjusting the digestion variables in order to find the most efficient cleavage protocol. Digestion time, papain and cysteine concentration play key roles in the digestion process, and so, it is fundamental to study their effect before stablishing a standard digestion protocol. In addition to the design of an efficient digestion protocol, the purification and recovery of pure digested Fabs is also an important step. After the cleavage of antibodies, there is a need to remove the ones that were not digested, Fc fragments, papain, small molecules (EDTA, cysteine, iodoacetamide) and small fragments that resulted from the digestion. To obtain pure digested Fab fragments is mandatory to have a robust purification scheme after the antibody digestion. The most traditional techniques to purify digested Fabs were vastly described in the **Chapter 2** and include the use of protein A to remove undigested antibodies and Fc followed by a diafiltration process, where papain, small molecules and fragments are removed.

In this chapter and in following ones, Fabs are produced by papain digestion of a polyclonal mixture of antibodies (Gammanorm®), where different types and classes are present. Gammanorm® is an antibody based therapeutic administered to

immunodeficient patients with difficulty in attaining the normal levels of antibodies [199]. The complexity of this antibody mixture created the need for a thorough study of the best digestion protocol, capable of digest most antibodies, independently of class or isotype. The first section of this chapter is focused on that, revisiting the conventional antibody digestion protocols, and design one capable to efficiently cleave different classes of antibodies. The effect of the three referred variables – digestion time, amount of papain and cysteine were studied. After stablishing the best digestion protocol, the other section of this chapter was to deliver pure Fabs present in the digestion mixture. Four different downstream schemes were designed, using protein A, protein L and centrifugal ultrafilters, in order to isolate the Fab fragments and make them suitable for the downstream studies developed under the scope of this thesis. In this chapter only antibodies from Gammanorm® are used and to simplify, the antibodies herein described will simple be referred as IgG.

This chapter contains sections that were published, as a research article, in the journal Separation and Purification Technology with the name Studies on the purification of antibody fragments (2018).

3.2. Materials and methods

3.2.1 Chemicals and biologicals

Phosphate buffered saline (PBS), Tris (hydroxymethyl)aminomethane (Tris), Sodium chloride (NaCl), citric Acid, Ethylenediaminetetraacetic acid (EDTA), L-cysteine, iodoacetamide and papain (≥ 10 units/mg protein) were obtained from Sigma Aldrich (St. Louis, MO/USA). Sodium dodecyl sulfate (SDS) and glycine were obtained from Bio-Rad (Hercules, CA, USA). Water used in all experiments was obtained from a Milli-Q purification system (Millipore, Bedford, MA/USA). Human immunoglobulin (IgG) for therapeutic administration (product name: Gammanorm®) was obtained from Octapharma (Lachen, Switzerland), as a 165 mg/mL solution.

3.2.2. Chromatographic resins and filtration devices

HiTrap™ Protein L and HiTrap™ Protein A HP were purchased as pre-packed 5 mL columns from GE Healthcare (Uppsala, Sweden). Amicon® Ultra-15 centrifugal filter units (NMWL of 10 kDa) were purchased from Merck Millipore.

3.2.3. Digestion protocols

The digestion protocol selected for the initial study was adapted from that reported in literature by Andrew *et al.* [112]. To evaluate the effect of digestion time and papain concentration the following conditions were selected: 2 g/L of IgG, 0.02 M of cysteine and 0.02 M of EDTA. The time of digestion was varied (4, 6, 8, and 24 hours) and for each digestion time, three concentrations of papain were tested (0.01, 0.02 and 0.1 mg/mL). The digestion occurred at 37˚C. To stop the digestion, a solution of 0.3 M of iodoacetamide was added to the digestion mixture to a final concentration of 0.03 M. To study the effect of cysteine, a concentration of 0.02 mg/mL of papain and a digestion time of 8 hours were chosen. The tested concentrations of cysteine were: 0, 0.01, 0.02 and 0.05 M.

To produce the Fab fragments for the downstream processes (DSP), the standard protocol was followed, and a digestion volume of 40 mL was processed. The major modification was the overnight digestion of the Fabs.

3.2.4. Chromatographic runs

All chromatographic experiments were performed in an ÄKTA™ Purifier 10 system (GE Healthcare). In all chromatographic runs, the conductivity, pH, and UV absorbance at 280 nm were continuously monitored. The data was acquired and processed by the software Unicorn 5.1. The flow-through and elution fractions were collected on a Fraction Collector Frac-950 (GE Healthcare).

3.2.5. Downstream processing

Four different DSP sequences were evaluated for the isolation of Fab fragments from the digestion mixture. DSP 1 included a protein A step followed by a protein L step; DSP 2 included a diafiltration step before purification by protein L; DSP 3 included a Protein L step followed by a protein A step; and DSP 4 included a protein A step followed by concentration.

In the chromatographic runs (protein A or protein L), 2 mL of sample were injected, either from the digestion mixture or collected pools. Adsorption occurred at pH 7.4 using a 20 mM sodium phosphate buffer with 150 mM NaCl; and elution was triggered by decreasing the pH to 2.5 using 0.1 M citrate buffer. In all runs, both flow-through and elution peaks were collected until the UV 280 absorbance reached the baseline. All elution fractions were neutralized with 3 M Tris pH 9. Regarding DSP 2, an initial ultrafiltration/diafiltration was performed in a 10 kDa centrifugal filter, in which 3 mL of digestion mixture was 4× diafiltered against PBS. For the DSP 4, the protein A flow-through samples were collected and 3× concentrated to a final volume of 2.5 mL. All the centrifugation and diafiltrations were performed in a fixed angle rotor centrifuge, during 10 min (each time) at 3000 *g* and 17˚C. All the steps in the four downstream schemes were performed in triplicate. Samples collected from the flow-through and elution steps were pooled and analysed with protein L chromatography.

3.2.6. Analytical methods

3.2.6.1. Digestion efficiency

The samples from the different digestion protocols tested were subjected to an analytical protein A chromatography step using a PA Immuno-Detection sensor cartridge from Applied Biosystems (Foster City, CA, USA). The adsorption buffer was PBS (pH 7.4) and the elution buffer was 12 mM HCl, 150 mM NaCl (pH 2–3) [200]. A calibration curve was prepared using standard Gammanorm® IgG solutions (in the range from 5 to 1000 mg IgG/mL). Digestion efficiency was determined based on the reduction of the

area of the elution peak. For 100% digestion, the elution peak area should decrease by 67%, assuming that both Fab and Fc fragments have the same molecular weight and that the digestion one IgG molecules yields two Fab and one Fc fragments.

3.2.6.2 Chromatographic recovery yield

The quantification of Fab fragments present in the pools collected during the downstream processes schemes were subjected to an analytical protein L chromatography using a POROS® CaptureSelect® LC Kappa Affinity Column from Applied Biosystems The adsorption buffer was PBS (pH 7.4) and the elution buffer was 12 mM HCl, 150 mM NaCl (pH 2–3). A calibration curve was prepared using standard human IgG solutions, normalized in terms of Fab fragments concentration (range from 3.3 to 660 mg Fab/mL).

The lack of a universal method to quantify the generated Fab fragments was the major challenge when designing the downstream experiments. An analytical protein L column was selected, which is able to bind Fab fragments but also undigested IgG with kappa light chain. This methodology will influence the tested purification yields, since it will quantify both molecules. This will particularly affect the quantification of Fab fragments in the initial feed where both molecules are present. After the undigested IgG is removed, the quantification will be accurate but yields will always be underestimated. However, the error will be present in all the purification steps, and for the purpose of this study, this type of quantification method is suitable to make a comparison between the different downstream schemes selected to isolate Fab fragments from an IgG digestion mixture.

3.2.7 Protein electrophoresis

The characterization of the fractions collected during each digestion protocol and chromatographic run was done by sodium dodecyl sulphate polyacrylamide gel electrophoresis (SDS-PAGE) [201]. Samples from collected pools were diluted with 2× Laemmli Sample Buffer from Bio-Rad. Diluted samples were applied in a 12% acrylamide gel prepared from a 40% acrylamide/2% bis-acrylamide stock solution (29:1) (Bio-Rad), and ran at 90 mV using a running buffer at pH 8.3, containing 25 mM Tris-

HCl, 0.192 M glycine and 0.1% SDS. To detect the protein bands, the gels were stained with BlueSafe purchased from NZYTech (Lisbon, Portugal).

3.3 Results and discussion

3.3.1. Enzymatic digestion of a mixture of human IgG

Amongst the several protocols available in the literature to generate Fab fragments by proteolytic digestion using papain [107,112,202,203], the protocol published by Andrew *et al.* [112] was selected for further optimization studies, since it was simpler, inexpensive and used relatively small amounts of IgG. In order to evaluate the efficiency of human IgG digestion, three key parameters were selected and studied for digestion optimization: digestion time, concentration of papain and concentration of cysteine.

In a first approach, the digestion time and the amount of papain were varied. Three concentrations of papain – 0.01, 0.02 and 0.1 mg/mL – and four digestion times – 4, 6, 8, and 24 hours were chosen, while the concentration of cysteine was kept at 0.02 M. The efficiency of the different digestion protocols was evaluated by an indirect method based on analytical protein A chromatography, that allows to estimate the mass of whole IgG present. At time zero, the IgG present in the digestion mixture is intact, corresponding to the maximum elution absorbance peak. When the digestion starts, the IgG in the mixture is cleaved, and consequently, the area of the elution peak decreases as the two Fab fragments generated are not able to bind to Protein A, and only the Fc fragment and intact antibodies are. Thus, if all antibodies are digested (100% digestion), the elution peak area should decrease by 67%. By comparing the different areas obtained from the different digestion mixtures, it is then possible to evaluate the efficiency of the digestion protocol. The results obtained are presented in **Figure 3.1**.

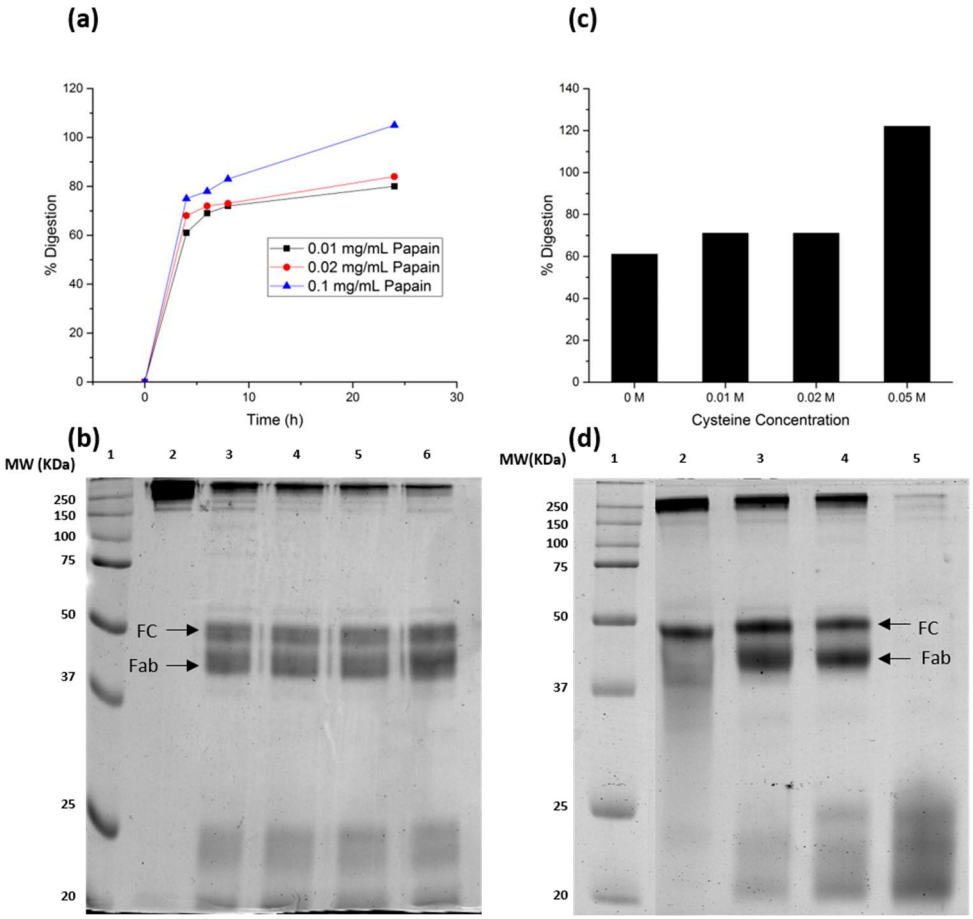

Figure 3.1 Digestion of IgG with different concentrations of papain and cysteine. (**a**) Cleavage of IgG during different digestion times and with increasing concentrations of papain. (**b**) SDS-PAGE gel of the digestion of IgG with 0.02 mg/mL of papain. Lane 1 – Molecular weight marker, Lane 2 – Digestion mixture at 0 h, Lane 3 – Digestion mixture at 4 h, Lane 4 – Digestion mixture at 6 h, Lane 5 – Digestion mixture at 8 h, Lane 6 – Digestion mixture at 24 h. (**c**) Mass of intact IgG after 8 hours incubation with 0.02 mg/mL of papain and different concentrations of cysteine (initial mass of IgG was 1.5 mg). (**d**) SDS-PAGE gel of the digestion of IgG with increasing concentrations of cysteine. Lane 1 – Molecular weight marker, Lane 2 – Digestion mixture with 0 M of cysteine, Lane 3 – Digestion mixture with 0.01 M of cysteine, Lane 4 – Digestion mixture with 0.02 M of cysteine, Lane 5 – Digestion mixture with 0.05 M of cysteine.

According to the results in **Figure 3.1a**, there is a clear relation between the amount of papain and the efficiency of digestion, with more IgG being cleaved when higher amounts of papain are present. It is also possible to observe that while the digestion is time dependent, more than 60% of the IgG is digested during the first four hours and more than 70% after 8 hours of digestion. When 0.01 and 0.02 mg/mL of papain are used, the results are very similar. Nevertheless, with 0.02 mg/mL of papain the digestion is slightly more efficient (higher digestion rate). For 0.1 mg/mL of papain, there is a higher digestion

of IgG, however, after 24 h of digestion, the mass of antibody binding to protein A is lower than the theoretical minimum, thus suggesting that probably there is some undesired degradation or overdigestion of IgG. This result suggests that, in terms of time and reagent consumption, using higher amounts of papain and longer digestion times may not be desirable when compared to a faster digestion (8 hours) using lower amounts of papain. For this reason, in further digestion optimizations the selected parameters were 0.02 mg/mL of papain and 8 h of digestion. The SDS-PAGE gel in **Figure 3.1b** corroborates the results shown in **Figure 3.1a** for a papain concentration of 0.02 mg/mL. In the beginning of the digestion (lane 2) there are no Fab or Fc fragments and only the whole antibody band is visible. Fab or Fc fragments appear after 4h of digestion (lane 3) and their concentration remains nearly constant over the digestion time. The bands at the end of the gel, between 25 and 20 kDa, correspond to degraded fragment forms that should be avoided.

The other parameter studied was the amount of cysteine in the digestion mixture. Cysteine is known to enhance the stability of papain and increase its activity in different applications [204]. The effect of cysteine in the digestion of a mixture of IgG was evaluated by testing different amounts of the amino acid. For a digestion of 8h using 0.02 mg/mL of papain, increasing concentrations of cysteine – 0, 0.01, 0.02, and 0.05 M – were tested. From the results presented in **Figure 3.1c** and **3.1d**, it is visible that the digestion is enhanced by the presence of cysteine. This effect is not so evident in **Figure 3.1c**, with the digestion efficiency increasing only 10 percentage points in the presence of 0.01 or 0.02 mg/mL cysteine, but is clear in **Figure 3.1d** (lane 2), where the two typical bands corresponding to the Fab and Fc fragments are not easily detected (only one band is visible that does not exactly correspond to either Fab or Fc), confirming that cysteine is needed for papain activation [110]. The digestions performed with 0.01 and 0.02 M of cysteine showed a similar IgG digestion profile, with the characteristic Fab and Fc bands visible. The major difference was observed in the presence of 0.05 M of cysteine, with the results suggesting an overdigestion of IgG with Fab and Fc fragments almost completely degraded. This fact could be further observed in the SDS-PAGE gel (**Figure 3.1d**, lane 5), where the two characteristic bands of Fc and Fab fragments are not present, while small molecular weight fragments are present in a higher concentration. Considering that the results obtained with 0.01 M and 0.02 M of cysteine are not significantly different, we chose to continue with a concentration of 0.02 M, as a higher

amount of cysteine could help to stabilize papain, thus making the digestion protocol more robust [110].

3.3.2. Downstream processes to isolate Fab fragments after digestion

While for intact antibodies an effective purification relies on the use of protein A affinity chromatography, for Fab fragments there is still no consensual method for effectively performing their purification. The lack of the Fc region does not allow protein A to bind Fab fragments by affinity interactions. However, protein A chromatography is traditionally used after the digestion of IgG to eliminate undigested IgG and Fc fragments derived from the digestion mixture [146,154]. To remove the other components present in the digestion mixture, a dialysis or diafiltration step can be performed, which can be followed by a concentration step [112]. In this work, the goal was to evaluate the best downstream process (DSP) to isolate Fab fragments after the digestion protocol. For that, we used protein A and protein L chromatography, and centrifugal filter units with 10 kDa of pore size. **Figure 3.2** illustrates the four downstream schemes studied.

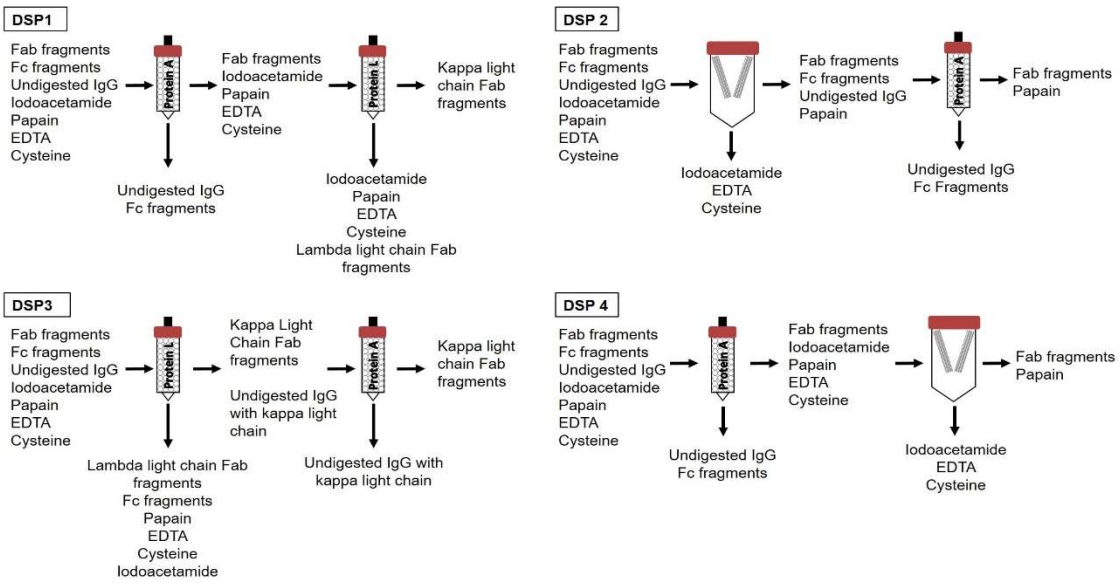

Figure 3.2 Different downstream processes designed to isolate the Fab fragments after the IgG digestion.

DSP 1 and 3 are purification schemes with chromatographic steps only, using both protein A and L columns. Since protein L is present in the purification process, the final products are Fab fragments with kappa light chain, those with lambda light chain are eliminated during the purification process, which is an inherent disadvantage of protein L based schemes. However, taking into consideration that the largest number of mammalian IgG (around two thirds) is composed of kappa light chain [138], DSP 1 and DSP 3 can be seen as representative methods to purify Fab fragments after a digestion protocol. Both processes are very similar in terms of recovery yields (see **Table 3.1**), showing considerable Fab losses, which can be explained by three factors: the first, and most relevant, is related with the ability of protein L to bind both Fab fragments and undigested IgG, which will lead to an overestimation of the initial concentration of Fab fragments and consequently to lower yields (if a digestion efficiency of around 70% is assumed, the successful elimination of undigested IgG will cause a decrease in yield of around 30%, and consequently the maximum recovery yield will be 70%); the second is the possible presence of kappa light chain classes with lower affinity for protein L [205]; the third can be attributed to the fact that Protein A is reportedly able to bind some types of Fab fragments through the constant light chain [146].

Table 3.1 Fab recovery yields of the purification steps comprising the four DSP designed for isolating kappa light chain Fab fragments from the IgG digestion mixture

Process	Yield (%)		
	Step 1	Step 2	Total
DSP1: Protein A - Protein L	62 ± 2	69 ± 2	43 ± 2
DSP2: DF/UF - Protein A	86 ± 5	67 ± 2	58 ± 4
DSP3: Protein L - Protein A	66 ± 1	78 ± 2	52 ± 2
DSP4: Protein A - DF/UF	58 ± 1	94 ± 5	54 ± 3

DSP 2 and 4 schemes are very similar to those used in the majority of IgG digestion protocols, but a membrane ultrafiltration process was performed instead of using dialysis. In this work, the use of an ultrafiltration step before and after protein A was evaluated. It is important to highlight that the use of protein A as the only chromatography step to isolate Fab fragments from an IgG digestion mixture needs always to be accompanied by a diafiltration/concentration process, in order to eliminate small molecular weight impurities such as cysteine and iodoacetamide. The removal of papain is more

problematical, and it may not be completely removed, even with a use of a 30 kDa membrane filter (papain molecular weight is approximately 23 kDa).

Making an overall evaluation of the different downstream schemes, it is possible to conclude that all the four schemes produce similar results. DSP 2 and DSP 4, with only one chromatographic step, exhibit slightly higher recovery yields, although the 10 kDa UF membrane is unable to remove the inactivated papain. DSP 1 and 3 both contain one affinity resin – protein L – for the capture of the desired product and other affinity resin – protein A – for the capture of the major impurities (Fc and undigested IgG) and thus both guarantee that the final products are pure kappa light chain Fab fragments. The SDS-PAGE gel in **Figure 3.3** shows the protein profile in each fraction collected during DSP 1 and 3. For DSP1 (**Figure 3.3a**) one can observe that in lane 3 there are only Fab fragments (~45 kDa), while in lane 4 it is possible to see three bands: the undigested IgG (on the top) and two bands between 50 and 37 kDa, that correspond to different Fc fragments from the IgG mixture. The final product of this DSP is present in lane 6 and it is possible to see that the Fab fragment is practically pure, within the sensitivity of the SDS-PAGE gel. Regarding the DSP3 (**Figure 3.3b**), in lane 4, the Fc fragments were successfully removed by protein L but there are still whole antibody molecules present, which were then successfully removed by protein A. Lane 5 shows almost pure Fab fragments (~45 kDa) without undigested IgGs. It is important to highlight that there is a major need for a universal process able to bind all types of Fab fragments and not only kappa light chain types.

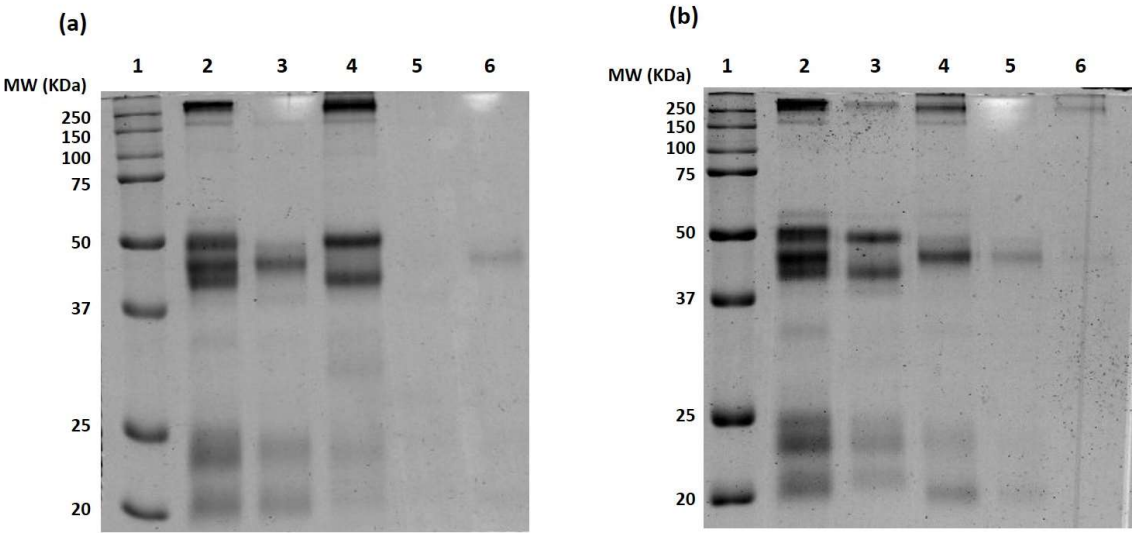

Figure 3.3 SDS-PAGE gel of the fractions collected after DSP1 and 3. (**a**) DSP 1. Lane 1 – Molecular weight marker, Lane 2 – Digestion Mixture, Lane 3 – Protein A flow-through, Lane 4 – Protein A elution, Lane 5 – Protein L flow-through, Lane 6 – Protein L elution. (**b**) DSP 3. Lane 1 – Molecular weight marker, Lane 2 – Digestion Mixture, Lane 3 – Protein L flow-through, Lane 4 – Protein L elution, Lane 5 – Protein A flow-through, Lane 6 – Protein A elution.

3.4. Conclusion

In this chapter, Fab fragments were successfully obtained by proteolytic digestion of whole human serum antibodies using papain. The digestion protocol was optimized in terms of time, papain and cysteine concentrations. The concentration of papain is particularly relevant for long digestion times (*e.g.* 24 h), however, the cleavage rate of IgG is more pronounced during the first 8 hours, where lower amounts of papain can be used without compromising the final result. The concentration of cysteine is also a critical factor, with low amounts leading to incomplete digestion and high amounts causing overdigestion with the degradation of antibodies into very small fragments. The optimised protocol (0.02 mg/mL of papain in the presence of 0.02 M cysteine, for 8 hours) allows the digestion of more than 70% of the IgG present in the digestion mixture. Regarding the designed downstream processing schemes to recover the Fabs after digestion, the tested combinations provided similar recovery yields. In order to guarantee the presence of only Fabs in the final product, schemes where two affinity chromatographic steps are involved are the best choice, however the presence of protein L chromatography will only allow the purification of kappa light chain Fabs. When protein A chromatography and a

centrifugal filter are used, there is no limitation regarding the type of Fabs in the final product, however, the pore size of the centrifugal unit used must allow the rejection of the Fab fragments (~50 kDa) and, simultaneously, the permeation of the papain (~23 kDa) used for the digestion, which did not happen when a pore size of 10 kDa was used. One possible solution is to use larger pore size unit (*e.g.* 30 kDa). Being all the tested purification scenarios very similar in terms of performance, the ultimate choice of the optimal downstream processing scheme should be made depending on the intended application.

In further chapters of this thesis Fabs are generated from the digestion of the Human IgG present in Gammanorm®. The work herein developed created the tools for an efficient digestion and purification platform for the Fab fragments, that will play a central role, as the main biologics of this thesis. With the described universal digestion protocol and subsequent downstream process is possible to ensure the cleavage of this Human IgG is efficient and the resulted Fabs have high degree of purity.

Chapter 4

Development of phage biopanning strategies for the discovery of Fab-binding peptide affinity ligands: an evolutionary approach to universality

4.1. Introduction

Recently, Fabs and mAb-derived alternatives such as single-chain variable fragments, nanobodies, bispecifics and conjugated mAbs [12] have emerged as powerful new therapeutic modalities. While mAbs and some the mAb-derived alternatives are amenable to protein A capture and platform downstream processes, at present there is no consensus on a universal platform for downstream processing for Fab therapeutics[130]. Protein L and single domain camelid antibodies have been applied as affinity solutuions for Fab purifications. Biological ligands, such as peptides, have been successfully used as affinity capture agents for downstream applications [140]. Their high stability, ease of engineering and high throughput screening capability makes them attractive candidates for affinity bioseparations [206]. Further, they can offer advantages when compared to protein domain ligands such as lower cost, ease of column regeneration, potentially higher chromatographic binding capacities and reduced immunogenicity [207].

To discover an affinity peptide ligand, one can employ combinatorial screening of a peptide library coupled with a strategically designed biopanning scheme. The most frequently used combinatorial screening techniques are phage display, mRNA display and high-throughput molecular simulations [208]. Phage display is a powerful technique, where highly diverse libraries of recombinantly engineered bacteriophage particles are used to display peptides at the N-termini of their pIII coat proteins [209]. This arrangement enables a vast library of affinity ligands, consisting of up to ~10^9 unique transformants, to be rapidly screened. Once a fraction of the peptide-displaying phages binds to the desired target, they are selected, amplified and subjected to several rounds of increasingly stringent selection steps (i.e. biopanning) to discard the weaker candidates and shortlist the peptides that bind strongly and selectively to the target protein [210].

The efficacy of this process is dependent on both the diversity of the peptide phage library and the specific biopanning scheme that is employed [211]. For library generation, two possible routes have been explored: (1) premade commercially available random phage libraries consisting of linear or cyclic 7-mer peptides [212], or linear 12-mer peptides [213]; or (2) a rationally designed phage library based on specific information of peptide binding to the target protein or a consensus motif to the target [210,214]. For biopanning, it is critical to include important steps such as negative selections and orientation of the target molecule [215,216] as well as steps relevant to the specific application such as wash and elution conditions for affinity chromatography.

In the current work, three different phage biopanning strategies are employed to identify affinity peptides for Fab purification. While the first screen focuses on the identification of peptides for a single Fab the second identifies peptides for multiple kappa Fabs. In both approaches, protein L beads are used to bind Fab fragments in a fixed orientation and NHS functionalized magnetic beads are employed in the final biopanning round to enable the evaluation of low pH elution conditions. Peptide sequences obtained using the two panning strategies are then synthesized and the binding of these peptides to different Fabs are evaluated using fluorescence polarization. The single Fab biopanning approach is shown to yield a peptide ligand with similar binding affinities to two different forms of the Fab (recombinant and post papain digestion) as well as the intact antibody. On the other hand, the biopanning strategy for multiple Fabs yields a peptide ligand that exhibits affinity for all three kappa fabs, indicating that it may be a good lead for the development of a more general affinity reagent for recombinant kappa Fabs. The third biopanning strategy was designed with the intention to find peptides with an affinity to a broader number of Fabs. To accomplish that, undigested kappa light chain Fabs, digested kappa light chain Fabs and digested lambda light chain Fabs were used in the biopanning scheme. The peptide sequences obtained from the third strategy, were synthesized and the peptides evaluated towards its ability to universally bind Fab fragments. The outcome was two peptides showing affinity towards all the digested Fab fragments used in this experiment. Finally, a proof of concept is presented using an affinity peptide column for Fab purification from a complex cell culture fluid (CCF) mixture.

This chapter contains sections published, as a research article, in the journal *Biotechnology Progress* with the name Development of phage biopanning strategies to identify affinity peptide ligands for kappa light chain Fab fragments (2019). Part of the work herein developed resulted from a highly collaborative effort with Doctor Akshat Mullerpatan [217].

4.2. Materials and methods

4.2.1. Materials

Pierce NHS-Activated magnetic beads, Pierce Protein-L magnetic beads, Pierce immobilized papain (agarose) and MagnaRack were ordered from ThermoFisher Scientific (Scoresby, VIC, Australia). MabSelect Sure, Tricorn empty chromatography column (5 mm × 50 mm), NHS Sepharose FF Resin and HiTrap Protein-L were obtained from GE (Uppsala, Sweden). Amicon® Ultra-15 centrifugal filter units (NMWL/MWCO of 30 and 100 kDa) were ordered from Merck Millipore (Darmstadt, Germany). Sodium hydroxide, L-cysteine, sodium phosphate, sodium sulfate, Ethylenediaminetetraacetic acid (EDTA), triisopropylsilane (TIPS), trifluoroacetic acid (TFA), dichloromethane (DCM) and acetonitrile were purchased from Sigma Aldrich (St. Louis, MO/USA). Dimethylformamide (DMF), piperidine (AGTC Bioproducts), N-methylpyrrolidone (NMP), activator 2-(1*H*-benzotriazol-1-yl)-1,1,3,3-tetramethyluronium hexafluoro-phosphate (HBTU) and methyl-tertiary-butyl ether (MTBE) were ordered from AGTC Bioproducts (Wilmington, MA). All 20-fluorenylmethoxy carbonyl (Fmoc) amino acids were obtained from 21st Century Biochemicals (Marlborough, MA). Fmoc-Lys-FAM-OH was obtained from AAT Bioquest (Sunnyvale, CA). 10X SDS PAGE buffer, Kaleidoscope Precision-Plus protein gel ladder, Bio-Rad AnykD polyacrylamide gel and SDS-PAGE system were procured from Bio-Rad Laboratories. Yeast extract was obtained from Amresco, while Bacto-tryptone, Bacto-agar were obtained from BD. The Ph.D.-12™ Phage Display Peptide Library Kit was purchased from New England Biolabs (Ipswich, MA).

The Fab fragments employed in this work included Fab A, Fab D and Fab E from NovoNordisk, and Fab Z, whose cell stock was kindly donated by Prof. P. Tessier. In

addition, intact mAb A and mAb 10 from NovoNordisk, mAb 2, 3 and 9 are from MedImmune, mAb 7 and 8 from BMS and mAb 11 and 12 from Merck were employed.

4.2.2. Fab Z expression and purification

A 5 ml culture tube was inoculated with the Fab Z BL21DE3 cell stock and grown overnight. It was then subcultured into flasks containing 200 ml auto-induction media. The cultures were then incubated with shaking at 225 rpm at 37^0C for 48 hours to allow for cell growth and protein expression, and the expressed protein was secreted into the media. The culture was centrifuged to pellet the cells and clear the supernatant containing media. The media was then 0.22 μm filtered and loaded onto a HiTrap protein L column on an ÄKTA Explorer system to purify the expressed Fab Z. The loaded column was washed with PBS pH 7.4, before eluting it from the column using citric acid pH 2.5. The eluted Fab solution was immediately adjusted to neutral pH using a 2 M Tris pH 9 buffer. The Fab was then concentrated and buffer exchanged into PBS pH 7.4 using 30 kD MWCO Amicon centrifugal filter units. SDS-PAGE analysis of the concentrated Fab solution (denaturing and non-reducing conditions) indicated the presence of considerably pure Fab.

4.2.3. Digestion of mAbs and purification of Fabs post digestion

All the digested Fabs employed in this work were digested and purified using the same protocol. A solution of 20 mg/mL of mAb was digested for 15 hours according to the protocol suggested by the supplier of the immobilized papain beads. Once digestion was complete, the digested Fabs were purified from the digestion mixture, using the MabSelect sure resin (GE) to remove residual mAb A and Fc fragments generated by digestion. 800 μl of resin slurry was washed three times with phosphate buffered saline (PBS) and incubated with the digestion mixture, for 1h, at room temperature under gentle stirring. The supernatant was then collected and concentrated using 30kD MWCO Amicon centrifugal filter units. The purity and size of the digested Fabs were assessed using SDS-PAGE in denaturing, non-reducing conditions.

4.2.4. On-bead Fab Immobilization immobilization

A combinatorial phage display library of 12-mer peptides fused to the minor coat protein (pIII) of M13 phage (New England Biolabs) was employed for biopanning to identify peptide binders against Fab fragments. Two different screens were performed, using the same phage library in 1.5 mL plastic Eppendorf tubes. Two types of Fab immobilization were conducted using two types of magnetic bead: (1) Pierce^{TM} protein L beads and (2) Pierce^{TM} NHS-activated magnetic Beads. Fab immobilization was performed according to the protocol prescribed by the bead supplier's manuals. For the protein L magnetic beads, the Fab was incubated for 1 hour at room temperature (RT), to promote efficient binding of the Fab to the bead and the prescribed elution step was omitted since the Fabs needed to remain immobilized onto the bead. Prior to immobilization, the tubes used were blocked with 5 mg/mL BSA and washed four times with PBS.

4.2.5. Single Fab target (SFT) phage biopanning approach

As shown in **Figure 4.1a**, the first round of screening (first positive) was performed by adding 10^{11} plaque forming units (pfu) to 200 µl of PBS pH 7.4 to the tube containing Fab A immobilized on the protein L magnetic beads, and incubated for 1 hour at RT. To ensure the removal of unbound and weakly bound phage, the following 10 washes were performed: 4× PBS + 0.1% Tween (PBST); 3× PBS + 0.5% Tween (PBS2T); 3× PBST. Bound phage were then eluted with 500 µL 20 mM citrate pH 3 for 15 min at RT, separated from the beads and immediately neutralized with 1M Tris pH 9. Phage amplification and purification were done according to the NEB phage display manual. First, the amplified phage from the first positive round were diluted to a concentration of 10^{11} pfu/200 µl (equal to concentration prior to first positive) and incubated for 40 min at RT in a BSA blocked tube containing protein L magnetic beads (first negative). The supernatant was then collected and applied to the second positive screen containing Fab A immobilized on the protein L magnetic bead. The incubation lasted 45 min, and the unbound and poorly bound phage were removed by applying 10 washes: 2× PBST; 2× PBS2T; 2× PBST + 300 mM Na_2SO_4; 2× PBS2T; 2× PBST. Bound phage was eluted and amplified as described previously. The amplified phage from the second positive, was diluted to a concentration of 10^{11} pfu/200 µl and subjected to a second negative

selection (second negative), equal to the first one. The supernatant from this step was collected and incubated for 40 min against Fab A immobilized on NHS beads (third positive). The wash and elution conditions for positive round 2 were applied to the third positive round. Three dilutions of the eluate (10×, 100× and 1000×) were prepared. *E. coli* cultures were infected with each dilution and plated on to LB/IPTG/Xgal plates. 50 distinct blue plaques corresponding to the M13 bacteriophage were randomly and carefully picked and amplified in *E. coli* cultures. Each culture was centrifuged and the supernatant containing amplified unique phage was submitted for sequencing.

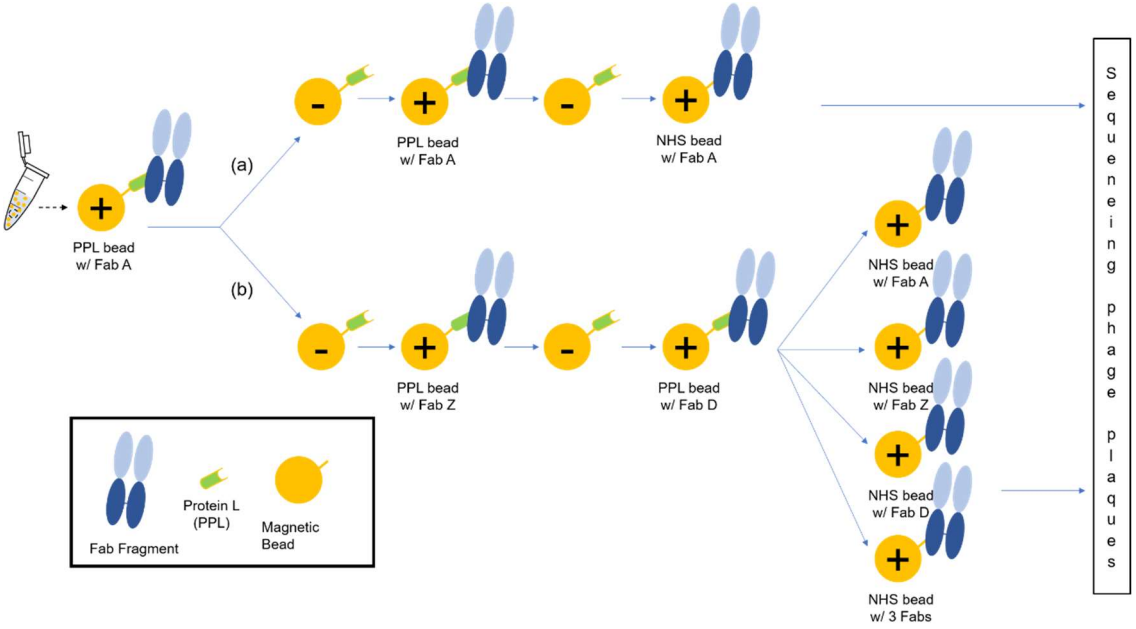

Figure 4.1 Two phage biopanning approaches used in this work to identify peptides toward Fab fragments. (**a**) Single Fab target (SFT) phage display scheme, (**b**) Multiple Fab target (MFT) phage display scheme.

4.2.6. Multiple Fab target (MFT) phage biopanning approach

As shown in **Figure 4.1b**, the first round of screen (first positive) was the same as for the SFT approach. Amplified phage from the first positive was diluted to a concentration of 10^{11} pfu/200 µl and incubated thrice (first negative) in: (1) BSA blocked tube, for 1 hour at RT; (2 and 3) protein L magnetic beads, without Fab, for 50 and 40 min, respectively, at RT. In each incubation, the supernatant of the previous step was used. The supernatant after the first set of negative rounds was collected and incubated with Fab Z immobilized on protein L magnetic beads, for 1 hour at RT (second positive). The unbound and poorly

bound phage was washed 10 times: 1× PBS; 3× PBST; 1× PBS + 300 mM Na_2SO_4; 3× PBST; 2× PBS. Bound phage was eluted, amplified and purified has described previously. All the amplified phage from the second positive (concentration of 10^{11} pfu/200 µl) was used in a second negative selection round, similar to the first negative (second negative). The supernatant of the second negative was collected and incubated with Fab D immobilized in protein L magnetic beads, for 45 min at RT. The unbound and poorly bound phage was washed 10 times: 1× PBS; 1× PBST; 1× PBS2T; 1× PBS + 300 mM Na_2SO_4; 2× *E. Coli* cell culture supernatant (CCF) - incubated for 5 min each, RT; 1× PBS + 300 mM Na_2SO_4; 1× PBS2T; 1× PBST; 1× PBS. Bound phage was eluted, amplified and purified as described previously. The amplified phage from the third positive was diluted to a concentration of 10^{11} pfu/200 µl and added to four different tubes containing NHS beads (fourth positive) with: (1) a mixture of the three used Fabs, (2) Fab A, (3) Fab Z and (4) Fab D. In each the incubation time was 45 min at RT and 10 washes were done: 1× PBS; 1× PBST; 1× PBS2T; 1× PBS + 300 mM Na_2SO_4; 1× PBS2T; 1× CCF - incubated for 5min; 3× PBST; 1× PBS. The unamplified phage eluate from the final biopanning round in each phage biopanning effort were subjected to plaque titering. Similar to the previous biopanning effort (**section 4.2.5**), 50 distinct blue plaques corresponding to the M13 bacteriophage were randomly and carefully picked, amplified in *E. coli* and submitted for sequencing.

4.2.7. Complete Fab target (CFT) phage biopanning approach

As shown in **Figure 4.2**, the first round of screen (first positive) was performed by adding 10^{11} plaque forming units (pfu) to 200 µl of PBS pH 7.4 to the tube containing Fab 1 immobilized on the protein L magnetic beads, and incubated for 1 hour at RT. To ensure the removal of unbound and weakly bound phage, the following 10 washes were performed: 1× PBS; 3× PBST; 2× PBS2T; 3× PBST; 1× PBS. Bound phage was eluted, amplified and purified has described previously. After the first positive, the biopanning is divided into two branches: the kappa light chain and the lambda light chain branch. The only difference between a branch and the other is the Fabs used. Amplified phage from the first positive was diluted to a concentration of 10^{11} pfu/800 µL and incubated thrice (first negative) in: (1) BSA blocked tube, for 1 hour at RT; (2 and 3) protein L magnetic beads, without Fab, for 50 and 40 min, respectively, at RT. In each incubation, the

supernatant of the previous step was used. The supernatant after the first set of negative rounds was collected, divided and incubated with Fab 2 (kappa brunch) and Fab 3 (lambda brunch) immobilized on NHS beads, for 2 hours at RT (second positive). The unbound and poorly bound phage was washed 10 times: 1× PBS, 1× PBST; 2× PBS2T; 300 mM Na_2SO_4; 2× PBS2T; 1× PBST; 1× PBS. The last step of the wash was done in a new tube, previously blocked with BSA. Bound phage was eluted, amplified and purified has described previously. Amplified phage, from both branches, were diluted to a concentration of 10^{11} pfu/400 µL and used in a second negative selection round, similar to the first negative (second negative). The supernatant of both second negatives was collected and incubated with Fab 4 immobilized in NHS beads, for 2 hours at RT (third positive). The unbound and poorly bound phage was washed 10 times: 1× PBS; 1× PBST; 2× PBS2T; 2× PBST; 2× PBS2T; 1× PBST; 1× PBS. Bound phage was eluted, amplified and purified as described previously. Amplified phage, from both branches, was diluted to a concentration of 10^{11} pfu/400 µL and incubated with Fab 5, immobilized in NHS beads, for 2 hours at RT (fourth positive). The unbound and poorly bound phage was washed 10 times: 1× PBS; 2× PBST; 2× PBS2T; 1× CCF - incubated for 5 min each, RT; 2× PBS2T; 1× PBST; 1× PBS. The unamplified phage eluate from the final biopanning round in each phage biopanning branch were subjected to plaque titering. Similar to the previous biopanning effort (**section 4.2.5**), 40 distinct blue plaques (from kappa and lambda branch) corresponding to the M13 bacteriophage were randomly and carefully picked, amplified in *E. coli* and submitted for sequencing.

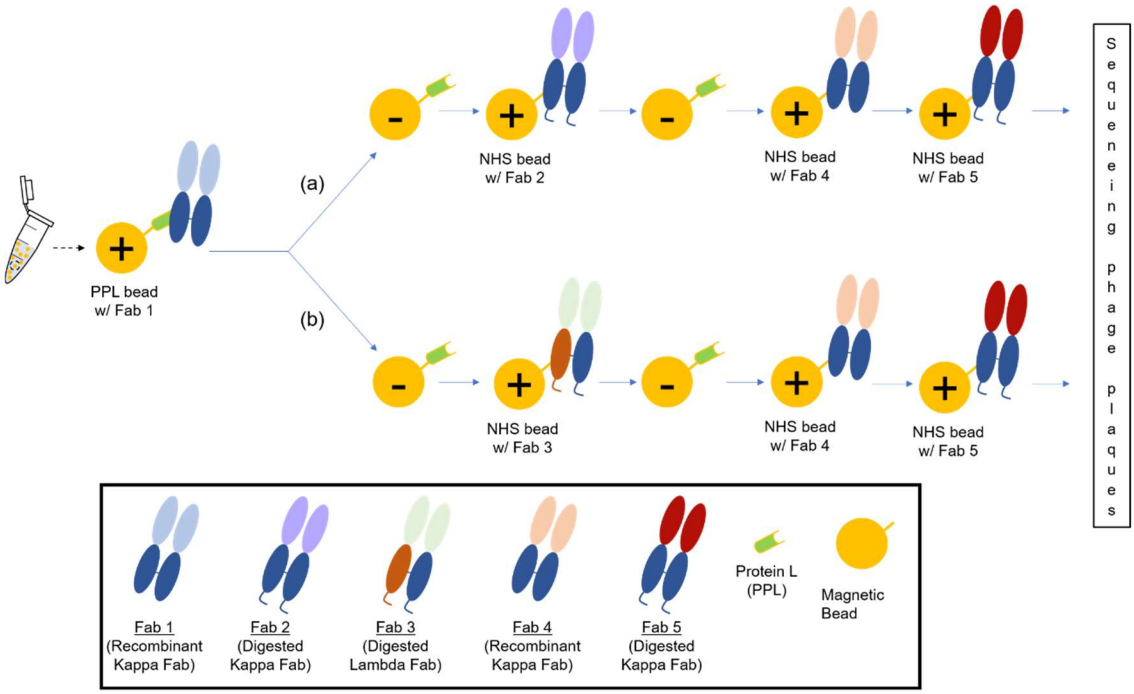

Figure 4.2 Complete Fab target (CFT) phage biopanning. (a) kappa light chain branch, (b) lambda light chain branch.

4.2.8. Solid phase labeled peptide synthesis

All peptides were synthesized by solid phase peptide synthesis on the Intavis AG Multipep RS in a 96-well plate format. Fluorenylmethoxycarbonyl (Fmoc) chemistry was used to synthesize the peptides on 8 mg per well of NovaPEG Rink Amide Resin. The C-terminal amino acid in each case was the Fmoc-Lys-FAM-OH. The FAM dye was functionalized to the amine group of the lysine sidechain. The fluorescent dye here has an excitation wavelength of 495 nm and emission wavelength of 519 nm. The synthesis followed the conventional deprotection-activation-reaction-capping scheme as mentioned elsewhere [218]. Post synthesis, the amino acid protecting groups were removed and the peptides were cleaved from the solid support using a cocktail of solvents comprising trifluoroacetic acid, water, triisopropyl silane and 2,2′-(ethylenedioxy)di-ethanethiol. The peptides were then purified by two precipitation cycles using cold methyl tert-butyl ether. Each peptide was finally reconstituted and dissolved in a solution of 20% acetonitrile in water. Solution pH or acetonitrile content was modified to aid the dissolution of partially soluble peptides. Peptide purity was determined by reversed phase liquid chromatography (RPLC) on a Waters ultra-performance liquid chromatography (UPLC) system using a Waters BEH C_{18} RPLC column.

4.2.9. Initial FP screen

4.2.9.1. SFT and MFT peptides

After peptide synthesis, all peptides were subjected to an initial binding screen against Fab A. Since fluorescence polarization detects binding via the rotational relaxation time of the molecule, the smaller species is usually labelled to ensure a large signal. The labelled peptide was diluted in PBS to prepare a stock solution of 500 nM. Fab A was diluted in PBS to two different concentrations (2 μM and 20 μM). Concentrations of peptide and Fab A were measured using a NanoDrop UV Spectrophotometer (Harlow Scientific). The level of binding was evaluated using fluorescence polarization (FP) by mixing equal volumes (20μL) of the peptide and each Fab concentration in a 384 well black plate, resulting in a final peptide concentration of 250 nM. In addition, a control experiment containing equal volumes of peptide and PBS buffer was performed. All the measurements were carried out in duplicate, and the plate was incubated for 2h at room temperature with gentle shaking. The parallel and perpendicular fluorescence intensities were measured using a Biotek Synergy 5 plate reader (excitation filter: 485/20 nm, emission filter: 528/20 nm; dye excitation: 496 nm and dye emission: 519 nm) at room temperature. The peptides that exhibited the highest FP change were selected for further studies.

4.2.9.2. CFT peptides

After peptide synthesis, all peptides were subjected to an initial binding screen against three Fabs (Fab 3, Fab 4 and Fab 7) and one mAb (mAb 7). The labelled peptide was diluted in PBS to prepare a stock solution of 500 nM. All the Fabs and mAb were diluted in PBS to a concentration of 20 μM. Concentrations of peptide Fabs and mAbs were measured using a NanoDrop UV Spectrophotometer (Harlow Scientific). The level of binding was evaluated using fluorescence polarization (FP) by mixing equal volumes (20 μL) of the peptide and each Fab/m concentration in a 384 well black plate, resulting in a final peptide concentration of 250 nM. In addition, a control experiment containing equal volumes of peptide and PBS buffer was performed. All the measurements were

carried out in duplicate, and the plate was incubated for 2h at room temperature with gentle shaking. The parallel and perpendicular fluorescence intensities were measured using a Biotek Synergy 5 plate reader (excitation filter: 485/20 nm, emission filter: 528/20 nm; dye excitation: 496 nm and dye emission: 519 nm) at room temperature. The peptides that exhibited the highest FP change were selected for further studies.

4.2.10. Assessment of K_D for peptide-Fab interaction

Lead peptides determined from the initial FP screen of each phage display strategy were evaluated for a full binding curve. The peptide concentration was kept the same as in the initial screen, while serial dilutions of the Fab spanning 0 µM to 150 µM were used for the experiment (for the determination of SFT phage lead peptides K_D, Fab A concentration ranged from 0 to 360 µM). Sample preparation and FP measurements were similar to the ones described previously. The obtained binding curves were fitted to a 4-parameter logistic equation (**Equation 4.1**) and the K_D values were determined[219].

$$Y = \frac{(A - D)}{\left(1 + \left(\frac{X}{C}\right)^{B}\right)} + D$$

Equation 4.1 4 parameter logistic curve equation used to fit binding curve data. A = response at zero analyte concentration, B = slope factor, C = inflection point representing K_D, D = response at infinite analyte concentration

For the CFT phage lead peptides, more than one full binding curve was done. In total 10 binding curves were done with different Fabs, both digested and expressed. The followed protocol was the equal to the ones applied in the MFT phage lead peptides. The binding curves obtained for the CFT peptides were normalized by subtracting the FP value of peptide in PBS.

4.2.11. A5 and C7 alanine-scanning mutagenesis

The A5 (WHYNWQDVSDRQ) and C7 (HQNHHSTFWEIY) peptides were synthesized (as described in **section 4.2.8**) with single point mutations. Twelve versions of each peptide were synthesized, each containing a systematically single point alanine mutation.

After peptide synthesis, full binding curves for every mutated version of A5 and C7 were accomplished.

4.2.12. Synthesis, purification and immobilization of B1

The B1 peptide (WIPNSEFEHERTK) was synthesized in 8 wells of a 96 well plate using Fmoc chemistry with a C-terminal lysine (K) residue for NHS-aided immobilization via the free amine in the lysine side chain. Initial peptide purity was determined by UPLC and subjected to further purification by reversed phase HPLC using a Waters C_{18} RPLC column. A linear gradient of 0-70% acetonitrile in water was employed to purify the peptide from other impurities to achieve > 95% pure peptide. Pure peptide fractions were pooled and lyophilized. The resulting solid form of the peptide was dissolved in PBS (immobilization buffer). The peptide was immobilized on the NHS Sepharose FF beads (GE) according to the supplier´s protocol. The resin bead functionalization yield was quantified from mass balance using reversed phase UPLC analysis.

4.2.13. Purification of Fab A by B1 affinity chromatography

The functionalized resin was packed into a Tricorn chromatographic column, with a packed bed volume of 0.5 mL. Flow rates for the equilibration, binding, washing and elution steps were maintained at 0.25 mL/min. All chromatographic experiments were carried out on an ÄKTA Explorer system. The column was equilibrated with PBS pH 7.4 (binding buffer), followed by the injection of 0.1-0.15 mg of Fab A spiked into a mock *E. coli* cell lysate. Washing with the binding buffer was performed until UV A280 baseline occurred. Elution was conducted with 20 mM citric acid, pH 2.5, until UV A280 baseline was achieved. A final strip was performed using 70% ethanol. Six chromatography repeat experiments were performed to assess the reusability of the peptide-functionalized resin. 0.5 mL fractions were collected for all experiments. The purity and yield of Fab A were determined by UPLC analysis and also visualized using denaturing non-reducing SDS-PAGE.

4.3. Results and discussion

4.3.1. First two phage display strategies – Single and multiple Fab target phage display

This chapter involved the identification of affinity peptides against Fab fragments. As described in the materials section, four different Fabs were employed: Fabs A, D, E and Z. Additional variations of Fab A were also used, namely murine Fab A, intact mAb A and Fab A obtained from enzymatic digestion of mAb A. While the sequences of Fabs A, E and murine Fab A are presented elsewhere[220] we are not able to disclose the sequences of Fabs D and Z due to IP constraints. Prior to carrying out the biopanning procedure, all the Fabs employed in this work were subjected to sequence alignment. The results indicated that while Fabs A, D, Z and murine Fab A possessed identical constant domain (heavy and light) sequences, Fab E bore 99.1% similarity to the other Fabs in the constant domains[220]. On the other hand, significant differences were observed among the variable domains of all the Fabs.

Two phage display screening approaches against Fab fragments were employed to identify peptide leads for affinity-based separations. The first focused on the identification of an affinity peptide for a single Fab while the second screen identified peptides for multiple Fab biologics. A commercial 12-mer M13 phage display library (NEB) was employed for phage biopanning against the Fabs. This dodecapeptide library has a complexity of 10^9 different peptides, which permits the high-throughput screening of a vast number of peptide options against a single target[221].Instead of carrying out the phage display experiments in the traditional plate format, which involves physical adsorption of the target to the well surface, the Fabs were either bound to protein L functionalized magnetic beads or immobilized on NHS functionalized beads. Protein L is known to bind the V_L region of Fabs and has been extensively employed for Fab purification[222]. The use of protein L to bind Fab fragments for this screen resulted in a fixed orientation of the Fab and minimized the chance of phage binding to the V_L region[223]. While binding to the protein L enabled a focused selection, it made elution screening difficult due to dissociation of the Fabs from the immobilized protein L at low pH. In order to overcome this limitation, NHS functionalized magnetic beads were

employed in the final biopanning round in both screening protocols to enable proper evaluation of elution conditions.

4.3.1.2. Single Fab target (SFT) phage display

The first phage display strategy was focused on the discovery of affinity peptides for Fab A (**Figure 4.1a**). A key component of this screen was the use of immobilized protein L which binds to the light chain of the Fab, proximal to the CDR. This resulted in the exposure of more conserved regions such as C_L and C_H1 to the phage during the screen. As seen in the figure, five rounds of panning were used; three positive selections with Fab A as target and two negative selections. For the first two positive rounds, Fab A was bound to protein L functionalized beads, while the last positive round employed covalent immobilization of the Fab on NHS beads. The negative selections were included to eliminate nonspecific binding of the phages to plastic, protein L, magnetic beads and/or BSA. The first negative selection was performed after the first positive panning rather than before, to avoid losing promising phage candidates that may have possessed significant binding to the target.

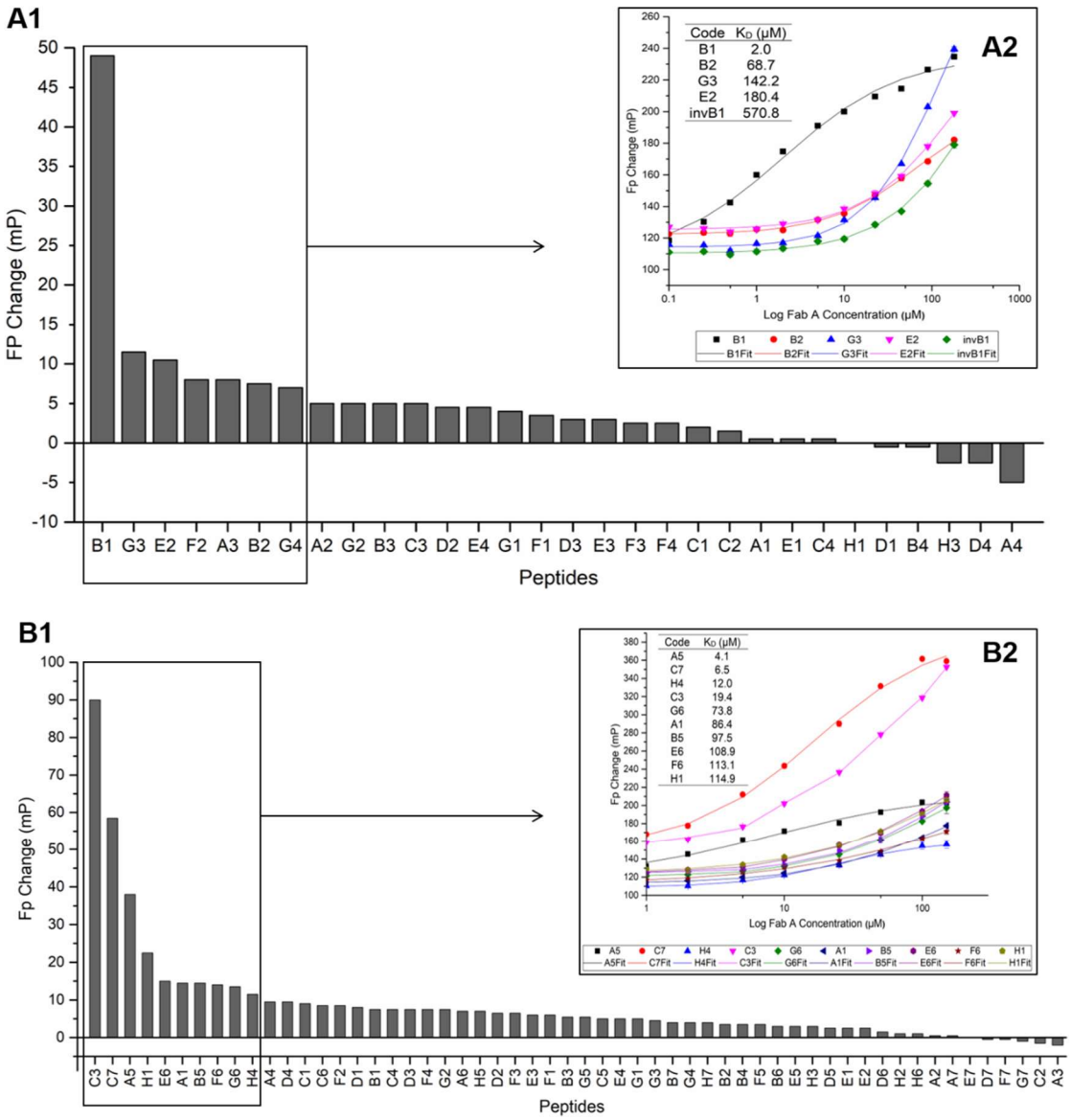

Figure 4.3 (**A1**) Initial binding screen of the peptides obtained after the SFT phage screening. (**A2**) Full binding curves for the lead candidates and their respective dissociation constants. (**B1**) Initial binding screen of the peptides obtained after the MFT phage screening. (**B2**) Full binding curves for the lead candidates and their respective dissociation constants. (Note: Fab A was used as target in all screens).

4.3.1.3. SFT phage display – Screened peptides

Once the biopanning was completed, 50 plaques were randomly selected, and the phage was sequenced. Interestingly, out of the 50 obtained sequences, 23 shared the same 12-mer peptide sequence – B1 (WIPNSEFEHERT) – which indicated that this specific peptide could potentially be a strong candidate for the target. The fluorescently labelled versions of the 28 unique peptides from this screening were then synthesized in a peptide

synthesizer. The inverted sequence of B1 was also synthesized to check for sequence/orientation bias. A single Fab A concentration (10 μM) fluorescence polarization screen was then performed on this set of peptides to shortlist the top candidates. Six peptides were selected based on the FP signal (**Figure 4.3A1**) with B1 exhibiting the highest change. The binding curves were then determined for four of these peptides as well as the inverted version of B1 (note: two of the peptides were not included in this analysis due to lack of sufficient purity). These experiments were carried out with a peptide concentration of 250 nM and Fab A concentrations ranging from 0 to 180 μM. The dissociation constants (K_D) resulting from these plots are also provided in the Figure. The results (**Figure 4.3A2**) agreed qualitatively with the initial FP screen, with B1 having the lowest dissociation constant (K_D) of 2 μM, and the other peptides having K_D values greater than 50 μM. The results also clearly demonstrated that the orientation of the B1 peptide was critical, with the inverted B1 peptide having the weakest binding. The affinity of B1 was higher than previously identified small molecule affinity ligands for Fabs [142] and comparable to peptide affinity ligands for other applications [224]. These results validated the efficacy of our screening protocol for the identification of peptides specific to a single Fab target.

4.3.1.4. B1 - Binding affinity towards different Fabs

There are two ways of producing Fab fragments – using proteolytic enzymes such as papain to cleave whole mAbs [113], or using expression systems that ensure the correct production and assembly of these biomolecules[154]. The Fab A biomolecule used during the phage display was expressed and produced using a mammalian cell system (as described elsewhere [225]). It was of interest to evaluate if B1 had similar binding behaviour against Fab A obtained by papain digestion as well as the intact mAb A. Accordingly, FP experiments were carried out as described in the methods section and the results (**Figure 4.4**) were found to be similar across all three Fab A formats with K_D values on the order of 2 μM. These results confirmed that peptide B1 binds to the Fab region of mAb A and that there is minimal difference in the binding to the two types of Fab fragments (non-digested and digested).

As discussed above, our screening protocol employed protein L functionalized beads, which should bias phage binding to more conserved regions in the Fab such as C_H1 and C_L. In order to evaluate whether this affinity peptide had utility for binding other Fabs, its binding to two additional Fabs was examined. This included a murine variant of Fab A, which shared its CDR region with humanized Fab A but was composed of a different framework, and a Fab with high sequence homology to Fab A – Fab E, but containing different CDR loops (PDB ID: 4LKX[226]). As can be seen in **Figure 4.4**, peptide B1 exhibited good binding to the murine version of Fab A with only a small increase in K_D to 6.1 µM. On the other hand, minimal binding was observed to Fab E indicating that binding likely involved the CDR loops. Thus, these results indicate that peptide B1 is specific to Fab A containing biomolecules and that binding is likely focused in the CDR region, thus reducing its broader specificity. These results are not particularly surprising since the first biopanning protocol only employed the single Fab A target.

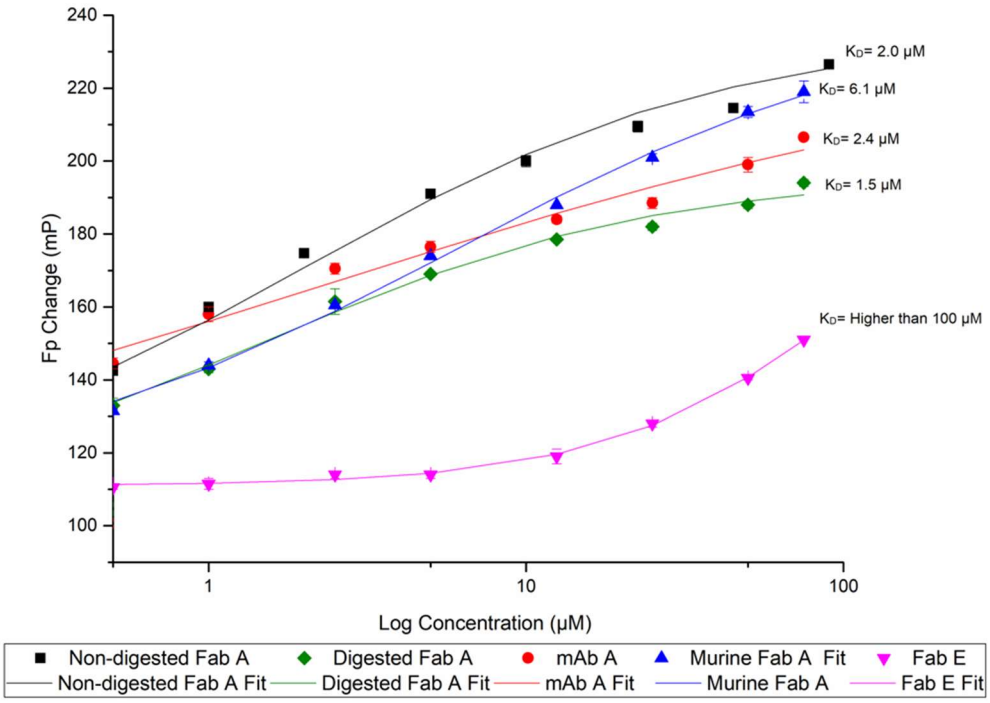

Figure 4.4 Binding curves of B1 peptide for different Fab fragments and a mAb. The respective dissociation constants are indicated

4.3.1.5. Multiple Fab target (MFT) phage display

In the Fab A display scheme (**Figure 4.1a**), the only region inaccessible to the phage was the protein L-binding region of the Fab. However, despite being proximal to the CDR loops [153,227], this approach did not result in any peptide binders to the more conserved regions of the Fab. A new phage screening strategy (**Figure 4.1b**) was thus developed which employed four positive biopanning rounds using three recombinant kappa Fab fragments (Fab A, Fab Z and Fab D) with different CDR regions and identical C_H1 and C_L regions. The intention behind this approach was to promote the binding of phages to the constant regions of kappa light chain Fab fragments. Moreover, negative selections employed in this biopanning scheme were made more stringent, with a total of six negative screening steps. In addition, an *E. coli* CCF wash step was employed during the Fab D and final biopanning round to screen out nonspecific binders which would also bind to impurities present in the crude CCF [228]. The last step of the scheme was divided into four parts, one for each Fab and one for an equimolar mixture of the three Fabs, to avoid bias to a particular Fab. Peptides resulting from this multi-step screening protocol were expected to bind to all three Fabs, likely at common regions.

The peptide sequences from the phage strategy were subjected to a similar evaluation using FP with Fab A and the results are shown in **Figure 4.3B1**. The sequences obtained from this new screening approach displayed a higher diversity than those resulting from the single Fab screen. It is also worth noting that peptide B1 was absent from this more extensive screen, indicating that the CDR regions of Fab A were likely screened out in this biopanning approach. After the initial single point experiments, the ten peptides which showed the most significant FP change were further evaluated to obtain the full binding curves and K_D values. The ranking obtained from these curves (**Figure 4.3B2**) was in agreement with the initial FP screen and the top two peptide binders, A5 (WHYNWQDVSDRQ) and C7 (HQNHHSTFWEIY), were determined to have K_D values of 4.1 μM and 6.5 μM, respectively.

4.3.1.6. A5 and C7 - Binding affinity towards different Fabs

It was then of interest to compare the binding affinities of the selected peptides A5 and C7 to other forms of Fab A, namely, intact mAb A, digested Fab A and murine Fab A. In addition, a control recombinant Fab (Fab E), was also evaluated. The results of this analysis are presented in **Figures 4.5** and **4.6** for A5 and C7, respectively. As can be seen in these figures, the K_D values for the binding of these peptides to all other forms of Fab A as well as the control Fab E were dramatically higher (i.e. lower affinity) as compared to the recombinant Fab A. This is in sharp contrast to the results obtained with B1, where comparable binding was observed for all forms of Fab A. The fact that A5 and C7 do not bind strongly to these other forms of Fab A could indicate that the binding region is not located in the CDR region.

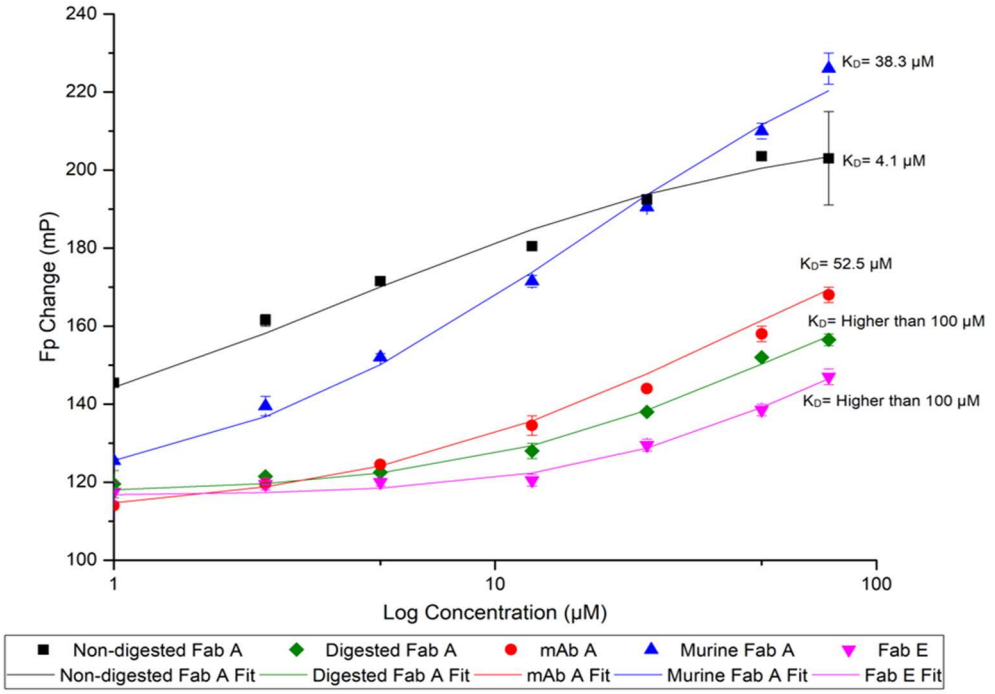

Figure 4.5 Binding curves of A5 peptide for different Fab fragments and a mAb. The respective dissociation constants are indicated

The reduced binding affinity to the intact mAb A, may be due to steric effects such as conformational changes[229] that could inhibit the binding of these peptides to sites near the hinge region. The decrease in binding affinity to the digested form of Fab A was surprising since it should have a very similar sequence to the recombinant Fab A. This difference in affinity could originate from the cleavage site of papain in the hinge region

of mAb A. Papain has two putative cleavage sites in human antibodies; the first at histidine (224)/threonine (225) and the second at glutamic acid (233)/leucine (234)[111]. This can result in digested Fabs having different residues at the C terminus (in C_H1) as compared to recombinant Fabs. In addition, if the cleavage reaction does not go to completion, this difference can be more pronounced. Subtle structural differences between digested and non-digested Fabs could also be playing a role in the decreased binding of A5 and C7 to the digested Fab A.

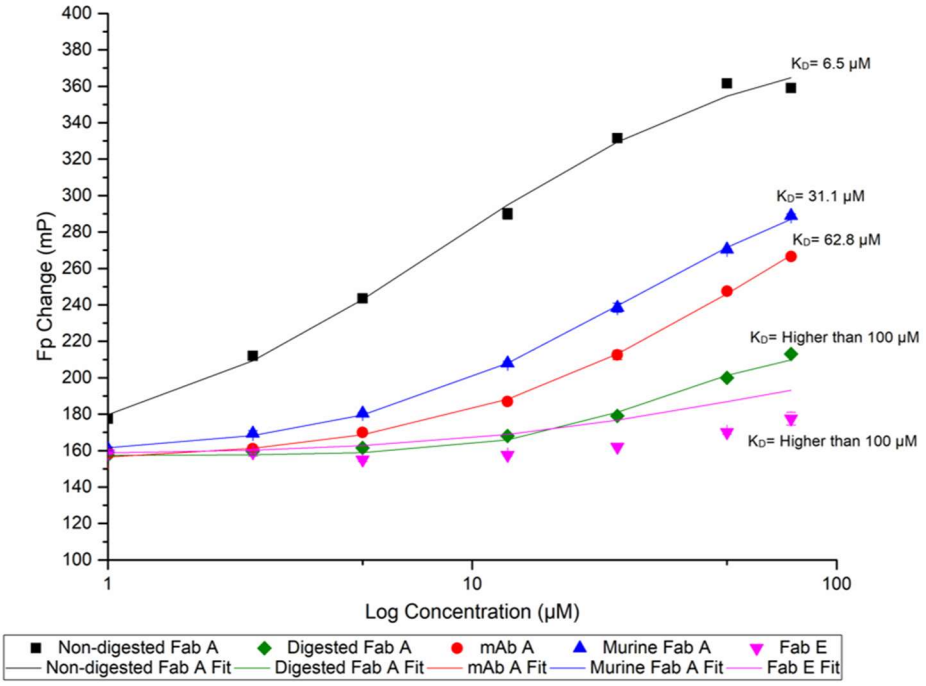

Figure 4.6 Binding curves of C7 peptide for different Fab fragments and a mAb. The respective dissociation constants are indicated

As can be seen in the figures, Fab E had negligible binding to these peptides. Since the only difference between Fab E and Fab A is in the CDR region, it is likely that the CDR region of Fab A is playing some role in contributing to the binding of peptides A5 and C7. However, the fact that the digested and whole mAb versions of Fab A have significantly reduced binding, indicates that the CDR region is not solely responsible for binding and that the conserved regions (i.e. V_L, C_L, C_H1 and framework region of V_H) may also be contributing. Interestingly, the murine Fab A was found to have the second highest binding for this set of molecules behind recombinant Fab A, with a K_D of 31 μM and 38 μM for peptides C7 and A5, respectively. The main difference between murine

Fab A and recombinant Fab A lies in the framework region of the V_H domain (60% similarity). This difference and any related conformational changes may be contributing to the reduced binding of the murine Fab A as compared to the recombinant Fab A. Clearly, further work with computational docking and/or biophysical studies will be required to more clearly determine the binding region(s) for these peptides.

We then examined the binding of peptides A5 and C7 to the two additional recombinant Fabs (Fab D and Fab Z) used in the positive rounds of the MFT phage display screen (**Figure 4.7**). As can be seen in the figure, while Fab Z (used in the second positive screen) exhibited moderate affinity with peptide A5 (K_D = 7.4µM), it showed significantly lower affinity with peptide C7 (K_D > 100µM). Peptide A5 was then evaluated with Fab D (used in the third positive screen of scheme MFT phage display) and some affinity (albeit lower) was also observed. These results indicated that peptide A5 was able to bind to all three Fabs employed in the screen with K_D values of 4.1, 7.4 and 37.7 µM for Fabs A, Z and D, respectively. This is in contrast to the results obtained with peptide C7 which was found to have moderate affinity only for Fab A. The ability of peptide A5 to bind to these three Fabs is encouraging and indicates that it may have potential as an affinity reagent for recombinant kappa Fabs. These results also indicate that in contrast to the first biopanning approach, the incorporation of multiple Fab targets in the second biopanning protocol and appropriate negative selections can result in the identification of a more generic affinity peptide reagent.

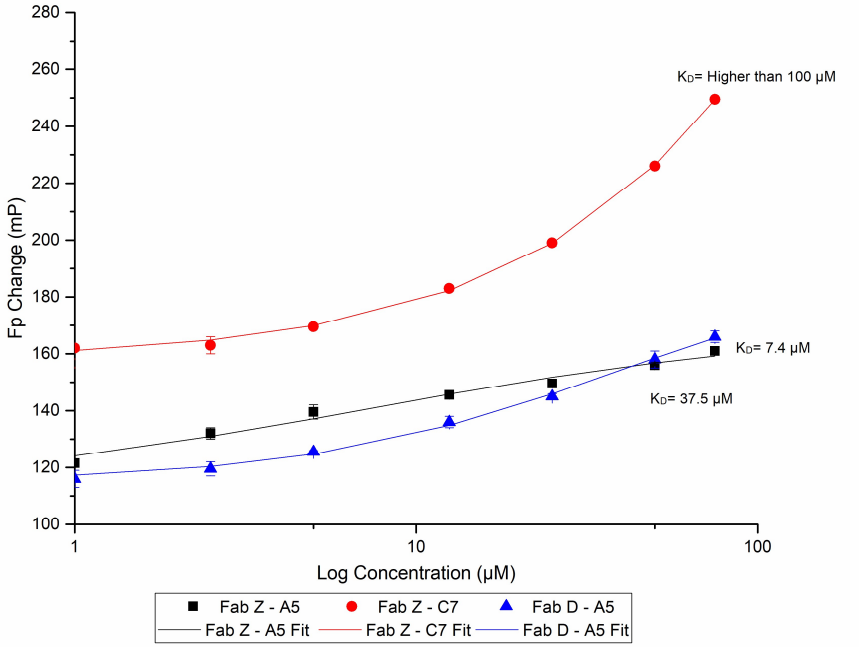

Figure 4.7 Binding curves of A5 with Fab Z and Fab D, and C7 with Fab Z. The dissociation constant obtained in each curve is indicated.

4.3.2. A5 and C7 alanine-scanning mutagenesis

Alanine scan is a commonly used method to study proteins, specially the influence of certain amino acids in their structure and/or activity [230,231]. It is traditionally used in enzymes, to evaluate their activity and binding sites [232] in antibodies to evaluate key amino acids responsible for the recognition of epitopes [233,234] or in other protein affinity studies [235]. Alanine-scanning mutagenesis is based on a systematic substitution of the original amino acid by an alanine and analyze the putative alterations that this mutation cause – in both protein structure and activity. Alanine is frequently used for this systematic amino acid replacement once it removes all the side-chains past the β-carbon, making it possible to deduce the effect of a specific side-chain in the studied protein [236]. Glycine is also a common amino acid for this type of assays, however the flexibility conferred by this amino acid can promote conformational changes, making the evaluation of the scanning mutagenesis more complex [237]. In addition to the use of alanine-scan in proteins, their use to study peptides is also a common procedure [238]. In this study, A5 and C7 were subjected to a single alanine point mutation to evaluate the effect of each amino acid in the binding to a Fab target, in this case, Fab A.

The results obtained with the alanine scan for A5 are summarized **Figure 4.8**. The original K_d for A5, calculated in previous sections (**section 4.3.6**) is 4.1μM. When alanine substitutes the original amino acid at positions 2 and 4, there is a decrease of K_d, 3.6 μM and 3.4 μM respectively, when this substitution is made on position 1 and 3, the K_d stays practically identical, 4.2 μM and 4.5 μM respectively. On contrary, when alanine substitutes the other amino acids (position 5 to 12), there is an increase of the K_d, and a decrease of affinity. Regarding C7 (**Figure 4.9**), only when the original amino acid at position 6 is substituted, there is a slight decrease in the K_d, from 6.5 μM to 6.4 μM. Mutations at positions 1 to 5 and position 7 promotes small increases in the original K_d, but not very pronounced. From position 8 to position 12, alanine mutation promotes a more pronounced increase in the K_d, decreasing affinity towards Fab A. Interestingly, for both peptides the crucial region for the binding to Fab A is closer to the C-terminal. Alterations of the amino acids closer to this region (from position 5 for A5 and from position 7 for C7) promotes a decrease of affinity, and the mutated peptides are less likely to bind Fab A as efficiently than the original. On the other hand, changes in the amino acids closer to the N-terminal region did not have significant impact on the binding to

Fab A, and in some cases, it promotes a stronger interaction. For the A5 peptide, the first five amino acids appeared to have less influence in the binding to Fab A, for C7, alterations in the first seven promotes no significant changes in its propensity to bind Fab A. Another interesting note is the higher effect caused by the alanine mutations of A5 when compared to C7. Changes in the A5 K_d are more accentuated than in C7. Probably in A5 the last amino acids are more important for the binding, while in C7 the influence of binding is distributed over the twelve amino acids.

Position	AA replaced	Peptide	K_d (μM)
Original (A5)	-	**WHYNWQDVSDRQ**	4.1
1	W	AHYNWQDVSDRQ	4.2
2	H	WAYNWQDVSDRQ	3.6
3	Y	WHANWQDVSDRQ	4.5
4	N	WHYAWQDVSDRQ	3.4
5	W	WHYNAQDVSDRQ	50.6
6	Q	WHYNWADVSDRQ	17.6
7	D	WHYNWQAVSDRQ	29.1
8	V	WHYNWQDASDRQ	34.7
9	S	WHYNWQDVADRQ	25.0
10	D	WHYNWQDVSARQ	26.8
11	R	WHYNWQDVSDAQ	51.9
12	Q	WHYNWQDVSDRA	22.8

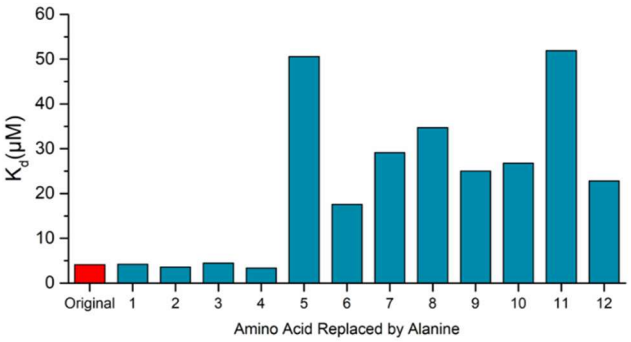

Figure 4.8 Table and bar graph summarizing the A5 alanine mutation results. In the table it is highlighted the point alanine mutation occurred in each amino acid of A5. The dissociation constant of the mutated versions of A5, towards Fab, is also indicated. In the graph it is possible to compare the effect of each alanine-mutation on the K_d of the twelve mutated A5 versions. To compare the results obtained with the alanine-mutations, the K_d of the original A5 towards Fab A, is present in both table and graph.

Position	AA replaced	Peptide	K_d (μM)
Original (C7)	-	**HQNHHSTFWEIY**	6.5
1	H	AQNHHSTFWEIY	7.4
2	Q	HANHHSTFWEIY	7.8
3	N	HQAHHSTFWEIY	7.1
4	H	HQNAHSTFWEIY	7.1
5	H	HQNHASTFWEIY	10.0
6	S	HQNHHATFWEIY	6.4
7	T	HQNHHSAFWEIY	8.9
8	F	HQNHHSTAWEIY	16.9
9	W	HQNHHSTFAEIY	23.2
10	E	HQNHHSTFWAIY	21.7
11	I	HQNHHSTFWEAY	17.4
12	Y	HQNHHSTFWEIA	37.6

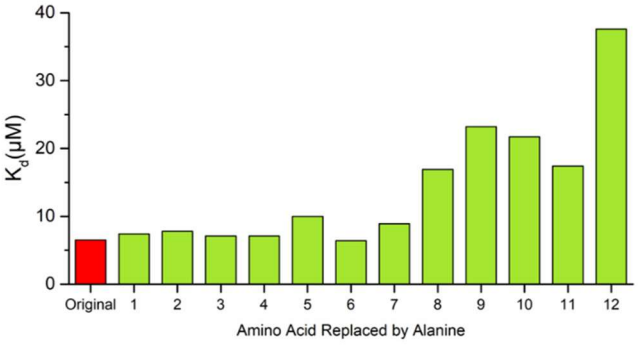

Figure 4.9 Table and bar graph summarizing the C7 alanine mutation results. In the table it is highlighted the point alanine mutation occurred in each amino acid of C7. The dissociation constant of the mutated versions of C7, towards Fab, is also indicated. In the graph it is possible to compare the effect of each alanine-mutation on the K_d of the twelve mutated C7 versions. To compare the results obtained with the alanine-mutations, the K_d of the original C7 towards Fab A, is present in both table and graph.

With these single-point alanine mutation assays it was possible to understand that not all the amino acids of A5 and C7 are fundamental in the binding to Fab A. In both peptides the region more affected by the alanine mutation is closer to the C-terminal region. These results could be a coincidence related to the nature of both peptides, or a bias created by the structure of the phage, isolated during the rounds of biopanning, that displayed the peptide on its surface, with the C-terminal region more available to bind to the target Fab. The N-terminal, closer to the phage, can putatively be more inaccessible. It is less likely that this result is based on the nature of the amino acids (hydrophobicity or charge) closer to the C-terminal region, once they do not show significant resemblances.

For the purpose of this work, find peptide affinity ligands for downstream applications, the assays completed here were useful to comprehend the influence of certain amino acids in the binding of a peptide to a target. For future experiments, it could be worth to do a deeper mutational study, by replacing with other amino acids, and understand if it is possible to increase the affinity of A5 and C7 peptides, towards Fab A or, if possible, towards a higher number of Fabs. Another future evaluation that could be made, having

in consideration these results, is the number of amino acids needed to promote an efficient binding to the target. For example, test if the absence of the initial amino acids in A5 and C7 affect the binding to Fab A and how.

4.3.3. Third phage strategy - Complete Fab target phage display

The results achieved in previous sections highlighted the importance of phage biopanning in the discover of high affinity peptides. The correct design of panning strategies allows to find peptides specific to different regions of the same biomolecule. The peptides discovered in previous sections (**4.3.3.** and **4.3.5**.) – B1, A5 and C7, are moderate affinity binders, able to target different regions of the same Fab fragments – Fab A. Despite A5 is herein considered a pseudo-affinity binder for kappa light chain Fabs, it lacks specificity to other classes of Fabs, including, digested Fabs, lambda Fabs and other types of kappa Fabs (i.e. Fab E). Having in consideration the lack of a broader specificity found in the peptides discovered, and the possibilities that a correct bioapanning strategy can offer, a third and more robust biopanning strategy was conceived. In this a higher variety of Fab targets was considered, including undigested kappa light chain Fabs, digested kappa light chain Fabs and digested lambda light chain Fabs. The goal intended with this strategy is to tackle all the intrinsic Fab variety (digested vs undigested and kappa vs lambda) in order to obtain a universal peptide affinity binder. **Table 4.1** summarizes all Fabs used for the CFT phage display and in the fluorescence polarization studies done with the peptides discovered during this biopanning.

Table 4.1 List of Fabs used in the CFT Phage Display (biopanning and FP screening). Information regarding the form (digested/expressed), type of light chain (Kappa/Lambda) and producing host is provided.

Fab	Form	Light Chain	Host
Fab 1	Expressed	Kappa	*E. coli*
Fab 2	Digested	Kappa	CHO
Fab 3	Digested	Lambda	CHO
Fab 4	Expressed	Kappa	HEK
Fab 5	Digested	Kappa	CHO
Fab 6	Expressed	Kappa	HEK
Fab/mAb 7	Digested	Kappa	CHO
Fab 8	Digested	Kappa	CHO
Fab 9	Digested	Kappa	CHO
Fab 10	Digested	Kappa	HEK
Fab 11	Digested	Kappa	CHO
Fab 12	Digested	Kappa	CHO

4.3.3.1 Complete Fab Target (CFT) Phage Display

The third phage strategy (**Figure 4.2**) was named Complete Fab Target (CFT) once it aims to put under the same scope a vast variety of Fab fragments formats. In this, two biopanning branches were created, one (kappa branch – **Figure 4.2a**) where exclusively kappa light chain Fabs were used (digested and expressed) and other (lambda branch – **Figure 4.2b**) where one lambda light chain Fab is employed, followed by two kappa Fabs. In each strategy four positive rounds of biopanning were involved, each one using a different Fab fragment. The first round of biopanning, common to both branches, uses protein L to immobilize the kappa light chain Fab. Upon branching, the following rounds of positive selections employs NHS beads. The immobilization on NHS beads, instead of protein L, as it was done in the previous two phage strategies, has two reasons. Firstly, Fabs with lambda light chain have no affinity towards protein L, therefore they cannot be immobilized on protein L functionalized beads. To maintain consistency, in subsequent rounds, NHS beads were used to immobilize the employed Fabs. Secondly, NHS beads have a lower ligand density than protein L magnetic beads, this will promote a decrease of Fabs on the NHS bead, creating the necessary conditions for an increase on phage

competition, and possibly finding higher affinity peptides. Decrease in target density is recommended to obtain higher affinity phage clones, and so higher affinity peptides [239]. Other difference applied in this biopanning strategy was the use of a higher phage volume (400 µL instead of 200 µl) to promote a higher binding of phage. The same type of negative selections (BSA blocked beads and tubes) and washes (with *E. coli* CCF) applied in the MFT were applied here in the CFT.

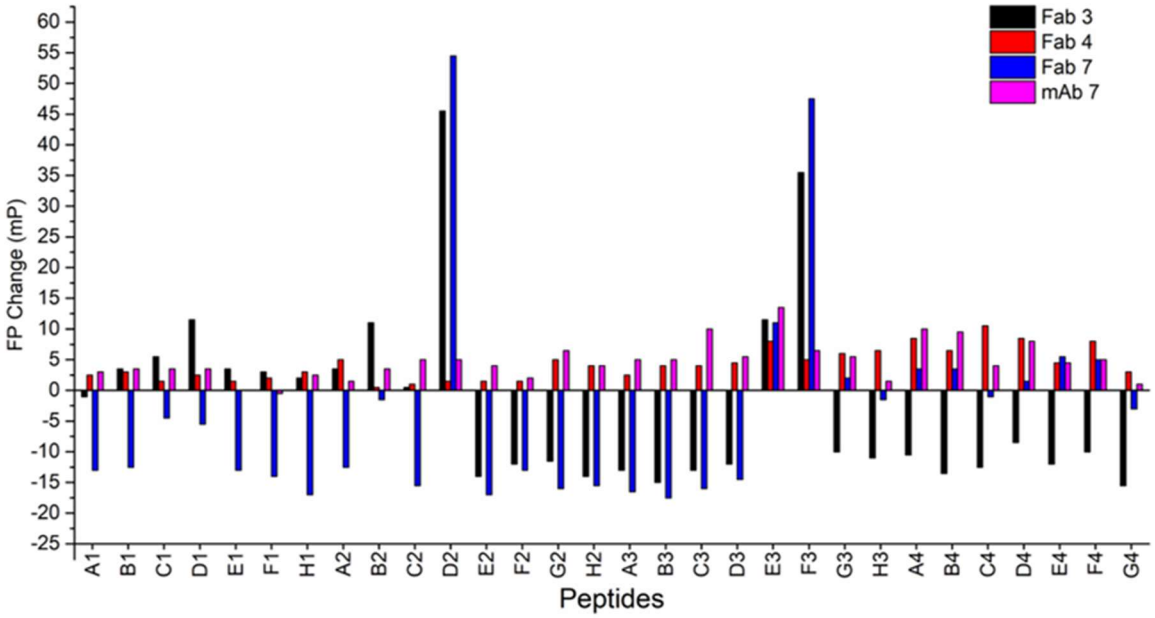

Figure 4.10 Initial binding screen of the peptides obtained after the CFT phage screening. The 30 peptides were tested screened against two digested Fabs (3 and 7), a expressed Fab (Fab 4) and a monoclonal antibody (mAb 7). Fab 7 was derived from mAb 7.

From each obtained phage eluates, 40 unique colonies were sent for sequencing. The presence of several common sequences, led to the synthesis of 30 unique labelled peptides, as it was done in previous sections (**section 4.2.8**). An initial fluorescence polarization screen was complete to short-list peptides and find lead candidates for further affinity studies. In this initial FP study, instead screening the labelled peptides against only one Fab, likewise done previously, the screening was completed against three Fabs and one mAb. All the other variables in the initial FP screen were kept. The results obtained are present in **Figure 4.10**. After an initial evaluation is possible to notice that a very small FP change is observed in most of the peptides screened, suggesting low affinity peptide binders or false positives, unsuccessfully screen out during the biopanning. Nevertheless, and making a more thorough analysis of the results, it is possible to short-list some peptides that show FP change, higher than 8 mP, for more than two tested

proteins, such as A4, E3, D2 and F3. Despite low FP change, E3 peptides was the only candidate that show similar binding across the four tested proteins. Peptide A4, produce low FP changes for two out of four biomolecules, while D2 and F3 show a considerable FP change for other two biomolecules. It is interesting to point out that the Fabs showing higher binding to A4 are an expressed Fab and a mAb, while D2 and F3 are showing a large FP variation only with digested Fab fragments. From this screen the top-rated peptides chosen for further consideration were A4, E3, D2 and F3.

4.3.3.2. A4, D2 and F3 - Binding affinity towards ten different Fabs

To guarantee that the peptides selected have a high affinity towards a broad range of Fabs, an exhaustive set of Fab biomolecules was used to determine dissociation constants and evaluate the universal binding hypothesis. Fabs used in this study are listed on **Table 4.1**. Out of ten tested Fabs, two (Fab 4 and 6) are produced by host expression, while the other eight are obtained by papain digestion of their respective mAb version. The results obtained with E3 will not be shown, since it demonstrated affinity values (K_d > 100 μM) and binding curves characteristic of a weak affinity binder. Regarding A4 (**Figure 4.11** and **Table 4.2**), it showed an affinity of 10.66 μM only towards Fab 6, not being considered a universal binder. In opposition, D2 and F3 possess binding curves characteristic of higher affinity binders, when compared to A4 and E3. Both D2 and F3 show high binding affinities to all digested Fab fragments tested but did not bind to the expressed ones **(Figure 4.12** and **Table 4.2**). The trend demonstrated by these two peptides is very similar to the eight tested digested Fab fragments, with both peptides having similar dissociation constants for the same Fabs. All the K_d values calculated by fitting the binding curves to a 4-logistic equation are present on **Table 4.2**.

Table 4.2 Dissociation constants (in µM) obtained for each peptide-Fab interaction for the peptides A4, D2 and F3. The highlighted boxes indicate weak (>100 µM) affinity between peptides and Fabs.

Fab	A4	D2	F3
Fab 2	>100	5.52	1.42
Fab 3	>100	20,37	27.45
Fab 4	>100	>100	>100
Fab 6	10.66	>100	>100
Fab 7	>100	3.93	5.00
Fab 8	>100	3.03	4.38
Fab 9	>100	4.34	5.78
Fab 10	>100	21.13	26.17
Fab 11	>100	3.64	5.14
Fab 12	>100	7.31	10.66

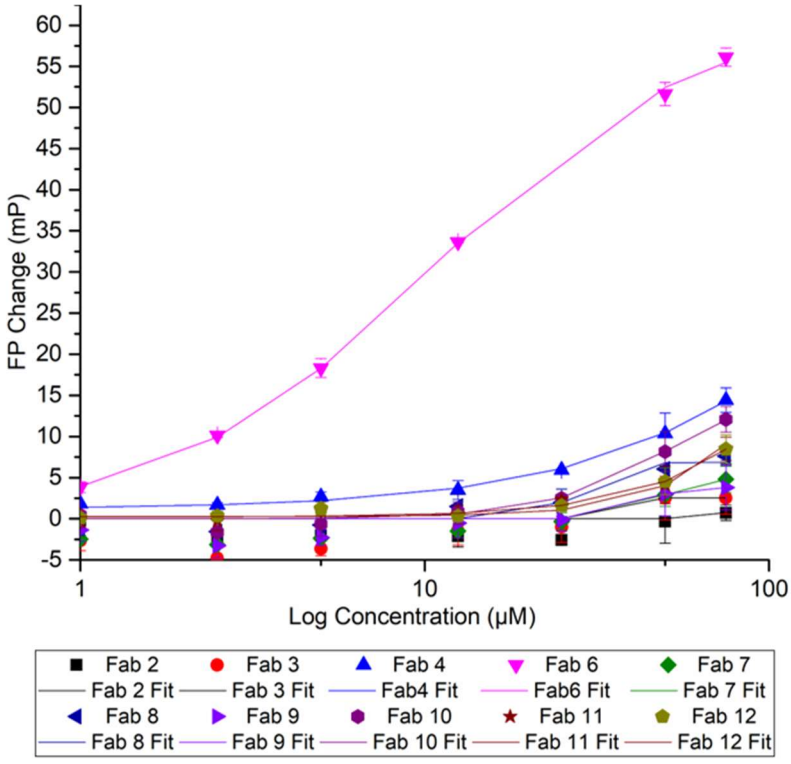

Figure 4.11 Binding curves for A4 with different Fab fragments - digested and expressed.

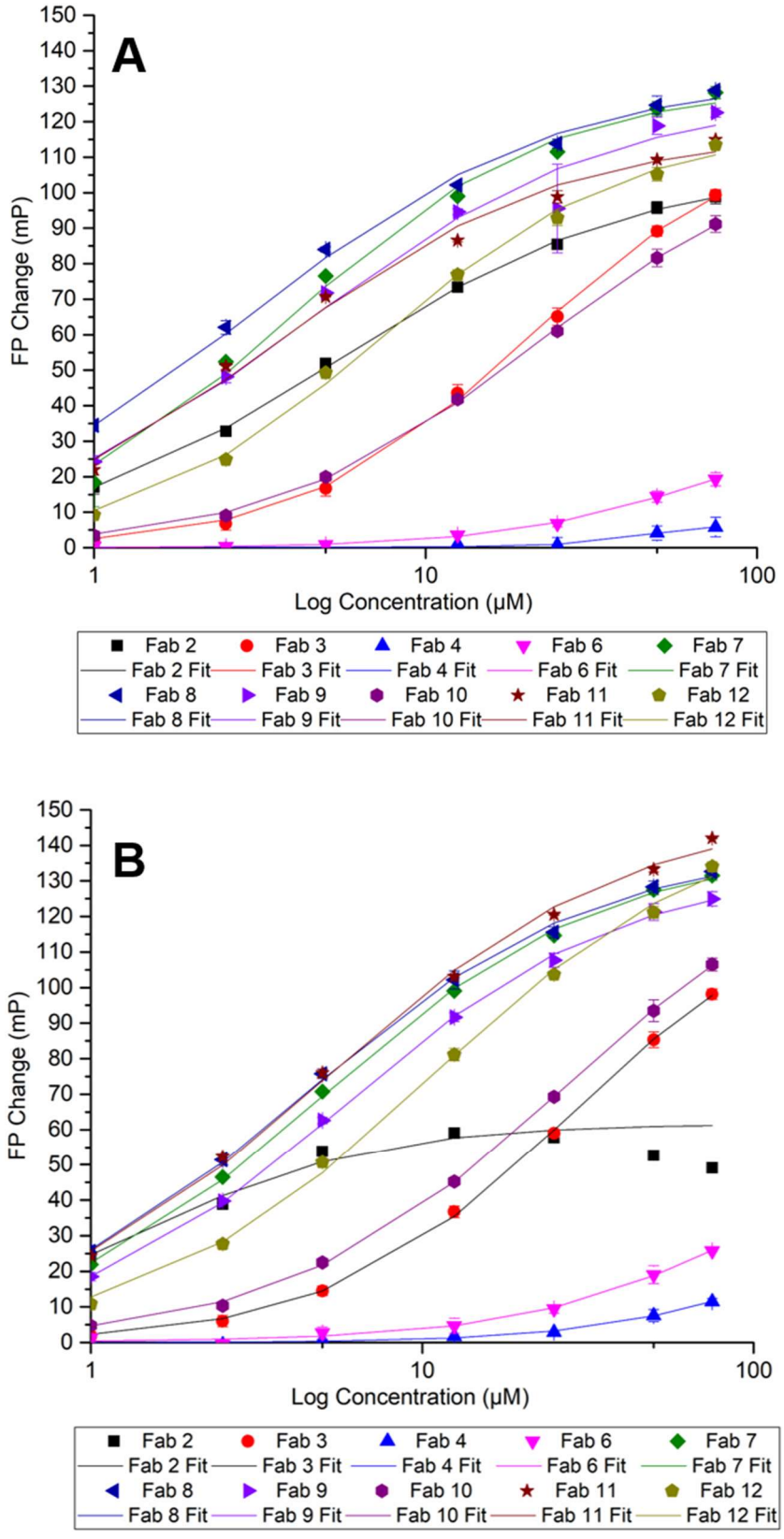

Figure 4.12 Binding curves for (**A**) D2 and (**B**) F3 with different Fab fragments - digested and expressed.

The results obtained herein with D2 and F3 are encouraging. Their ability to bind eight different digested Fab fragments, including one with lambda light chain (Fab 3), is enough to classify D2 and F3 as universal binders for digested Fab fragments. However, the lack of affinity towards expressed Fabs is a surprise. A possible explanation for these results could be related with the papain digestion procedure, used to generate all the digested Fabs here employed. It is likely that D2 and F3 are recognizing and binding to a common sequence, or structural motif, present in all the digested Fabs, perhaps a region closer to the site where papain cleaves mAbs, near the hinge region. Furthermore, the complete lack of affinity towards expressed Fabs, may indicate subtle differences of the C-terminal regions - place where papain cleaves mAbs, of the constant domains between the digested and expressed Fabs. These differences could be the key to understand why D2 and F3 binds exclusively to digested Fab fragments. The affinity variances between digested and expressed is also present in previous sections of this chapter, creating the idea that the difference between express and digested Fabs is more pronounced that is commonly referred. Like A5 and C7, D2 and F3 have different binding behaviour to the same Fab but with different origin. Fab 6 and 10 targets the same epitope, and share the same sequence, however, D2 and F3 are only able to bind the digestion version of this biomolecule (Fab 10) not the expressed one (Fab 6), corroborating the hypothesis of changes during the digestion that could interfere with the binding of peptides.

Out of all the peptides found with this work, D2 and F3 are the ones that show a broader specificity to bind Fab fragments. Despite having affinity only towards digested Fabs, one can theorize the application of these peptides as possible capture solutions for digested Fabs. Traditionally, digested Fabs are purified from a digestion mixture using a protein A step, where Fc and undigested antibodies are removed. This step is generally followed by a second step, that may differ from process to process. The use of D2 and F3 can thus be used as main capture step, to bind digested Fab fragments, and so replacing the affinity step based on Protein A (**Figure 4.13**).

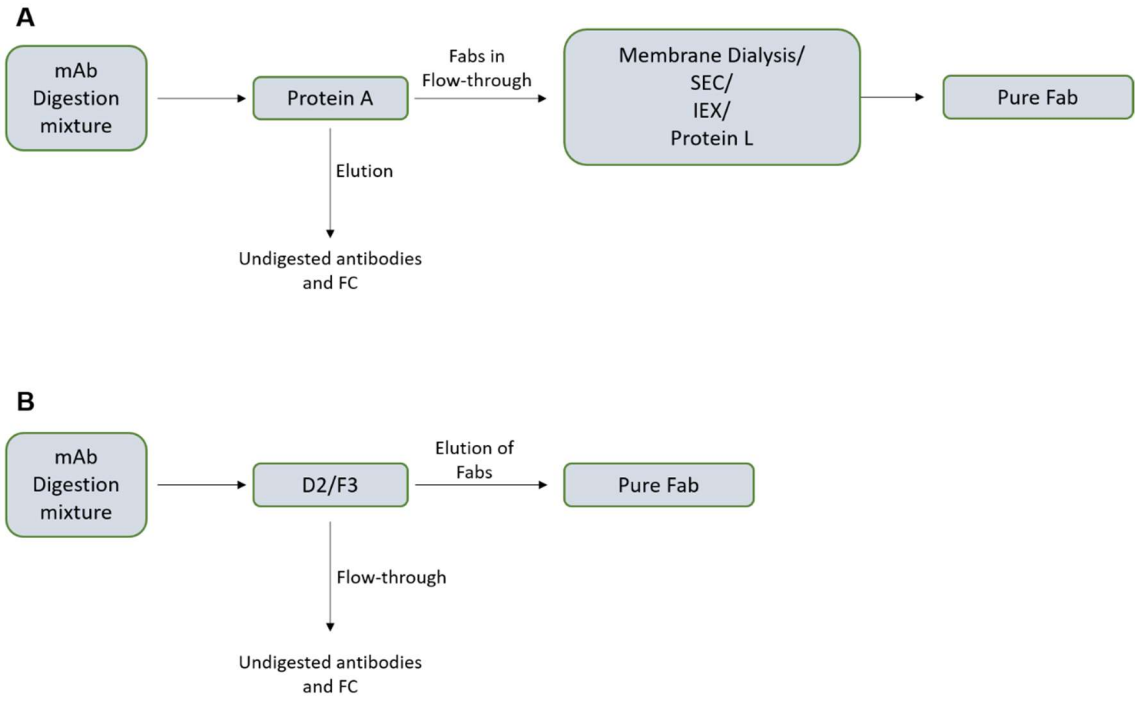

Figure 4.13 Two possible downstream processes for digested Fab fragments (**A**) Traditional scheme, using protein A as the main purification step. (**B**) Implementation of D2/F3 peptides as a solution for the purification of digested Fabs.

4.3.4. Proof of Concept Purification of Fab A

While the dissociation constants of the interactions of the identified affinity peptides to the Fabs in this chapter were on the order of 10^{-6} M, protein L is known to bind more strongly to Fabs, with K_D values of < 10^{-7} M[130]. However, it is well known that in addition to binding affinity, selectivity and ease of elution are critical components of the identification of effective affinity ligands for the chromatographic purification of biological products. Accordingly, we carried out a proof of concept study to demonstrate that the B1 peptide, which showed the highest affinity towards Fab A in the initial screens, could be successfully employed in a column format for Fab purification from a complex feed. As described in the methods section, peptide B1 was immobilized onto an NHS activated Sepharose Fast Flow resin with a final ligand density of 2 µmol/mL. The resulting peptide resin was then employed for the purification of Fab A spiked into a crude *E. coli* cell lysate. RP-UPLC chromatograms of Fab A spiked into the CCF, the flow-through pool and the elution pool are presented in **Figure 4.14** (**A** and **B**). As can be seen, while the flow-through pool contained negligible amounts of Fab A, the elution

pool contained primarily the highly purified Fab A. Based on the peak areas from this analysis, this single chromatographic step resulted in a Fab A purity of greater than 90% and a recovery of 84% (both purity and recovery were obtained by UPLC chromatogram peak integration). SDS-PAGE analysis was also carried out and the results also indicated significant purification of Fab A from the complex feed (**Figure 4.14C**). It is also important to note that the elution of Fab A from this immobilized peptide column was carried out under relatively mild conditions (pH 5 as compared to the typical pH 2.5 for elution from protein L). This affinity chromatography experiment was repeated 5 times on the same resin and very similar levels of purity and recovery were achieved, indicating that this affinity resin may have utility for multiple cycles of operation. This proof of concept purification using an affinity peptide column demonstrates that peptides identified from the phage screening procedure can be effectively employed for Fab affinity purification with minimal process development at the column scale.

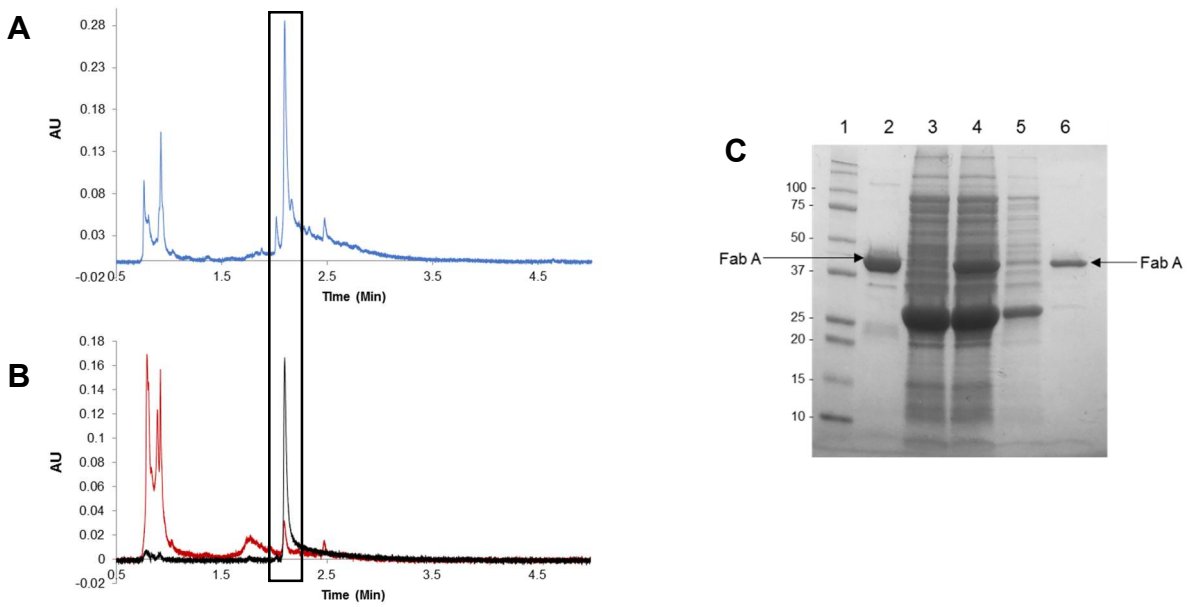

Figure 4.14 (**A**) UPLC chromatograms depicting Fab A spiked into *E. coli* cell lysate (blue) and (**B**) Flow-through fraction of peptide B1 chromatographic experiment (red) and purified Fab A (> 80%) in eluate fraction (black). The black rectangle denotes Fab A, before and after purification by B1 peptide affinity chromatography. (**C**) SDS-PAGE (reducing conditions) of the fractions of purification of Fab A from E. coli CCF. 1 – Ladder; 2 – Pure Fab A; 3- E. coli CCF; 4- *E. coli* CCF spiked with Fab A; 5- Flow-through pool; 6 – Elution pool.

4.4. Conclusion

In this chapter, three different approaches to find peptides for the purification of Fab fragments were designed and evaluated. In the first two phage biopanning strategies, using protein L and NHS magnetic beads, the peptide sequences obtained were synthesized and the binding of these peptides to different Fabs were evaluated using fluorescence polarization. A biopanning strategy focusing on a single Fab (Fab A) yielded a peptide ligand which displayed similar binding affinities to two different forms of the Fab (recombinant and post papain digestion) as well as the intact antibody. This peptide also exhibited affinity for a murine variant of Fab A which had the same CDR region, but a different framework. In contrast, minimal binding was observed to a Fab with high sequence homology to Fab A but containing different CDR loops, indicating that this peptide was specific to Fab A containing biomolecules and that binding was focused primarily in the CDR region. The second biopanning strategy, using three Fabs, yielded a peptide ligand that exhibited affinity for all three Fabs, indicating that it may have potential as a more general affinity reagent for recombinant kappa Fabs. In the third biopanning strategy, the know-how acquired in the previous two was applied, especially in the design of the phage scheme, where more diverse Fabs (digested and undigested, kappa and lambda) were employed. Additionally, the fluorescence polarization assays were more exhaustive, using an increased number of biomolecules with higher diversity. The chief outcome of the third phage biopanning were two peptides – D2 and F3. These showed high affinity towards eight different digested Fab fragments (both kappa and lambda), being considered universal peptide binders for digested Fab fragments. A possible application for D2 and F3 is the replacement of the traditional protein A step when Fab fragments are produced by papain digestion. Finally, an affinity peptide column was developed, and its efficacy was demonstrated for Fab purification from a complex CCF mixture. The results presented in this paper demonstrate that different protein L based phage biopanning strategies can be effectively employed to identify affinity peptide leads for specific Fab and kappa Fab purifications. Future work will refine our biopanning techniques to further improve peptide discovery for kappa Fabs and will include more detailed experimental and modelling studies to better identify the binding regions for these affinity reagents. Optimization of peptide immobilization and column operating conditions will also be carried out to further improve the performance of the developed Fab affinity peptide columns.

Chapter 5

Debottlenecking process development using a microfluidic high-throughput platform

5.1. Introduction

The production and purification of mAbs has no secrets. Recent improvements in upstream and protein A technology led to the creation of a robust and efficient platform to produce mAbs. For Fab fragments, there still a long way to trail, in both upstream and downstream. Focusing on the last, protein L is the prefer choice to purify Fab fragments, however, its inability to bind all Fab classes and typical harsh elution conditions makes this purification solution not as reliable as protein A is for antibodies. The main focus of this thesis is to find purification alternatives for Fab fragments, as it was done in previous chapters with peptides. In this, another alternative is presented, the use of multimodal chromatography as a downstream solution for these antibody derivatives.

Traditionally, chromatography is based on one type of interaction, such as affinity, ion exchange, hydrophobic interaction and size exclusion. Recently, the idea of using more than one type of physicochemical interaction (e.g., charge and hydrophobicity) produced a new chromatographic mode named multimodal chromatography [240]. This new purification concept combines in one ligand multiple modes/types of interaction. The structure and properties of the ligand will establish the nature of the interaction and the strength that each will have [241]. The core novelty of these new ligands is the possibility of having in one single ligand a combination of ionic, hydrophobic, hydrogen bonding or Van der Waals interactions. The heterogeneity of multimodal (or mixed-mode) chromatography offer some advantages when compared to the single interaction chromatography including, higher selectivity, capacity, efficiency, and salt-tolerance [242,243]. Making a comparison with protein domain-based ligand, multimodal ligands are cheaper, offer milder operating conditions and the screening of new ligand alternatives is easier [244–246]. Multimodal chromatography is already an implemented purification tool [247,248]. Currently there is a vast choice of commercially available resins offering ligands with different moieties and structure [243]. Another indicator of the value of

multimodal chromatography is the development of several ligands for specific purification application, as well as the increasing number of publications focusing on the use of this type of chromatography [249].

Multimodal chromatography promotes increased selectivity and flexibility when compared to traditional chromatography modes. The complexity of interactions holds great potential towards the purification of biomolecules, however, the same complexity creates a major limitation, the binding interaction between the ligand and the target is not as intuitive as in the single interaction chromatography. The presence of more than one moiety requires a deep study on the best binding and elution conditions to understand which variables are essential for an efficient purification [250,251]. The intrinsic nature of the biomolecule and physicochemical properties of the ligand will make each purification procedure unique, thus a thorough evaluation of the best chromatographic conditions is mandatory. To implement a multimodal chromatography step, in a downstream process, a fast and reliable high-throughput (HT) system need be employed to screen the ideal operational conditions. This screen must have in consideration numerous variables: pH, conductivity, salt concentration, phase modifiers and type of impurities.

To do an exhaustive and fast process development of multimodal ligands/resins several high-throughput technologies have been employed, including, resin slurry in a microplate, resin tips and miniature columns [252,253]. The last two required the use of automated liquid handlers and precise robotic setups, that could increment the cost of the process development [254,255]. The use of resin slurries in 96-well plates is the most traditional choice to study protein and ligand interaction, in both academia and industry, however the handling of this high-throughput format could be difficult and may interfere with the process development assays. In this chapter a new high-throughput platform, based on microfluidics, is presented. The relative novelty of this type of HT solution requires a detail introduction about microfluidics, including device fabrication, and a brief state of the art of the use of this technology in chromatography.

5.1.1. Microfluidics and microfabrication

Miniaturization of systems has experienced a tremendous progress since the 1970s, leading to the fabrication of devices, with dimensions of micrometers and nanometers, for a broad range of applications [256]. This trend has created the means for microfluidics (the study of fluid movement through micron-sized chambers and channels) to become an important player in the intersection of chemistry, physics, biology and engineering [257]. Microfluidic systems has the advantage of reduced process costs, small process volumes, reproducibility, small footprint, automation, and short process time, making microfluidic platforms (**Figure 5.1**) attractive for a range of life-sciences applications, especially in the field of biotechnology and/or bioanalysis[258]. Microfluidic platforms (biochips) can be designed to perform a myriad of tasks including, toxin detection, DNA and protein sequence analysis, clinical and forensic analysis, molecular and medical diagnostics for biological, biomedical and chemical applications.

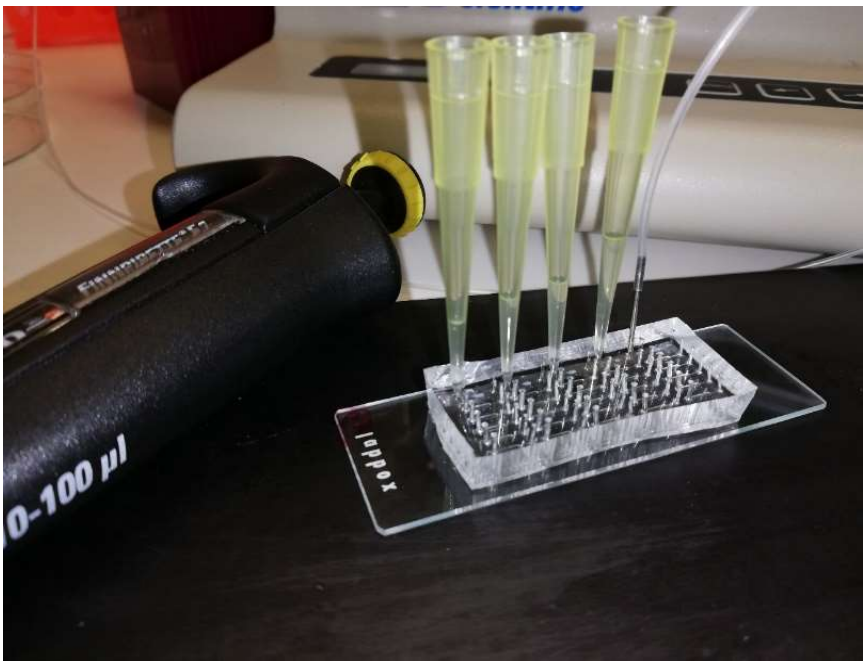

Figure 5.1 Microfluidic device used in the assays

One of the features making the production and development of microfluidic based technology a promising tool is the ability of delivering results within short periods of time, consequence of the readiness which is possible to fabricate microfluidic structures. To produce them two processes are commonly used: photolithography and

soft-lithography. With the first, the desired pattern of the microfluidic chip is designed and transformed into a mold, using photosensitive film and selectively exposing it to radiation [259]. In the second, the mold produced is used to fabricate and replicate microstructures [260]. Poly(dimethylsiloxane) (PDMS), or silicone elastomer, is the most common material used in the fabrication of the microfluidic devices. When compared to other materials (glass or silicon), PDMS has numerous advantages, including low-cost, low-toxicity, flexibility and transparency. Additionally, being impermeable to water, permeable to gases and non-toxic to cells, PDMS is compatible with biological studies. Finally, a user point-of-view feature, it is very easy to work with, making the fabrication of PDMS structures a relatively simple and timeless task [261]. All these features make PDMS the most popular material for the fabrication of microfluidic chips, using soft-lithography.

The microfluidic production process can be divided into three main parts (**Figure 5.2** [262]), hard mask fabrication, mold fabrication and PDMS sealing and casting:

(1) The hard mask fabrication starts with deposition of a thin aluminum layer onto a glass substrate, followed by the deposition of a photoresist layer. After, the microfluid pattern, previously designed using a design software, is transferred by direct write lithography (DWL) to the photoresist layer. The exposed parts of the photoresist are developed, exposing the aluminum layer, which is removed by wet chemical etching with standard aluminum etchant. The last step of mask fabrication is the removal of the remaining photoresist with acetone. The result of this first step is a hard mask that will be used to create the microfluidic mold.

(2) The mold fabrication also initiates with a deposition of a photoresist layer, but this time onto a silicon substrate. The previously produced mask is aligned with the photoresist layer, forming a stack that is exposed to UV light. The defined patterns and features are then transferred to the layer by selectively hardening or sensitizing the film. The photoresist layer can now be processed in two ways (depending on the type of photoresist): the exposed regions can remain or be developed away. In the end of this step, the molds can be reused several times and create several similar structures.

(3) The last step of microfluidic structures production is the pouring of PDMS onto the mold. When the PDMS is poured, it polymerizes by increasing the temperature until approximately 70°C, being then peeled off from the mold. Once peeled, the PDMS retains the negative of the features in the mold. The final step is the sealing of the structure, in order to allow the liquid to flow. The PDMS structures are exposed to an air plasma, to oxidize the surface and generating hydroxyl groups, that in contact with an PDMS slab or a glass substrate will create covalent siloxane bonds and so making an irreversible sealing.

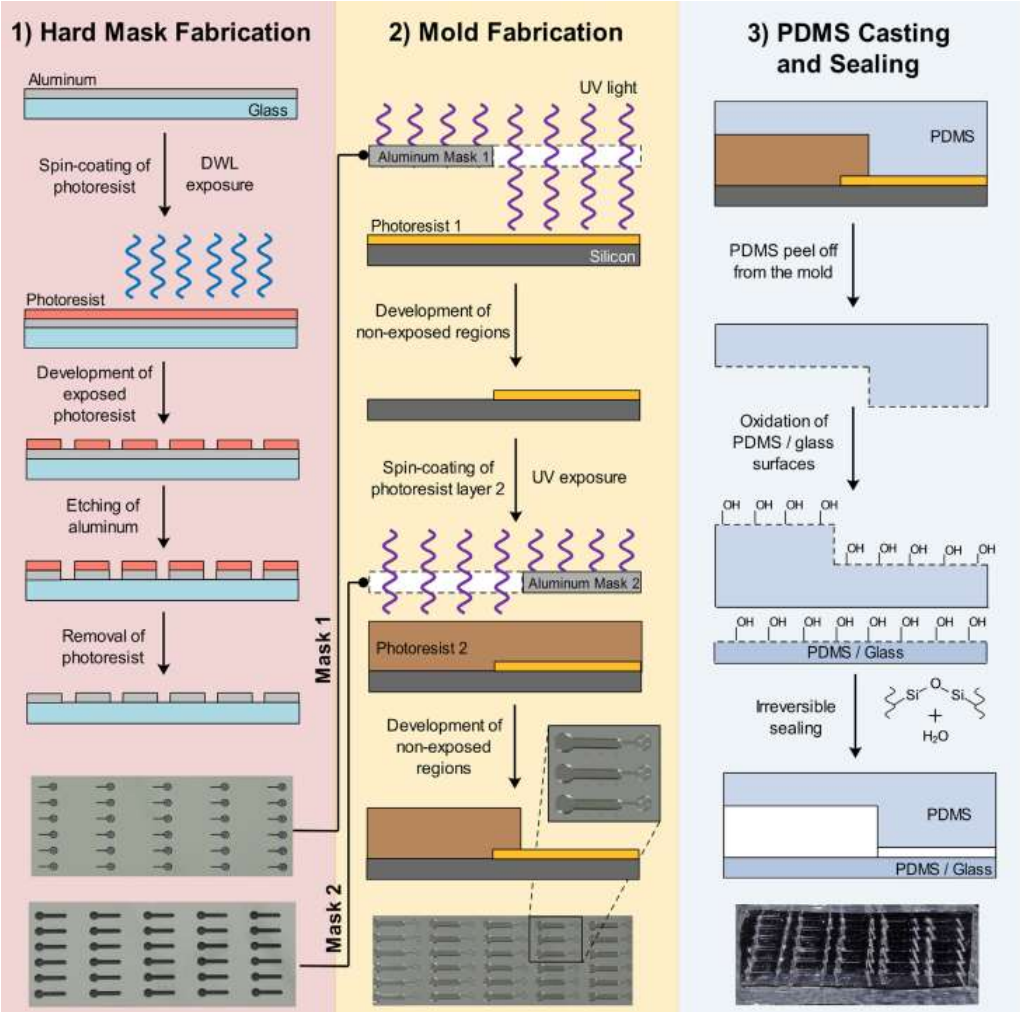

Figure 5.2 Schematic representation of the steps involved in the production of the microfluidic device used for thesis [262].

A brief summary of the main steps involved in a microfluidic device fabrication was made herein. The mask and mold used for this work were idealized, designed and produced by Doctor Inês Pinto, at INESC-MN. The complete and detailed protocol for the production of the microfluidic structure used in this work can be found elsewhere [262].

5.1.2. Chromatographic microfluid applications

Liquid chromatography has benefited with the increase popularity of microfluidics. In fact, in the last two decades, an increase of chromatography operations applied in microfluidic devices has been observed. Reasons for this are the development of novel microfluidic fabrication technologies (soft-lithography) and the use of new and more flexible materials (PDMS). With the correct design and fabrication techniques is possible to adapt different types of chromatography approaches (analytical or preparative) and techniques (e.g. screen of binding/elution conditions, dynamic binding capacity) to microfluidic devices. To illustrate the range of possibilities when microfluidics is combined with chromatography, some examples of chromatographic microfluid applications will be discussed.

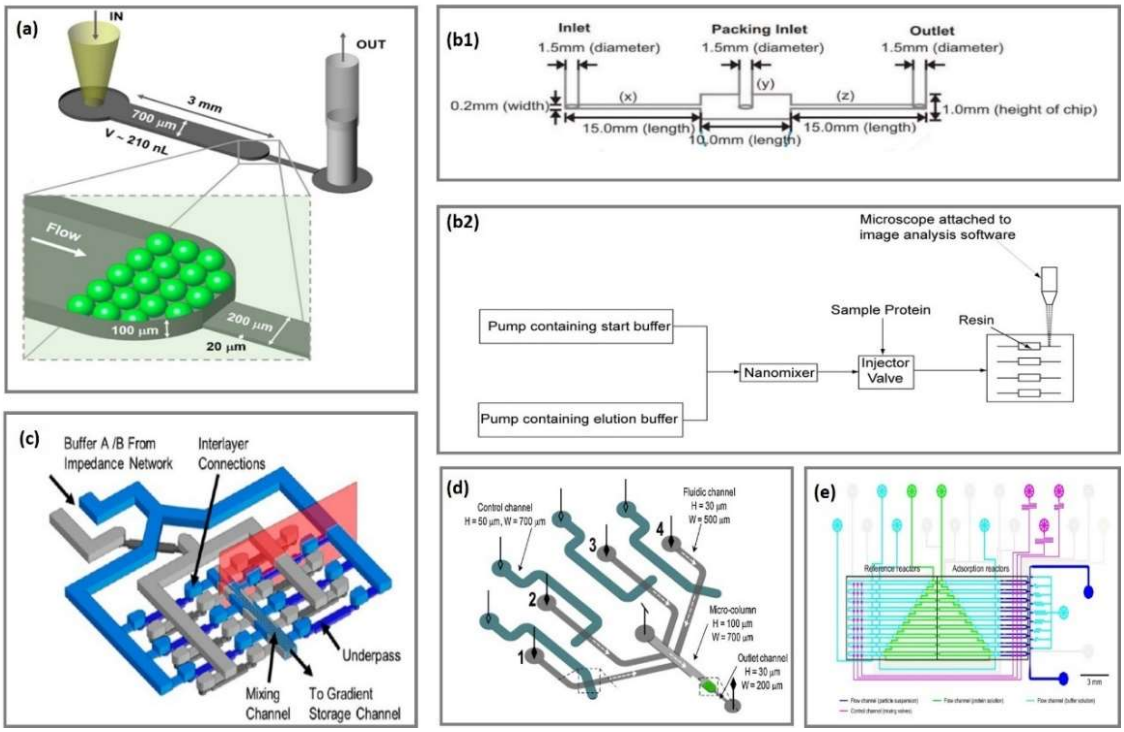

Figure 5.3 Examples of different microfluidic devices for chromatographic purposes. (**a**) Schematic representation of Pinto *et al.* HT screen platform [263]. (**b1** and **b2**) Schematic representation of the microfluidic columns used by Shapiro *et al*. [264,265] (**c**) Schematic representation of the integrated microfluidic system developed by Huft *et al.* [258] (**d**) Schematic representation of the regenerable microfluidic structure planned by Pinto *et al*. [266]. (**e**) Schematic overview of the microfluidic device designed by Rho *et al*. [267].

The complexity of the chromatographic setup is proportional to the complexity of the desired application. An example of a simple device is the one developed Pinto *et al*., a

high-throughput microfluidic platform [263]. This was created as an alternative to the current formats used in the HT screen of chromatographic resins and conditions - microtiter plates, micropipette tips and miniature columns. The key feature of this device is the difference of height of the two channels (**Figure 5.3a**). Having a larger (100 μm) and a smaller (20 μm) channel, the beads will be trapped, creating a packed bed with the interface in the region of the taller channel. When the liquid flows, by applying a negative pressure at the outlet, the beads will be trapped against the 20 μm gap (interface between the larger and smaller channel) with minor distortion or compression. In this work, Pinto *et al.* used this HT screen device to study the behavior of a multimodal resin (Capto MMC) in the purification of a monoclonal antibody [263]. The application of this platform was validated at macroscale by comparison with pre-packed resins. With this microfluidic solution is possible to do a complete study of the ideal chromatographic conditions for the purification of any molecule, assuming a previous labelling procedure.

The work of Shapiro *et al*. [264,265] was motivated by the urge to improve the speed of downstream solutions validation. In his works two different microchips were created (**Figure 5.3b1 and 5.3b2**), both operated at a flow rate comparable to the ones used at bench scale. The first had the goal of quantifying the protein breakthrough, frontal adsorption chromatography, using standard preparative beads. The second, an evolution of the first chip, was designed to do both dynamic binding and separation studies, of a model protein and a mixture of proteins, using the same beads. The difference of the two chips is their complexity, in the first the beads are packed in a microfluidic column (W = 0.15 mm; L = 10 mm; H = 1 mm) and using fluorescence microscopy it is possible to visualize the binding of the model protein (lysozyme) to the preparative beads (SP Sepharose Fast Flow). The work with the first chip was extended to a more complete analysis of the binding and elution conditions of the same protein and a mixture (hen egg white proteins). To accomplish this, the chip was "updated" with the insertion of a nanomixer to control the injection of binding and elution buffer. The results obtained in both works, using two different chips, showed good quantitative agreement between the microfluidic column and the 2-mL and 30-mL laboratory scale columns.

In the previous chromatographic microfluidic examples, there was an increase of device complexity, while the first was used for a HT screen approach, the second was used to do a deeper study of a chromatographic resin. The work developed by Huft *et al*. is an example of an even more complex device (**Figure 5.3c**) [258]. It describes the

development of a fully integrated microfluidic system on a PDMS microdevice by combining all the elements (sample loading, gradient generation and mixing, parallel sample separation, and fraction recovery) needed to deliver a complete chromatographic process, with high yield and low dilution. With this device is possible to perform both analytical and preparative techniques, including the separation and selective recovery of low molecular weight DNA. The fabrication of this chip was possible due to the used of microvalves, made by multilayer soft-lithography, that reconfigure liquid flow path and modulate the flow of the buffers. The control of the vales for sample recover was made by fluorescence detection. Another example of a complex chromatographic microfluidic device is present in the work of Pinto *et al*. (**Figure 5.3d**) [266]. An integrated and regenerable microfluidic platform, based on pneumatically-actuated valves and chromatography cycles was constructed. With this device is possible to do all the common chromatographic steps – resin equilibration, adsorption, elution and resin regeneration, in one device, using a pneumatic control system. A final example of a complex microfluidic device, used to evaluate a fast batch adsorption characteristic of biomolecules on beads, was designed by Rho *et al*. (**Figure 5.3e**) [267]. This device is completely automated and can do all the necessary steps needed for a complete batch study using too a pneumatic control system.

A brief overview of some chromatography based microfluidic applications was done. With precise engineering work and the application of the correct microfluidic technology (e.g. UV detectors, microvalves, fabrication materials, pumps, channel design) is possible to use the know-how developed in traditional liquid chromatography and applied it in microfluidic systems. The range of possible chromatographic microfluidic applications and solutions is vast and there is still space to improve both bench and micro scale chromatography.

In this chapter, two different concepts were combined to find a purification alternative for Fab fragments - multimodal chromatography and microfluidics. An HT system based on microfluidics was applied to study the binding of Fab fragments to eleven different multimodal resins. For each ligand, three pH values (5,7, and 9) and five different NaCl concentrations were tested (0, 50, 100, 150 and 200 mM), in a total of fifteen conditions per resin. In order to accomplish a thorough multimodal process development, for each resin the binding of impurities (*E. coli* lysate and CHO supernatant) and model proteins (Fc fragment, IgG and BSA) were also evaluated in the same conditions as the ones used

for Fabs. Once all the resins were evaluated, the results obtained with the microfluidic platform required validation. This was done by three different approaches. The first was made by comparing multimodal chromatography with affinity-based chromatography. The same type of microfluidic assays was done with protein L, the affinity ligand traditionally used to purify kappa light chain Fab fragments. The second was made by comparing the results obtained with Capto MMC resin in microfluidics and as a resin slurry, in a 96-well plate. Having this resin in two different HT system formats it was possible to confirm Fab binding results and evaluate two different screening platforms. Secondly, five multimodal resins were selected, packed in a normal chromatographic column and the binding of Fab fragments and complex mixtures were evaluated at a bench-scale in an ÄKTA Purifier system. Having validated the microfluidic chromatographic experiments, a downstream process, based on two multimodal resins was designed and evaluated.

This chapter contains sections that were published, as a research article, in the journal Separation and Purification Technology with the name Studies on the purification of antibody fragments (2018). Part of the results obtained in this chapter resulted from a highly collaborative work with Doctor Inês Pinto and MSc. Mariana São Pedro, from BERG-iBB.

5.2. Materials and methods

5.2.1. Chemicals and biologics

Phosphate buffered saline (PBS), tris (hydroxymethyl)aminomethane (Tris), sodium chloride (NaCl), citric acid, sodium bicarbonate, sodium carbonate, ethylenediaminetetraacetic acid (EDTA), L-cysteine, iodoacetamide and papain (≥ 10 units/mg protein) were obtained from Sigma Aldrich (St. Louis, MO/USA). Sodium phosphate dibasic and monobasic, sodium acetate and acetic acid 100% were purchased from AppliChem PanReac (Darmstadt, Germany). Sodium dodecyl sulfate (SDS) and glycine were obtained from Bio-Rad (Hercules, CA, USA). Water used in all experiments was obtained from a Milli-Q purification system (Millipore, Bedford, MA/USA). Human

immunoglobulin G (IgG) for therapeutic administration (product name: Gammanorm®) was obtained from Octapharma (Lachen, Switzerland), as a 165 mg/mL solution.

5.2.2. Chromatographic resins and filtration devices

HiTrap™ Protein L and HiTrap™ Protein A HP were purchased as pre-packed 5 mL columns from GE Healthcare (Uppsala, Sweden). Carboxymethyl Sepharose™ Fast Flow, Capto MMC, Capto Adhere and HiTrap™ Heparin Sepharose™ HP were purchased as bulk resins, also from GE Healthcare. HEA, PPA and MEP HyperCel™ Sorbents were purchased as bulk resins from Pall Lifesciences (NY, USA). Nuvia cPrime, Nuvia aPrime, CHT™ Ceramic Hydroxyapatite XT, and CHT™ Ceramic Hydroxyapatite Type I Media were kindly offered by Bio-Rad (Hercules, CA, USA) as pre-packed resins. TOYOPEARL MX-Trp-650M was kindly offered by Tosoh Bioscience GmbH (Stuttgart, Germany) as bulk resin. Eshmuno® HCX was purchased as bulk resin from Merck Millipore (Darmstadt, Germany). Amicon® Ultra-15 centrifugal filter units (NMWL of 10, 30 and 100 kDa) and Amicon® Ultra-0.5 centrifugal filter units (NMWL of 10 and 100 kDa) were purchased from Merck Millipore.

5.2.3. Sample labelling

5.2.3.1. IgG labelling with Alexa 430

IgGs from Gammanorm® mixture were conjugated, before digestion, to the amine-reactive dye Alexa Fluor® 430 (A430) NHS ester, obtained from Thermo Fisher Scientific (Waltham, MA, USA), whose maximum excitation and emission wavelengths are 430 nm and 545 nm, respectively. The IgG mixture was first diluted in 0.1 M sodium bicarbonate buffer to a concentration of 20 mg/mL and it was added to the reactive dye solution in a volume ratio of 4:1. The reaction was incubated for one hour in the dark at room temperature. The non-conjugated dye was then removed in a series of 10 diafiltration steps with PBS using Amicon® Ultra-0.5 centrifugal filter units (NMWL of 10 kDa), centrifuged at 14000 *g* for 10 min, until a clear permeate was obtained.

5.2.3.2. IgG labelling with BODIPY NHS ester

Two different BODIPY (BPD) molecules were used to label IgGs from Gammanorm® mixture. Before digestion, BDP FL NHS ester and BDP TMR NHS ester, both obtained from Lumiprobe GmbH (Hannover, Germany), were used to label IgG, separately. The maximum excitation and emission of the first dye are 503 nm and 509 nm, respectively, while the second are 545 and 570 nm, respectively. The labelling procedure applied is similar for both. The IgG mixture was first diluted in 0.1 M sodium bicarbonate buffer to a concentration of 10 mg/mL and it was added to the reactive dye solution in a volume ratio of 20:1. The reaction was incubated for four hours in the dark at room temperature. The non-conjugated dye was then removed in a series of diafiltration steps with PBS using Amicon® Ultra-0.5 centrifugal filter units (MWCO of 100 kDa), centrifuged at 14000 *g* for 5 min, until a clear permeate was obtained.

5.2.3.3. BSA, *E. coli* lysate and CHO supernatant labelling with BODIPY TMR NHS ester

To prepare BSA, *E. coli* lysate and CHO supernatant conjugated with BDP TMR NHS Ester, a similar protocol described by Pedro *et al.*[268]. was followed. Firstly, the dye was mixed with a solution of the biological sample (7.5 mg/mL in 0.1 M sodium bicarbonate) in a proportion of 1:2 volume ratio of sample to reactive dye solution, in a vortex for 3 seconds. During this bioconjugation step, 10% w/w PEG 3350 was added to help with dye solubilization and, therefore, prevent the formation of aggregates. Then, the reaction was incubated overnight in the dark with mild agitation at 4ºC. Finally, in order to remove the non-conjugated dye, the final solution was washed with PBS in a series of 8 diafiltration steps using Amicon Ultra-0.5 mL centrifugal filter units (MWCO of 10 kDa), centrifuged at 14,000 ×*g* for 5 minutes. Both *E. coli* lysate and CHO supernatant were concentrated using an Amicon Ultra-0.5 mL centrifugal filter units (MWCO of 3 kDa).

5.2.4. Digestion protocol

Fab fragments used in this chapter were generated by digestion of a mixture of IgG - Gammanorm®. Two digestion protocols, based on the work developed previously (**Chapter 3**) and by Andrew *et al.* [112], were employed. The differences applied had the goal of increasing digestion yield. All the changes were considered and validated during the design of the digestion protocol (**Chapter 3**).

5.2.4.1. Digestion protocol 1

This digestion protocol was done for the initial microfluidics studies where multimodal was compared with cation exchange chromatography. The digestion conditions were the following: Alexa 430 labelled IgG at a concentration of 2 g/L, 0.02 M of cysteine, 0.02 M of EDTA, 0.02 mg/mL of papain and a digestion volume of 40 mL. The digestion was done for 8h. Digestion stopped with 0.3M of iodoacetamide.

5.2.4.2. Digestion protocol 2

This digestion protocol was done for the microfluidic high-throughput screen using multimodal resins (with labelled IgG), for the microplate, bench-scale result validation and for the two column downstream experiments (with non-labelled IgG). The digestion conditions were the following: IgG (labelled with BDP-NHS FL or non-labelled) at a concentration of 2 g/L, 0.02 M of cysteine, 0.02 M of EDTA, 0.1 mg/mL of papain and a digestion volume of 50 mL. The digestion was done overnight (approximately 16h). Digestion stopped with 0.3M of iodoacetamide.

5.2.5. Downstream processing of digested Fc and Fab fragments

The purification of Fab fragments after the digestion was based on the work developed on **Chapter 3**. For Fabs produced using the Digestion protocol 1, the purification protocol was the DSP 3, described on Chapter 3 (**section 3.3.2.**). The Fabs produced using Digestion Protocol 2, the purification was based on the DPS 1 described on Chapter 3

(**section 3.3.2**.), with point alterations. All digestion mixture was loaded onto a protein A column on an ÄKTA Purifier system. Column was previously equilibrated with PBS, and after completely injection of the digestion mixture, elution was done by decreasing the pH to 2.5 using 0.1 M citrate buffer. Both flow-through and elution peaks were collected until the UV 280 absorbance reached the baseline. protein A flow-through fraction was then injected in protein L. The purification procedure and the buffers used for protein A were the same. The pH of the elution samples was neutralized with 2 M Tris-HCl, pH 9. The elution peak, containing kappa light chain Fabs, was collected and concentrated with a 30 kD MWCO Amicon centrifugal filters. For experiments where Fc fragment where needed, the elution peak of protein A was collected. To separate the Fc from undigested IgG, a 100 MWCO Amicon centrifugal filters was used, and the permeate (where Fc is) was concentrated and buffered exchanged with a 30 MWCO Amicon centrifugal filters. Both labelled and non-labelled kappa light chain Fabs and Fc fragments were produced and purified using the same methodology.

5.2.6. Microfluidics

5.2.6.1. Structure fabrication

The micro-columns (3×0.7 mm) used in the microfluidic studies were fabricated using PDMS soft-lithography. The PDMS was purchased from Dow-Corning (Midland, MI/USA) as a Sylgard 184 elastomer kit. The aluminum hard mask, SU-8 mold and PDMS structures were fabricated according to the procedure reported by Pinto *et al.* [263].

5.2.6.2. Microcolumn packing

The resins under study were suspended in a 1-2% (v/v) slurry in a 33% (v/v) polyethylene glycol (PEG) 8000 solution (Sigma-Aldrich, St. Louis, MO/USA). After bead homogenization, beads were inserted and packed in the micro-columns by pulling the liquid from the outlet using a syringe pump (Model NE-1002X, New Era Pump System, Inc.). All solutions were made to flow through the micro-columns by applying a negative

pressure at the outlet. Once the packing was completed, the micro-columns were washed with 50 to 70 µL of the buffer composition to be tested.

5.2.6.3. Microfluidic binding experiments: initial microfluidics study - multimodal vs cation -exchange

A volume of 30 µL of labelled Fab fragments, resulted from the IgG digestion (Digestion protocol 1) and purified using DSP 3, at a concentration of 30 µg/mL was inserted in the micro-column and adsorbed to all tested resins. For all the resins, the binding conditions screened included both pH (5 – 9) and conductivity (no salt added – 8 mS/cm) variations. For pH 5, an additional conductivity of 20 mS/cm was also tested. For pH 5 and 6, the buffering agent was 10 mM acetate, for pH 7 and 8, the buffering agent was 10 mM phosphate, and for pH 9, 10 mM carbonate buffer was used. The conductivities were measured with a handheld CO 300 conductivity meter from VWR. Conductivities were adjusted with a concentrated solution of NaCl at 6 M.

5.2.6.4. Microfluidic binding experiments: multimodal high-throughput screening of multimodal resins

A volume of 30 µL of labelled samples (Fab and FC fragments, IgG, BSA, *E. coli* lysate and CHO supernatant) at concentration of 60 µg/mL was inserted in the micro-column and adsorbed to all tested resins. For all the resins and all samples, the binding conditions screened included three pH (5, 7 and 9) and five salt (NaCl) concentration (0; 50; 100; 150; and 200 mM). For pH 5, the buffering agent was 50 mM acetate, for pH 7, the buffering agent was 50 mM phosphate, and for pH 9, 50 mM carbonate buffer was used.

5.2.6.5. Fluorescence monitoring and image analysis

An inverted fluorescence microscope (Olympus CKX41) coupled to a CCD color camera (Olympus XC30) was used to continuously monitor the assays performed in the micro-columns. The filter cube provided a band pass excitation of 460-490 nm and a long pass emission of 520 nm. The fluorescence signal from the beads inside the micro-columns

was acquired with an exposure time of 1 s, 17× gain (no gain for the experiments described on **section 5.2.6.4**) and a 4× objective. Images were analyzed using ImageJ software (National Institutes of Health, USA), and the fluorescence emission values were obtained by averaging the entire end-section of the micro-columns [269].

5.2.7. High-throughput screening with 96-well filter plate

PreDictor™ Capto MMC plates, kindly provided by GE Healthcare, were used to screen Fab fragments binding conditions to Capto MMC. The pH and salt conditions were the same described on **section 5.2.6.4**. The protocol followed was the one suggested by the suppliers, with the 1h incubation time under agitation. Pure Fab concentration was 150 μg/mL in a volume of 200 μL. After incubation, no elution procedure was executed, the unbound Fab was collected to measure its concentration. All the binding conditions were made in triplicate. Before and after the procedure Fab concentration was measured by UV at 280 nm.

5.2.8. Protein electrophoresis

The characterization every IgG digestion and the two step purification scheme was done by SDS-PAGE [201]. Samples from collected pools were diluted with 2× Laemmli Sample Buffer from Bio-Rad. Diluted samples were applied in a 12% acrylamide gel prepared from a 40% acrylamide/2% bis-acrylamide stock solution (29:1) (Bio-Rad), and ran at 90 mV using a running buffer at pH 8.3, containing 25 mM Tris-HCl, 0.192 M glycine and 0.1% SDS. To detect the protein bands, the gels were stained with BlueSafe purchased from NZYTech (Lisbon, Portugal). If necessary (low protein concentration) a silver protocol was applied as follows: (1) 2h fixation in 30% ethanol, 10% acetic acid; (2) 10 min wash with 30% ethanol; (3) 2×10 min wash with MilliQ water; (4) 1 min sensitization with 0.02% sodium thiosulfate; (5) 3×30 s wash with MilliQ water; (6) 30 min staining with 0.15% silver nitrate; (7) 1 min wash with MilliQ water; (8) development in 3% sodium carbonate, 0.05% formaldehyde; (9) 15 min wash with 5% acetic acid.

5.2.9. Isoelectric focusing

Isoelectric focusing (IEF) was performed to evaluate the isoelectric point of Fabs, Fc and whole antibody with and without conjugated label. The IEF was performed using a Pharmacia PhastSystem separation module (Amersham Biosciences) in a precast homogeneous polyacrylamide gel (PhastGel® IEF 3-9 with 50x46x0,45 mm) from GE Healthcare. The gel running program included a 75 Vh prefocusing step at 2000 V, sample application at 200 V for 15 Vh, and a focusing step at 2000 V for 410 Vh. Once run is over, the gel is silver stained. Both running and staining procedure was previously reported by Olsson *et al.* [270].

5.2.10. *E. coli* lysate and supernatant production

To do an HT screen of the binding conditions of a *E. coli* lysate to multimodal resins a recombinant green fluorescent protein (GFP) producing *E. coli* was used. Cells were cultured according to the supplier protocol (Biomedal, Spain) [271]. Initially, a pre-inoculum was cultured overnight and under constant agitation (250 rpm) at 37°C in LB medium supplemented with ampicillin (100 mg/L). This culture was then used to inoculate 50 mL of cell medium at an initial OD600 of 0.1. This second culture was completed under the same operational and buffer conditions. In order to increase the amount of impurities, cells were left in culture for three days. The culture was then centrifuged at 4000 g for 15 min at 4°C and the cells pelleted. The pellet was resuspended in 10 mL PBS and subjected to sonication for 10 min. Lysed cells were centrifuged for 15 min at 15000 g and the supernatant was collected. This *E. coli* strain was transformed to produce GFP, however, for the purpose of this work, there was no inducer step, being the production of GFP practically inactivated. This lysate was used in both microfluidics and ÄKTA experiments.

To study the behavior of multimodal resins with a cell culture fluid – unprocessed supernatant containing a high amount of impurities, an *E. coli* supernatant was produced as it described on the work by Silva-Santos *et al.* [272].

5.2.11. CHO supernatant production

To screen the binding conditions of a CHO supernatant to multimodal resins, cell culture extracts from FreeStyle™ CHO-S cell line obtained from Life Technologies (Carlsbald, CA, USA) were used. This cell line can grow in suspension in a defined serum-free medium. Cell expansion was performed using a FreeStyle™ CHO Expression Medium, supplemented with 8 mM $_{L}$-glutamine and 0.5% (v/v) antibiotics (50 U/mL penicillin and 50 µg/mL streptomycin) obtained from Thermo Scientific (Waltham, MA, USA). After 3 days of culture, cell supernatant was collected by centrifugation (12°C for 8 min at 1250 g). All this procedure was made by Marta Carvalho from SCERG-iBB.

5.2.12. Chromatographic runs

5.2.12.1 Microfluidics confirmation at bench-scale

Binding studies of pure Fabs to five selected multimodal resins (Capto MMC, MEP, PPA, ToyoPearl 650M TRP and CHT XT) were made at the bench-scale using an ÄKTA™ Purifier 10 system (GE Healthcare). In all the chromatographic runs, columns were equilibrated, before injection, with binding buffer (50 mM acetate/phosphate buffer pH 5/7). Upon equilibration, 200 µL of pure Fabs (1 mg/mL) was injected. The loaded column was washed with the binding buffer for 4 CV (1 CV = 1 mL) before an elution step. The elution step was made by salt gradient (5CV) or step. The salt elution buffer is the same as the binding buffer, with 1 M of NaCl. In point experiments a pH elution step was made with 0.1 M citric acid pH 3. In the end of the elution, a column strip was made with 0.5 or 1 M of sodium hydroxide (NaOH) or 0.5 M phosphate pH 7. In all chromatographic runs, the conductivity, pH, and UV absorbance at 280 nm were continuously monitored. The data was acquired and processed by the software Unicorn 5.1. The same type of experiments, using the same buffers, done with pure Fab fragments was done with *E. coli* supernatant, and Fab spiked in *E. coli* lysate, but only in three resins (PPA, ToyoPearl 650M TRP and CHT XT). For CHT XT these last set of chromatographic runs were done at pH 6.5 and 7. For PPA, two elution modes were done, using salt and pH gradient. The pH of every injection made was adjusted with 0.1 M citric acid, pH 3 or 2 M Tris-HCl, pH 9.

5.2.12.2. Two step multimodal downstream process

Four two-step downstream schemes based on three multimodal resins were design. In the first step of every scheme, columns were equilibrated, before injection, with binding buffer (50 mM acetate/phosphate buffer pH 5/7). Upon equilibration, 200 µL of pure Fabs (1 mg/mL) spiked into *E. coli* cell lysate was injected. The elution step varies with each column, it could be salt, or pH based, and gradient (5CV) or step. The salt elution buffer was the same as the binding buffer but with 1 M of NaCl, if it is a pH elution step the buffer is 100 mM citric acid pH 3. In the end of the elution, a column strip was made with 0.5 M of sodium hydroxide (NaOH) or 0.5 M phosphate (for CHT XT). All flow-through and elution fractions were collected. For the second step of the purification scheme, 2 mL of the flow-through or elution fraction was injected into the second multimodal resin. The binding and elution procedures are the same as the first purification step. In all chromatographic runs, the conductivity, pH, and UV absorbance at 280 nm were continuously monitored. The data was acquired and processed by the software Unicorn 5.1. The flow-through and elution fractions were collected on a Fraction Collector Frac-950 (GE Healthcare). The pH of every injection made was adjusted with 0.1 M citric acid, pH 3 or 2 M Tris-HCl, pH 9. Quantification of the Fabs present in each fraction is made accordingly to the procedure described in **section 3.2.6.2**. A characterization of the samples was made using an SDS-Page gel, stained with silver staining protocol.

5.3. Results and discussion

5.3.1. Initial microfluidic studies: multimodal vs cation-exchange experiments

There is a myriad of processing choices to purify Fab fragments, such as affinity techniques like protein A or protein L described previously, but none of them is a universal method, as they typically depend on the type of Fab fragment. In particular protein L, which is the gold standard for Fab fragments purification, has several limitations, namely harsh elution conditions, inability to bind to lambda light chains and to distinguish between Fab fragments and non-digested IgG. Alternative possibilities to

address these limitation include ion exchange chromatography and, more recently, multimodal chromatography [113].

Since a standard process for the purification of Fab fragments is yet to be established, there is a pressing need for developing efficient high-throughput screening tools that allow for a rapid study of different non-affinity chromatography resins under different operating conditions. To address these issues, a microfluidic-chromatographic column with 210 nL (**Figure 5.4a**) was fabricated in house using soft-lithography techniques, as a highly efficient high-throughput screening tool, for the optimization of binding conditions of a mixture of fluorescently labelled Fab fragments. Chromatographic beads are packed inside a microchannel (**Figure 5.4a**) and continuously monitored under a fluorescence microscope. In general terms, the operating procedure in these micro-columns can find a parallel to a conventional chromatography assay and includes the following sequence of steps: (i) packing of the beads; (ii) equilibration with the adsorption buffer to be tested; (iii) flow of the Fab-containing solution; and (iv) elution of the bound Fab fragments. By using this approach, it is possible to perform a rapid process optimization (within a few minutes) with results that can be further extrapolated to macro-scale, being thus possible to have a first overview about the performance of different resins for the binding of Fab fragments [263]. This type of experiment allows for a faster and simple screening of the best Fab fragment binding conditions in a way that can be extrapolated for a larger recombinant Fab purification platform. To validate microfluidics as a suitable tool to screen chromatographic conditions and choose between cation exchange or multimodal as a chromatographic mode to capture Fab fragments, an initial proof of concept study was completed.

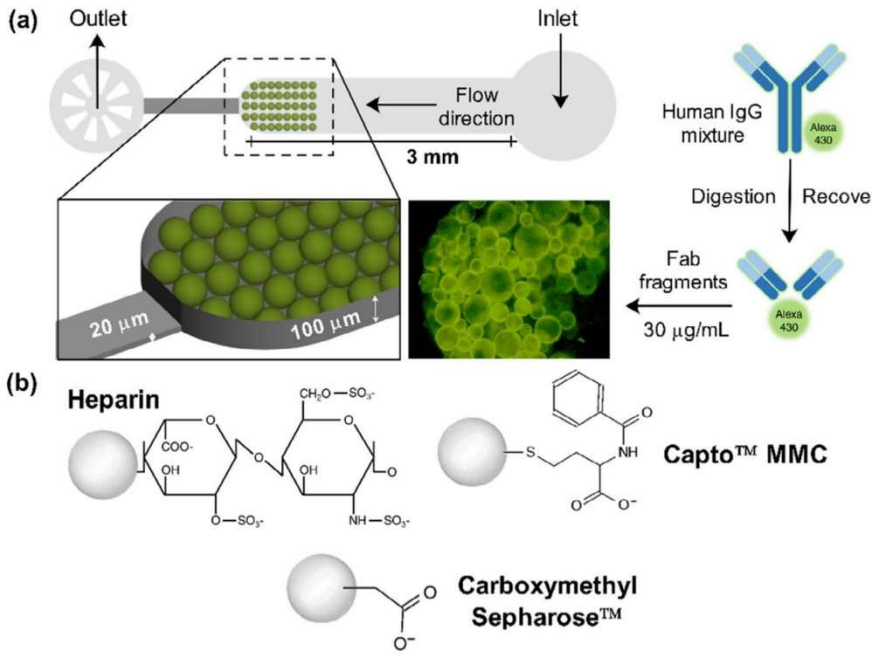

Figure 5.4 General schematics of the micro-columns used for the optimization of capture of Fab fragments by different chromatography resins. (**a**) Detail of the interface region of the two microfluidic channels at different heights for bead packing. (**b**) Molecular structure and name of the analysed ligands, commercially available as functionalized agarose or cellulose beads.

5.3.1.1. Binding to cation exchange resins

The CEX resins evaluated were carboxymethyl (CM) Sepharose and heparin Sepharose, which have been previously reported as a capture medium for the purification of monoclonal antibodies [263]. The screening conditions included buffers with pH values varying from 5 to 9 and conductivities ranging from the value measured with no NaCl addition (intrinsic conductivity of the buffering agent) up to 8 mS/cm. By analyzing the results presented in **Figure 5.5**, it was possible to evaluate the adsorption kinetics of the labelled Fab fragments from the increase in fluorescence over time, by calculating the slope from the moment the fluorescence starts to increase until it reaches a plateau.

Comparing both CEX resins, it is clear that heparin is able to bind Fab fragments more efficiently than CM, especially at lower pH values (pH = 5 and 6). This result is expected for two reasons: (i) heparin has a higher density of negative charges, and (ii) heparin beads are much smaller (30 μm compared to 90 μm average size of the CM beads), having a higher charge distribution [273] and promoting a stronger electrostatic interaction between the immobilized ligand and the Fab fragments. These assumptions are supported

by the information provided by the resin suppliers, according to which there is approximately 6 mg of carboxymethyl ligand per mL of resin against 10 mg of heparin ligand per mL of resin. Analyzing individually the CM resin, only in conditions where the pH is 5 and no salt is added to the buffer there is binding of Fab fragments. Since the fragments used have a pI of about 9, the surface of the Fab molecules is highly positive at pH 5, thus justifying the increased binding efficiency of CM measured at this pH value. A small increase in salt concentration at pH 5 (for example from ~ 0.6 to 2 mS/cm) precludes binding of Fabs to the resins, which extends also to other pH values, making this resin highly salt intolerant. Furthermore, when the pH is increased, CM is unable to bind the fragments, as a consequence of the low negative charge density of the ligand [274]. The global surface charge of the Fab fragments decreases when the pH increases. This decrease makes CM unable to bind the fragments. The profiles obtained at pH 8 and 9 (results not shown) were very similar to the ones obtained at pH 7. It is important to highlight that when the obtained slopes are close to zero, this means that the detection limit of the used equipment was reached, and the amount of Fab fragments adsorbed to the beads cannot be detected. An example of this are the adsorption curves measured at conductivities above 4 mS/cm, all resulting in fluorescence values that do not increase significantly above the background.

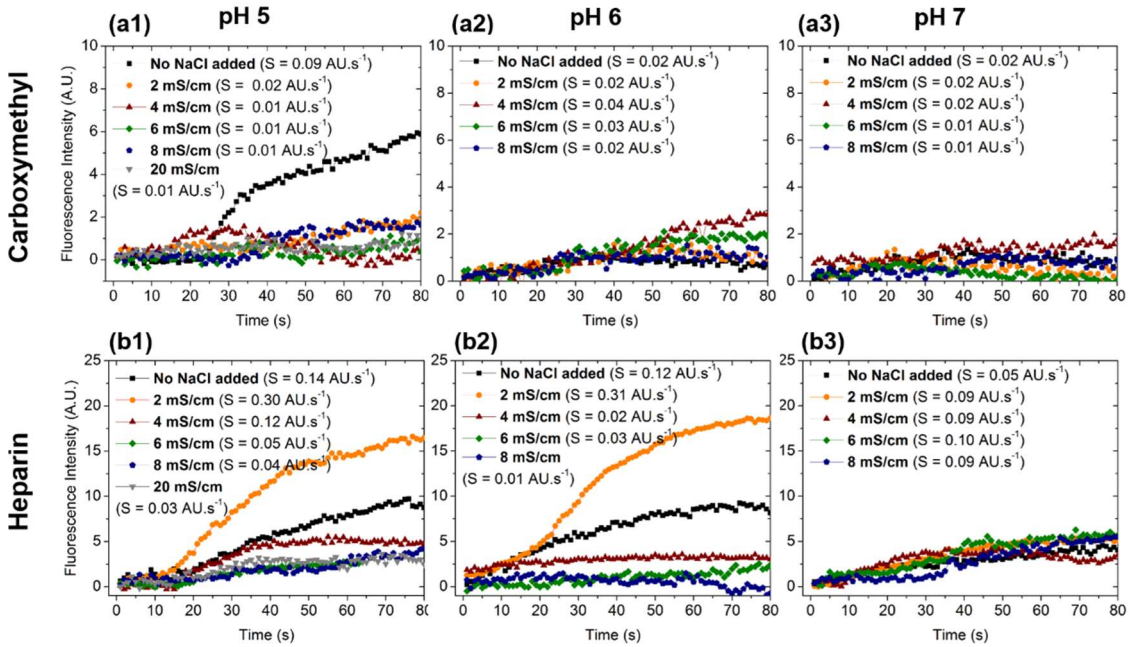

Figure 5.5 Fluorescence measured over time while a Fab fragment solution (30 µg/mL) was flowed continuously through the cation exchange resins under different pH values and conductivities. (**a1-a3**) Carboxymethyl resin at pH 5, pH 6 and pH 7, respectively. (**b1-b3**) Heparin resin at pH 5, pH 6 and pH 7, respectively. The slopes of the linear region of the different curves are indicated in brackets.

Differently from CM ligands, heparin resins are strong cation exchangers [275], with almost two times higher charge density, and the result here obtained proved that difference. At pH 5, below conductivity values of 4 mS/cm, there is a significant adsorption of Fab fragments to the beads. However, at 6 mS/cm and above, the adsorption slopes remain approximately unchanged up to 20 mS/cm, at which occurs a complete screening of the electrostatic interactions between the ligand and the Fab fragments. It is important to highlight that when no NaCl is added to the adsorption buffer at pH values of 5 and 6, the binding of Fab fragments is less pronounced than when the working buffers have a conductivity of 2 mS/cm. A hypothesis for this observation is that there is a need for a slightly higher conductivity to promote a more stable adsorption of Fab fragments to the heparin ligands. At pH 6, the adsorption profiles are very similar to the ones at pH 5, the major difference being the relatively lower binding capacity at a conductivity of 4 mS/cm, due to a lower density of negative charges of Fab fragments at pH 6 compared to pH 5. At pH values of 7 and above, there were no significant differences in adsorption behaviours between each conductivity value, all being very close to the noise threshold.

Considering that the binding mechanism of the analysed resins occurs mainly through ionic interactions, the results obtained herein were expected [275,276]. CM was shown to be less efficient than heparin in binding Fab fragments through the assessment of the fluorescence intensity. In addition, the working conditions of CM are more limited in terms of salt tolerance. Although low salt tolerance is an intrinsic characteristic of ion exchangers, heparin showed a relatively higher binding capacity at conductivity values up to 4 mS/cm, due to a higher charge density and ligand density in this resin.

5.3.1.2. Binding to a multimodal resin

The multimodal resin chosen to determine if the high-throughput studies herein developed will be based on CEX or multimodal chromatography was Capto MMC. The pH and conductivity conditions used for the evaluation of the multimodal resins are the same as those used in the study of the CEX resins and the obtained results are shown in **Figure 5.6**.

Capto MMC is a multimodal cation exchanger resin comprising a phenyl-, a sulphur- and a carboxyl- group as main moieties. This ligand displays three major types of interactions

- electrostatic, thiophilic and hydrophobic. The results obtained here are in accordance with previous reports showing that as the pH increases and approaches the pI of the target molecule, the binding capacity of the Capto MMC ligand decreases [277]. The effect of the conductivity on binding capacity suggest that this multimodal ligand is significantly more salt tolerant than a pure CEX ligand, particularly at pH 5 where significant binding, compared to that of heparin ligand, is obtained up to 20 mS/cm. At pH 7 and 9, the salt tolerance property of Capto MMC can still be observed, although the overall magnitude of the binding reduces as the pH value increases until almost no adsorption is observed at pH 9 and 8 mS/cm. The results obtained with Capto MMC corroborate other studies with monoclonal antibodies, in which the optimal binding was obtained at pH values 3.5 units below the isoelectric point of the target mAbs [247]. Regarding the higher salt tolerance, it may be justified by the presence of phenyl groups that promote hydrophobic interactions with the Fab fragments when higher conductivities are used, resulting in a higher adsorption than if only electrostatic interactions were present [277]. However, in the presence of reduced electrostatic interactions (pH = 9) and if the amount of salt is sufficiently high (8 mS/cm) Capto MMC starts losing its salt tolerance [263], since the hydrophobic interactions alone are not sufficient to maintain an effective binding.

The use of a microfluidic-based approach proved to be a fast and convenient method for a first screening of the best conditions to bind Fabs envisioning the purification of recombinant fragments. The results obtained showed that multimodal resins are a superior choice than pure cation exchange resins, since they are more salt tolerant and provide a more effective binding of the Fabs.

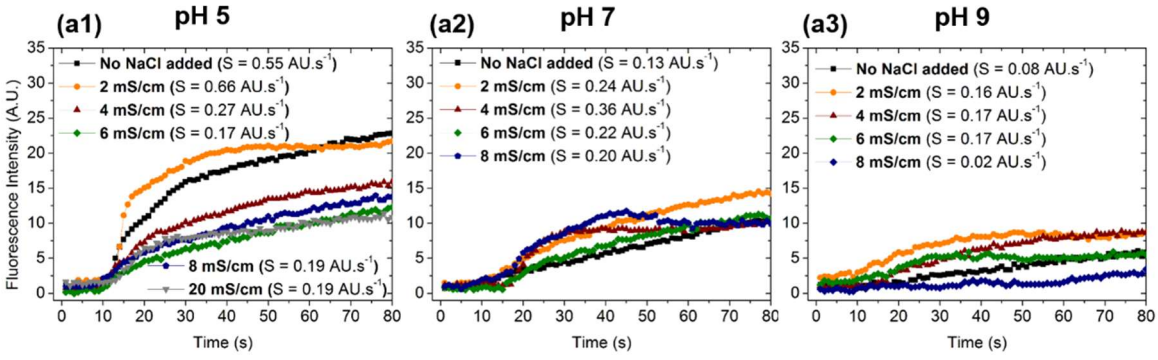

Figure 5.6 Fluorescence measured over time while a Fab fragment solution (30 µg/mL) was flowed continuously through Capto MMC resin under different pH values (**a1-a3** - pH 5, pH 7 and pH 9, respectively) and conductivities. The slopes of the linear region of the different curves are indicated in brackets.

5.3.2 Effect of the dye

The Alexa Fluor 430 dye used on the first set of experiments has an inherent negative charge promoting a decrease of the pI of the target protein. Additionally, and because this dye targets primary amines present on lysine residues, Alexa 430 will also neutralize the positive charge of these amino acids. The combination of these two factors will promote a significant decrease on pI making Fab biomolecules more negative than naturally are [268].

To avoid a decrease of Fab positive charges, other amine reactive dye was used, BODIPY (BDP). In comparison with Alexa 430, BDP has the advantage of being a neutral molecule, promoting no charge difference upon conjugated with the target molecule. The putative effect will be only present by the conjugation with lysine, that may interfere with the global charge of the molecule. To evaluate the possible pI change, an isoelectric focusing of the Fabs and Fc present after the digestions of the IgG present in Gammanorm was made (**Figure 5.7**). The results demonstrate that Fabs (both kappa and lambda) and Fc suffer no significant pI change when conjugated to BDP molecule. These results are corroborated by the work of *Pedro et al.* [268], where Alexa 430 and BDP were used to label the same IgG mixture. Despite the different BDP conjugation (NHS vs maleimide) the labelled IgG had negligible charge modification, in contrast to the Alexa 430 conjugation that promoted a significant reduction of the pI.

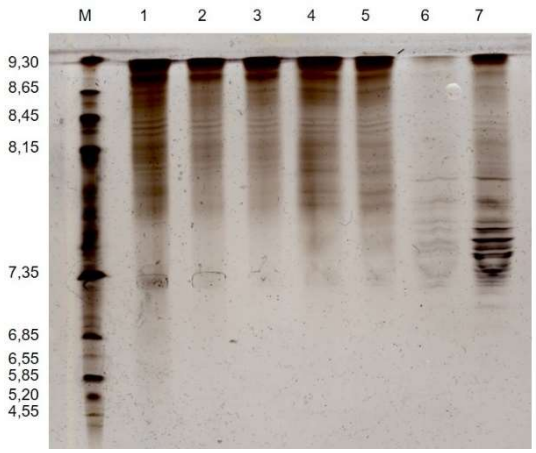

Figure 5.7 Isoelectric focusing gel for labeled and non-labelled Fab and Fc fragments. **M** - Marker; **1** - Labelled kappa Fabs (BDP FL NHS); **2** - Non-labelled kappa Fabs; **3** - Labelled kappa Fabs (BDP TMR NHS); **4** - Non-labelled lambda Fabs; **5** - Labelled lambda Fabs (BDP TMR NHS) ; **6** - Non-labelled Fc fragments; **7** - Labelled Fc fragments (BDP TMR NHS).

In further experiments, all the biological samples will be labelled with BDP using NHS click chemistry. To avoid charge variations the degree of labelling will be kept low, specially for the single proteins tested. Another change in the protocol is the increase of concentration of the target studied. This had the propose of increasing the fluorescence and have a more intense signal, the standard concentration will be 60 µg/mL, two times higher than the one used in the previous section (**section 5.3.1**).

5.3.3. High-throughput screen of multimodal resins binding conditions: a microfluidic approach

With the promising preliminary results, where the use of multimodal chromatography to bind Fab fragments outperformed cation-exchange chromatography a thorough HT screen was delineated to study the binding of Fab fragments to different multimodal resins. Eleven multimodal resins (**Table 5.1**) were then selected and tested for the binding of Fab fragments, other proteins (IgG, Fc and BSA) and two types of complex mixtures (*E. coli* lysate and CHO supernatant). For each study (ligand and sample), three pH values (5, 7 and 9) and five different NaCl concentrations were tested (0, 50, 100, 150 and 200 mM), in a total of fifteen conditions per resin. The results obtained with multimodal ligands were compared with protein L, the traditional choice to the majority purify Fab fragments.

Table 5.1 List of the multimodal resins used in this work with selected features summarized.

Trade Name	Referred	pKa	Particle Size (μM)	Ligand density	Description
Nuvia cPrime	Nuvia cPrime	4.46 [278]	70 ± 10	110 - 150 μmol/mL	Hydrophobic cation exchange
TOYOPEARL MX-Trp-650M	Toyo	N/A	50 - 100	120 μmol/mL	Hydrophobic cation exchange
Capto MMC	Capto MMC	4.6 [278]	36 - 44	70 - 90 μmol/mL	Hydrophobic cation exchange
Eshmuno® HCX	Eshmuno	N/A	75 - 95	170 - 300 μmol/ml	Hydrophobic cation exchange
Nuvia aPrime 4A Media	Nuvia aPrime	N/A	50 ± 10	100 ± 20 μmol/mL	Hydrophobic anion exchange
Capto™ adhere	Capto Adhere	N/A	36 - 44	90 - 120 μmol/mL	Hydrophobic anion exchange
MEP HyperCel	MEP	4.85	80 - 100	80-125 μmol/mL	Hydrophobic anion exchange
HEA HyperCel	HEA	10	80 - 100	>50 μmol/mL	Hydrophobic anion exchange
PPA HyperCel	PPA	6.00 - 7.00	80 - 100	>50 μmol/mL	Hydrophobic anion exchange
CHT Ceramic Hydroxyapatite Type I	CHT Type I	N/A	40	N/A	Anion and cation exchange
CHT Ceramic Hydroxyapatite XT	CHT XT	N/A	40	N/A	Anion and cation exchange

In previous section (**section 5.3.1**), the binding estimation was made by calculating the slope from the moment the fluorescence starts to increase until it reaches a plateau. For this set of experiments, a new quantification method was applied, the binding of fluorescently labelled samples to the resins is evaluated by the fluorescence value at the plateau, as this parameter is related with the binding capacity of the ligand. Upon injection of the labelled samples, the fluorescence increases over time, as a result of the binding to the beads. After a certain period, the fluorescence reaches a stable state – a maximum of fluorescence. This maximum is the parameter chosen to compare different chromatographic experiments. Different binding conditions will have different maximum values. An example of adsorption kinetics curves is present on **Figure 5.8**, where the binding of Fab fragments to TOYOPEARL MX-Trp-650M at pH 5, with different salt concentrations, is plotted. Analyzing the fluorescence level over time, it is clear the effect of salt. Lower salt concentrations promote higher fluorescence values, and vice versa, meaning that TOYOPEARL MX-Trp-650M binds more Fabs when the salt concentration is lower. The fluorescence difference will generate different maximum values (different plateau), and an adequate comparison can be made. The maximum values (Fmax) presented in the figure are calculate by fitting he fluorescence data overtime with the Hill function (**Equation 5.1**). The fluorescence curves on **Figure 5.8** increases in a sigmoidal manner, making possible to apply the Hill equation, and obtain the value where each curve reaches a fluorescence saturation. The Hill equation is generally applied to study kinetics reactions and was initially applied to describe the binding of oxygen to hemoglobulin [219,279,280]. In this chapter all the fluorescent binding curves will be fitted with a Hill function and the Fmax values will be used to compare different chromatographic runs. The plotting of the Fmax values will be made in the form of heatmaps.

$$F = \frac{F_{max} \times t^{n}}{(t_{0.5})^{n} + t^{n}}$$

Equation 5.1 Adapted Hill equation. *F* represents fluorescence of the beads, F_{max} is the maximum rate of reaction, *t* is the time, $t_{0.5}$ is the time that originates half of the F_{max} and n is the dimensionless Hill coefficient.

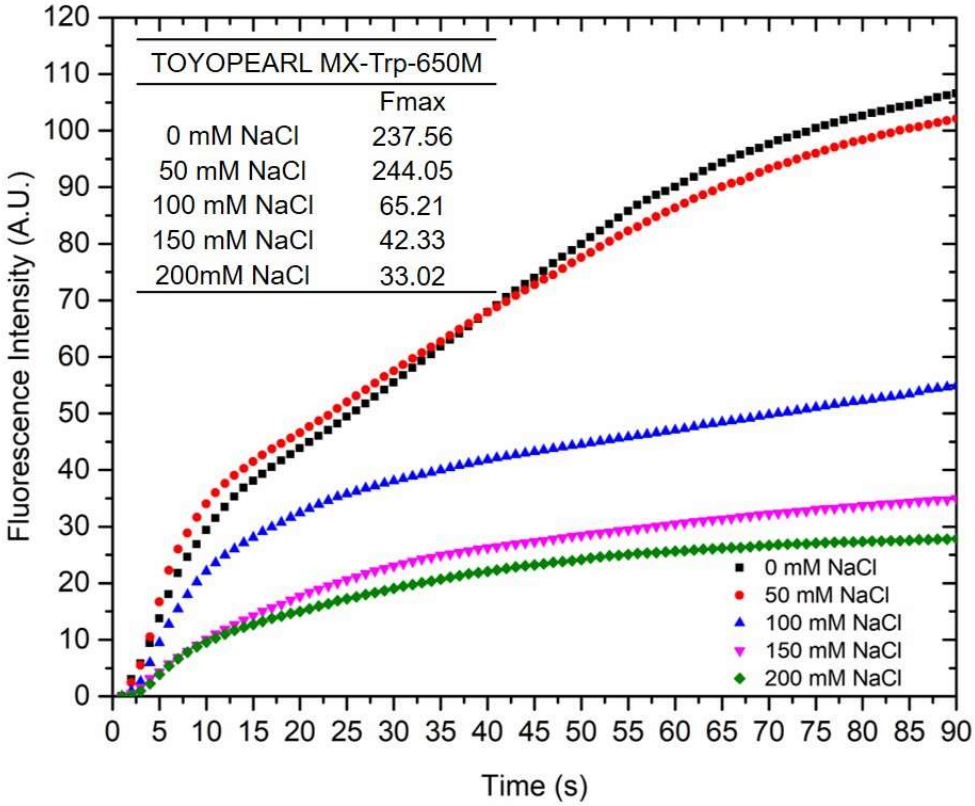

Figure 5.8 Example of the binding results obtained with the multimodal resins. Each fluorescent curve was fitted using the Hill equation and a Fmax value is determined.

5.3.3.1. Binding studies with Nuvia cPrime

Nuvia cPrime is a multimodal ligand with several groups capable making different type of binding interactions. The presence of a benzene ring will promote hydrophobic interactions, the amide and amine groups hydrogen-bonding and finally electrostatic interactions can be created by the carboxylate group. This ligand has already been applied in polishing applications [281]. Despite the relative novelty of this resins, its characterization is considerable, the effect of each ligand moiety was vastly studied, since Nuvia cPrime was used to design multimodal ligand candidates.

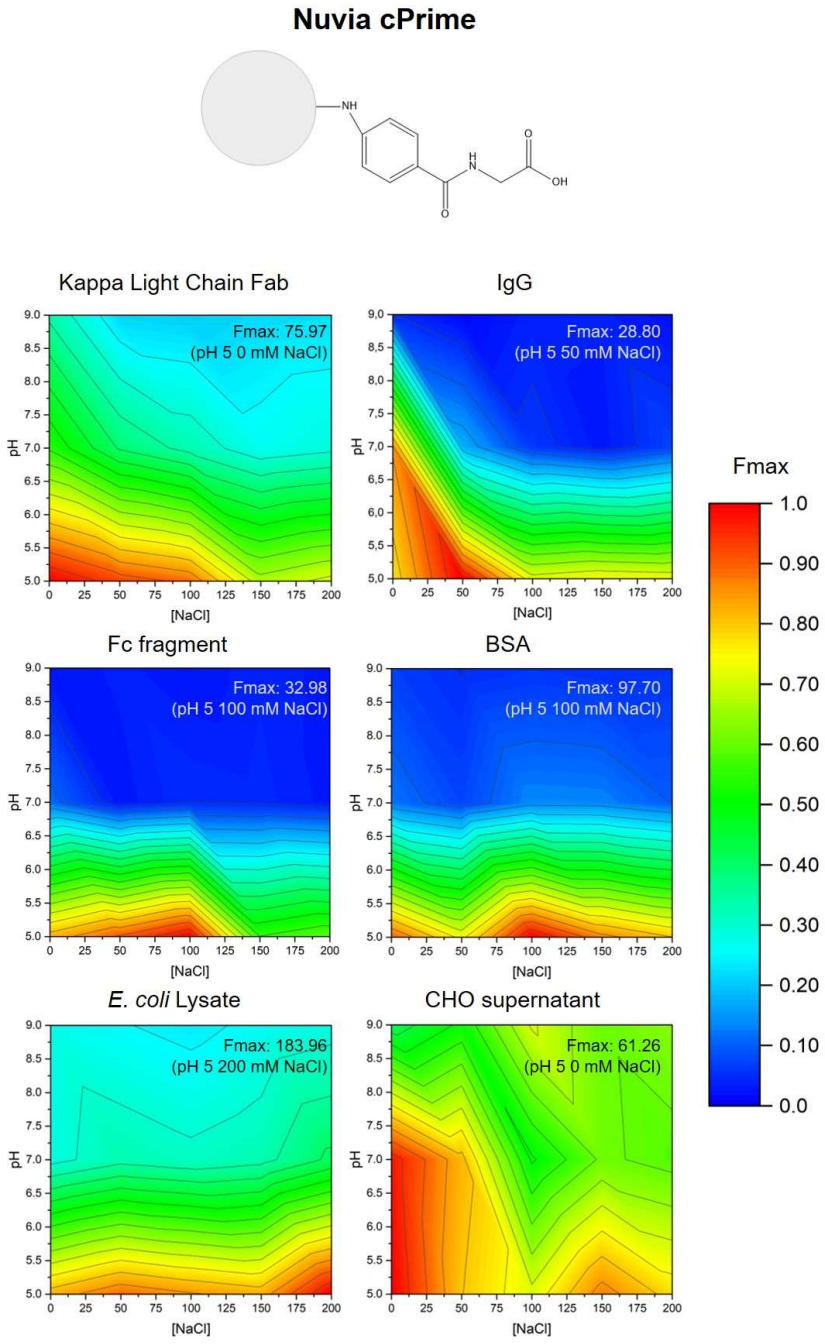

Figure 5.9 Heatmaps obtained for the binding of different labelled biomolecules (Fab and Fc fragments, IgG and BSA) and complex media (*E. coli* lysate and CHO supernatant) to Nuvia cPrime at different binding conditions. In all the heatmaps the highest Fmax and the conditions where it was obtained is indicated. All the Fmax values of the heatmaps were normalized using the highest value for each study.

The results obtained with Nuvia cPrime ligand are represented on **Figure 5.9**. Starting with Fab fragments, the binding is favored at pH 5 with low/moderate amount of salt. With a global pI between 7.5 and 9 (**Figure 5.7**), the polyclonal mixture of Fabs herein used is positively charged at pH 5, and so the binding to Nuvia cPrime is majorly driven by electrostatic interactions. When salt concentration increases, the binding starts to decrease, specially at higher pHs (7 and 9), where the global charge of Fabs is less positive. At higher salt concentrations, the hydrophobic interactions of this resin are strengthen [282] and Fabs bind to Nuvia cPrime by a combination of electrostatic and hydrophobic interactions. An increase of the binding pH generates a decrease of Nuvia cPrime ability to bind Fab fragments. At pH 7, these molecules start to be less positive and binding to the multimodal ligand is not as effective. The increase of salt, to pH 7, has the same effect seen previously at pH 5, however the electrostatic interactions are not as strong, and the binding of Fabs is lower. At pH 9, some Fabs have no charge while others are already negatively charged, and consequently the binding to this weak cation hydrophobic exchanger decreases. Nevertheless, as the majority of the Fab fragments used have relatively high pI (**Figure 5.7**), the binding at pH 9 is still considerable. The increase of salt concentration at pH 9 promotes a decrease the resin binding capacity as observed at the other two pHs.

Fab fragments are the target biomolecule of this study, however the application of multimodal chromatography requires an extensive optimization study. Consequently, to increase the knowledge of each resins, the binding to other biomolecules to multimodal ligands was evaluated. Having structural and chemical characteristics different from Fabs, IgG, Fc fragments and BSA were chosen as model proteins. Moreover, if Fab are produced by enzymatic digestion, IgG and Fc fragments can be considered impurities need to be removed after the enzymatic cleavage of antibodies. The binding profile of the three-model protein resembles the one obtained for Fab fragments: an increase of pH promotes a decrease of the binding capacity, and higher binding is achieved at lower salt concentrations. Making an analysis based on the pI of the three proteins, the polyclonal mixture of IgG is the one that has an higher pI (between 6 and 9), and so it shows higher pH tolerance when compared to Fc fragment (pI ~ 7 and 7.5) and BSA (pI ~ 5). These results corroborate what was previously discussed, Nuvia cPrime behaves mostly as ion-exchange ligand, at low salt concentrations. The increase of the salt concentration has lower effect on the binding at pH 5, for the three biomolecules, probably due to an

increase of the hydrophobic interactions. At pH 7 and above, BSA and Fc lose their binding affinity towards Nuvia cPrime, while IgG, more charged than the previous two, retains some binding. At pH 9, a negligible binding of IgG occurs, possible as a result of the presence of some positively charged patches in the biomolecule. It is interesting to note the lack salt tolerance, observed with IgG, for Nuvia cPrime at pHs higher than 7 and NaCl concentrations below 50 mM. At these conditions, the interaction is mainly driven by electrostatic interaction.

The heatmaps depicted in **Figure 5.9** indicate the highest Fmax obtained for each biomolecule/mixture used. However, these values can only be compared within the same labelled molecules. For example, with Nuvia cPrime, the highest Fmax obtained for Fab is 75.97 and for IgG is 28.80, these does not mean a higher binding of Fabs to Nuvia cPrime. The different molecules have different degrees of labelling (number of dye molecules coupled to a protein), and so the comparison of different samples for the same resin, even at the same condition, cannot be made. The values obtained act as a guideline, e.g., in this case, Fab fragments bind strongly to Nuvia cPrime at pH 5 with 0 mM NaCl while IgG bind strongly at pH 5 with 50 mM NaCl. Nevertheless, whenever the biological sample is the same, the comparison between different resins is possible.

The production of Fab fragments can be made using different cell hosts, with *E. coli* and mammalian cells being among the most popular. The implementation of quality by design (QBD) concepts requires an increasing process understanding and control. Robust analytical and HT purification techniques promote an intensive characterization not only of the target molecule but also the impurities present after the production process [283,284]. Having this concept in consideration, an HT screen of the binding conditions of an *E. coli* lysate and a CHO supernatant was made. Before discussing the results obtained with these two complex mixtures, it is relevant to clarify that the labelling of both lysate and supernatant was made without any type of sample processing. All the molecules present in the mixture that can be subjected to NHS click chemistry were labelled, including proteins, phospholipids, metabolites, among others. Additionally, having almost no information about the molecules present in the complex mixtures and to guarantee a proper labelling procedure, the labelling designed by Pedro *et al.* [268] was applied to ensure a high degree of labelling. These are the reasons for the high values of Fmax obtained with these two types of supernatants.

The results obtained for both lysate and supernatant follow the trend of the previous biomolecules, an increase of pH promotes a decrease of the binding capacity. For the *E. coli* lysate, Nuvia cPrime is salt tolerant at the three tested pHs, having no significant binding differences when the salt concentration increases. Regarding the CHO supernatant, the binding at both pH 5 and 7 is very similar, with a decrease in Fmax as the salt concentration increases. At pH 5, 150 mM of NaCl increases the binding, probably due to the presence of some impurities with propensity to bind the phenyl ring of the ligand at these conditions.

Making an overall evaluation of Nuvia cPrime, it is possible to verify a higher binding capacity at lowers pHs and a relative tolerance to salt until concentrations of NaCl close to 100 mM. As the pH increases, Nuvia cPrime loses binding ability, especially for lower pI proteins (BSA and Fc). For higher salt concentrations (> 100 mM of NaCl), there is also a decrease of the binding capacity, however, it is more salt tolerant than a traditional cation exchanger. At higher pHs, the ligand does not exhibit the same salt tolerance, proving that there must be a higher level of cooperation between electrostatic and hydrophobic interaction. Finally, the lack of clear differences on the heatmaps herein obtained can compromise the use of Nuvia cPrime as a downstream solution for Fabs.

5.3.3.2. Binding studies with Capto MMC

The binding experiments of Fab fragments to Capto MMC although already presented in **section 5.3.1.2** were repeated as the fluorophore was changed. The results obtained are present on **Figure 5.10**. Considering the heatmap for Fab fragments, there is a very good agreement with the previous analysis: at lower pHs Capto MMC has a higher binding capacity and is salt tolerant; upon increasing of the pH, the ligand starts losing its binding capacity and salt-tolerance.

The binding results of IgG, Fc and BSA to Capto MMC resembles the ones already discussed for Fabs fragments: higher binding and salt tolerance at lower pHs; increasing the pH causes a decreasing of the binding capacity and salt tolerance. It is interesting to observe that the binding of these three biomolecules is favored with the presence of salt (>50 mM NaCl), specially IgG and BSA. The pH and salt effect with the complex mixtures assays are also in agreement to what was observed for the other biomolecules.

The significant difference between them is the ability of Capto MMC to bind *E. coli* lysate impurities at a broader range of conditions, when compared to CHO supernatant. A higher salt concentration promotes a higher and pH-independent binding of *E. coli* lysate impurities, while for CHO supernatant, Capto MMC binds better at lower pH with either no NaCl added or at a salt concentration higher than 100 mM NaCl.

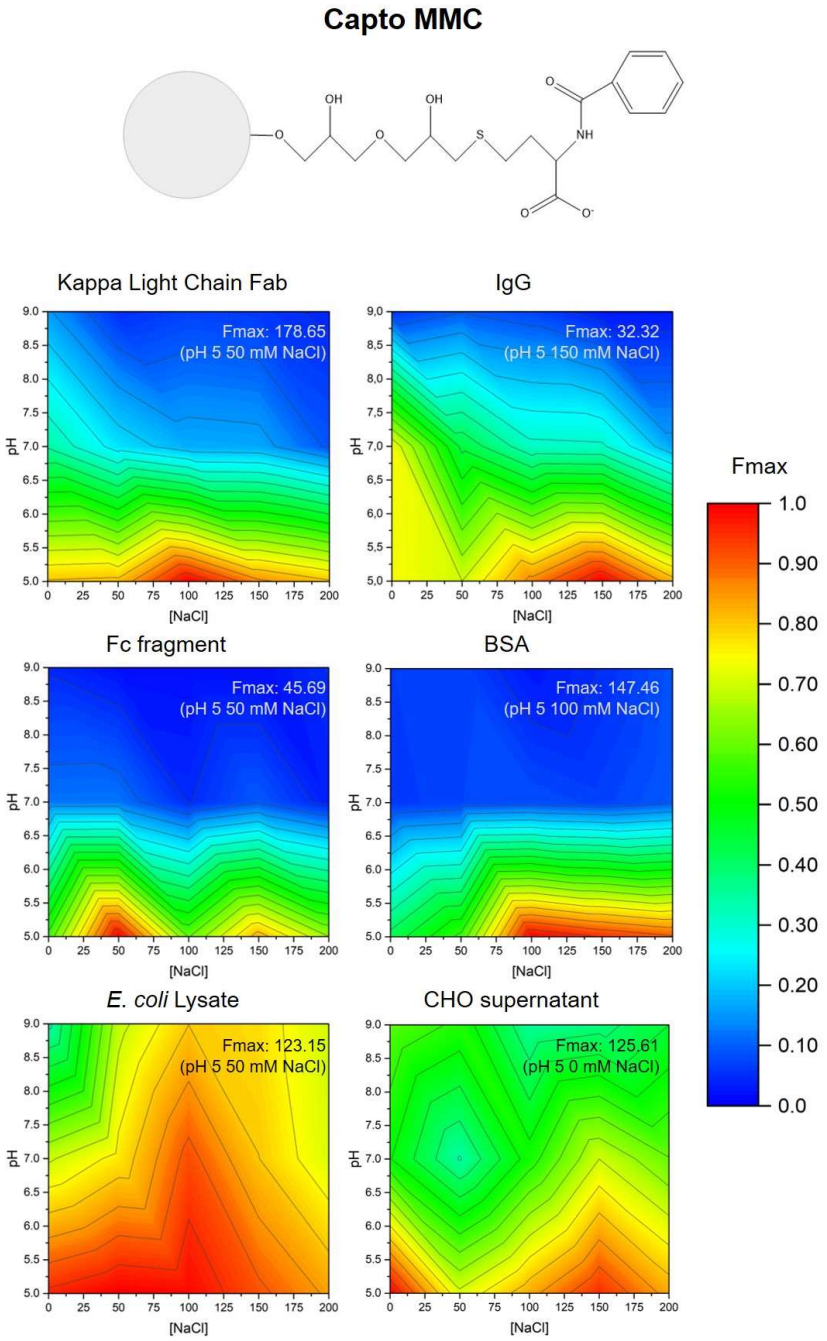

Figure 5.10 Heatmaps obtained for the binding of different labelled biomolecules (Fab and Fc fragments, IgG and BSA) and complex media (*E. coli* lysate and CHO supernatant) to Capto MMC at different binding conditions. In all the heatmaps the highest Fmax and the conditions where it was obtained is indicated. All the Fmax values of the heatmaps were normalized using the highest value for each study.

Capto MMC and Nuvia cPrime share very similar chemical moieties, a phenyl group, a peptide bond and a carboxyl group, in structurally different ligands, with Capto MMC containing an extra thioether group and thus able to participate in thiophilic interactions. The different arrangement of these moieties induces distinct presentation of hydrophobic and charged groups to the different biomolecules. The resemblance between both ligands was already examined and the influence of each ligand in binding and elution of proteins studied [282]. The results obtained herein confirmed what was previously reported. The presence of an extra aliphatic linker on Capto MMC increases the hydrophobic interactions, and thus the binding to proteins is stronger. Higher Fmax values (higher fluorescence and so stronger binding) were observed for all the single molecules tested - Fabs, IgG, BSA and Fc on Capto MMC than on Nuvia cPrime. Another factor contributing for a stronger interaction of Capto MMC is their significant structural flexibility in comparison to the planar structure of Nuvia cPrime [285]. The presence of negatively charged and hydrophobic groups interacting with positively charged and hydrophobic protein residues is similar in both resins, however, their different presentation, together with a higher degree of flexibility and extra thioether group in Capto MMC makes this resin a stronger binder than Nuvia cPrime. Stronger interaction is often related with difficult elution, reasons why Capto MMC is considered a sticky resin [156]. Despite promoting weaker interactions, Nuvia cPrime could be an alternative for Capto MMC once it can offer milder elution conditions.

5.3.3.3. Binding studies with Toyopearl MX-Trp-650M

TOYOPEARL MX-Trp-650M (referred in this work as Toyo) is a weak cation hydrophobic exchanger with a particularity of having a tryptophan residue on the ligand. The hydrophobic moiety of the amino acid is paired with a carboxylic acid, functioning as a weak cation exchange entity. The presence of a tryptophan, on the ligand structure, offers a unique hydrophobicity varying accordingly to the type of salt used [286]. Additionally, the interaction of amino acids with other molecules is dependent on their structure, and due to the presence of tryptophan, Toyo will have different affinities for structurally different molecules. These two factors make the understanding of the ideal binding conditions a fundamental study prior the implementation of a Toyo-based purification operation.

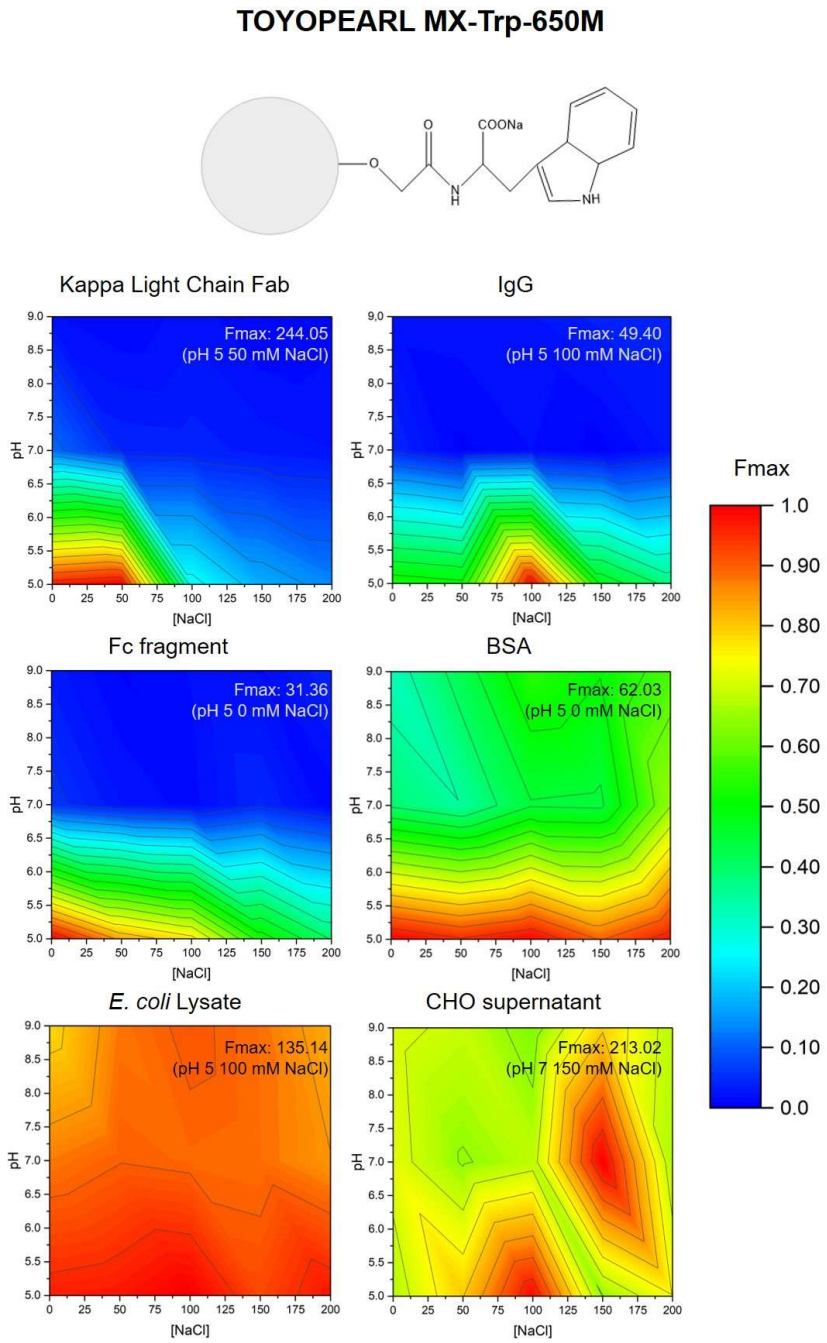

Figure 5.11 Heatmaps obtained for the binding of different labelled biomolecules (Fab and Fc fragments, IgG and BSA) and complex media (*E. coli* lysate and CHO supernatant) to Toyo at different binding conditions. In all the heatmaps the highest Fmax and the conditions where it was obtained is indicated. All the Fmax values of the heatmaps were normalized using the highest value for each study.

The results obtained with Toyo (**Figure 5.11**) show a similar binding profile as the two weak cation hydrophobic exchangers studied previously, but with lower salt tolerance. At pH 5 and low NaCl concentrations, the binding is stronger, especially for Fabs and Fc. The increase of salt and pH promotes a decrease in the binding to the ligand, except for

IgG which binds strongly at around 100 mM NaCl, pH 5. The binding profile observed for BSA is also similar to Nuvia cPrime and Capto MMC, however, at neutral and alkaline pHs (7 and 9) there is not an accentuated decrease of binding as previously observed. This difference between BSA and the antibody molecules (Fab, Fc and IgG) could be related to the hydrophobic interactions between tryptophan and this protein [286]. The structure of Toyo seems to have more affinity towards BSA, specially at neutral and alkaline pHs, which could be related with the availability of hydrophobic patches on the protein to interact with the amino acid on the ligand, at higher pHs and salt concentrations. Different affinities towards different biomolecules are thus created by the presence of the tryptophan. For antibody molecules (Fab, IgG and Fc) the interactions are majorly electrostatic and the presence of the tryptophan ligand may blocking the electrostatic interaction with the Toyo carboxylic group as the charge density of the antibody molecules decrease with the increase of the pH and proximity with their pI. For BSA, the ligand has a multimodal performance, depending on the chromatographic conditions.

Regarding the complex mixtures, all the fifteen conditions tested for *E. coli* lysate and CHO supernatant show high binding to Toyo. The only difference is the presence of two regions where the binding is higher for the CHO supernatant. This result was not expected, it was already herein observed that Toyo loses its binding ability at higher pHs and higher salt concentrations, however the data show the opposite: a relative high pH and salt tolerance in the binding of *E. coli* lysate and CHO supernatant. An explanation could be the high complexity and degree of labelling of the mixtures, promoting a strong and condition-independent hydrophobic interaction with the tryptophan on the ligand. Nevertheless, and having in consideration the data obtained here and in other works (e.g. Toyo was used to separate mAb monomers and dimers), this resin shows significant different binding behaviors which are welcome in a Fab downstream process [286].

5.3.3.4. Binding studies with Eshmuno HCX

Eshmuno HCX is a multimodal tentacular resin with the ability of creating hydrophobic, strong and weak electrostatic interactions and hydrogen bonding. The presence of tentacles on the bead promotes a more flexible binding allowing an easier access of the protein to the ligands. From all the ligands tested in this study, Eshumuno is the more complex, containing several aromatic rings, carboxylic groups and sulphate groups. The

features of this resin (high ligand density, the presence of several interacting groups and tentacular shape) makes the comparison to other resins a stimulating study to understand possible binding interactions on multimodal resins.

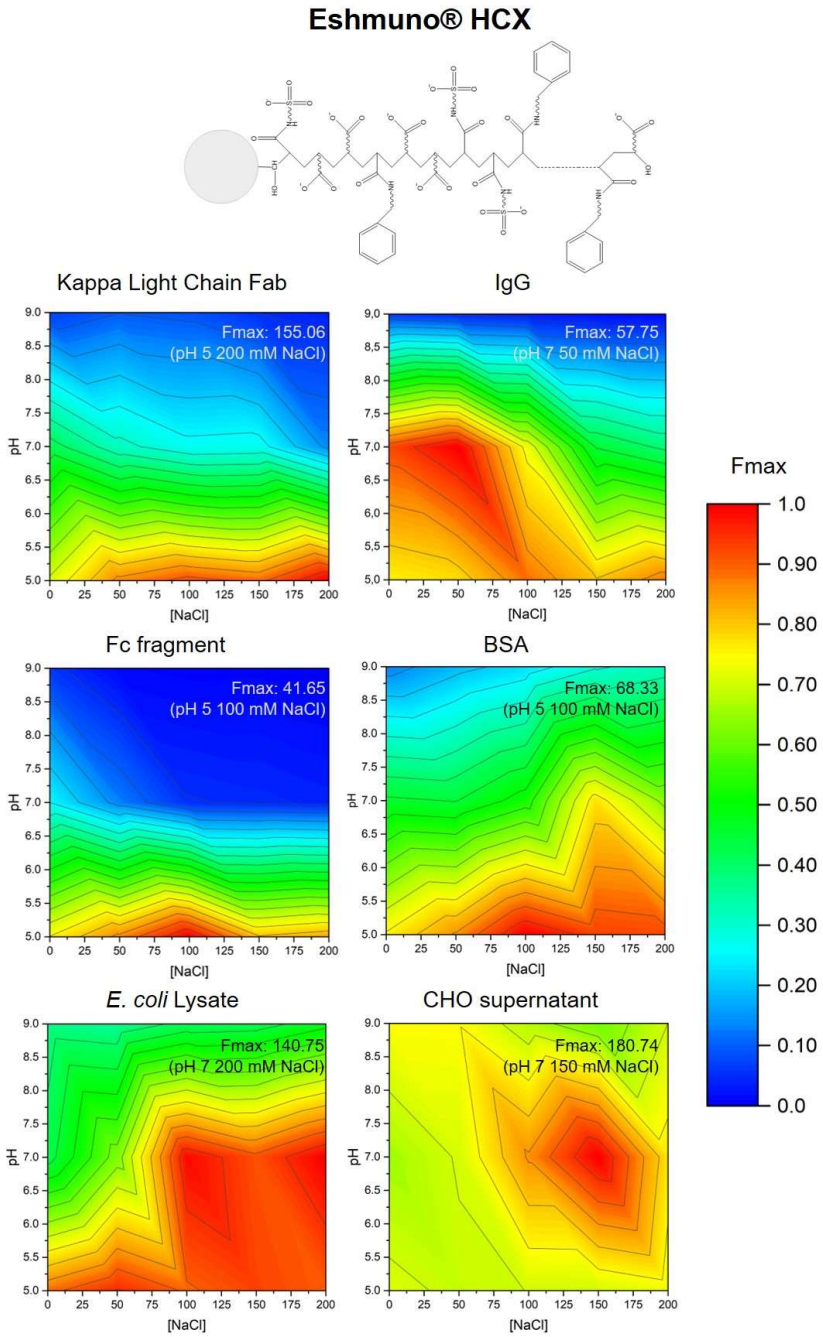

Figure 5.12 Heatmaps obtained for the binding of different labelled biomolecules (Fab and Fc fragments, IgG and BSA) and complex media (*E. coli* lysate and CHO supernatant) to Eshmuno at different binding conditions. In all the heatmaps the highest Fmax and the conditions where it was obtained is indicated. All the Fmax values of the heatmaps were normalized using the highest value for each study.

The results obtained with Eshmuno are represented on **Figure 5.12**. Despite their structural differences, the binding behavior of this ligand does not differ from the other three hydrophobic cation exchangers. With the increase of the pH, a decrease of the binding is observed for the four single proteins tested (Fab, Fc, IgG and BSA). However, the salt tolerance appears to be higher in this resin, specially at pH 5, where the increasing of the salt promotes a stronger interaction. The presence of several phenyl rings in a more charge dense environment may be responsible for this salt tolerance. At higher pHs, as the proteins become neutral and negatively charged, the interaction loses its strength and the binding is weaker. Having in consideration the tentacular shape of the resin, the results obtained with IgG are worth of a deeper analysis. At pH 7, in contrast to Fab and Fc, the binding is not affected, even with higher salt concentration (until 100 mM NaCl). Additionally, the highest Fmax value, obtained in all IgG experiments with cation exchangers multimodal resins, was achieve at pH 7 and 50 mM NaCl using Eshmuno (Fmax – 57.75). A possible explanation for this selectivity towards IgG is a consequence of two factors: the tentacular shape of the resin and the fact that IgG is the largest protein tested (150 kDa). The combination of these two may create the necessary conditions for an easier access to the hydrophobic regions of IgG allowing for a more specific binding to this protein. Regarding the complex mixture results, the increase of pH promotes a slight decrease of the binding of *E. coli* lysate, while the increase of salt, until pH 7 favors it. The binding to CHO supernatant resembles the one on Toyo, where a high binding region is present on a relative uniform binding profile.

The novelty of this resin makes the comparison with other works a difficult task. It is possible to validate the results herein observed once they do not vary significantly from data obtained with other hydrophobic cation exchanger resins. A deeper analysis is needed to complete comprehend its binding mechanisms, and the effect of the tentacular structure on multimodal interactions.

5.3.3.5. Binding studies with CHT ceramic hydroxyapatite resins

The natural adsorbent hydroxyapatite ($Ca_{10}(PO_4)(OH)_2$) was first described as a chromatographic solution in 1956 by Tiselius *et al*. [287], and despite the lack of novelty, hydroxyapatite technology has been evolving and applied in the purification of mAbs, bacteriophages and viruses [288]. The multimodal resin ceramic hydroxyapatite (CHT)

is based on a complex crystalline structure capable of adsorbing different protein, especially mAbs [289]. The mixed-mode characteristic of the resin is conferred by two groups: positively charge calcium residues (metal affinity) and negatively charged phosphate ions (cation exchange) [249,290]. In this study two types of CHT resins were tested, both commercialized by Bio-Rad: CHT XT and CHT Type I. The difference between the two is related with the production process, for CHT XT an extra jet milling process is executed to create more robust and size uniform beads (crystals).

The results obtained with these resins, presented on **Figure 5.13** and **5.14**, are very similar, with point differences probably caused by the difference in their structure – CHT XT has a more uniform bead distribution. Despite the supplier recommendation of using pH above 6.5, and considering the risk of bead disintegration, the binding at pH 5 was tested. At this pH is where both CHT resins binds strongly to all tested single proteins. When there is an increase of the pH, the binding decreases. However, Fabs that have a higher pI than the other proteins, show a higher resistance to the increase of pH. CHT resins seem to be salt tolerant at all tested pHs, with an increase of salt not significantly affecting the binding, as the pH does. The presence of positive and negative ions is responsible for the maintenance of a high binding capacity at salt concentration up to 200 mM NaCl. Finally, the lack of affinity toward the complex mixtures is a noteworthy result. The Fmax values obtained for the complex mixtures, for all multimodal resins tested, are high, however for CHT resins these values are the lowest. A negligible binding is achieved, being most of the values attributed to background fluorescent levels obtained upon the flow of the fluorescently labelled complex mixture.

The lack of affinity towards media impurities make this traditional chromatographic resin an option in a purification process. The small size of the CHT beads, the high binding capacity for Fab fragments and general high salt tolerance are ideal features for a Fab purification scheme, especially as a polishing step, as it was already vastly characterized [291].

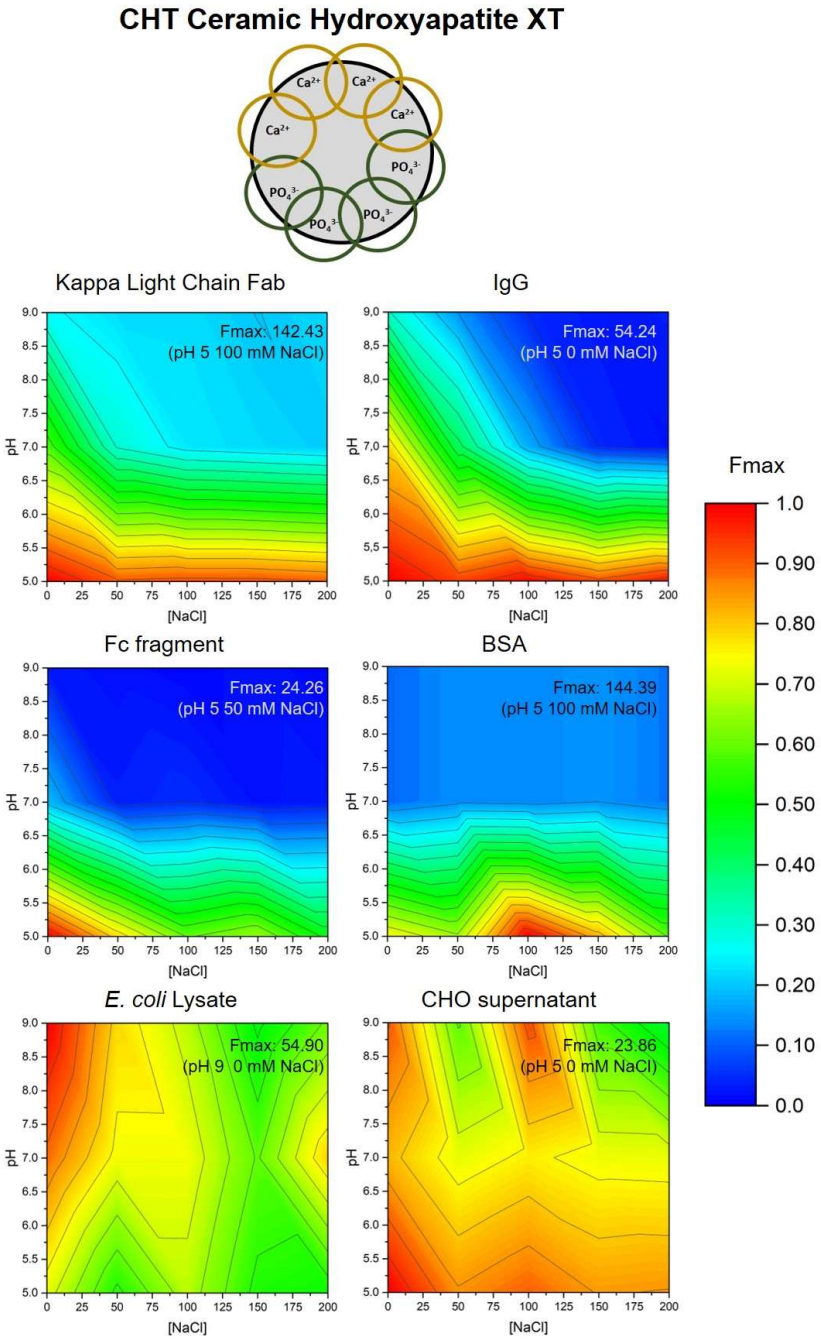

Figure 5.13 Heatmaps obtained for the binding of different labelled biomolecules (Fab and Fc fragments, IgG and BSA) and complex media (*E. coli* lysate and CHO supernatant) to CHT XT at different binding conditions. In all the heatmaps the highest Fmax and the conditions where it was obtained is indicated. All the Fmax values of the heatmaps were normalized using the highest value for each study.

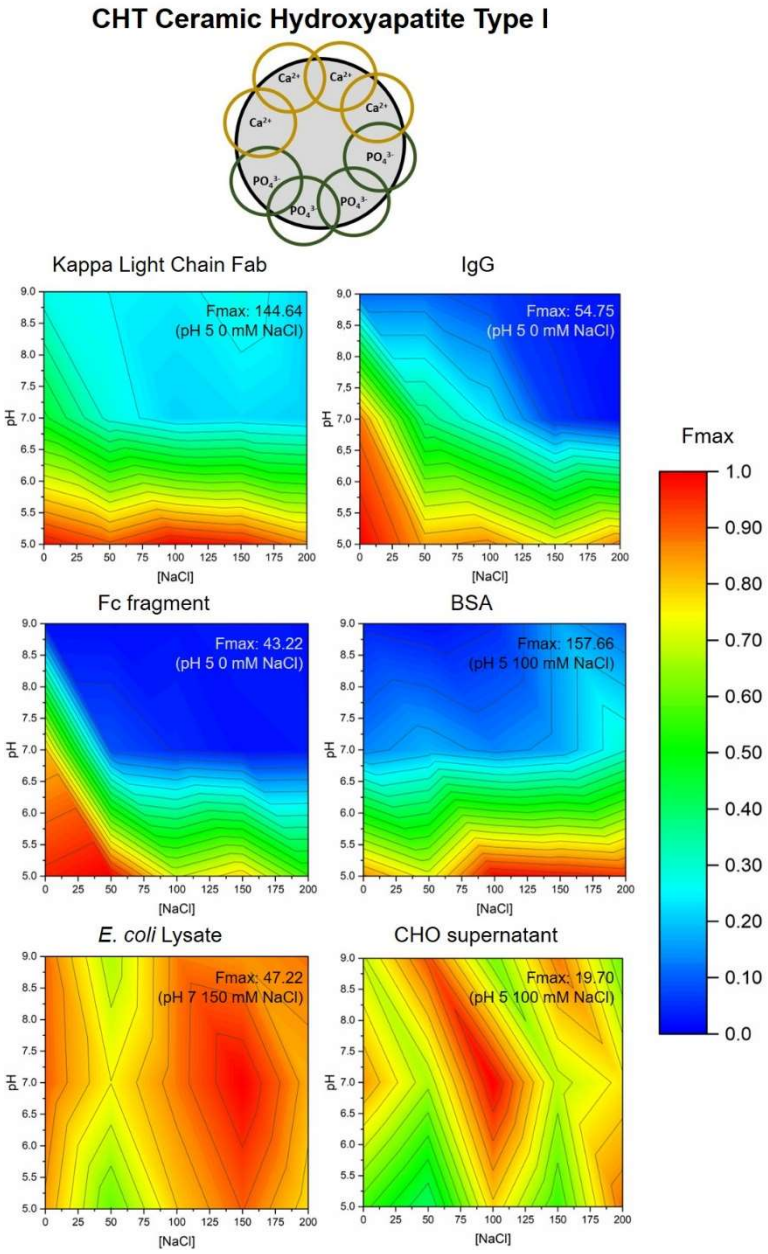

Figure 5.14 Heatmaps obtained for the binding of different labelled biomolecules (Fab and Fc fragments, IgG and BSA) and complex media (*E. coli* lysate and CHO supernatant) to CHT Type I at different binding conditions. In all the heatmaps the highest Fmax and the conditions where it was obtained is indicated. All the Fmax values of the heatmaps were normalized using the highest value for each study.

5.3.3.6. Binding studies with Capto Adhere

Unlike to the previous tested resins, Capto Adhere is a strong anion exchanger with a hydrophobic functionality. The presence of a quaternary amine, a phenyl and hydroxyl groups promotes electrostatic, hydrophobic and hydrogen bonding interactions, respectively. The results obtained with this ligand are represented on **Figure 5.15.**

The binding behavior of Fab fragments to Capto Adhere is the opposite to the one observed with the other cation multimodal ligands. The presence of a quaternary amine confers a constant pH-independent positive charge. At pH 5, Fab having a strong positive charge (pI around 8 – 9), cannot bind to the resin, due to charge repulsion. The behavior of Capto Adhere at pH 5 is majorly electrostatic, and the increase of salt do has no effect on the binding. With the increase of pH, there is a decrease of Fab charge, and consequently binding increases. At pH 9, Capto Adhere can successfully bind Fab fragment at all the tested salt concentrations. The salt-tolerance of the ligand is a well-studied characteristic, and the results herein obtained corroborate those ones [292]. At all tested pHs, an increase of the conductivity does not change the binding behavior of the resin, in some cases a higher NaCl concentration favors the binding of Fabs to Capto Adhere (i.e. pH 9 150 mM NaCl). For IgG and Fc fragments, the binding behavior is similar, the only difference being the existence of working conditions (salt and pH) where the binding is stronger. This only occurs at high salt concentration, possible as a result of a more pronounced exposure of hydrophobic amino acids and their availability to bind to the aromatic ring. The results obtained with antibody derived molecules agrees with the literature, the unexpected results were obtained with BSA. The binding of this protein is uniform at all the tested conditions, with two distinctive regions where it is stronger: pH 5 without salt and pH 7 with 200 mM of NaCl. The last condition is expected, once Capto Adhere is known to bind better at higher pHs and salt concentrations. The surprising result is the binding at all pH 5 tested conditions. The pI of BSA is 4.7, being thus only slightly negatively charged at pH 5, and so theoretically binding to Capto Adhere would be unfavorable. Two hypotheses can explain this result. The first is related with the labelling procedure. In fact, the presence of a dye could be interfering with the results by conferring the protein a stronger hydrophobic nature which could enhance the binding of BSA to Capto Adhere by increased hydrophobic interactions. The second is related with the stick nature of both ligand and BSA, consequence of their highly hydrophobic character. The

combination of a strong hydrophobicity moiety of Capto Adhere and the presence of several hydrophobic patches on BSA [293] could create the necessary conditions for a high binding even at non-expected conditions.

The complex mixtures results are constant at all pHs and salt concentrations, with a very high binding occuring independently of the tested conditions. It appears that both electrostatic and hydrophobic interactions are occurring, and the binding of the components present in *E. coli* lysate and CHO supernatant is a consequence of that combination. Probably the same phenomenon is occurring with BSA.

The ability of Capto Adhere to bind Fabs only at very basic conditions (pH 9) is not very appealling as a Fab purification solution. However, if operated in flow-through mode, it could be a resin to be taken in consideration. The ability of binding BSA and complex mixture at lower pHs supports the implementation of this chromatographic solution. Nevertheless, extra studies are needed to evaluate the purification of Fabs, in a flow-through mode.

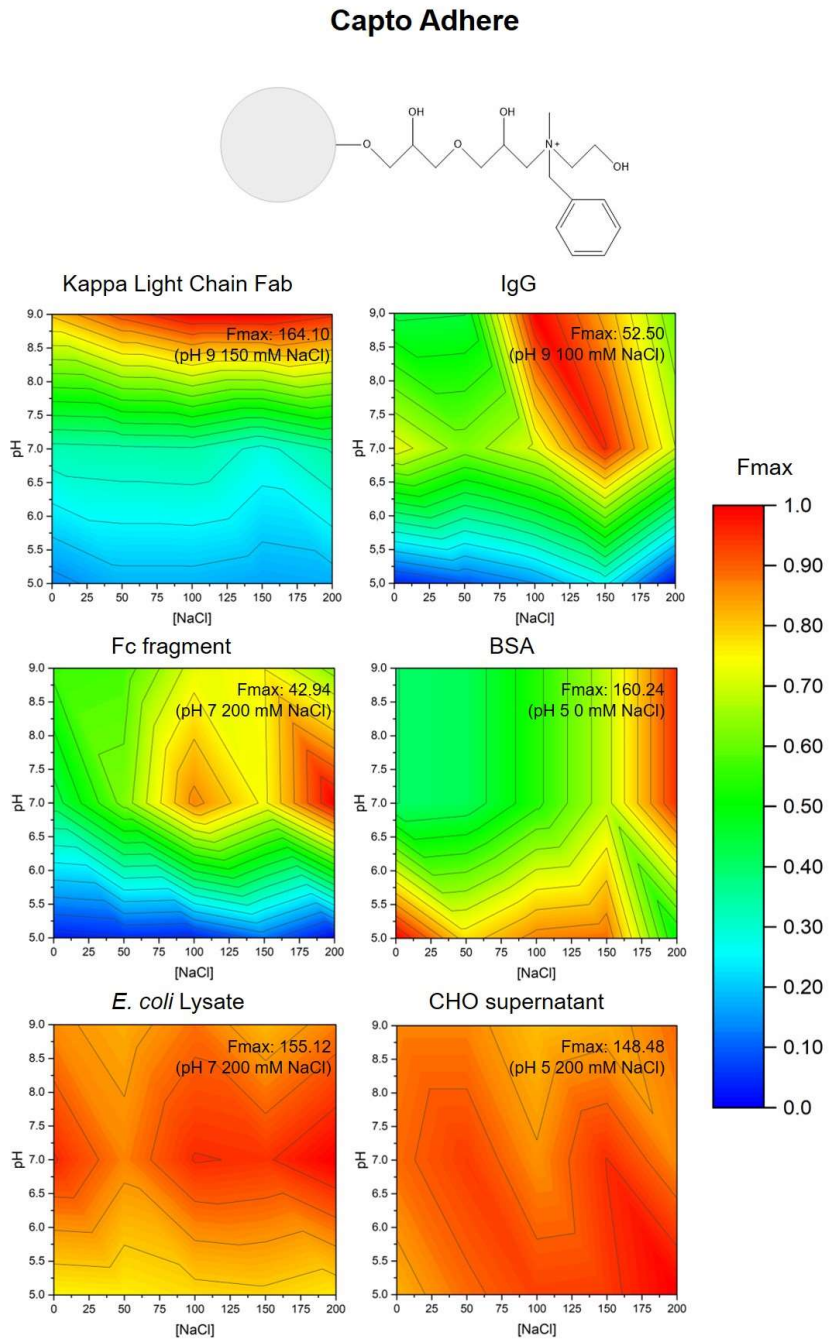

Figure 5.15 Heatmaps obtained for the binding of different labelled biomolecules (Fab and Fc fragments, IgG and BSA) and complex media (*E. coli* lysate and CHO supernatant) to Capto Adhere at different binding conditions. In all the heatmaps the highest Fmax and the conditions where it was obtained is indicated. All the Fmax values of the heatmaps were normalized using the highest value for each study.

5.3.3.7. Binding studies with Nuvia aPrime

Nuvia aPrime is anion exchange multimodal solution recently launched by Bio-Rad. This ligand shares similar groups with Capto Adhere, including an aromatic ring, a hydroxyl group and a quaternary amine. Despite their similarities, key features of the two ligands impact their binding behavior. Linker length and the proximity of interacting groups were two features studied in a comparison of Nuvia aPrime and Capto Adhere [294]. Robison *et al*. studied different anion exchange multimodal prototypes by comparing the retention of a protein library [294]. Differences between retention was observed as a consequence of different ligand flexibility, length, and availability of interacting moieties. Among all the prototypes, number 13 was the ligand that ended up being commercialized by Bio-Rad as Nuvia aPrime. In the microfluidic study herein discussed, Nuvia aPrime was also evaluated for different proteins but with a wider range of binding conditions. The obtained results are represented on **Figure 5.16**.

Analyzing the results obtained with Fab fragments, Nuvia aPrime shows higher binding with the increase of the pH. With a pI around 8-9, Fabs are only negatively charged at pH 9, and so capable to efficiently interacting to Nuvia aPrime. The electrostatic interaction between the resin and Fabs is balanced by the relative salt tolerance of the ligand. The application of salt has no negative effect on the binding, in some cases (i.e. pH 9, 50 mM NaCl) favours it. Regarding Fc fragments, the binding behavior is comparable to Fabs. The only difference is the pH value where Fc starts to have a more pronounce binding to Nuvia aPrime. Having a lower pI than Fabs, Fc start to bind at a lower pH. The results obtain for IgG show a higher pH tolerance than the other two antibody derivatives. Moreover, from all the tested resins, Nuvia aPrime is the one with higher affinity towards IgG, with a Fmax of 93.21 in the best condition – 150 mM NaCl, pH 9. This propensity to bind IgG, especially at higher pHs and higher salt concentrations, could be a result of strong hydrophobic interactions of this ligand to more available hydrophobic regions of whole antibody in comparison to the Fc and Fab fragments.

As observed for Capto Adhere, Nuvia aPrime exhibited a strong binding to BSA. This interaction was so marked that the microfluidic setup herein applied was not adequate to obtain trustworthy values. The fluorescence increase was constant, never reaching a plateau, and upon fitting the Hill function, the Fmax values were not acceptable. The lack of coherent Fmax values made the construction of the BSA heatmap impossible. To have

an idea about what is happening when BSA binds to Nuvia aPrime, heatmap shown on **Figure 5.16** was contruct with the fluoresncence value obtained at each condition at t= 90s. The results indicate a better binding of BSA to the multimodal resin at basic pHs (>7) with a salt concentration higher than 50 mM of NaCl. Regarding the *E. coli* lysate and CHO supernatant, the results are the similar to Capto Adhere. Probably the same type of interactions is occurring on Nuvia aPrime, and the hydrophobicity of these complex mixtures is creating a pH and salt independent binding to the ligand.

Nuvia aPrime is a novel multimodal purification option. Their structure and binding characteristics make this new ligand an alternative to Capto Adhere, commonly used in industrial applications. There is still a long path to take to completely understand the binding features of this new ligands. The results herein obtained, and the work developed by Robinson *et al.*, are promising, and the application of Nuvia aPrime as a purification step should be taken in consideration.

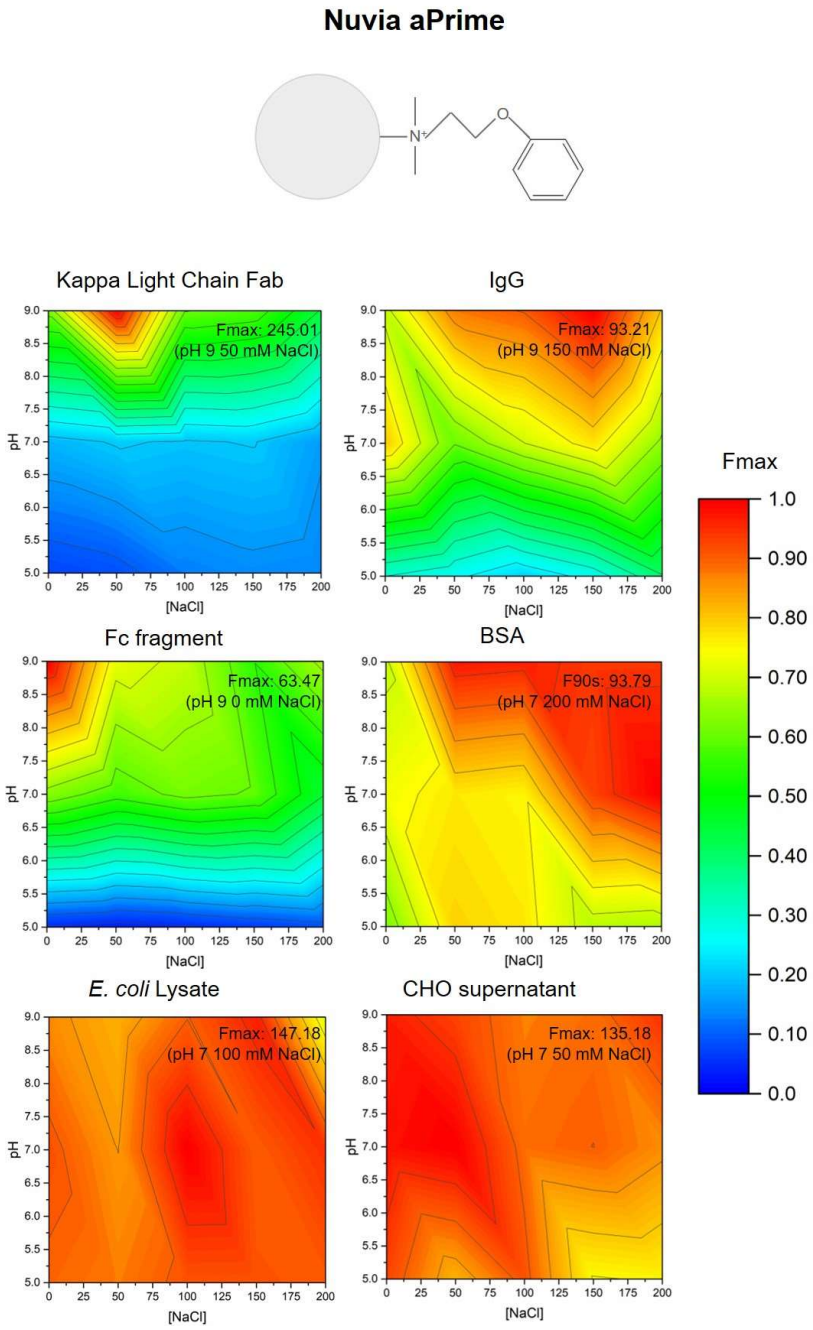

Figure 5.16 Heatmaps obtained for the binding of different labelled biomolecules (Fab and Fc fragments, IgG and BSA) and complex media (*E. coli* lysate and CHO supernatant) to Nuvia aPrime at different binding conditions. In all the heatmaps the highest Fmax and the conditions where it was obtained is indicated. All the Fmax values of the heatmaps were normalized using the highest value for each study. Because for BSA it was not possible to calculate the Fmax. the values used to construct the heatmap were obtained at t=90s of eahch condition.

5.3.3.8. Binding studies with HEA and PPA

Pall Life Sciences offers three type of anion exchangers multimodal resins: HEA, PPA and MEP. Focusing on the first two, HEA and PPA are quite similar ligands with a secondary amine and an hydrophobic group (hexyl for HEA and phenylpropyl for PPA) [295]. The comparison between these two ligands was already discussed elsewhere [296], and the overall conclusion is the similar behavior of HEA and PPA, with point operational conditions more suited for one or other resin.

The results obtained using the microfluidic approach to find the best binding conditions for HEA and PPA are presented on **Figure 5.17** and **5.18**. Comparing the binding of Fabs to the two resins, it increases with the increase of the pH for HEA and is constant at all pHs for PPA, with two regions where the binding is higher. The lack of an aromatic group in HEA makes this resin unable to bind positively charged proteins under low pH conditions. The charge repulsion is higher at low pH, and HEA is only able to bind Fabs at a pH where these biomolecules have a greater negative profile (pH 7 and 9). On the other hand, PPA having an extra hydrophobic moiety, can counterbalance the charge repulsion at lower pHs, establishing cation-π and hydrophobic interaction and the binding is favored when salt is present. This is the reason why at pH 5 with 150 mM NaCl the Fmax has the higher value on PPA (Fmax: 196.66). The results achieved with Fab fragments demonstrate a higher mixed-mode nature of PPA when compared to HEA, where the effect of electrostatic interaction is more present [296,297]. Differences in the hydrophobic groups of these ligands makes the presence of salt more important for PPA than for HEA. Regarding the binding to IgG and Fc, the profile obtained for Fabs was kept. For HEA, an electrostatic-driven behavior is observed, and an increase of the pH promotes an increase of the binding to both Fc and IgG. PPA binds to these two targets at higher pHs and salt concentrations. The ability to bind IgG, at any condition of this design experiment, except pH 5 with no salt, makes PPA an interesting resin for the binding of IgG biomolecules. Regarding BSA, the binding is similar for HEA and PPA, confirming previous results [298]. Generally, the binding to BSA is favored with at higher pHs in the presence of salt. Finally, for complex mixtures, the trend observed with Nuvia aPrime and Capto Adhere is kept, with a high binding independently of the pH or NaCl concentration.

Two ligands with similar structures had also an overall similar performance, with point conditions where the binding was favored. The more hydrophobic nature of PPA makes it more salt tolerant than HEA and suitable to purify biomolecules at high-sat conditions. Having noticeable different binding natures, HEA and PPA can be considered valuable options, independently or in combination, as alternatives to purify Fab fragments. The resolution of the HT platform herein applied is a noteworthy result. It was able to detect different binding conditions in ligands having a small difference between them.

5.3.3.9. Binding studies with MEP

The last anion exchange multimodal resin studied is MEP. This ligand possesses an alkyl (ethyl), an aromatic (pyridine) and a thio-ether group [295]. Unlike HEA and PPA, MEP has a protonable amine in the head group. MEP can be considered a biomimetic hydrophobic ligand due to their protein A like operation, specially the low pH elution [299]. MEP has a relatively low pKa (~5) having no charge at neutral pH, the binding to antibodies is mainly driven by hydrophobic interaction and hydrogen bonding. The elution is made by lowering the pH and so increasing the charge repulsion. This protein A-like feature makes MEP one of the most popular alternatives to purify mAbs [299,300].

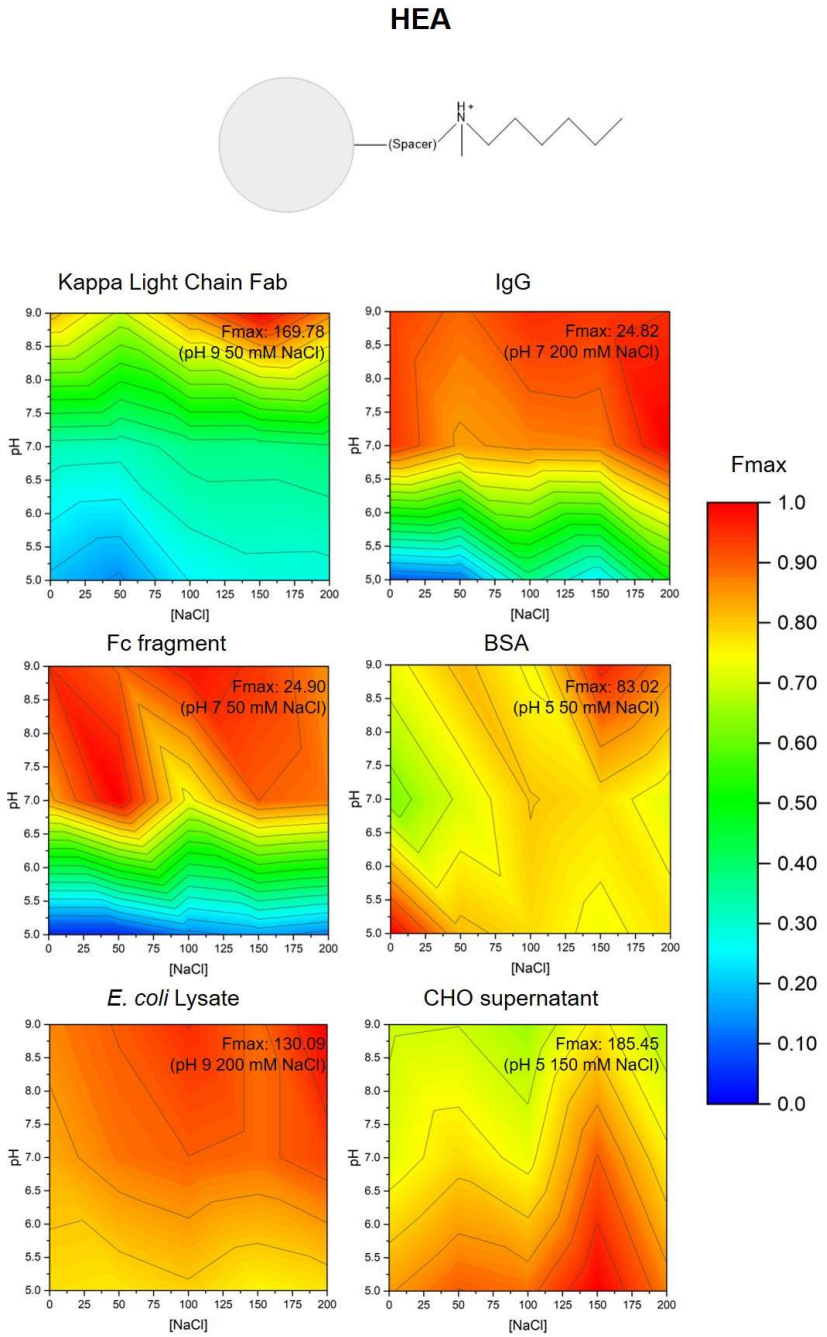

Figure 5.17 Heatmaps obtained for the binding of different labelled biomolecules (Fab and Fc fragments, IgG and BSA) and complex media (*E. coli* lysate and CHO supernatant) to HEA at different binding conditions. In all the heatmaps the highest Fmax and the conditions where it was obtained is indicated. All the Fmax values of the heatmaps were normalized using the highest value for each study.

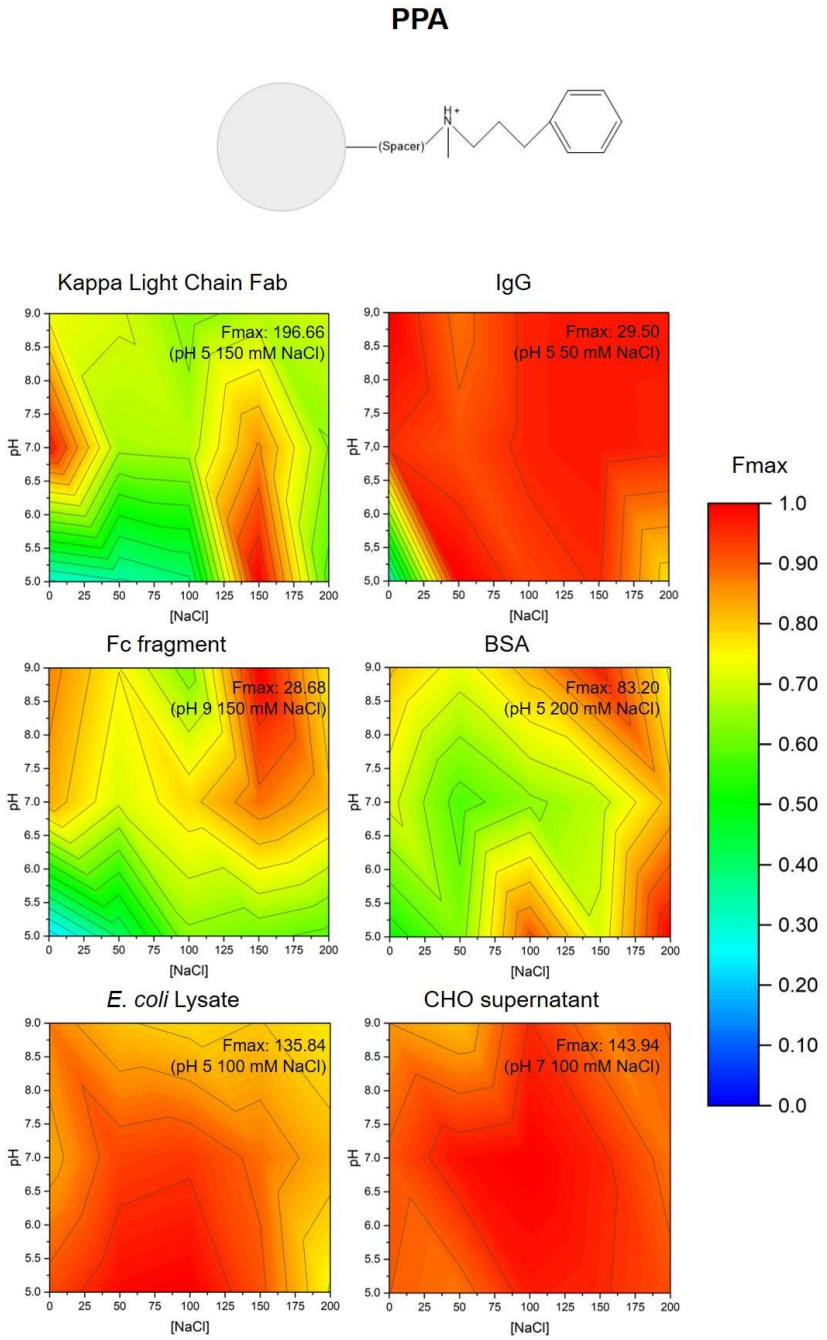

Figure 5.18 Heatmaps obtained for the binding of different labelled biomolecules (Fab and Fc fragments, IgG and BSA) and complex media (*E. coli* lysate and CHO supernatant) to PPA at different binding conditions. In all the heatmaps the highest Fmax and the conditions where it was obtained is indicated. All the Fmax values of the heatmaps were normalized using the highest value for each study.

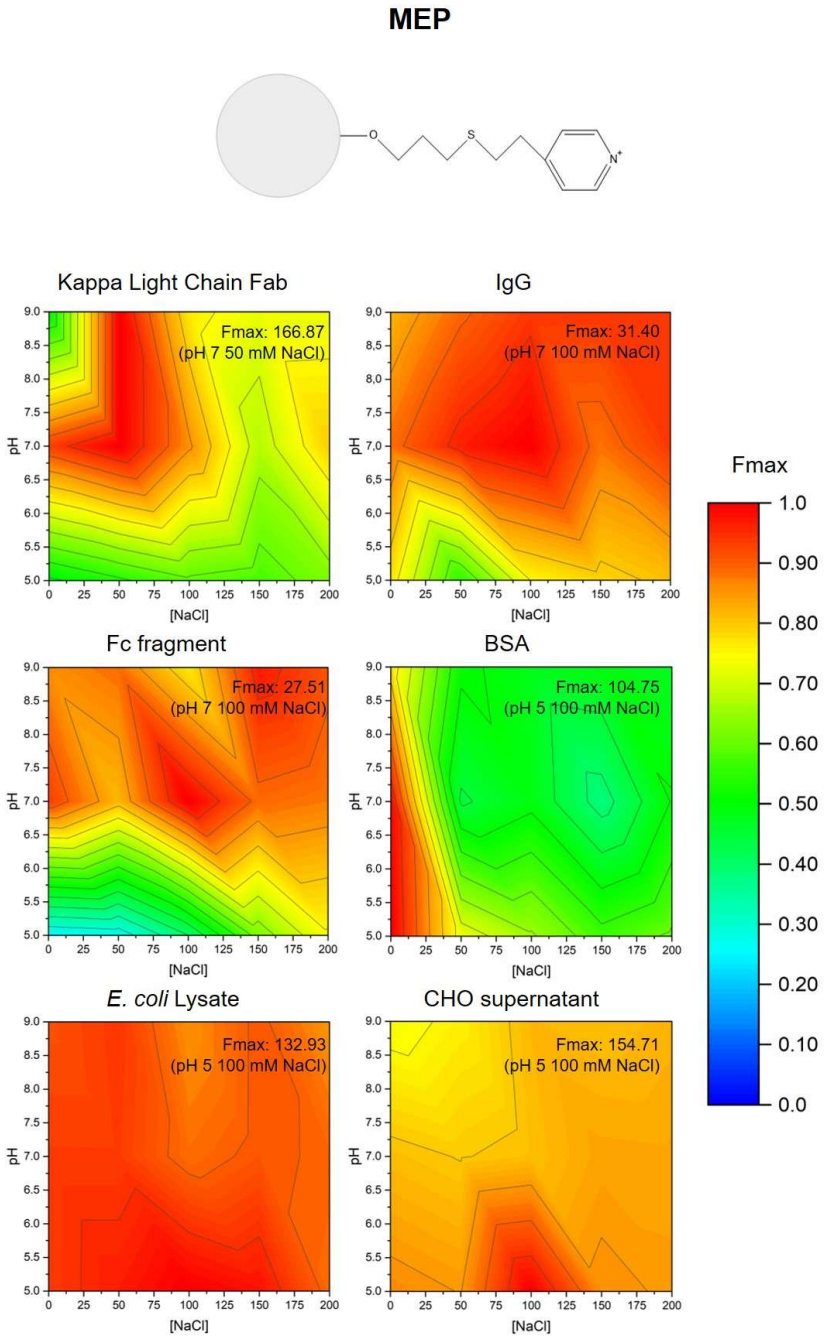

Figure 5.19 Heatmaps obtained for the binding of different labelled biomolecules (Fab and Fc fragments, IgG and BSA) and complex media (*E. coli* lysate and CHO supernatant) to MEP at different binding conditions. In all the heatmaps the highest Fmax and the conditions where it was obtained is indicated. All the Fmax values of the heatmaps were normalized using the highest value for each study.

The IgG results herein obtained for MEP (**Figure 5.19**) confirm what was referred previously, that MEP has a high affinity towards the polyclonal mixture of IgG used in these experiments, with an increasing binding at higher salt concentrations and pHs. Regarding the antibody fragments, Fc shows a binding profile similar to IgG, however lower binding occurs at acidic pHs. For Fabs, there is a region where the binding is highly favored (50 mM NaCl, pH 7). Probably the binding to IgG is a combination of interactions between hydrophobic residues of both Fc and Fab and the ligand, and it appears that the major interaction is occurring with the Fc region.

Regarding BSA, it binds strongly when there is no salt and an increase in salt concentration promotes a decrease in the binding of BSA. The inability of MEP to bind BSA has been reported in the literature, [301], however the data here presented show otherwise and despite the lower binding of BSA to MEP when the salt concentration is higher, there is still a certain level of interaction. Further studies should be performed to complete analyze this result. Nevertheless, the presence of the dye on BSA is a variable to be taken in consideration, specially having in consideration the results obtained with the other anion multimodal exchangers.

The complex mixture results do not differ from the previous results obtained with this samples. The wide range of impurities and the labelling procedure could be affecting the complete understanding of the binding forces occurring with both *E. coli* lysate and CHO supernatant. However, the comparison between different resins is accurate, and with the different Fmax values obtain is possible to have a preliminary analysis of the complex mixtures binding behavior.

The overall results for MEP showed a resin capable of distinguish between Fab fragments and whole IgG. Varying the pH and salt concentration and possibly the elution mode, it may be possible to separate Fab from other biomolecules after a digestion protocol. Moreover, the lack of salt tolerance when the binding to BSA (a model protein) could be a good indicator of the possible use of MEP to purify Fab fragments in a complex media scenario.

5.3.3.10. Binding studies with Protein L

Protein L was vastly described in this thesis as the main solution to purify Fab fragment s. In order to compare it with the multimodal resins herein suggested as possible new alternatives for the downstream process of Fabs, the same type of microfluidic screen was executed. Additionally, having an affinity solution so implemented in the industry, this set of experiments can be applied to validate the use of this HT platform and the binding conditions screening method. The results obtained with protein L are represented on **Figure 5.20**.

The protein L HT screening results were the expected, with complete binding to both Fab fragments and IgG observed at every condition tested. Having these two biomolecules kappa light chains, the binding occurs to protein L independently of the operational conditions. Unlike multimodal resins, where the interactions are based on electrostatic and/or hydrophobicity, protein L interaction is affinity-based, thus salt and pH have small effect on the binding to kappa light chain containing biomolecules. Regarding Fc fragments and BSA, having no affinity towards protein L, the results show negligible binding of these biomolecules. The highest Fmax values obtained for both proteins are the lowest of all the multimodal resins (11.41 for Fc and 12.67 BSA), result of putative unspecific binding to the protein L beads. In comparison to the other resins, the Fmax obtained in the screening of the best binding conditions for the complex mixture were also low. The Fmax obtained by *E. coli* lysate and CHO supernatant are a consequence of the high degree of labelling, being this result a consequence of intrinsic fluorescence of the samples.

All the protein L results were expected, specially the affinity towards the kappa light chain Fabs and the polyclonal mixture of IgG. The lack of affinity to bind Fc and BSA is also a predictable result. The set of assays developed with protein L, and confirmation of anticipated results, approve the applicability of this platform and experimental setup to screen chromatographic binding conditions. The only drawback is the need to do a prior labelling procedure of the tested samples, that may influence the binding results. Nevertheless, when comparing the same samples, the influence of the fluorescence dye is cancelled out, making the comparison between different conditions and resins a reliable and herein validated result.

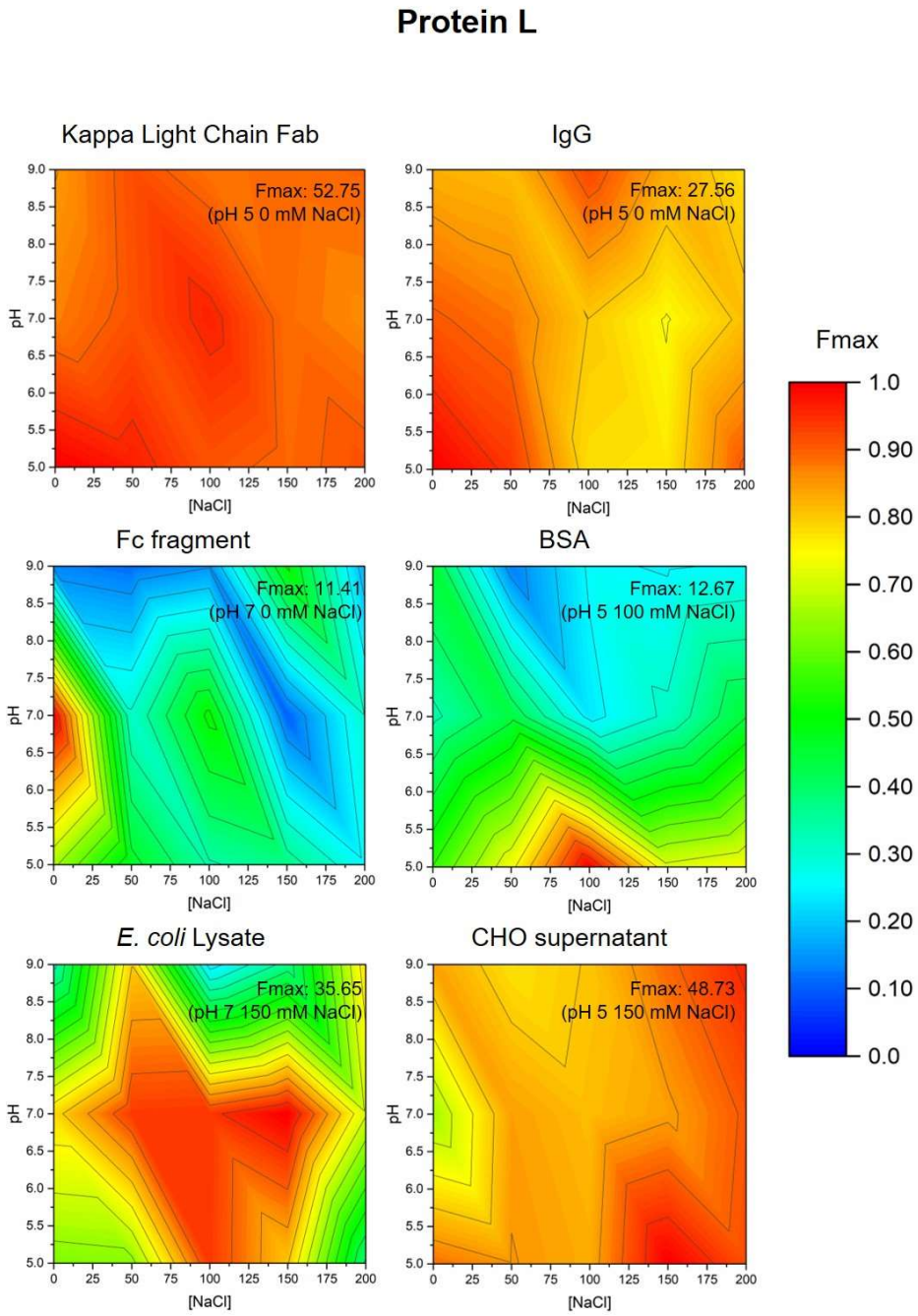

Figure 5.20 Heatmaps obtained for the binding of different labelled biomolecules (Fab and Fc fragments, IgG and BSA) and complex media (*E. coli* lysate and CHO supernatant) to Protein L at different binding conditions. In all the heatmaps the highest Fmax and the conditions where it was obtained is indicated. All the Fmax values of the heatmaps were normalized using the highest value for each study

5.3.4. High-throughput screening using 96-well microplate

The relative novelty associated with the use of microfluidics to screen chromatographic conditions demands extensive result confirmations. Previously, the use of a traditional and implemented affinity chromatographic technique (protein L) was applied to confirm and validate microfluidic results. Despite the added value brought by the referred study, it is interesting to compare different HT platforms. The use of 96-well plate format to screen for chromatographic binding and elution conditions is a well implemented technique, considered the standard methodology in HT chromatographic studies [302,303]. Herein, a disposable 96-well filter PreDictor™ plates, was used to compare the binding of Fab fragments to Capto MMC multimodal resin. The PreDictor™ plates are commercially available and accordingly to the type of study required, plates with different resins can be acquired. In this work, to compare the binding of Fabs, using different HT platforms, PreDictor MMC single medium plate was used. The wells of these plates are filled with 6 µL of Capto MMC resins, making them ideal for binding, elution and washing studies. The experiments done with the 96-well format were very similar to the ones on the microfluidic platform, with three differences: (1) there was no Fab labelling procedure, (2) all the binding conditions were done in triplicate and (3) the concentration of Fab was 0.15 mg/mL in a volume of 200 µL (vs 0.06mg/mL in 30 µL in microfluidics). The result obtained for the plate experiment is present on **Figure 5.21**. As expected, the binding of Fabs to Capto MMC is similar in both HT platforms, with the heatmap herein obtained presenting the same type of binding profile (**Figure 5.10**, **section 5.3.3.2**). The only surprising result is the low Fab binding percentage. A higher binding to Capto MMC would be expected, having in consideration the previous data analyzed in this thesis and in other works. This can be explained with the lack of process optimization, specially, the mixing and incubation step. The diffusion or contact of Fabs with the chromatographic beads may be compromised by an inadequate incubation time and/or mixing. Other hypothesis is the saturation of the beads, however, having Capto MMC a binding capacity of >45 mg BSA/mL resin, saturation is unlike to occur, since the amount of Fabs used was 0.5 mg/mL of resin. Despite of the low Fab binding percentage, the trend observed in microfluidics and plate format are the same: higher binding at low pHs and higher conductivities.

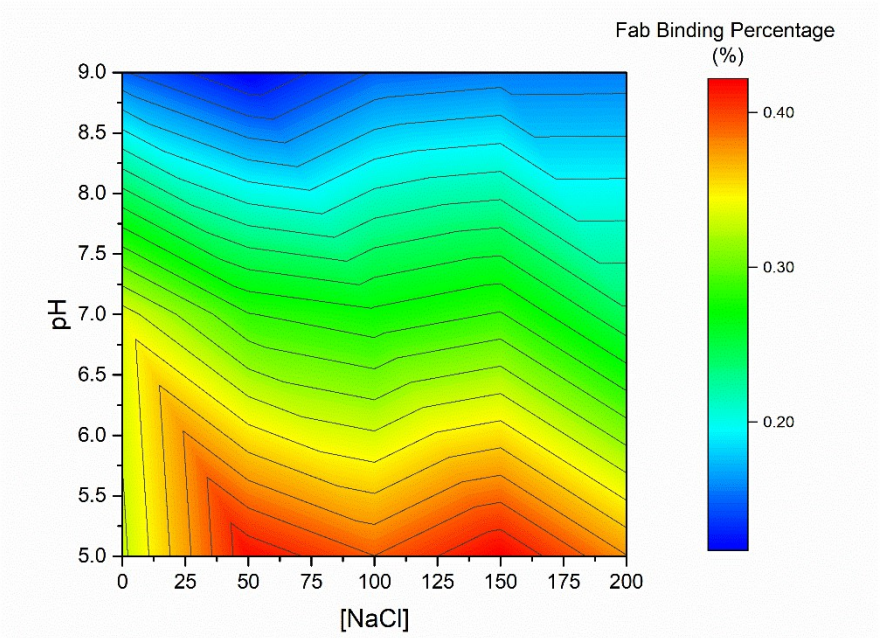

Figure 5.21 Heatmaps obtained for the binding of Fab fragments to Capto MMC resin slurry present on a 96-well filtered plate at different binding conditions.

Having tested the two HT platforms, an evaluation based on the user point-of-view can be made. Five parameters will be taken in consideration: labelling procedure, amount of sample and consumables, preparation time, equipment, and device (plate vs microfluidic) handling. The necessity of a fluorescent dye is the major limitation of the microfluidic approach herein explored. The need to add a fluorophore to the sample, in order to monitor its binding to the chromatographic bead, can influence the results by changing the charge and hydrophobic nature of the proteins. With the 96-well plate format there is no need for labelled samples, the evaluation of the binding was made by measuring the absorbance at 280 nm after and before a certain incubation time (in this case one hour). Regarding the quantities of sample and buffer needed, the microfluidic setup is the one that requires less amount of both sample and buffers. The concentration of protein used in microfluidic experiments was 60 µg/mL (30 µL) while for plate experiments was 150 µg/mL (200 µL). Additionally, the volume of buffer used to equilibrate the beads on the microfluidic setup is 50 - 70 µL (in excess – the microfluidic chamber has 210 nL) while to equilibrate the beads, on one well of the plate, at least 600 µL of buffer is needed. The amount of beads needed for the microplate assays is much higher than for the microfluidic experiments – 6 µL vs. 70 nL. In terms of preparation, a proper equilibration process is needed for both platforms, and because the volumes of microfluidics are smaller, the time needed to inject the beads, equilibrate them and start the data acquisition process is faster

than the microplate. All this handling takes around 7 minutes in the microfluidic assays. For plate assays the resin equilibration and incubation time is longer, and the process may take 2 to 3 hours. Nevertheless, for plate assays, it is possible to have 96 results all at once, while for microfluidics the results are obtained one by one. The equipment need for the microfluidic setup is a syringe pump and a microscope capable of tracking fluorescence over time. For 96-well plate experiments a centrifuge, a mixer and a UV-plate reader are needed. Finally, the handling of the microfluidic device is very intuitive, being the major problem the possibility of clogging the column upon packing it with the beads [262]. The handling of the plate needs to be more meticulous once the chance of cross-contamination of well is higher. Additionally, if the resin slurry is pipetted to the wells manually and not using a robot, the risk of errors is higher, once different quantities of resin could generate different data. The plate herein utilized was supplied by GE Healthcare, and the amount of resins was properly controlled, thus the error associated with resin slurry handling is not present. Other difference between the two systems is the binding mechanism. In the microfluidic device the flow of the samples is similar to a traditional packed-bed, while in the plate, the adsorption is based on batch. This difference may introduce higher variability to the plate systems, once the binding mechanisms of this is very distinct from the packed-bed. The comparison herein taken is summarized on **Table 5.2.**

Table 5.2 Comparison between the two High-throughput Systems used in this work.

	High-throughput Systems	
	Microfluidic Chromatography	96-well plate w/ resin slurry
Labelling	Yes	No
Sample	Low (60 µg/mL - 30 µL)	High (150 µg/mL - 200 µL)
Consumables	50 µL of buffer 70 nL of resin	600 µL of buffer 6 µL of resin
Preparation Time	4 min packing and equilibration 3 min data acquisition (one by one)	0.5 to 1h equilibration and sampling 1 to 2h incubation 5 min data acquisition (depend on the number of samples – maximum 96)
Equipment	Syringe pump Fluorescence microscope	Centrifuge Mixer Plate reader
Handling Problems	Clogging of the microcolumn	Cross-contamination

Taking in consideration the comparative analysis done and the results obtained it is possible to make a final evaluation of the two HT platforms applied. The possibility of obtaining fast results with low amounts of consumables is the major advantage of microfluidics. The limitation resides on the need of a labelling procedure. A poor characterization of its effect can influence the microfluidic results. Regarding the HT system based on 96-well filter plate, the quantity of consumables and preparation time is higher compared to microfluidics. However, it is possible to have 96 results almost at the same time and without needing samples with a fluorescent dye. The choice of the best system can be based on the equipment available, amount of sample and process time. Nevertheless, a conclusion can be taken, independently of the platform chosen, if the procedure is properly executed, the results will not differ from these two different HT approaches.

5.3.5. Bench-scale experiments

The application of the described microfluidic technology is a valuable instrument to do a fast screen of chromatographic operational conditions, narrow the number of possible resins and have an initial idea of the chromatographic mode to apply. Nevertheless, in chromatography, microfluidics cannot be applied without confirmation of main results with a bench-scale chromatographic system. Different variables such as flowrate, bead packing and residence time are different in both scales, and so the effect of those in the binding result must be confirmed. As the target biomolecules of this thesis are Fab fragments, the experiments at bench-scale were focused only on Fabs. These assays were performed in a 1 mL packed column, using a Fab concentration of 1 mg/mL in 200 µL. The binding occurred at pH 5 and 7, no salt, with the same type of buffer used in the microfluidic experiments. The elution was made by salt gradient elution, 5 CV, with 1 M of NaCl. For two resins (PPA and MEP) a pH elution step was made with 0.1 M citric acid pH 3. After the elution, a regeneration step with sodium hydroxide (or phosphate for CHT XT) followed by an equilibration step were done. Five resins were chosen for these studies were Toyo, Capto MMC, PPA, MEP and CHT XT.

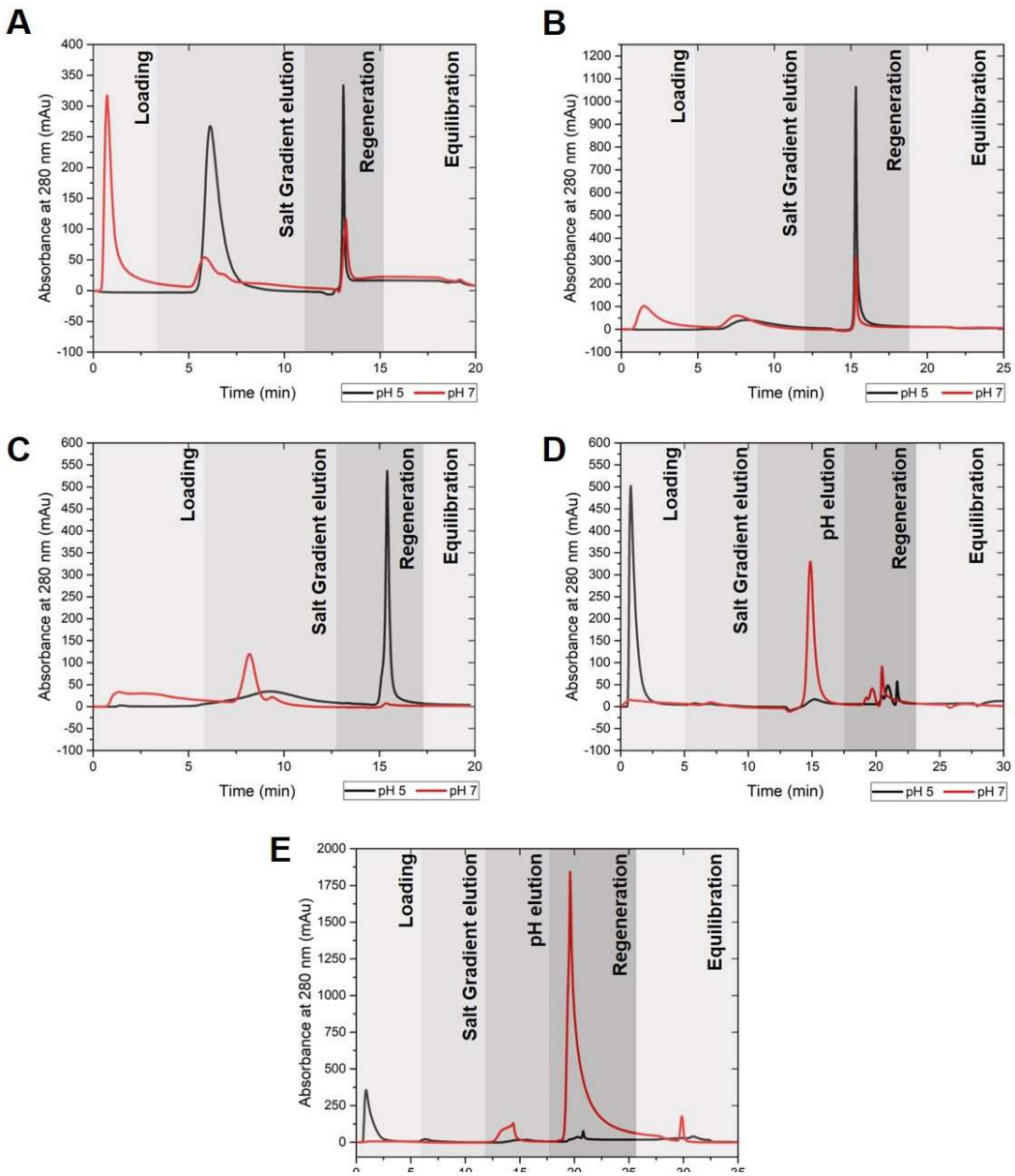

Figure 5.22 Chromatograms obtained in the microfluidic confirmation results using a bench-scale ÄKTA purifier system. The binding studies were done with pure Fab at two pHs (5 and 7) followed by a salt elution gradient. For PPA and MEP an extra pH elution step was done. **A** – Chromatograms obtained using Toyo. **B**- Chromatograms obtained using Capto MMC. **C** -Chromatograms obtained using CHT XT. **D** - Chromatograms obtained using PPA. **E** - Chromatograms obtained using MEP.

The two cation exchangers multimodal resins tested were Toyo and Capto MMC, and the resulted chromatograms are represented on **Figure 22A** and **22B**. The results confirm the trend observed previously, at pH 5 there is no flow-through peak, indicating a complete binding to both Toyo and Capto MMC. When the pH increases to pH 7, Toyo dramatically loses their ability to bind Fabs, and a high flow-through peak is observed. Regarding Capto MMC, it appears to be more pH tolerant, promoting more binding of Fabs to the

resin, when compared to Toyo, at pH 7. The salt elution on Capto MMC has practically no effect, the elution peaks at both pHs are very similar – corroborating the previous observed salt-tolerance. The hydrophobic nature of this ligand is noticeable with this elution mode, 1 M of salt is not enough to elute Fabs. These are only removed when the column is regenerated with NaOH. Salt elution with Toyo effectively elutes Fabs, specially at pH 5, the pH at which Toyo binds Fabs. The binding to this resin occurs majorly through electraostatic interaction, with Fabs being successfully eluted at higher ionic strengths. Upon column regeneration, some Fabs are removed from Toyo at both pHs, but more at pH 5, where Fabs bind stronger. It is important to highlight the usefulness of polyclonal Fabs in this set of experiments. The use of a mixture of Fabs, having different charge and structural characteristics is an advantage once it is possible to access "universal" binding and elution conditions, however, there will be some Fabs with distinct charge or structural differences that will bind differently to the resins. An example is the binding of some Fabs, at pH 7, that only elute at high salt concentration and or upon column regeneration.

The third multimodal resin used to confirm microfluidic results was CHT XT (**Figure 5.22C**). At pH 5, this resin binds strongly Fabs. Some Fab biomolecules partly elute upon salt gradient with 1 M of NaCl while others are only completely removed during column regeneration with 0.5 M of phosphate. Upon a pH increase, CHT loses its ability to bind Fabs and the presence of a broad flow-through peak is observed. The change of the ionic strength causes the elution of the majority of Fabs, and no peak appears during column regeneration.

PPA and MEP were the two anion exchange multimodal resins chosen. With PPA (**Figure 5.22D**), the binding only occurs at pH 7, while at pH 5, all the Fabs flow through the column. Based on the microfluidic results, this pH dependency is expected since the only region where Fabs do not bind to PPA is at pH 5 with no salt (**section 5.3.3.9**). The salt has little effect on the elution of Fab bound at pH 7, being those only eluted with an acidic pH elution step. The results obtained for MEP (**Figure 5.22E**) are also expected, with a high binding occurring at pH 5 and 7, with the last exceeding the first. The Fab elution from this resin, at pH 5, happens throughout salt and pH elution, where there is a leaking of the Fabs during both elution steps and regeneration. At pH 7, a small fraction of Fabs elute with the pH step, and the large majority is only removed during column regeneration. The elution of this resin is traditionally pH-based, in these experiments the

decision of performing a first salt elution gradient was to confirm the salt tolerance demonstrated by PPA and MEP during the microfluidic assays. Despite the result confirmation, the presence of a high salt concentration created the conditions for a stronger hydrophobic interaction, leading to the observed elution difficulties, even at low pH.

The results obtained in this experimental procedure confirm the ones obtained with microfluidics. The five selected resins show similar Fab binding profiles in both chromatographic setups. In further process development studies, Capto MMC and MEP resins will be discarded. The expected hydrophobic nature of the first makes the elution of Fabs a demanding task, the high binding at pH 7 and salt tolerance, suggested a possible elution protocol at undesired harsh pH and salt conditions. In the case of MEP, the inability to elute Fab at high-salt conditions could also affect the purification protocol, thus PPA was chosen as the anion exchanger multimodal resin. Toyo and CHT XT were also chosen since they can offer chromatographic opportunities for a multimodal based downstream protocol.

5.3.6. Multimodal chromatographic studies on *E. coli* cell culture fluid

The microfluidic approach applied in this work was subjected to different types of validation: use of protein L, comparison with other HT system and result confirmation with an ÄKTA purifier system. All these validations were made with single biomolecules in buffer solutions, which do not represent the environment where biomolecules are before any purification process. Additionally, the information acquired from the complex mixture microfluidic assays is not enough for a complete understanding of the binding behavior of these multimodal resins. In order to tackle this limitation, the three selected resins were used to study the binding of an *E. coli* supernatant, containing an abnormal amount of impurities (total protein concentration – 14.55 mg/mL). These experiments were similar to the ones already described for Fabs. In all experiments, 200 µL of the CCF were injected, at pH 5 (pH 6.5 for CHT to avoid bead disintegration) and 7, followed by a salt gradient elution step and finally a regeneration followed by an equilibration step. For PPA, an elution based on the pH was also done. The chromatograms resulted from these experiments are present on **Figure 5.23**.

In the results obtained for Toyo (**Figure 5.23A**), low binding of the components of the CCF to this resin is observed. Only at pH 5 there is some binding, possibly caused by charge interaction. With the increase of pH to 7, the global charge of impurities changes, and the repulsion phenomena starts to increase, blocking the binding to Toyo. At pH 5, after a salt gradient step, all the impurities are eluted with trace amounts removed during the regeneration step. Regarding CHT (**Figure 5.23B**), the results are clear, in both tested pHs, there is no binding of *E. coli* CCF impurities. The lack of affinity towards CCF impurities, in both resins, is a remarkable result, and in the case of CHT, this was previously noticed during the microfluidic experiments.

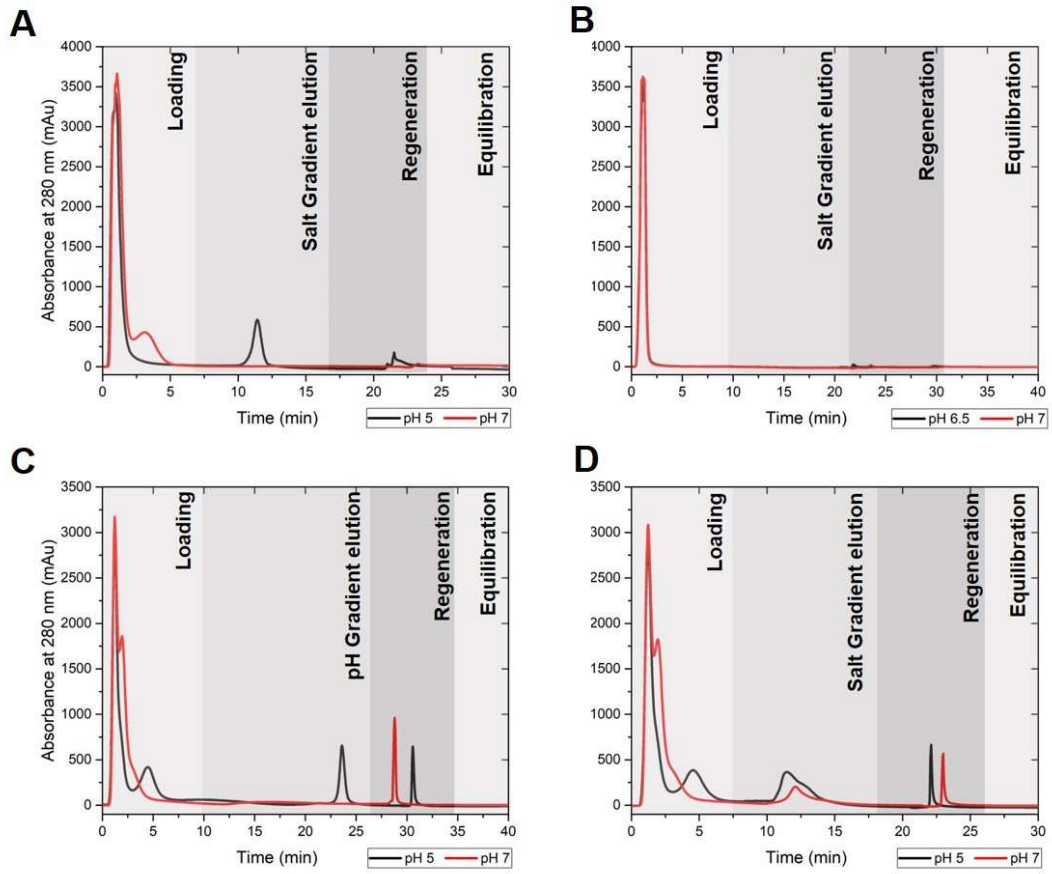

Figure 5.23 Chromatograms obtained upon injection of a *E. coli* supernatant in three different columns. The binding studies were done at two pHs followed by a salt elution gradient. For PPA an extra pH gradient assay was done. **A** – Chromatograms obtained using Toyo. **B**- Chromatograms obtained using CHT XT. **C** -Chromatograms obtained using PPA, pH gradient study. **D** - Chromatograms obtained using PPA, salt gradient study.

PPA has a pronounced mixed-mode nature and thus two elution modes were studied: pH and salt-elution. The presence of a high flow-through peak, at both pHs, suggest a low binding propensity of CCF impurities to PPA (**Figure 5.23C** and **5.23D**). However, the height of the flow-through peak indicates more binding to this resin than to Toyo or CHT.

When a pH linear gradient is selected as elution mode, there is an elution peak only for the adsorption at pH 5 (elution gradient from pH 5 to 9). On the contrary, in the pH gradient elution done for the adsorption at pH 7 (elution gradient from pH 7 to 3), there is no elution peak. This inability to elute impurities by decreasing the pH is a very interesting result, since in the previous section, Fabs were only eluted by decreasing the pH from 7 to 3. The salt gradient elution results are similar for both tested adsorption pHs, upon increasing of the salt concentration, elution occurs. The elution peak seems higher at pH 5, consequence of a higher binding of impurities at this pH. In all the regeneration steps, the presence of peaks is noticeable, probably there are impurities binding strongly to PPA.

The results herein obtained are promising. The lack of affinity towards *E. coli* CCF impurities, in all the three resins tested could be an important feature for potential multimodal downstream processes. The opportunity of combining different types of elution modes is also an advantage of the tested resins. Taking in consideration both Fab and *E. coli* CCF results, the next step is to understand the effect of the combination of the two during a multimodal purification process.

5.3.7. Multimodal chromatographic studies: Fab spiked into *E. coli* lysate

In this chapter an evolutionary and funneling approach was adopted to develop a Fab downstream process based on multimodal chromatography. The microfluidic and chromatographic studies developed on Toyo, CHT and PPA allowed a deeper understanding about potential binding and elution conditions to purify Fab fragments. In this section, the Fab fragments were spiked into a *E. coli* lysate to study if the effect of cell culture media will affect the previous results where Fabs were studied in pure buffer solutions. The chromatographic conditions chosen for each resin were based on the data obtained previously. In this section, instead of using cell culture fluid – unprocessed supernatant, an *E. coli* cell lysate was chosen as media, in order to mimic the most traditional method to produce Fab fragments, in the cytoplasm of an *E. coli*. To assure that the two types of complex mixtures generate similar results, an initial injection of the lysate was made to each resin. The chromatographic profile was equal to the ones obtained in the previous section, except for PPA, that showed a small percentage of

impurities in the flow-through that only eluted upon column regeneration (results not shown). Another difference was the higher UV values obtained on the previous section, consequence of the use of a more complex media. The results of Fabs spiked in *E.coli* lysate are present on **Figure 5.24**, the chromatograms were displayed parallelly to compare the different profiles. The first peak of each chromatograms corresponds to the flow-through, the second the elution and the last peak resulted from the stripping of the column. All the flow-through and elution peaks were collected and analyzed by SDS-PAGE (results not shown).

The data acquired previously, for Toyo, suggested a high Fab binding capacity at pH 5. Additionally, at this pH, a considerable percentage of CCF impurities were present in the flow-through. Having these results in consideration, the chosen binding pH was 5 and the elution mode was a salt gradient, in order take advantage of possible differences in the binding of both Fabs and impurities and separate them with a salt gradient. The chromatogram obtained for Toyo resembles the previous ones. The majority of impurities flow through the column, while Fab will bind. A 5 CV salt gradient is not enough to obtain two elution peaks, thus it is possible that Fabs are eluting with part of the lysate impurities. The presence of a relative high peak upon regeneration, present also during the Fab experiments on buffer, indicate and confirm a strong binding to Toyo at pH 5. The relative selectivity for Fab fragments is a fundamental feature for the implementation of Toyo as a purification solution. However, the presence of Fabs strongly bound to the column is a limitation of the operational conditions chosen, further elution studies need to be done to diminished the amount of Fab irreversible bound to Toyo.

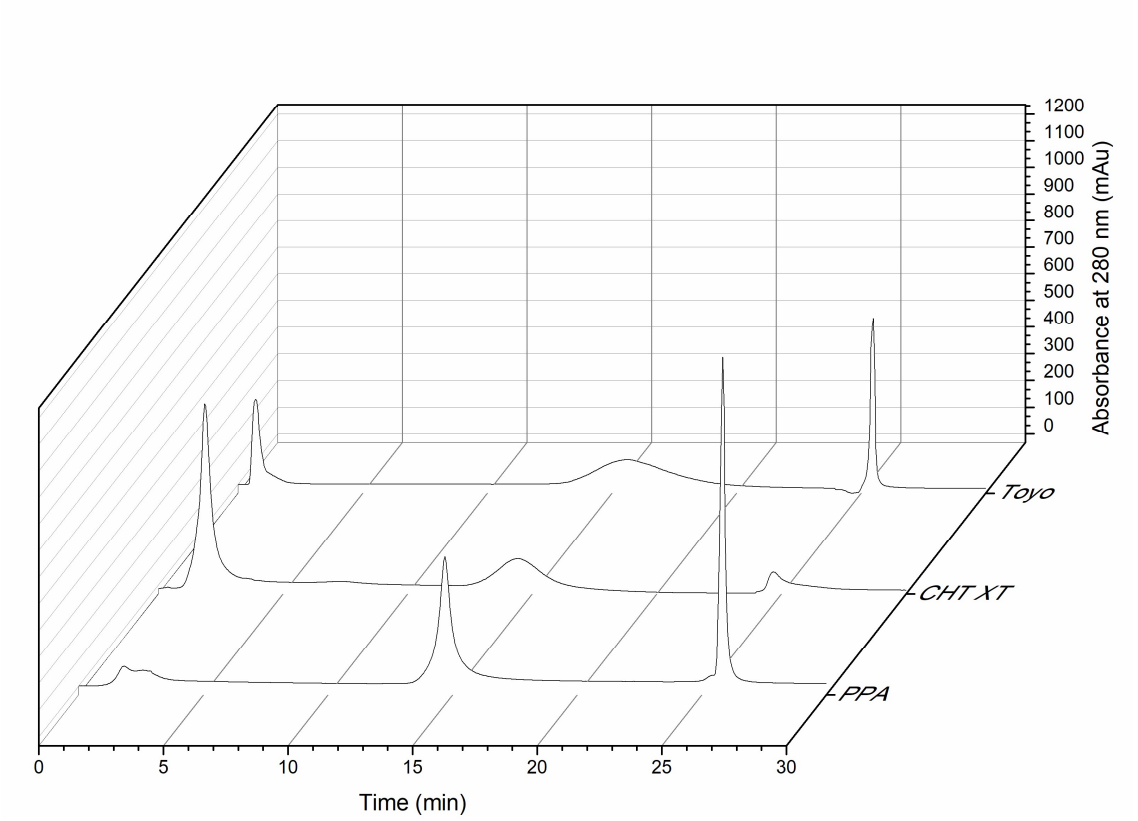

Figure 5.24 Chromatograms obtained upon injection of a Fab spiked into *E. coli* lysate in three different multimodal resins – Toyo, CHT XT and PPA.

Regarding the CHT resin, its inability to bind CCF impurities was also observed in this experiment where Fab was spiked in *E. coli* lysate. A sharp flow-thorough peak, containing impurities, is observed while Fabs are present is the elution peak. The results obtained previously were confirmed, CHT demonstrate a distinct selectivity towards Fab fragments. Having this result in consideration is important to highlight the importance of the effect binding pH for CHT resin. In **section 5.3.5**, the binding of Fab to CHT was made at pH 5 and 7, and two distinctive results were obtained. At pH 5, the strong binding to the column did not allow a proper salt elution step, while at pH 7, the binding was not so efficient, with only a small percentage of Fabs being able to bind to the column. In this chromatographic run, performed at pH 6.5, Fabs were more efficiently bound to the column and it was possible to elute them using the same salt gradient used previously. The need for an adequate process development is well characterized in this set of experiments. The studies herein described, conjugation between microfluidics HT system and bench-scale chromatography, can expedite the implementation of a downstream process without significant losses.

It was observed previously that PPA is able to bind Fabs at pH 7 and elute them by decreasing the pH. Also, the binding of impurities was less favorable at pH 7, and no elution was observed with deceasing pH gradient pH. Having these results into consideration, the Fabs present in the spiked *E. coli* lysate bound to PPA at pH 7 and eluted with a pH step gradient (pH =3). The absence of a flow-through peak and a sharp elution peak confirms the results previously obtained. With the SDS-gel (results not shown) was possible to observe a small percentage of Fab fragments in the flow-through peak, being the vast majority present on the elution peak, with a considerable degree of purity. Additionally, upon column regeneration, the lysate impurities are eliminated from the column. The ability to selective elute Fabs by decreasing the pH is a valuable PPA feature capable of separating impurities from Fabs.

5.3.8. Multimodal downstream process: two multimodal columns

The thorough process development described in this chapter had the goal of designing a purification process based on two different multimodal resins. Having in consideration all the data acquired, four different schemes were designed. The different resins and binding and elution conditions are schematized on **Table 5.3**. For each process the results will be qualitatively analyzed using a SDS-PAGE gel and quantitatively by percentage of Fab recovery and purity. The quantification and purity of Fabs was done using an analytical protein L column, as described previously (**section 3.2.6.2**). The work described lacks other analytical techniques, such as, DNA and toxin clearance and Fab activity after the purification process. Regarding the last one, the assessment of activity will be a difficult parameter to analyze since the Fabs applied in this study result from a digestion of a polyclonal mixture of IgGs.

Table 5.3 Schematization of the four purification processes based on two multimodal columns. In all processes, the binding and elution conditions are indicated for each column

Process number	First Step	Second Step
1	**PPA** Binding: pH 7 Elution: pH 3 (step)	**CHT XT** Binding: pH 6.5 Elution: 1 M NaCl (gradient, 5 CV)
2	**PPA** Binding: pH 7 Elution: pH 3 (step)	**Toyo** Binding: pH 5 Elution: 1 M NaCl (step)
3	**Toyo** Binding: pH 5 Elution: 1 M NaCl (step)	**PPA** Binding: pH 7 Elution: pH 3 (step)
4	**Toyo** Binding: pH 5 Elution: 1 M NaCl (step)	**CHT XT** Binding: pH 6.5 Elution: 1 M NaCl (gradient, 5 CV)

The first process was based of PPA and CHT XT. The gel electrophoresis results present of **Figure 5.25A** corroborate the quantification results present in **Table 5.4**. The first PPA step allowed a recovery of 51% of Fab in the elution with 80% purity (lane 3 gel A). The purity obtained in this first purification step was expected, since using the same operation conditions, in previous results, the majority impurities that bind to PPA only elute using a salt gradient and by regeneration of the column. The choice of a pH elution step had this in consideration, the ability to only elute Fab fragments. Regarding the recovery yield, a higher binding of Fabs to PPA was expected. A possible hypothesis could be related with the polyclonal nature of the Fab mixtures used, which confer them different

structural and electrostatic characteristics promoting different binding patterns. Nevertheless, in future studies, an increase of salt concentration when working with PPA may promote a stronger and universal binding to Fabs, avoiding the presence of 31% of Fabs in the flow-through. In the second step of this process, the yield results were surprising. Having in consideration both microfluidic and ÄKTA results, a higher yield of Fabs in the elution fraction would be expected (lane 4 and 5 gel A). An explanation could be related with the pH correction performed after the PPA elution, the addition of 2 M Tris-HCl pH 9 to the eluted fraction. The presence of Tris could be affecting the interaction between Fabs and the CHT resin and a low recovery yield is observed. Nevertheless, CHT seems to be an efficient resin to remove purities, since the purity of both flow-through and elution fraction is higher than 80% (lane 5 gel A).

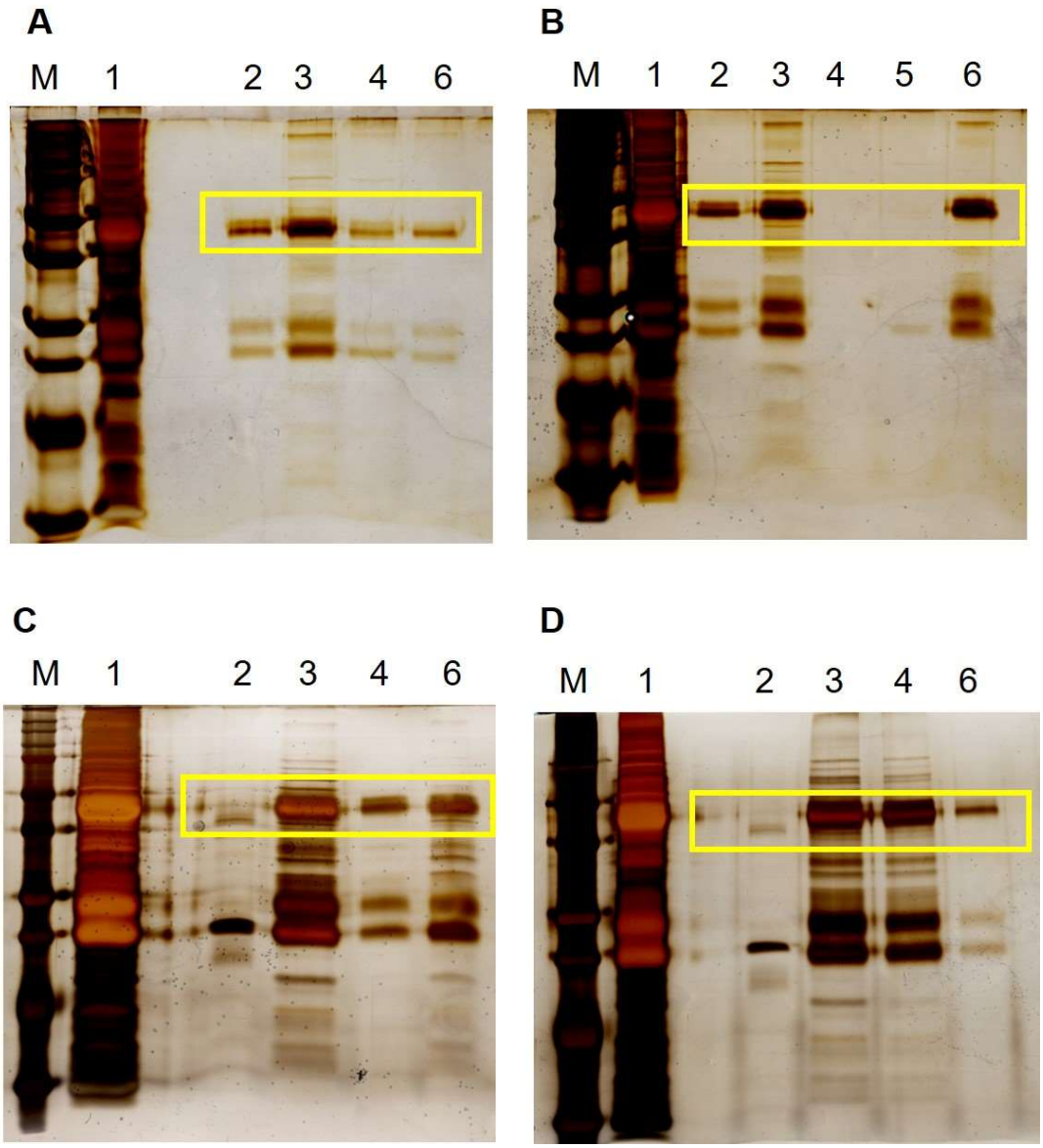

Figure 5.25 SDS-Page gel, stained with silver nitrate, of the pooled fractions collected during the two multimodal columns process. **A**, **B**, **C** and **D** corresponds to processes 1, 2, 3 and 4, respectively. The lanes are all the same: M- Ladder; **1**- Feed (Fab spiked in *E. coli* Lysate); **2** – Flow through fraction of the first column; **3**- Elution fraction of the first column; **4** – Flow-through fraction of the second column; **5**- Wash of second column; **6** – Elution of the second column. A yellow box was added to each gel to highlight Fab fragments – 50 kDa

Table 5.4 Fab recovery yields and purity of each step of the four designed purification processes. Both values were obtained using a protein L affinity column

Process	Columns	Fab Recovery Yield (%)	Purity (%)
1	PPA	**Flow-through** – 31 **Elution** - 51	**Flow-through** - 84 **Elution** – 80
	CHT XT	**Flow-through** - 88 **Elution** - 26	**Flow-through** - 83 **Elution** -86
2	PPA	**Flow-through** - 29 **Elution** - 60	**Flow-through** - 84 **Elution** - 72
	Toyo	**Flow-through** – 11 **Wash** - 2 **Elution** - 78	**Flow-through** – 61 **Wash** - 64 **Elution** - 89
3	Toyo	**Flow-through** - 0 **Elution** - 69	**Flow-through** - 29 **Elution** – 73
	PPA	**Flow-through** - 16 **Elution** - 61	**Flow-through** - 79 **Elution** - 84
4	Toyo	**Flow-through** - 5 **Elution** - 77	**Flow-through** - 37 **Elution** -72
	CHT XT	**Flow-through** - 120 **Elution** -7	**Flow-through** - 81 **Elution** - 86

In the second process, the two selected resins were PPA and Toyo. The PPA step in this process had the same results of the previous one (**Figure 5.25B** and **Table 5.4**). Regarding the Toyo step, a Fab recovery of 78% and 89% purity was an expected result, having in consideration the data previously obtained. The presence of Fabs irreversibly attached to the resin and the lack of affinity towards impurities are the main reasons for this recovery yield and purity, respectively. The obtained gel confirms the presence of a Fab fragment band practically without impurities (lane 6 on the gel B). The third process (**Figure 5.25C** and **Table 5.4**) has the same resins of the second, but in a different order. Having Toyo as a first purification step, the recovery increases slightly (69% vs 60%) while the purity is kept. The high binding of Fab to Toyo at pH 5 is a consistent result throughout this work being confirmed by the lack of Fabs in the flow-through fraction and the presence

of 30% strongly bounded to the resin. The second PPA step of the third process is not as efficient as the second Toyo step on the second process, especially to remove impurities (lane 5 on the gel C). With a recovery of 61% and a purity of 84%, proved to be a resin with the same performance in all the tested processes, including after a Toyo elution step where the salt concentration is higher.

The fourth process had Toyo and CHT as resins. The results (**Figure 5.25D** and **Table 5.4**) show a similar Toyo performance, especially when compared to the process three – 77% recovery, 72% purity. However, this good result was not followed by CHT, showing an elution recovery of 7%, all the Fabs are present in the flow-through fraction (lane 4 on gel D). CHT as polishing step can only be applied if the elution of the first step is not based on salt. The high conductivity of the Fab solution after elution from Toyo did not allow the binding of Fabs to CHT, compromising the overall fourth purification process.

From the four processes designed, the ones having Toyo and PPA resins are the ones with high purification efficiencies. The results achieved using CHT as polishing solution were not satisfied, more development needs to be done with this resin or use it as a first purification step. Regarding PPA and Toyo resins, the consistent results obtained in all the processes, confirming previous data and suggesting that these downstream solutions can be considerate good alternatives for the purification of Fabs. Nevertheless, having in consideration the incomplete recovery of Fabs and the general purity level around 80%, the use of a different chromatographic mode, such as ion exchange or hydrophobic interaction, replacing one of the multimodal steps, could be an interesting option for a more efficient Fab downstream process.

5.4. Conclusion

The most variable regions of an antibody biomolecule are the Fab fragments. The presence of the CDR loops makes each Fab a distinct biomolecule with specific structure, charge and accessibility of the hydrophobic regions [155]. Fabs can be produced using several cell systems or cleaved by enzymatic digestion, thus increasing the variability of these biomolecules. For antibodies, the lack of an efficient upstream alternative to mammalian cells and the use of protein A, targeting a conserved region, as the workhorse of the downstream process, makes the production of any type of mAb a well established

and implemented production process. In the case of Fabs, the different production options and their intrinsic variability compromises the efficient of the overall production process. Especially at the downstream stage, where protein L is the most common purification option. Despite being an affinity solution, it lacks the ability to bind lambda light chains Fabs, some kappa subtypes and traditionally is associated with harsh elution conditions. In this chapter, to tackle the variability obstacle, the possibility of designing a universal downstream process, based on multimodal chromatography was evaluated. When this chromatography mode is selected, and extensive optimization of the process conditions is typically required. In order to screen the best binding conditions of Fab fragments to different multimodal resins, a HT screen system, based on microfluidics was successfully evaluated. Additionally, the binding of different proteins and complex mixtures was also successfully studied. Overal,11 different multimodal resins were tested, for the binding of 4 different biomolecules and 2 complex mixtures, in a total of 15 binding conditions for each target biosample, in a total of 1080 binding experiments to find the best multimodal resins and binding conditions to purify Fab fragments.

The microfluidic approach had a preponderant role on this screen, once it allowed to obtain result within short periods of time and using very low amounts of consumables. The feasibility of this HT system was demonstrated by comparing the standard Fab purification method – protein L, and a well implement HT system, the 96-well filter plate. Furthermore, 5 multimodal resins were selected, and the binding studies at pH 5 and 7 were confirmed with a bench-scale chromatographic system. All these differnt confirmation studies, validated the microfluidic results. The data acquired during the microfluidic assays could be a valuable source of information for the purification of Fab fragments, once the majority of multimodal resins commercially available were characterized in terms of binding conditions. Moreover, the significance of microfluidics was confirmed, holding great applicability as an HT screening system. Regarding the limitations detected during the realization of this work, the most noticeable was the need to use a fluoresce dye to evaluate binding behaviors. The fluorophore can drastically change the characteristics of a targeted biosamples. Nevertheless, in the experiments performed, except for the complex mixtures, the influence of the dye was lessened by the use of uncharge labels and low degrees of labelling and by the thoroughness of the study.

A deeper analysis of the complex mixtures, specially its HCP and DNA/RNA content is fundamental to expedite the implementation of new chromatographic solutions at the

downstream process of biomolecules. The device herein described has one major limitation: the fluorescent-based detection mode. Despite being suitable for single molecules, the detection mode for complex mixture has still some weakness, specially the ability to distinguish between different biomolecules. Having in consideration the pressing need to ensure a complete study of all the impurities in a given production process, an upgrade of the microfluidic device could potentiate its application in an industrial scenario. One of the upgrades could be the implementation of UV sensors [304]. The design of a new microfluidic device able to detect label-free biomolecules, while keeping the speed and handling features could radically changes the way downstream process development is currently executed.

The result-based funneling process led to the selection of three multimodal resins. For these, a binding study targeting *E. coli* process impurities, and a lysate spiked with Fab was successfully accomplished. The results indicated an accentuated Fab selectivity, with the majority of impurities flowing through or irreversible bound to the column. With the data acquired, four two-column downstream processes, based on three resins was done. An overall evaluation of the results indicates a good recovery yield and efficient removal of impurities. The best process was the one where PPA was the first resins followed by Toyo. The results of the two-column processes agreed with all the previous results and demonstrated and accentuated level of consistency.

The process development approach executed in this chapter allowed to study the interaction of two complex variables. The use of microfluidics complemented with a bench-scale chromatographic system was a procedure capable of designing a downstream process within a short period of time and confirm the results obtained in each technique. Despite the good results obtained using multimodal chromatography, the implementation of other chromatographic modes to purify Fab could promote higher purification yields. Additionally, instead of acquiring results one by one, the application of a design of experiments approach could increase the output of data.

Chapter 6

Evaluation of phenylboronic acid as ligand to purify Fab fragments

6.1. Introduction

Boronic acid-based ligands have the ability of binding *cis*-diol containing biomolecules, making them a class of chromatographic affinity ligands – boronate affinity chromatography. Different applications, based on this interaction, have been explored which include the analysis of carbohydrates, the separation of sugars and the purification of several biomolecules such as glycoproteins, glycopeptides, nucleosides and nucleic acids [305]. One of boronic acid ligands is Phenylboronic acid (PBA), commonly used as a purification solution to capture antibodies [306]. Their ability to specifically recognize glycans, present on antibodies, made PBA a possible alternative to protein A affinity chromatography as the main capture step for mAbs. Several studies focused on this hypothesis demonstrated the ability of PBA to purify mAbs, from a cell culture fluid, with high recovery yield and purity [306]. Additionally, being PBA a synthetic ligand, its implementation on an antibody downstream process would promote economic savings, when compared to the more expensive protein A[307].

The complexity of PBA allows this ligand to bind biomolecules by several types of interactions. The predominant one, responsible to bind *cis*-diol groups, is a reversible covalent ester bond [308]. The presence of N-linked oligosaccharides, at the asparagine residue on C_H2 domain of the Fc region of antibodies, allows the interaction between PBA and these glycoproteins. Different sugars are present on Fc, including fucose, galactose and mannose, all containing 1,2-*cis*-diol groups capable of forming covalent ester bonds with PBA [306]. Depending on the pH, this ligand can adopt different conformations, promoting different *cis*-diol interactions (**Figure 6.1**). In acidic environments (pH < pKa), boronic acids have a trigonal planar form that can be altered to a tetrahedral boronate anion, upon hydroxylation, when in alkaline environments (pH > pKa). Both conformations retain the ability to interact with diol compounds, however, the tetrahedral equilibrium constant is higher when compared to the trigonal one ($K_{eq\text{-}tet}$

> $K_{eq\text{-}trig}$), making the interaction at acid conditions less favourable [309]. Additionally, the presence of an aromatic ring on the PBA structure is responsible for hydrophobic interactions and π-π interactions [310]. Moreover, electrostatic interactions between boronates and diols are also prone to occur, through coulombic attraction or repulsion. Other interactions include hydrogen bonding and charge transfer. The last one is likely to happen in acidic conditions, as a result of the presence of a free orbital in boron atom, in the trigonal uncharged form. This free orbital can serve as an electron receptor and a coordination interaction can occur, promoting a Lewis acid-base type of interaction [308].

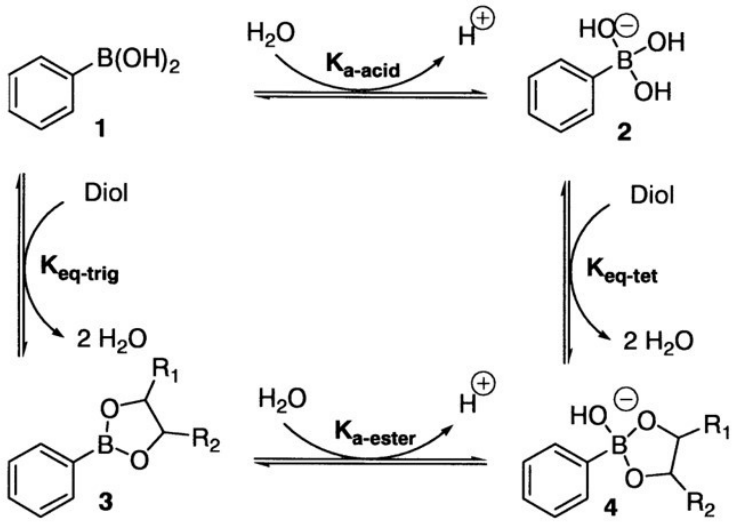

Figure 6.1 Schematization of the different PBA forms at different environment pHs and upon interaction with diol [317].

PBA ligand, as a purification tool, was vastly characterized and applied in our group. Several studies including fundamental characterization [311], purification of different biomolecules [312], thorough mAbs process development [313] and economical studies have been made [307]. However, there was stil. space for another study: the use of PBA as a purification tool for an antibody derivate biomolecule – Fab fragments. Like Fc fragments, Fabs, when produced in mammalian cell lines or after antibody digestion, have sugar molecules on their structure, and theoretically, are able to interact with PBA. However, the interaction responsible for the binding of antibodies to PBA is commonly stated to occur in the Fc region. Having this in consideration, the work developed in this chapter has two main goals: (1) understand whether PBA can be applied in the purification of Fab fragments produced in mammalian cell lines and/or after an antibody digestion process and (2) understand the influence of Fc and Fab fragments in the binding

of a antibodies to PBA. To accomplish this, and considering the multimodal nature of PBA, the approach applied in the previous chapter was repeated. In addition to the microfluidic binding studies, in different pHs and salt concentrations, microfluidic elution studies were also executed, with different elution agents. The microfluidic results were evaluated, and a bench-scale confirmation was made in an ÄKTA purifier system. The studies herein executed targeted both Fc and Fab fragments, and the best results were also compared with whole antibodies.

This chapter contains sections published, as a research article, in the journal Separation and Purification Technology with the name Studies on the purification of antibody fragments (2018) [113]. The work herein developed resulted from a highly collaborative effort with the Master student Miguel Ambrósio. Part of the results showed in this chapter were executed during his Master Thesis.

6.2. Materials and methods

The studies developed in this chapter were similar to the ones on **Chapter 5**. The only differences were: (1) use of lambda light chain Fab fragments (2) microfluidic elution studies and (3) ÄKTA confirmation studies. Gammanorm and CHO labelling protocol (see **section 5.2.3**), IgG digestion protocol (see **section 5.2.4**), kappa light chain Fabs and Fc fragments purification from the digestion mixture (see **section 5.2.5**), microfluidic structure fabrication, microcolumn packing, and microfluidic binding studies (see **section 5.2.6**) followed the previous described protocol. To avoid unnecessary repetition of identical protocols, those will not be here described. Minor alterations will be referred on the results and discussion section of this chapter. The materials and biologics were also the same. The ones applied in the different procedures of this chapter will be referred in its specific section.

6.2.1. Production of lambda light chain Fab fragments

Lambda light chain Fabs used in these chapter were produced by digestion of a polyclonal mixture of IgG (Gammanorm®). The lambda Fabs were purified from the digestion mixture as it is described on **Section 5.2.4**. This class of Fabs do not bind to protein L, so

the flow-through sample was concentrated, and buffer exchanged with a 30 MWCO Amicon centrifugal filters. Both labelled and non-labelled lambda light chain Fabs were produced and purified using the same methodology.

6.2.2. Microfluidic elution studies

The microfluidic elution studies follow the same methodology for microcolumn packing and microfluidic binding studies (see **section 5.2.6**) with an extra elution step. In this, the elution solution flow through the column, were kappa or lambda light chain Fabs are bound to the beads, and the decrease of fluorescence is monitored and recorded (as described on **section 5.2.6.3**). The beads applied in this study were aminophenylboronate P6XL resin, purchased from Prometic Bioseparations (Canada). The elution buffers were Tris, D-Sorbitol, Urea, Magnesium Chloride (all from Sigma Aldrich (USA)), Arginine (ACROS organics (USA)) and Guanidine Hydrochloride (Invitrogen (USA)). All were used in different concentrations.

6.2.3. Confirmation of the microfluidics studies at bench-scale

6.2.3.1 Binding studies

Binding studies of pure Fab (kappa and lambda) and Fc fragments and CHO supernatant to aminophenylboronate P6XL resin were made at bench-scale using an ÄKTA™ Purifier 10 system (GE Healthcare). In all the chromatographic runs, the column was equilibrated, before injection, with binding buffer (50 mM Acetate/Phosphate/Carbonate buffer pH 5/7/9 with variable NaCl concentrations). Upon equilibration, 200 µL of pure Fabs/Fc (1 mg/mL) and CHO supernatant were injected, individually. The loaded column was washed with the binding buffer for 7 CV (1 CV = 1 mL) before an elution step with 1M Tris-HCl, pH 8.5. In all chromatographic runs, the conductivity, pH, and UV absorbance at 280 nm were continuously monitored. The data was acquired and processed by the software Unicorn 5.1.

6.2.3.2 Elution studies

Elution studies of pure Fab (kappa and lambda) and Fc fragments and IgG, all at 1mg/mL (200 µL) were made at bench-scale using an ÄKTA™ Purifier 10 system (GE Healthcare). The binding of all samples to aminophenylboronate P6XL resin was performed using the same binding buffer, 50 mM Phosphate, pH 7. The loaded column was washed with the binding buffer for 7 CV (1 CV = 1 mL) before an elution step. A 10 CV gradient elution was executed using different elution agents (tris-HCl, sorbitol, arginine). In the end of the elution, a column strip was made with 1M Tris-HCl, pH 8.5 and a regeneration step with 1 M NaOH was also performed. In all chromatographic runs, the conductivity, pH, and UV absorbance at 280 nm were continuously monitored. The data was acquired and processed by the software Unicorn 5.1.

6.3. Results and discussion

6.3.1. Initial Microfluidic studies with Phenylboronic acid resin

To access the ability of phenylboronic acid (PBA) to bind digested Fabs, an initial microfluidic binding study was performed. This first screen was done in parallel with the one described on **section 5.3.1**, where the comparison between multimodal and cation exchange ligands was done. All the chromatographic conditions were the same and the kappa light chain Fabs (purified after digestion with protein A and protein L) were labelled with Alexa Fluor® 430. The results obtained for this initial screen are represented on **Figure 6.2** [113].

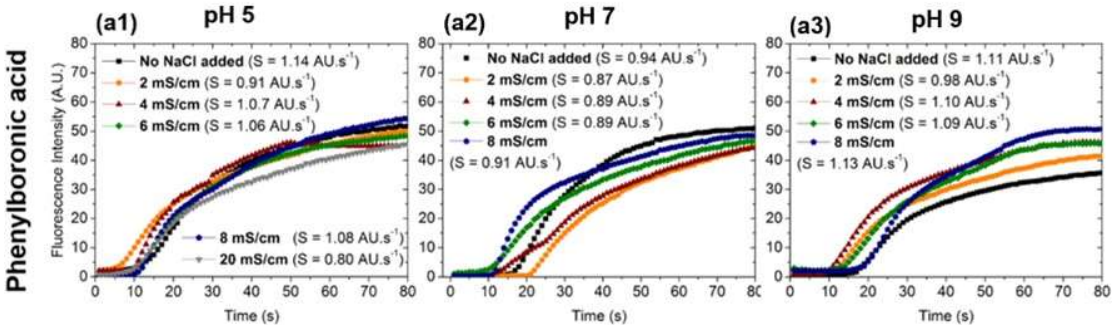

Figure 6.2 Fluorescence measured over time while a Fab fragment solution (30 μg/mL) was flowed continuously through the PBA resin under different pH values (**a1-a3** – pH 5, pH 7 and pH 9, respectively) and conductivities. The slopes of the linear region of the different curves are indicated in brackets

The results obtained with the PBA resin showed high binding capacities in all the conditions tested. The obtained slopes are very high (at least twice as higher as the slopes obtained with Capto MMC – **Figure 5.5**) and similar for different pH and conductivity conditions, with variations within the error of the method. These results were rather surprising, since it was assumed beforehand that the glycosylation level of Fab fragments under study were lower than in the whole antibodies, and thus the affinity interactions with the PBA ligand, would be lower when compared and described for glycosylated proteins, including antibodies [313]. There are three possible explanations for these results. The first is the presence of N-glycans in the Fab portion [314] of the digested IgGs is enough to form covalent ester bonds between the boronic acid ligand and the cis-diol molecules in the Fab fragments. Nevertheless, N-glycans are only known to occur on 15% to 25% of the Fab fragments [49] and thus this hypothesis alone cannot explain the high binding of Fab fragments to the PBA ligand. The second hypothesis is based on non-affinity interactions that can occur between Fabs and the PBA ligand, which include: charge transfer, hydrophobic, electrostatic, and hydrogen bonding. This could be an explanation for the effective binding of Fab fragments in different conditions, for example: high conductivities can promote hydrophobic interactions; and high pH values enhance electrostatic interactions between the hydroxyboronate anion (pKa = 8.8, tetrahedral conformation; sp^3 hybridization) and Fabs, while low pH values promote charge transfer coordination with the boron atom (trigonal conformation; sp^2 hybridization) [315]. If this last hypothesis is correct, phenyl boronate is acting purely as a multimodal ligand, with different types of interactions dominating depending on the experimental conditions. The third explanation is related with the dye used to label the

Fabs – Alexa Fluor® 430. As it was demonstrated in other works [268], Alexa dyes are responsible for an accentuated change in the pI and hydrophobicity of the molecules. The universal binding obtained with PBA could be a result of the presence of the dye on Fab fragments, promoting a stronger interaction with the resin. If this is the case, the affinity of PBA towards the fluorophores must be mitigated by using a different dye such as BDP TMR NHS. A more thorough study on the use of phenyl boronate to purify Fabs needs be performed in order to further understand the effect of the dye and which are the main interactions involved in the adsorption of these biomolecules to the resin.

6.3.2. Hight throughput microfluidic biding studies with phenylboronic acid resin

The initial results with PBA, where its universal ability to bind Fabs was demonstrated, were thought-provoking. The ability to selective bind glycoproteins is well documented, however, the high binding observed at every condition studied, especially at different pHs, were surprising. To better understand the interaction between PBA and Fabs, a new set of experiments was conceived. A thorough study was executed, where the binding to PBA resins was tested not only towards kappa Fabs, but also to lambda, Fc fragments and IgG. CHO supernatant, as a complex media was also evaluated. To minimize the effect of the fluorophore on the experiments, BDP TMR was used to label all the biomolecules and complex mixture used in this section of the work. With the knowledge acquired in the previous chapter, the use of this dye will not interfere significantly with the results. Additionally, the degree of labelling of the single biomolecules was kept low, to mitigate as much as possible the effect of the dye, like in **Chapter 5**. The binding conditions, pH and NaCl concentration were similar to the ones used previously (**section 5.2.6.4**), with the exception of an extra binding condition, at all the pHs, where the NaCl concentration was 1 M. This result will not be present in the heatmaps, and it was performed to confirme the salt-tolerance of PBA. In this study only CHO supernatant will be tested as a complex mixture once the putative Fabs produced on *E. coli* will not be glycosylated. The data acquired (treated as described on **section 5.3.3**) with this new set of experiments are present on **Figure 6.3**.

The first conclusion upon analysis of all the heatmaps present of **Figure 6.3** is the pH dependency of PBA to bind the antibody fragments. With an increase of pH, the binding to this resin drastically decays, especially for the two classes of Fabs and Fc fragments. The effect is present also on IgG, however at a lower extense. The constant binding, even at high pH, observed previously (**Figure 6.2**) was not observed in these studies. This can be related with the modification caused on Fab by the conjugation with the Alexa Fluor® 430. This alteration increased the hydrophilic nature to the labelled Fabs, increasing the interaction with the aromatic moiety of PBA, creating the conditions for a universal binding to the ligand. The decrease binding observed for Fabs on **Figure 6.3**, at higher pHs is an expected result. At pH 9, both ligand and the biomolecules are negatively charged, creating a strong electrostatic repulsion phenomenon and hindering the binding through *cis*-diol groups present in Fabs, Fc and IgG [308]. Because Fabs labelled with Alexa Fluor® 430 had a higher degree of labelling, thus higher hydrophobicity, the binding at pH 9 was still able to occur, mainly through hydrophobic interaction. Additionally, since Alexa Fluor® 430 labelled Fab can make the necessary surface contact with the ligand, possibly covalent ester bond is also occurring.

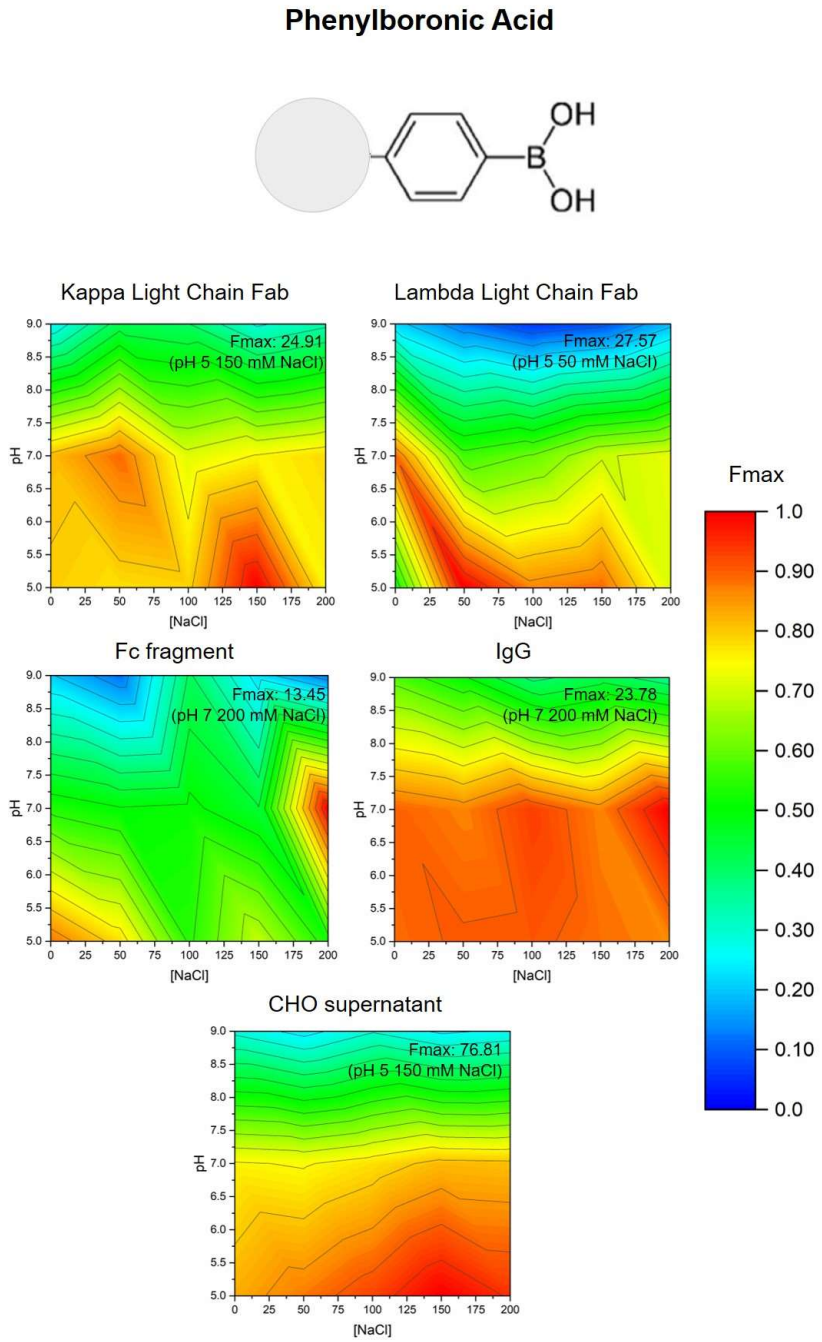

Figure 6.3 Heatmaps obtained for the binding of different labelled biomolecules (Fab and Fc fragments, IgG) and CHO supernatant to PBA at different binding conditions. In all the heatmaps the highest Fmax and the conditions where it was obtained is indicated. All the Fmax values of the heatmaps were normalized using the highest value for each study.

The binding at pH 5 and 7, for the two classes of Fabs, is comparable. Small binding differences are observed, at different NaCl concentrations, while keeping the overall binding behavior. At these pHs, the neutral trigonal configuration of PBA can interact with the Fabs through the *cis*-diol groups present on this digested antibody fragemnts.

Hydrophobic interactions, caused by the aromatic ring on PBA, may also be promoting the binding to Fabs, specially at higher salt concentrations. Electrostatic interactions are less likely to occur, since when using buffers with 1 M of NaCl (results not shown) the binding at all the pHs was not affected, proving the salt-tolerant nature of PBA. Furthermore, at pH 5 and 7, the empty orbital in the boron atom could be promoting charge transfer by becoming a Lewis acid capable and accepting a pair of electrons from a Lewis base [316]. The putative presence of carboxylate groups (e.g. aspartate and glutamate) and uncharged primary amines (e.g. glutamine, asparagine), could be source of those Lewis base electrons [308]. For Fc fragments, the results also suggest a constant binding to all the salt concentrations tested at pH 5 and 7, except at two distinct regions where the binding is higher. It is possible that the same type of interactions occurring with Fab fragments is also occurring with Fc. The presence of a lower percentage of N-glycans on these fragments, in comparison to whole IgG, promotes interactions not only based on the *cis*-diol groups, but also based on charged and/or hydrophobic putatively patches more available on the Fc, which may explain why the stronger binding occurring at pH 5 with no salt and at pH 7 with 200 mM of NaCl – the two red regions on Fc heatmap. Regarding IgG, the binding is salt tolerant and constant for all the experiments done at pH 5 and 7. The PBA affinity towards *cis*-diol groups on IgG is well documented and could be the main responsible for the interaction [317], although secondary charge transfer, hydrogen bonding and hydrophobic interactions may also be occurring, but not with the specificity and strength of the covalent ester bond. Finally, for CHO supernatant, the pH also shows great impact on the binding. An increse of the pH promotes a decreasing of the binding of this complex mixture. The high binding at pH 5 and 7 is not an expected result, since this resin has a documented selectivity towards mAbs in cell culture fluid [306,317]. Nevertheless, having in consideration the results obtained with the complex mixtures on **Chapter 5**, the relative low Fmax values (76.81 at 150 mM, pH 5) obtained for the CHO supernatant is encouraging of a low affinity for the impurities present of the media toward PBA. Additionally, the high degree of labelling and the presence of several impurities capable of being labelled by NHS-click chemistry, promotes an increase of this complex mixture hydrophobicity, creating the conditions for an atypical binding to PBA.

The results obtained on this section agree with the general data present in other works where PBA is used as a purification/selection solution for antibodies. At lower pHs (5 and 7) the presence of *cis*-diol moieties on the target biomolecules promote an effective binding to PBA through covalent ester bond. A good example are the results obtained with whole IgG biomolecules which with glycan molecules available to bind to PBA, and thus promoting a constant binding at all the salt concentrations tested at pH 5 and 7. In the case of Fabs, the analysis is more complex. The percentage of N-glycans on Fabs is lower when compared to whole antibodies, and so the binding to PBA is not mainly driven by covalent ester bond, hydrophobic, charge transfer and others may be playing an important role. The same happens for Fc. Moreover, the different binding profile obtained with kappa and lambda Fabs can be a consequence of a N-glycans variability on different classes and types of Fabs. The use of a polyclonal mixture of Fabs and Fc can also generate different binding patterns to PBA. Other factor promoting difference on the binding to IgG, Fab and Fc is the digestion. Despite not affecting the structure of sugars [318], after digestion both Fabs and Fc could be structurally rearranged, and the availability of sugars altered. A final comment can be made by analysing the heatmaps of the two antibody fragments herein studied. The regions where Fabs binds less to PBA are the same regions where Fc binds better, and vice-versa. With this analysis and the heatmap obtained for IgG, it is possible to generate the hypothesis of a cooperative binding, between the Fab and Fc, in the binding of antibodies to PBA.

6.3.3. Hight throughput microfluidic elution studies with Phenylboronic acid resin

The binding between PBA and *cis*-diol containing biomolecules is complex. The diversity of interaction modes makes the study of the chromatographic operational conditions a challenge. The binding of Fabs to PBA was hypothesized to be mainly driven by the covalent ester bond, formed upon binding to the N-glycans present on these biomolecules. Secondary interactions are possible to occur, especially hydrophobic interactions or charge transfer. With this information, an elution microfluidic study was designed to find the ideal elution agents and to infer about the type of interaction between PBA and Fabs (kappa and lambda). The elution agents selected were arginine, tris, sorbitol, magnesium chloride ($MgCl_2$), guanidine and urea. Sodium chloride, a traditional salt elution agent,

was not considered once PBA was able to bind Fabs with different pHs buffers containing 1 M of NaCl. The elution studies followed the same microfluidic protocol as the binding, with an extra step, where the selected elution buffer flows in the microcolumn and a decrease of fluorescence is observed. Binding of Fabs to PBA occurred at pH 7 with no salt (50 mM phosphate, pH 7). All the elution buffers were at pH 8.5 and had 150 mM of Tris (except the Tris buffer). The quantification of the different elution conditions is made by calculation the slopes of the elution curves in the initial 15 seconds. The elution curves obtained in this study are represented on **Figure 6.4** and **6.5**. In all the graphs, the curve correspondint to only the binding buffer is represented (black squares, 50 mM phosphate pH 7).

Arginine is generally used to ensure a mild elution of antibodies from protein A. In the presence of this amino acid, the aggregation after elution is less prone to occur, and the eluted unfolded antibodies can refold back to its native state [319]. Additionally, boronate affinity columns are described to purify arginine containing peptides [320]. Having these in consideration, arginine was applied to elute kappa and lambda Fabs from PBA resin. The results on **Figure 6.4** show a decrease of fluorescence over time when arginine is used as an elution agent, for the two classes of Fab fragments. Higher concentrations of arginine promote faster elution ratios, however, for concentrations higher than 500 mM the difference is no longer significant. Differences in the elution of kappa and lambda Fabs can be observed, with the last, showing higher slopes values, and being more affected by the presence of arginine. This difference can be caused by the difference availability of N-glycans, or other interactions patches on Fabs, that promote different competition between them and arginine. Nevertheless, despite the different elution rates, in both classes of Fabs, the fluorescence reaches the same level. The results showed here demonstrate the applicability of arginine as Fabs elution agent from PBA. This amino acid could be responsible for a competition, with Fabs, at the boron atom, promoting the disruption of the ester covalent bond. Additional, arginine can be responsible for disrupting several types of interactions, including, hydrogen bonding, π-π and hydrophobic, making it an agent for protein desorption mechanisms [292].

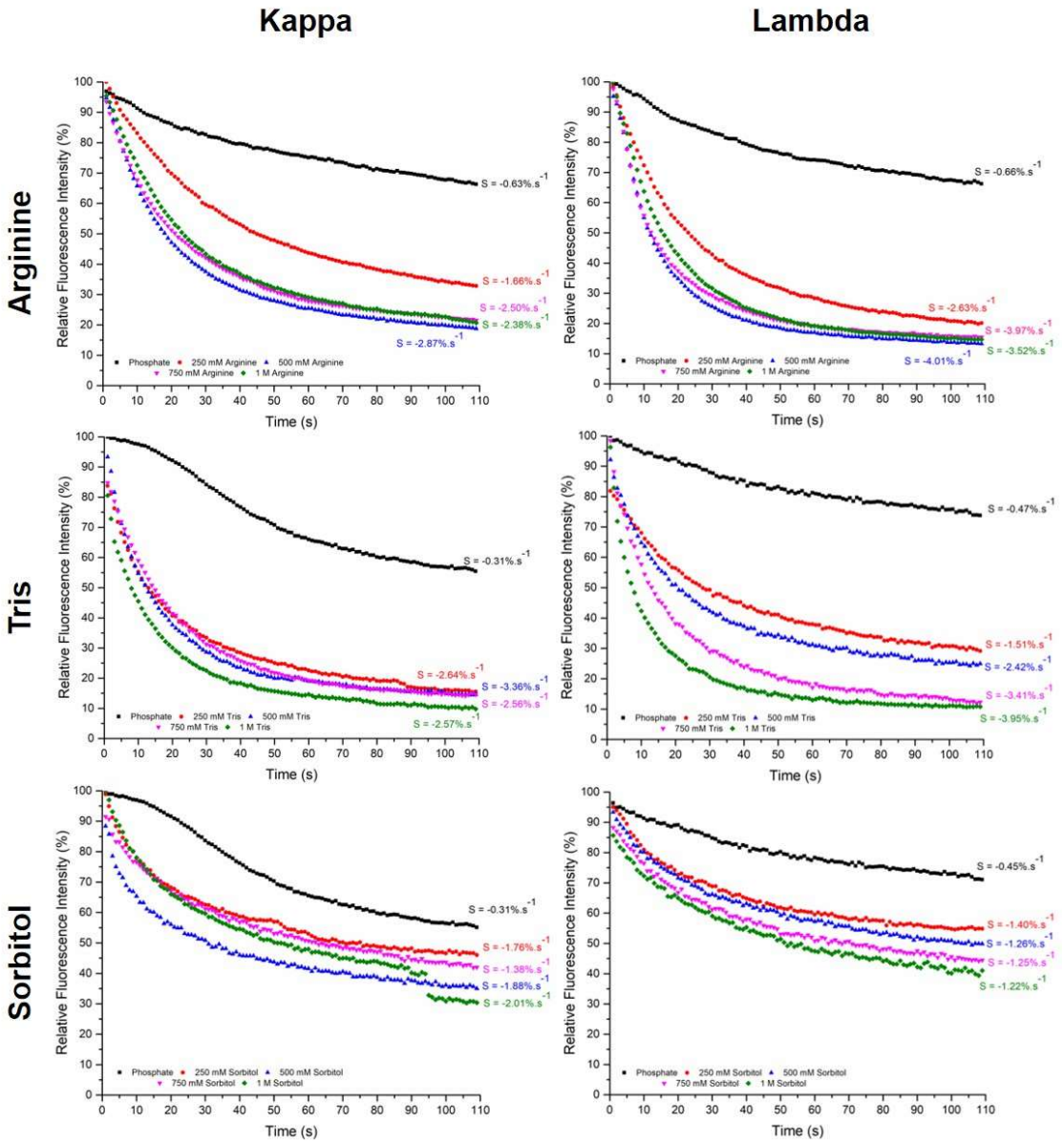

Figure 6.4 Fluorescence measured over time of Fab fragment elution from a PBA using different elution agents (arginine, tris and sorbitol), after adsorption using 50 mM phosphate at pH 7 as binding buffer. The slopes obtained in the linear region for each condition are indicated

The use of Tris to disrupt specific and non-specific interactions with PBA was previously reported for mAbs [317]. Tris is a *cis*-diol competitor and thus can be used as an elution agent for boronate affinity chromatography. The same is true for sorbitol, despite being less effective than Tris, it can also compete for *cis*-diol interactions. The results for these two elution agents, present of **Figure 6.4**. Comparing both, the results obtained for Tris showed faster elution rates when compared to sorbitol. Both show concentration dependency upon elution, with faster elution occurring at higher concentrations. These results are expected, the same performance has already been described [317].

Sorbitol is only able to compete for *cis*-diol interactions, and consequently its strength is not as high as it is for Tris. Comparing the two classes of Fabs, Tris seems to elute faster kappa than lambda Fabs, while for sorbitol there is no differences between the tested Fabs.

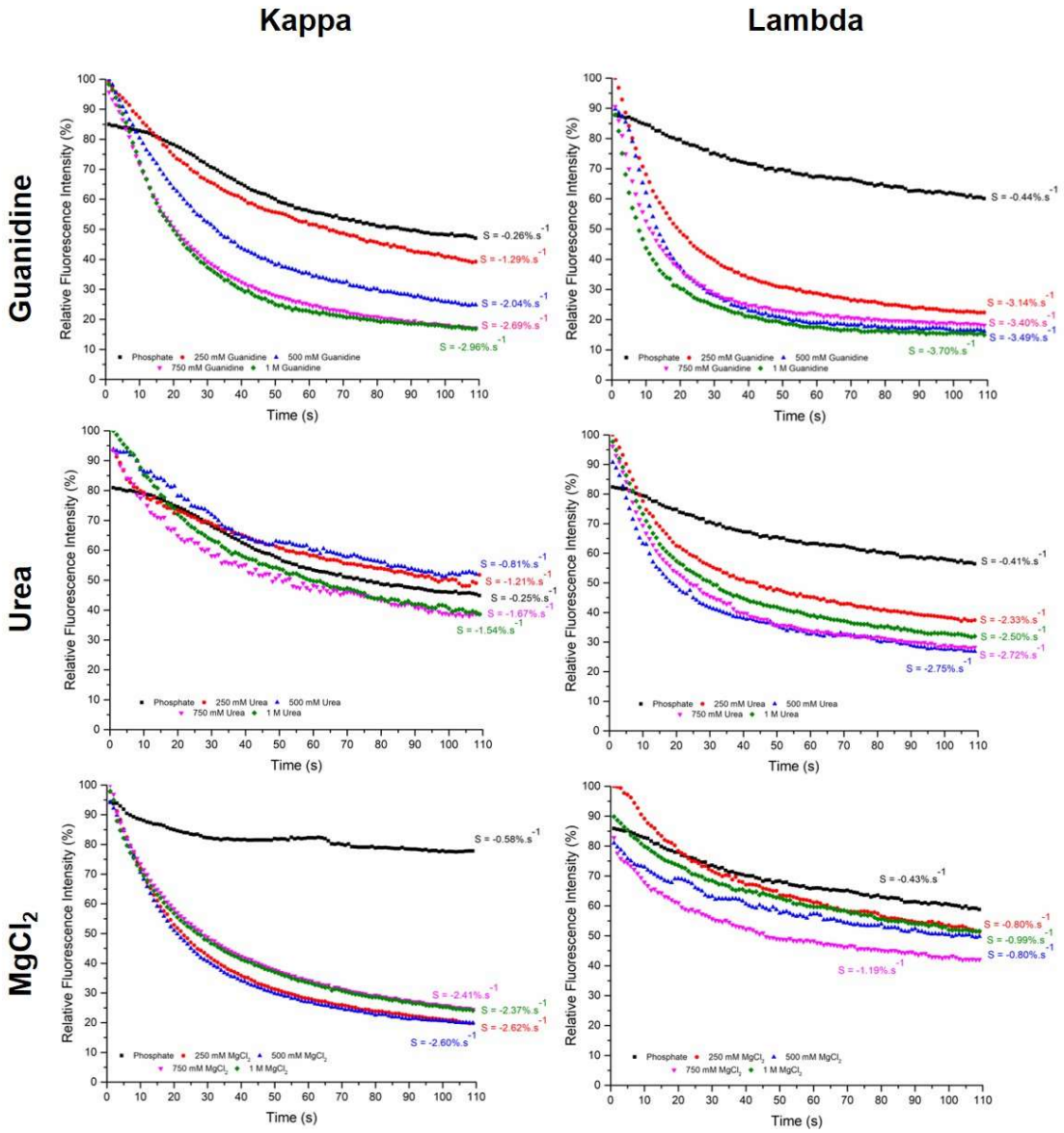

Figure 6.5 Fluorescence measured over time of Fab fragment elution from a PBA using different elution agents (guanidine, urea and magnesium chloride), after adsorption using 50 mM phosphate at pH 7 as binding buffer. The slopes obtained in the linear region for each condition are indicated.

Urea and guanidine are two denaturating and chaotropic agents commonly used as elution agents [321,322]. Their ability to disrupt hydrogen bonds and hydrophobic interactions is limited by their propensity to denature proteins impairing their biological activity. Nevertheless, a relative low concentration of both was tested (until 1 M) to access their

applicability in the elution of Fabs. Interestingly, urea and guanidine have more effect on the elution of lambda Fabs than kappa (**Figure 6.5**). For the last, urea is the elution agent where slower elution rates were observed, and the fluorescence did not decrease above 40%. The same happened for lambda Fabs, but with faster elution rates. For guanidine, the elution rate is also faster for lambda than for kappa Fabs, however, lower fluorescence levels are achieved. With these results it is possible to hypothesize that lambda Fabs are more prone to denaturation by the tested agents, and so, eluted faster and more easily. Kappa Fabs being more stable [37], are not so affected by urea or guanidine, and the elution is not as efficient. Another conclusion related with the type of predominant interaction can be taken. Urea and guanidine are known to disrupt different kinds of interactions, except the *cis*-diol, being kappa Fabs more resistant to these elution agents, it is possible that the predominant interaction of this class of Fabs with PBA is the covalent ester bond. The opposite for lambda Fabs, being easily eluted with urea and guanidine, the major interactions present, upon binding with PBA, could be hydrogen bonding, charge transfer and/or hydrophobic, easily disrupted by urea and guanidine.

Magnesium chloride is also a chaotropic agent applied in the elution of antibodies [322]. Its ability to disrupt hydrogen bonding and other type of interactions was considered in this HT elution screen. The result with this agent shows almost no impact on the elution of lambda Fabs, and a considerable impact on kappa (**Figure 6.5**). The presence of this salt, even is low concentrations, is enough to promote a high degree of elution for kappa light chain Fabs. Probably, a rearrangement of the ligand and/or kappa Fabs, in the presence of magnesium chloride is promoting the disruption of hydrogen bonds or hydrophobic interaction, creating the necessary conditions for an efficient elution. For lambda, the elution curves have approximately the same slope as the binding buffer, proving the low effect of magnesium chloride on the elution. The results obtained with this elution agent are an ideal example of the complexity of PBA ligand. Like urea and guanidine, sodium magnesium is a chaotropic agent, however, for the first two the class of Fabs more prone to be eluted were lambda, while for magnesium chloride, kappa Fabs are more easily eluted. A deeper study focusing not only on the elution of Fabs but also in the binding could clarify the main interactions involved in the binding of these antibody fragments do PBA. An appropriate tool for this study could be thermodynamics, already applied for mAbs and PBA [311].

With the HT screen results herein developed it was possible to narrow the choices for elution agents. *Cis*-diol competitors, such as tris, arginine and sorbitol outperformed urea, guanidine and magnesium chloride in the elution of Fabs. The first three, know to disrupt specific and non-specific PBA interactions, showed no significant differences between kappa and lambda Fabs, proving to be more universal elution agents than urea, guanidine and magnesium chloride. Considering the results obtained with tris, arginine, and sorbitol and their low of impact on the tertiary structure of Fabs these agents will be tested at bench scale. Regarding the applicability of microfluidics to screen for elution conditions, the overall evaluation is positive. The only limitation, besides the labelling with a fluorophore, is related with the contact time between the elution buffer and the sample bounded to the resin. To minimize the photobleaching effect, the superficial velocity used for elution is considerbly high (above 1200 cm/h) and could compromise the elution by not allowing the necessary contact time between the buffer and the target/resin. A possible solution could be the implementation of a microfluidic platform with a UV sensor, promoting the realization of binding and elution experiments without the need of a fluorescent dye.

6.3.4. Confirmation of microfluidic binding studies on a bench-scale ÄKTA purifier system

The chromatographic microfluidic approach applied in this thesis is a method to rapidly screen different operation conditions and select the best for further studies. Despite the productiveness of this type of platform, the confirmation using a bench-scale chromatographic column is always needed to access if the chromatographic results were influenced by different experimental scales (micro vs bench). The PBA data acquired with microfluidics was compared in a packed column, containing 1 mL of resin. These studies were focused on the two classes of Fab fragments, kappa and lambda, Fc fragments and CHO supernatant. Five binding conditions were selected: pH 5 with 150 mM NaCl, pH 7 with 0, 50 and 150 mM NaCl and pH 9 with 150 mM NaCl. After the

binding, an elution step, with 1 M Tris-HCl pH 8.5 was performed. The chromatographic results are represented of **Figure 6.6**.

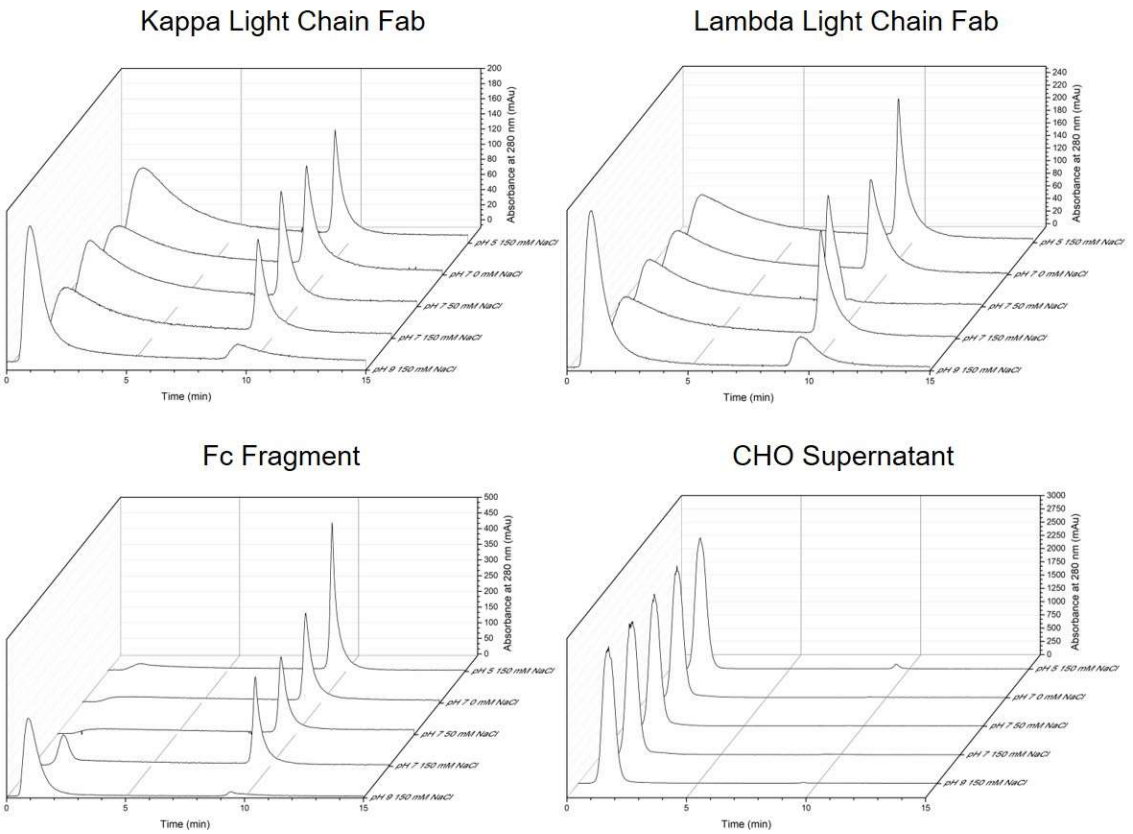

Figure 6.6 PBA binding studies confirmation at bench-scale. Chromatograms obtained after injection of different samples on a 1 mL PBA packed column. Kappa and Lambda Fabs, Fc fragments and CHO supernatant were injected, at different binding condition and eluted with 1M Tris-HCl.

For the same binding conditions, the chromatograms of kappa and lambda Fabs were similar (**Figure 6.6**). At pH 5 and 7 (at all NaCl concentrations), it is possible to observe a wide flow-through peak followed by a sharp elution peak. The chromatograms, at these pHs and salt concentrations, have the same profile and approximately the same peak height, corroborating the microfluidic results where no significant differences were observed at pH 5 and 7, at the tested salt concentrations. Several interactions may be involved in this binding, as previously discussed. At pH 9, a large flow-through peak is observed as a result of a reduced binding of both classes of Fabs to PBA, caused mainly by electrostatic repulsion between Fabs and the ligand [308]. The same result was observed on microfluidics. The higher binding capacity at pH 5 and 7, and salt tolerance was observed in the two chromatographic approaches taken, confirming the binding

results for kappa and lambda light chain Fabs. However, the wide flow-through peak observed in the bench-scale chromatographic studies, for kappa and lambda Fabs, at pH 5 and 7, was suprising and may be related with the use of a polyclonal mixture of Fabs during these experiments. These were produced by digestion of antibodies present on Gammanorm® mixture, which is composed by several types and classes of IgGs (59% IgG1; 36% IgG2; 4.9% IgG3; 0.5% IgG4 and at maximum 82.5 μg/mL of IgA). The diversity of this antibody polyclonal mixture, with different classes and subtypes, is transferred to the digested Fabs, which add to the already variable nature of Fabs (result of the presence of CDRs), create a mixture of biomolecules structurally variable. The characteristic Fab structural variability will create different binding to the PBA, especially if the interaction is occurring through the N-glycans on Fabs. The sugars availability to bind to the resin will be dependent on Fab structure, with different Fabs having different level of sugar exposure. The wide flow-through peak is a consequence those structural differences present of the Fab mixture, there are Fabs without N-glycans and the binding simple does not occur. This difference was not detectable in the microfluidic studies, once the Fabs not binding to the beads were not monitored. The application of a detection point, capable of detecting the flow through fluorescence could have given more information about this result, increasing the sensibility of the HT platform.

The Fc results (**Figure 6.6**) follow the same trend as the Fab fragments, higher binding at pH 5 and 7, at all NaCl concentrations, and no binding at pH 9. At pH 7 with 150 mM of NaCl, a higher flow-through peak is observed, however upon calculating the areas under the curves, the ratio between the elution peak and the total peak areas is not significant and lays within the error of the technique (results not shown). The difference between flow-through peaks of Fc and both Fab fragments, suggest a higher affinity of PBA towards the last, confirming previous works where the main interaction between PBA and mAbs is reported to happen at the C_H2 domain of the Fc region. In terms of structural variability, in comparison to Fabs, Fc display a relative constant structure, thus, even in the presence of a polyclonal mixture of Fcs the binding to PBA is constant. To compare binding results of antibody fragments with a whole antibody, an injection of IgGs present on Gammanorm® was done, at pH 7 with no salt (results not shown). The result was a total absence of flow-through, and a sharp elution peak. Despite PBA being able to bind more Fc than Fabs, there are some Fc fragments not binding to the ligand and flowing through the column. The flow-through peaks observed with the two types of antibody

fragments, and its absence with whole antibodies, may indicate a collaborative binding, between Fc and Fab to PBA, as previously referred.

CHO supernatant was the final binding study realized on an ÄKTA purifier system with PBA (**Figure 6.6**). The results are clear, in all tested conditions, there is no elution peak, the most of impurities do not bind to the column. This result is expected, as the PBA selective towards mAbs present in cell culture supernatant was previously described [306]. The difference between these results and the microfluidic ones was also present in the multimodal resin study, and it is mainly caused by the already discussed extreme labelling procedure. Nevertheless, the relative low Fmax values, in comparison to the multimodal resins, was indicative of a low binding of CHO supernatant impurities to PBA, as it was confirmed.

6.3.5. Confirmation of microfluidic elution studies on a bench-scale ÄKTA purifier system

The confirmation experiments done on the previous section were repeated, this time to validate the elution of kappa and lambda Fabs, Fc fragments and IgG from PBA. The binding occurred at pH 7 (50 mM phosphate buffer), with no salt, and the elution, for all the elution agents was done by a gradient elution step of 10 CV (1 CV = 1 mL). The chosen elution agents were tris, arginine and sorbitol. All the elution buffers were at the same pH (=8.5), and concentration (1 M). In sorbitol and arginine buffers, 150 mM of Tris-HCl was added as buffering agent. For all the injected samples, the use of 150 mM tris, as a buffering agent, was tested in a control chromatographic run. All the results are present of **Figure 6.7**.

For the two classes of Fab fragments results are similar, tris and sorbitol, with similar elution peaks outperformed arginine (**Figure 6.7**). The use of 150 mM of Tris has a small effect on the elution, not only of Fabs but also of Fc and IgG, confirming that arginine and sorbitol, at 1 M concentration, are the major players in the elution. These elution results were expected. Indeed, during the microfluidic studies, the buffers more capable to elute Fab fragments were the three selected for this study. However, the similar results obtained with tris and sorbitol were not observed in the microfluidic studies, where tris had a better performance. This difference could be related with the low contact time at

microscale between the elution agent and the chromatographic beads. At normal scale, the linear velocity is slower (156 cm/h), and the contact is more efficient, promoting a better elution. The results obtained with arginine show an elution peak not as high and sharp as the other two elution agents. Probably the same elution effect is happing, competition with the N-glycans of Fabs causing elution, however, arginine appears to be a weaker competitor for this interaction. The presence of a wide elution peak with arginine corroborates this hypothesis.

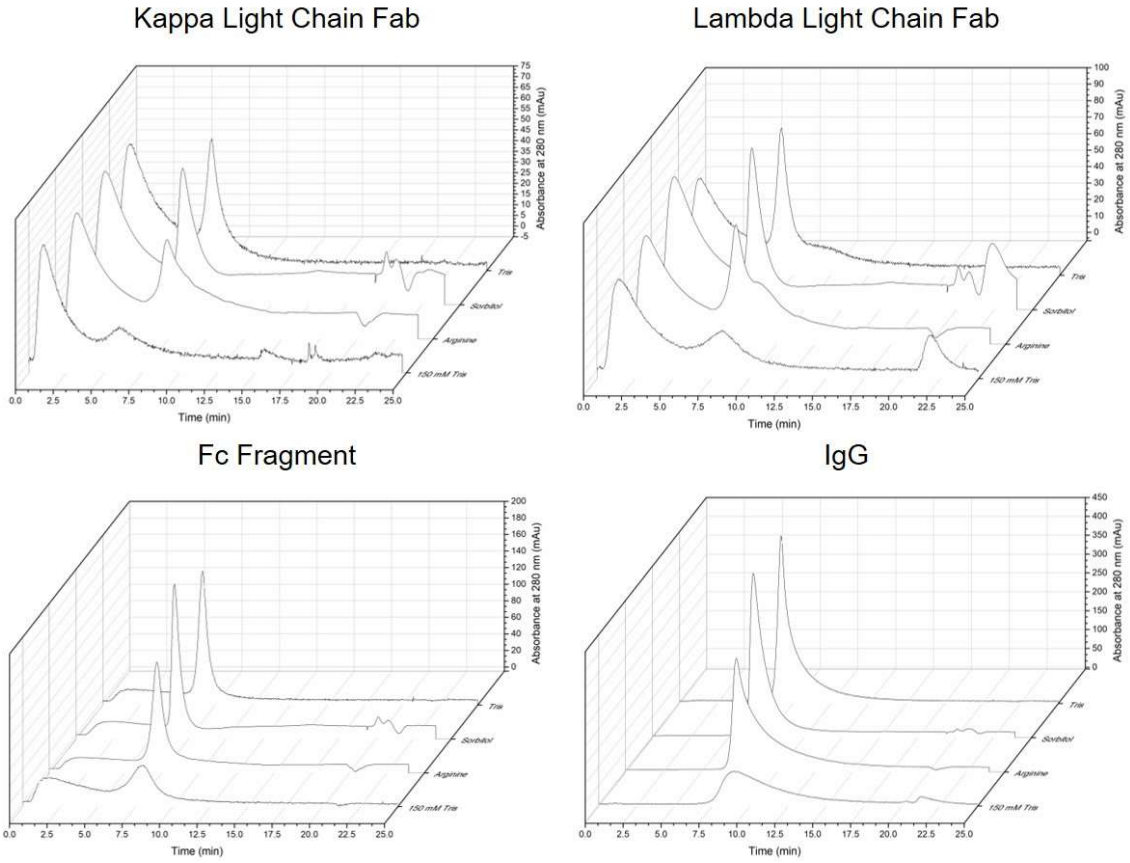

Figure 6.7 PBA elution studies confirmation at bench-scale. Chromatograms obtained after injection of different samples on a 1 mL PBA packed column. Kappa and Lambda Fabs, FC fragments and IgG were injected at the same binding conditions (50 mM Phosphate, pH 7, no salt). Elution was made using a 10 CV gradient, with different elution agents.

Similarly to Fabs fragments, from the three tested elution buffers, tris and sorbitol elute more efficiently both Fc fragments and IgG (**Figure 6.7**). For both biomolecules, higher peaks are obtained with these two elution agents, while for arginine a smaller peak is observed. Having in consideration the same trend observed in all the tested targets, the hypothesis of arginine being a weaker competitor for the covalent ester bonds, in comparison to tris or sorbitol, fits all the data acquired in these experiments. Other result observed is the sharper elution peak, obtained with the three agents, for Fc. A justification

for this could be related with the diversity of the IgG mixture used. Different biomolecules bind differently to PBA, and so the elution does not occur at the same buffer concentration, resulting in a wider elution peak. For Fc, the level of similarity is higher, promoting similar binding and elution and consequently generating sharper peaks.

The general results obtained with microfluidics were confirmed at bench-scale. Tris and sorbitol for all the biosamples tested were more efficient elution agents then arginine. These are responsible to act as competitors for the cis-diol interactions which appear to be the leading interaction for all the antibody fragments tested [317]. To increase the elution efficiency, especially with arginine, the combination of more than one elution agent could promote higher elution yields.

6.4. Conclusion

A microfluidic approach was employed to study the binding of Fabs and Fc to PBA and understand if this ligand can be a solution for the purification of Fab fragments. The microfluidic binding results, for all the tested antibody biomolecules, had the same binding profile: constant binding at pH 5 and 7, at all the salt concentration tested, and loss of binding upon increasing the pH to 9. This result was expected since, at pH 9, kappa Fabs, lambda Fabs, Fc fragments and IgG are negatively charged, like PBA, creating a strong charge repulsion, not allowing the interaction to occur. At pH, 5 and 7, being PBA neutral, hydrogen bonding, charge transfer, hydrophobic and *cis*-diol interactions can occur between the ligand and the tested antibody molecules. It is likely that *cis*-diol interaction is playing a central role in the binding to PBA. The presence of N-glycans in all the biomolecules tested can promote a strong covalent ester bond between them and the ligand. The bench scale ÄKTA results confirmed the salt tolerance of PBA, and the more efficient binding at pH 5 and 7. The presence of wider flow-through peaks, for the two classes of Fabs tested, in contrast to ones for Fc, suggests a higher affinity for PBA to bind the last than the firsts. This result was not observed during the microfluidic results. The extreme variable nature of Fabs, kappa and lambda, and the use of polyclonal mixture of these, could be the reasons behind this result. Nevertheless, if just one Fab is used, the presence of exposed N-glycans could promote an efficient binding to PBA, and this resin can be applied to purify a single monoclonal Fab. Regarding the elution microfluidic

studies, six elution agents were tested. As expected, tris, arginine and sorbitol outperformed the others. These elution agents are *cis*-diol interaction competitors, responsible to break the bonding between N-glycans on Fabs and the PBA. Having this in consideration, tris, arginine and sorbitol where selected to bench-scale studies. The results were similar for Fabs, Fc fragment and IgG, with tris and sorbitol displaying similar results and outperforming arginine.

With the results obtained in this chapter is possible to take three main conclusions. The first concerns the binding of antibodies to PBA, the results achieved in this chapter point to Fc as the main region responsible for this interaction. The presence of higher and wider flow-through peaks when Fabs were injected in PBA column, in comparison to the partly absence of flow-through peaks in Fc injections, indicate a stronger interaction between the Fc region of antibodies and PBA. Fabs may also be involved, but with a minor influence. The second conclusion is related with the variability of Fab fragments. The presence of CDRs and the structural variability of all the classes and subclasses make Fab fragments an extreme variable biomolecule. This will have impact on the exposure of N-glycans, and consequently interfering with the binding to PBA. With the results obtained here, PBA seemed to be a solution of purify Fab fragments, however an initial binding study is needed to access if the N-glycans present on the Fab are exposed to bind to PBA. Finally, the similar binding and elution profiles obtained for Fabs, Fc and IgG, do not allow the use of this resins as a purification solution after antibody digestion with papain. PBA was not able to selective bind any tested antibody biomolecule. The only possible approach is to purify Fab fragments in flow through mode, however, this will only be possible if after mAb digestion, the N-glycans on Fab cannot bind to PBA. If Fabs are produced using a mammalian cell system, being this capable of doing post-translational modification, PBA could be used as a purification tool, if the sugars have and acceptable level of exposure. The lack of selectivity corroborates the general hypothesis of PBA binding to Fabs and Fc by the sugars present on their structure.

Chapter 7

Conclusions and Future Work

Conclusion

The variable nature of Fab fragments creates obstacles in the design of universal downstream process. In this thesis, the focus was to tackle this limitation and explore new solutions to purify this class of antibody biomolecules. Two different experimental routes were taken. In the first, an affinity-based solution, peptides capable of selectively bind Fab fragments were discovered and developed. The second, based on process development, a high-throughput method to find the ideal operational condition to purify Fab fragments, using multimodal chromatography, was designed and applied.

The variability of Fab fragments is also a consequence of the different production processes that can be adopted to generate this biomolecule. Before the study of new purification alternatives, a universal antibody digestion protocol, capable of cleaving a polyclonal mixture of antibodies, and generate Fab fragments, was developed. The result was the establishment of a standard digestion protocol, where essential digestion variables were adjusted to efficiently produce digested Fab fragments from a polyclonal mixture of IgG. Additionally, different purification protocols, to obtain pure digested Fabs, were evaluated. In the end of this initial study, a standard digestion and purification protocol was conceived, and applied to generate pure digested Fabs. The idealization of the protocol to produce pure digested Fabs was one the pillars of this thesis and can be considered an initial approach for procedures where Fab fragments are generated by papain digestion of antibodies.

Production cost, selectivity and flexibility are some of several advantages of peptides as affinity ligands. To take advantage of those, different phage display biopanning strategies were idealized to screen and find peptides capable to bind Fab fragments. The different biopanning schemes designed resulted from the acquired know-how obtained in each screening procedure. With this evolutionary phage display biopanning approach, five different Fab-peptide binders were found: B1, A5, C7, D2 and F3. The first three were able to bind the same Fab fragments, but in different regions. With the ability to bind

three different kappa light chain Fabs, A5 was considered a pseudo-universal Fab binder. B1 and C7 had only affinity towards one Fab fragment. D2 and F3 were considered universal binder for digested Fabs, these two peptides showed high affinity towards all the Fabs produced by enzymatic digestion with papain. B1 was further tested as a ligand on a chromatographic column, being able to purify a Fab, spiked into a *E. coli* cell culture fluid, with a recovery and purity of more than 80%. The ability to use peptides as chromatographic ligands was proved in this thesis. The correct design of a phage display biopanning scheme play a pivotal role in the process of discovering affinity peptide binders. The approach herein developed allowed to target different regions of Fab fragments in order to find universal peptides. Despite none of the five peptides can be considered universal, the experience and the know-how acquired during the three realized biopanning creates good perspectives for future phage display procedures targeting more conserved regions of Fabs and finding universal peptide binders. Nevertheless, taking in consideration the results obtained with B1 peptide and the overall process, from phage display to column immobilization, one month and a half was enough to generate a reliable and reproductible peptide-affinity chromatographic based solution.

Multimodal chromatography was the second solution evaluated to purify Fab fragments. To fully understand the binding mechanisms in this type of chromatography a time-consuming process development must be taken to find which operation conditions promote a more efficient purification. The complexity of multimodal ligands in combination with the extreme variable nature of Fabs, created the need to develop a high-throughput system capable of expeditiously characterize several multimodal resins to bind Fabs. This need was solved with a microfluidic platform capable of screening different chromatographic conditions in a manner of minutes. With this, a thorough process was designed to study the ideal binding conditions (pH and salt concentration) of a polyclonal mixture of kappa light chain Fab fragments to eleven different multimodal resins. Additionally, binding to other proteins (Fc fragments, BSA and IgG) and two types of complex mixtures (*E. coli* lysate and CHO supernatant) was also study. More than one thousand binding results were obtained, being all the results confirmed and validated by: microfluidic studies on protein L (the standard method to purify Fabs), other high-throughput platform and at a normal bench-scale with a packed-bed column. With all this information, four different two-multimodal column process was designed, being this able to remove the majority of impurities and achieving good recovery yields. The combined

complexity of both Fabs and multimodal ligands was successfully mitigated and simplified using a microfluidic approach. This allowed the acquisition of a large amount of chromatographic data within a short period of time. All the gather information was accurately processed, and the conditions for an efficient purification scheme were promptly found.

The reported ability to bind antibodies, led to the design of studies to evaluate if phenylboronic acid can be applied to purify Fab fragments. A microfluidic approach was also adopted in the evaluation of these pseudo-multimodal ligand. The results were enlightening, phenylboronic acid can bind Fabs using the same interactions as the ones used to bind antibodies. However, due to the extremely variable nature of Fabs, phenylboronic acid is only able to bind Fabs if the N-glycans are available/exposed on their structure. In the case of mAbs and Fc, the binding to phenylboronic acid occurs via the C_H2 fragment of the last, being this a constant region in the vast majority of antibodies, the interaction is not as variable as it is for Fabs, where the sugars can have different levels of exposure. More studies need to be done to confirm this hypothesis, specially, using a monoclonal Fab fragment instead of using a polyclonal digested mixture. Nevertheless, if the N-glycans are exposed and available to bind phenylboronic acid, this resin can be used to purify Fabs as it is to purify mAbs.

A long road needs to be trailed to apply peptides or multimodal ligands as alternatives to the traditional domain-based chromatography, specially protein A, G and L. Despite its high-cost and traditional harsh elution conditions, their affinity, selectivity and vast application makes the efforts for the implementation of alternatives a difficult task. Nevertheless, the work developed during this thesis proved that peptides and multimodal ligands, can be seen as true alternatives in the purification of Fab fragments, an important class of antibody derivatives. With the correct and target-oriented application of screening techniques, such as phage display and high-throughput process development, it is possible screen for a peptide ligand or chromatographic conditions capable of efficiently purify Fab fragments. The work described in this thesis can be considered a valuable contribution for the development of new purification technologies, not only for Fab fragments, but to other biomolecules.

Future work

The search for better alternatives to purify Fab fragments was the main goal of this thesis. The work developed could help in the development and implementation of peptide affinity chromatography and multimodal chromatography as downstream solutions. In order to increase the robustness of the data acquired here, future experiments can be made. For the peptide affinity chromatography four future projects can be designed:

1) Development of a new biopanning strategy, where a scFV is used as a negative selection. With this, the peptides with affinity to the variable regions of Fabs will be discarded. The positive selections consists on a Fab containing the same variable regions.
2) Development of a coupling method to immobilized D2 and F3 on a resin and evaluate its applicability in the purification/quantification of digested Fabs.
3) Development of further mutational studies to evaluate if A5 and C7 can be transformed to bind more classes of Fab fragments.
4) Development of a more oriented peptide phage display, with the design of a specific peptide library. This will can be constructed having in consideration all the peptide motifs found during the three realized phage display biopannings.

Regarding the multimodal chromatography studies, there is also space to improve the work developed, and this include:

1) Implementation of a design of experience approach to study additional chromatographic operation conditions for Fab fragments.
2) Development of downstream strategies including other types of chromatography modes, such as ion-exchange.
3) Development of a microfluidic device, with a UV sensor, to realize chromatographic binding and elution studies without the need to do a target labelling procedure.
4) Study the effect of phase modifiers in the purification of Fab fragments.
5) Use of different monoclonal Fabs, preferentially with different levels of N-glycans exposure, to confirm the use of phenylboronic acid as a Fab purification solution.

Bibliography

[1] K. Tsumoto, Y. Isozaki, H. Yagami, M. Tomita, Future perspectives of therapeutic monoclonal antibodies, Immunotherapy. 11 (2019) 119–127. https://doi.org/10.2217/imt-2018-0130.

[2] M. Toporkiewicz, J. Meissner, L. Matusewicz, A. Czogalla, A.F. Sikorski, Toward a magic or imaginary bullet? Ligands for drug targeting to cancer cells: principles, hopes, and challenges, Int. J. Nanomedicine. 10 (2015) 1399–1414. https://doi.org/10.2147/IJN.S74514.

[3] P. Holliger, P.J. Hudson, Engineered antibody fragments and the rise of single domains, Nat. Biotechnol. 23 (2005) 1126–1136. https://doi.org/10.1038/nbt1142.

[4] J.G. Elvin, R.G. Couston, C.F. van der Walle, Therapeutic antibodies: Market considerations, disease targets and bioprocessing, Int. J. Pharm. 440 (2013) 83–98. https://doi.org/10.1016/j.ijpharm.2011.12.039.

[5] C. Rader, Overview on concepts and applications of Fab antibody fragments, Curr. Protoc. Protein Sci. Chapter 6 (2009) Unit 6.9. https://doi.org/10.1002/0471140864.ps0609s55.

[6] L.S. Wolfe, C.P. Barringer, S.S. Mostafa, A.A. Shukla, Multimodal chromatography: Characterization of protein binding and selectivity enhancement through mobile phase modulators, J. Chromatogr. A. 1340 (2014) 151–156. https://doi.org/10.1016/j.chroma.2014.02.086.

[7] J. Yan, Q.-L. Zhang, D.-Q. Lin, S.-J. Yao, Protein adsorption behavior and immunoglobulin separation with a mixed-mode resin based on p-aminohippuric acid, J. Sep. Sci. 37 (2014) 2474–2480. https://doi.org/10.1002/jssc.201400520.

[8] A.L. Nelson, J.M. Reichert, Development trends for therapeutic antibody fragments, Nat. Biotechnol. 27 (2009) 331–337. https://doi.org/10.1038/nbt0409-331.

[9] J.M. Reichert, Antibodies to watch in 2016, MAbs. 8 (2016) 197–204. https://doi.org/10.1080/19420862.2015.1125583.

[10] B.B. Haab, Methods and applications of antibody microarrays in cancer research, PROTEOMICS. 3 (2003) 2116–2122. https://doi.org/10.1002/pmic.200300595.

[11] R.W. Bennett, An Antibody Modified Automated Enzyme-Linked Immunosorbent Assay-Based Method for Detection of Staphylococcal Enterotoxin*, J. Rapid Methods Autom. Microbiol. 16 (2008) 320–329. https://doi.org/10.1111/j.1745-4581.2008.00138.x.

[12] A.L. Nelson, Antibody fragments: hope and hype, MAbs. 2 (2010) 77–83.

[13] M.L. Chiu, G.L. Gilliland, Engineering antibody therapeutics, Curr. Opin. Struct. Biol. 38 (2016) 163–173. https://doi.org/10.1016/j.sbi.2016.07.012.

[14] A.N.C. Weir, A. Nesbitt, A.P. Chapman, A.G.P.P. Antoniw, A.D.G. Lawson, Formatting antibody fragments to mediate specific therapeutic functions, Biochem. Soc. Trans. 30 (2002) 512–516. https://doi.org/10.1042/bst0300512.

[15] A. Constantinou, C. Chen, M.P. Deonarain, Modulating the pharmacokinetics of therapeutic antibodies, Biotechnol. Lett. 32 (2010) 609–622. https://doi.org/10.1007/s10529-010-0214-z.

[16] T.L. Kirley, K.D. Greis, A.B. Norman, Selective disulfide reduction for labeling and enhancement of Fab antibody fragments, Biochem. Biophys. Res. Commun. 480 (2016) 752–757. https://doi.org/10.1016/j.bbrc.2016.10.128.

[17] C.T. Mendler, L. Friedrich, I. Laitinen, M. Schlapschy, M. Schwaiger, H.-J. Wester, A. Skerra, High contrast tumor imaging with radio-labeled antibody Fab fragments tailored for optimized pharmacokinetics via PASylation, MAbs. 7 (2014) 96–109. https://doi.org/10.4161/19420862.2014.985522.

[18] W. Wang, E. Wang, J. Balthasar, Monoclonal Antibody Pharmacokinetics and Pharmacodynamics, Clin. Pharmacol. Ther. 84 (2008) 548–558. https://doi.org/10.1038/clpt.2008.170.

[19] P. Chames, M.V. Regenmortel, E. Weiss, D. Baty, Therapeutic antibodies: successes, limitations and hopes for the future, Br. J. Pharmacol. 157 (2009) 220–233. https://doi.org/10.1111/j.1476-5381.2009.00190.x.

[20] S. Bournazos, J.V. Ravetch, Fcγ receptor pathways during active and passive immunization, Immunol. Rev. 268 (2015) 88–103. https://doi.org/10.1111/imr.12343.

[21] A. Frenzel, M. Hust, T. Schirrmann, Expression of recombinant antibodies, Front. Immunol. 4 (2013) 217. https://doi.org/10.3389/fimmu.2013.00217.

[22] T. Omasa, M. Onitsuka, W.-D. Kim, Cell engineering and cultivation of chinese hamster ovary (CHO) cells, Curr. Pharm. Biotechnol. 11 (2010) 233–240.

[23] S.M. Schatz, R.J. Kerschbaumer, G. Gerstenbauer, M. Kral, F. Dorner, F. Scheiflinger, Higher expression of fab antibody fragments in a CHO cell line at reduced temperature, Biotechnol. Bioeng. 84 (2003) 433–438. https://doi.org/10.1002/bit.10793.

[24] R. Jalalirad, Production of antibody fragment (Fab) throughout Escherichia coli fed-batch fermentation process: Changes in titre, location and form of product, Electron. J. Biotechnol. 16 (2013) 9–9. https://doi.org/10.2225/vol16-issue3-fulltext-15.

[25] H. Nakamura, N. Oda-Ueda, T. Ueda, T. Ohkuri, Introduction of a glycosylation site in the constant region decreases the aggregation of adalimumab Fab, Biochem. Biophys. Res. Commun. 503 (2018) 752–756. https://doi.org/10.1016/j.bbrc.2018.06.071.

[26] H. Yamaji, T. Manabe, K. Watakabe, M. Muraoka, I. Fujii, H. Fukuda, Production of functional antibody Fab fragment by recombinant insect cells, Biochem. Eng. J. 41 (2008) 203–209. https://doi.org/10.1016/j.bej.2008.04.017.

[27] K. Mori, H. Hamada, T. Ogawa, Y. Ohmuro-Matsuyama, T. Katsuda, H. Yamaji, Efficient production of antibody Fab fragment by transient gene expression in insect cells, J. Biosci. Bioeng. 124 (2017) 221–226. https://doi.org/10.1016/j.jbiosc.2017.03.007.

[28] C.D. Wilde, K. Peeters, A. Jacobs, I. Peck, A. Depicker, Expression of antibodies and Fab fragments in transgenic potato plants: a case study for bulk production in crop plants, Mol. Breed. 9 (2002) 271–282. https://doi.org/10.1023/A:1020306917914.

[29] J.K.-C. Ma, P.M.W. Drake, P. Christou, The production of recombinant pharmaceutical proteins in plants, Nat. Rev. Genet. 4 (2003) 794–805. https://doi.org/10.1038/nrg1177.

[30] F. Li, N. Vijayasankaran, A. (Yijuan) Shen, R. Kiss, A. Amanullah, Cell culture processes for monoclonal antibody production, MAbs. 2 (2010) 466–479. https://doi.org/10.4161/mabs.2.5.12720.

[31] P. Chames, D. Baty, Bispecific antibodies for cancer therapy, MAbs. 1 (2009) 539–547.

[32] S.K. Gupta, P. Shukla, Microbial platform technology for recombinant antibody fragment production: A review, Crit. Rev. Microbiol. 43 (2017) 31–42. https://doi.org/10.3109/1040841X.2016.1150959.

[33] H.F. Liu, J. Ma, C. Winter, R. Bayer, Recovery and purification process development for monoclonal antibody production, MAbs. 2 (2010) 480–499. https://doi.org/10.4161/mabs.2.5.12645.

[34] R.L. Fahrner, H.L. Knudsen, C.D. Basey, W. Galan, D. Feuerhelm, M. Vanderlaan, G.S. Blank, Industrial Purification of Pharmaceutical Antibodies: Development, Operation, and Validation of Chromatography Processes, Biotechnol. Genet. Eng. Rev. 18 (2001) 301–327. https://doi.org/10.1080/02648725.2001.10648017.

[35] E. Garber, S.J. Demarest, A broad range of Fab stabilities within a host of therapeutic IgGs, Biochem. Biophys. Res. Commun. 355 (2007) 751–757. https://doi.org/10.1016/j.bbrc.2007.02.042.

[36] D. Röthlisberger, A. Honegger, A. Plückthun, Domain Interactions in the Fab Fragment: A Comparative Evaluation of the Single-chain Fv and Fab Format Engineered with Variable Domains of Different Stability, J. Mol. Biol. 347 (2005) 773–789. https://doi.org/10.1016/j.jmb.2005.01.053.

[37] R. Toughiri, X. Wu, D. Ruiz, F. Huang, J.W. Crissman, M. Dickey, K. Froning, E.M. Conner, T.P. Cujec, S.J. Demarest, Comparing domain interactions within antibody Fabs with kappa and lambda light chains, MAbs. 8 (2016) 1276–1285. https://doi.org/10.1080/19420862.2016.1214785.

[38] S. Fekete, D. Guillarme, P. Sandra, K. Sandra, Chromatographic, Electrophoretic, and Mass Spectrometric Methods for the Analytical Characterization of Protein Biopharmaceuticals, Anal. Chem. 88 (2016) 480–507. https://doi.org/10.1021/acs.analchem.5b04561.

[39] A. Teplyakov, G. Obmolova, T.J. Malia, J. Luo, S. Muzammil, R. Sweet, J.C. Almagro, G.L. Gilliland, Structural diversity in a human antibody germline library, MAbs. 8 (2016) 1045–1063. https://doi.org/10.1080/19420862.2016.1190060.

[40] T. Teerinen, J. Valjakka, J. Rouvinen, K. Takkinen, Structure-based stability engineering of the mouse IgG1 Fab fragment by modifying constant domains, J. Mol. Biol. 361 (2006) 687–697. https://doi.org/10.1016/j.jmb.2006.06.073.

[41] C.L. Townsend, J.M.J. Laffy, Y.-C.B. Wu, J. Silva O'Hare, V. Martin, D. Kipling, F. Fraternali, D.K. Dunn-Walters, Significant Differences in Physicochemical Properties of Human Immunoglobulin Kappa and Lambda CDR3 Regions, Front. Immunol. 7 (2016). https://doi.org/10.3389/fimmu.2016.00388.

[42] R.F. Montaño, S.L. Morrison, Influence of the Isotype of the Light Chain on the Properties of IgG, J. Immunol. 168 (2002) 224–231. https://doi.org/10.4049/jimmunol.168.1.224.

[43] J.C. Almagro, I. Hernández, M.C. Ramírez, E. Vargas-Madrazo, Structural differences between the repertoires of mouse and human germline genes and their evolutionary implications, Immunogenetics. 47 (1998) 355–363. https://doi.org/10.1007/s002510050370.

[44] V. Morea, A. Tramontano, M. Rustici, C. Chothia, A.M. Lesk, Conformations of the third hypervariable region in the VH domain of immunoglobulins11Edited by I. A. Wilson, J. Mol. Biol. 275 (1998) 269–294. https://doi.org/10.1006/jmbi.1997.1442.

[45] H. Shirai, A. Kidera, H. Nakamura, Structural classification of CDR-H3 in antibodies, FEBS Lett. 399 (1996) 1–8. https://doi.org/10.1016/S0014-5793(96)01252-5.

[46] D. Kuroda, H. Shirai, M. Kobori, H. Nakamura, Structural classification of CDR-H3 revisited: A lesson in antibody modeling, Proteins Struct. Funct. Bioinforma. 73 (2008) 608–620. https://doi.org/10.1002/prot.22087.

[47] R.L. Stanfield, A. Zemla, I.A. Wilson, B. Rupp, Antibody elbow angles are influenced by their light chain class, J. Mol. Biol. 357 (2006) 1566–1574. https://doi.org/10.1016/j.jmb.2006.01.023.

[48] C. Lizak, Y.-Y. Fan, T.C. Weber, M. Aebi, N-Linked Glycosylation of Antibody Fragments in Escherichia coli, Bioconjug. Chem. 22 (2011) 488–496. https://doi.org/10.1021/bc100511k.

[49] F.S. van de Bovenkamp, L. Hafkenscheid, T. Rispens, Y. Rombouts, The Emerging Importance of IgG Fab Glycosylation in Immunity, J. Immunol. 196 (2016) 1435–1441. https://doi.org/10.4049/jimmunol.1502136.

[50] G.R. Kleemann, J. Beierle, A.C. Nichols, T.M. Dillon, G.D. Pipes, P.V. Bondarenko, Characterization of IgG1 immunoglobulins and peptide-Fc fusion proteins by limited proteolysis in conjunction with LC-MS, Anal. Chem. 80 (2008) 2001–2009. https://doi.org/10.1021/ac701629v.

[51] A. Bondt, Y. Rombouts, M.H.J. Selman, P.J. Hensbergen, K.R. Reiding, J.M.W. Hazes, R.J.E.M. Dolhain, M. Wuhrer, Immunoglobulin G (IgG) Fab glycosylation analysis using a new mass spectrometric high-throughput profiling method reveals pregnancy-associated changes, Mol. Cell. Proteomics MCP. 13 (2014) 3029–3039. https://doi.org/10.1074/mcp.M114.039537.

[52] F.S. van de Bovenkamp, L. Hafkenscheid, T. Rispens, Y. Rombouts, The Emerging Importance of IgG Fab Glycosylation in Immunity, J. Immunol. 196 (2016) 1435–1441. https://doi.org/10.4049/jimmunol.1502136.

[53] C. Magdelaine-Beuzelin, C. Pinault, G. Paintaud, H. Watier, Therapeutic antibodies in ophthalmology: old is new again, MAbs. 2 (2010) 176–180.

[54] T.S. Raju, B.J. Scallon, Glycosylation in the Fc domain of IgG increases resistance to proteolytic cleavage by papain, Biochem. Biophys. Res. Commun. 341 (2006) 797–803. https://doi.org/10.1016/j.bbrc.2006.01.030.

[55] K. Zheng, M. Yarmarkovich, C. Bantog, R. Bayer, T.W. Patapoff, Influence of glycosylation pattern on the molecular properties of monoclonal antibodies, MAbs. 6 (2014) 649–658. https://doi.org/10.4161/mabs.28588.

[56] X. Robert, P. Gouet, Deciphering key features in protein structures with the new ENDscript server, Nucleic Acids Res. 42 (2014) W320-324. https://doi.org/10.1093/nar/gku316.

[57] P. Gouet, E. Courcelle, D.I. Stuart, F. Métoz, ESPript: analysis of multiple sequence alignments in PostScript, Bioinforma. Oxf. Engl. 15 (1999) 305–308.

[58] K. Lebozec, M. Jandrot-Perrus, G. Avenard, O. Favre-Bulle, P. Billiald, Quality and cost assessment of a recombinant antibody fragment produced from mammalian, yeast and prokaryotic host cells: A case study prior to pharmaceutical development, New Biotechnol. 44 (2018) 31–40. https://doi.org/10.1016/j.nbt.2018.04.006.

[59] P. Hossler, S.F. Khattak, Z.J. Li, Optimal and consistent protein glycosylation in mammalian cell culture, Glycobiology. 19 (2009) 936–949. https://doi.org/10.1093/glycob/cwp079.

[60] M.N. Baeshen, A.M. Al-Hejin, R.S. Bora, M.M.M. Ahmed, H.A.I. Ramadan, K.S. Saini, N.A. Baeshen, E.M. Redwan, Production of Biopharmaceuticals in E. coli: Current Scenario and Future Perspectives, J. Microbiol. Biotechnol. 25 (2015) 953–962. https://doi.org/10.4014/jmb.1412.12079.

[61] A. Gaciarz, J. Veijola, Y. Uchida, M.J. Saaranen, C. Wang, S. Hörkkö, L.W. Ruddock, Systematic screening of soluble expression of antibody fragments in the cytoplasm of E. coli, Microb. Cell Factories. 15 (2016) 22. https://doi.org/10.1186/s12934-016-0419-5.

[62] S. Sahdev, S.K. Khattar, K.S. Saini, Production of active eukaryotic proteins through bacterial expression systems: a review of the existing biotechnology strategies, Mol. Cell. Biochem. 307 (2008) 249–264. https://doi.org/10.1007/s11010-007-9603-6.

[63] C.-J. Huang, H. Lin, X. Yang, Industrial production of recombinant therapeutics in Escherichia coli and its recent advancements, J. Ind. Microbiol. Biotechnol. 39 (2012) 383–399. https://doi.org/10.1007/s10295-011-1082-9.

[64] H.-P. Meyer, D.R. Schmidhalter, Microbial Expression Systems and Manufacturing from a Market and Economic Perspective, (2012). https://doi.org/10.5772/29417.

[65] Z.A. Ahmad, S.K. Yeap, A.M. Ali, W.Y. Ho, N.B.M. Alitheen, M. Hamid, scFv Antibody: Principles and Clinical Application, J. Immunol. Res. (2012). https://doi.org/10.1155/2012/980250.

[66] M. Venturi, C. Seifert, C. Hunte, High level production of functional antibody fab fragments in an oxidizing bacterial cytoplasm11Edited by J. Karn, J. Mol. Biol. 315 (2002) 1–8. https://doi.org/10.1006/jmbi.2001.5221.

[67] A. de Marco, Strategies for successful recombinant expression of disulfide bond-dependent proteins in Escherichia coli, Microb. Cell Factories. 8 (2009) 26. https://doi.org/10.1186/1475-2859-8-26.

[68] M. Hust, T. Jostock, C. Menzel, B. Voedisch, A. Mohr, M. Brenneis, M.I. Kirsch, D. Meier, S. Dübel, Single chain Fab (scFab) fragment, BMC Biotechnol. 7 (2007) 14. https://doi.org/10.1186/1472-6750-7-14.

[69] T. Fujii, T. Ohkuri, R. Onodera, T. Ueda, Stable Supply of Large Amounts of Human Fab from the Inclusion Bodies in E. coli, J. Biochem. (Tokyo). 141 (2007) 699–707. https://doi.org/10.1093/jb/mvm075.

[70] A. Basu, X. Li, S.S.J. Leong, Refolding of proteins from inclusion bodies: rational design and recipes, Appl. Microbiol. Biotechnol. 92 (2011) 241–251. https://doi.org/10.1007/s00253-011-3513-y.

[71] R. Levy, R. Weiss, G. Chen, B.L. Iverson, G. Georgiou, Production of correctly folded Fab antibody fragment in the cytoplasm of Escherichia coli trxB gor mutants via the coexpression of molecular chaperones, Protein Expr. Purif. 23 (2001) 338–347. https://doi.org/10.1006/prep.2001.1520.

[72] K.J. Jeong, S.H. Jang, N. Velmurugan, Recombinant antibodies: engineering and production in yeast and bacterial hosts, Biotechnol. J. 6 (2011) 16–27. https://doi.org/10.1002/biot.201000381.

[73] S.C. Makrides, Strategies for achieving high-level expression of genes in Escherichia coli., Microbiol. Rev. 60 (1996) 512–538.

[74] C.-C. Hsu, O.R. Thomas, T.W. Overton, Periplasmic expression in and release of Fab fragments from Escherichia coli using stress minimization, J. Chem. Technol. Biotechnol. 91 (2016) 815–822. https://doi.org/10.1002/jctb.4672.

[75] L.A. Fernández, I. Sola, L. Enjuanes, V. de Lorenzo, Specific Secretion of Active Single-Chain Fv Antibodies into the Supernatants of Escherichia coli Cultures by Use of the Hemolysin System, Appl. Environ. Microbiol. 66 (2000) 5024–5029.

[76] K.Y. Kwong, C. Rader, E. coli expression and purification of Fab antibody fragments, Curr. Protoc. Protein Sci. Chapter 6 (2009) Unit 6.10. https://doi.org/10.1002/0471140864.ps0610s55.

[77] S. Corisdeo, B. Wang, Functional expression and display of an antibody Fab fragment in Escherichia coli: study of vector designs and culture conditions, Protein Expr. Purif. 34 (2004) 270–279. https://doi.org/10.1016/j.pep.2003.11.020.

[78] R. Levy, K. Ahluwalia, D.J. Bohmann, H.M. Giang, L.J. Schwimmer, H. Issafras, N.B. Reddy, C. Chan, A.H. Horwitz, T. Takeuchi, Enhancement of antibody fragment secretion into the Escherichia coli periplasm by co-expression with the peptidyl prolyl isomerase, FkpA, in the cytoplasm, J. Immunol. Methods. 394 (2013) 10–21. https://doi.org/10.1016/j.jim.2013.04.010.

[79] M.P. DeLisa, D. Tullman, G. Georgiou, Folding quality control in the export of proteins by the bacterial twin-arginine translocation pathway, Proc. Natl. Acad. Sci. U. S. A. 100 (2003) 6115–6120. https://doi.org/10.1073/pnas.0937838100.

[80] G. Walsh, Biopharmaceutical benchmarks 2014, Nat. Biotechnol. 32 (2014) 992–1000. https://doi.org/10.1038/nbt.3040.

[81] G. Yin, E.D. Garces, J. Yang, J. Zhang, C. Tran, A.R. Steiner, C. Roos, S. Bajad, S. Hudak, K. Penta, J. Zawada, S. Pollitt, C.J. Murray, Aglycosylated antibodies and antibody fragments produced in a scalable in vitro transcription-translation system, MAbs. 4 (2012) 217–225. https://doi.org/10.4161/mabs.4.2.19202.

[82] H.-J. Kang, H.-J. Kim, M.-S. Jung, J.-K. Han, S.-H. Cha, Optimal expression of a Fab-effector fusion protein in Escherichia coli by removing the cysteine residues responsible for an interchain disulfide bond of a Fab molecule, Immunol. Lett. 184 (2017) 34–42. https://doi.org/10.1016/j.imlet.2017.02.008.

[83] S. Chu, X. Zhu, N. You, W. Zhang, F. Zheng, B. Cai, T. Zhou, Y. Wang, Q. Sun, Z. Yang, X. Zhang, C. Wang, S. Nie, J. Zhu, M. Wang, The Fab Fragment of a Human Anti-Siglec-9 Monoclonal Antibody Suppresses LPS-Induced Inflammatory Responses in Human Macrophages, Front. Immunol. 7 (2016). https://doi.org/10.3389/fimmu.2016.00649.

[84] J. Chatellier, M.H. Van Regenmortel, T. Vernet, D. Altschuh, Functional mapping of conserved residues located at the VL and VH domain interface of a Fab, J. Mol. Biol. 264 (1996) 1–6. https://doi.org/10.1006/jmbi.1996.0618.

[85] S.A. Masri, H. Rast, W.-G. Hu, L.P. Nagata, D. Chau, S. Jager, D. Mah, Cloning and expression in E. coli of a functional Fab fragment obtained from single human lymphocyte against anthrax toxin, Mol. Immunol. 44 (2007) 2101–2106. https://doi.org/10.1016/j.molimm.2006.09.007.

[86] M.A. Meehl, T.A. Stadheim, Biopharmaceutical discovery and production in yeast, Curr. Opin. Biotechnol. 30 (2014) 120–127. https://doi.org/10.1016/j.copbio.2014.06.007.

[87] T.I. Potgieter, M. Cukan, J.E. Drummond, N.R. Houston-Cummings, Y. Jiang, F. Li, H. Lynaugh, M. Mallem, T.W. McKelvey, T. Mitchell, A. Nylen, A. Rittenhour, T.A. Stadheim, D. Zha, M. d'Anjou, Production of monoclonal antibodies by glycoengineered Pichia pastoris, J. Biotechnol. 139 (2009) 318–325. https://doi.org/10.1016/j.jbiotec.2008.12.015.

[88] R.T. Burtet, M.A. Santos-Silva, G.A.M. Buss, L.M.P. Moraes, A.Q. Maranhão, M.M. Brigido, Production of a recombinant Fab in Pichia pastoris from a Monocistronic expression vector, J. Biochem. (Tokyo). 142 (2007) 665–669. https://doi.org/10.1093/jb/mvm226.

[89] N. Ponomarenko, S.D. Chatziefthimiou, I. Kurkova, Y. Mokrushina, Y. Mokrushina, A. Stepanova, I. Smirnov, M. Avakyan, T. Bobik, A. Mamedov, V. Mitkevich, A. Belogurov, O.S. Fedorova, M. Dubina, A. Golovin, V. Lamzin, A. Friboulet, A.A. Makarov, M. Wilmanns, A. Gabibov, Role of κ→λ light-chain constant-domain switch in the structure and functionality of A17 reactibody, Acta Crystallogr. D Biol. Crystallogr. 70 (2014) 708–719. https://doi.org/10.1107/S1399004713032446.

[90] B. Gasser, M. Maurer, J. Gach, R. Kunert, D. Mattanovich, Engineering of Pichia pastoris for improved production of antibody fragments, Biotechnol. Bioeng. 94 (2006) 353–361. https://doi.org/10.1002/bit.20851.

[91] A.M. Gonçalves, A.Q. Pedro, C. Maia, F. Sousa, J.A. Queiroz, L.A. Passarinha, Pichia pastoris: a recombinant microfactory for antibodies and human membrane proteins, J. Microbiol. Biotechnol. 23 (2013) 587–601.

[92] V. Puxbaum, D. Mattanovich, B. Gasser, Quo vadis? The challenges of recombinant protein folding and secretion in Pichia pastoris, Appl. Microbiol. Biotechnol. 99 (2015) 2925–2938. https://doi.org/10.1007/s00253-015-6470-z.

[93] F.S. Hartner, C. Ruth, D. Langenegger, S.N. Johnson, P. Hyka, G.P. Lin-Cereghino, J. Lin-Cereghino, K. Kovar, J.M. Cregg, A. Glieder, Promoter library designed for fine-tuned gene expression in Pichia pastoris, Nucleic Acids Res. 36 (2008) e76–e76. https://doi.org/10.1093/nar/gkn369.

[94] D. Ning, X. Junjian, Z. Qing, X. Sheng, C. Wenyin, R. Guirong, W. Xunzhang, Production of recombinant humanized anti-HBsAg Fab fragment from Pichia pastoris by fermentation, J. Biochem. Mol. Biol. 38 (2005) 294–299.

[95] B. Gasser, D. Mattanovich, Antibody production with yeasts and filamentous fungi: on the road to large scale?, Biotechnol. Lett. 29 (2007) 201–212. https://doi.org/10.1007/s10529-006-9237-x.

[96] X. Garcia-Ortega, P. Ferrer, J.L. Montesinos, F. Valero, Fed-batch operational strategies for recombinant Fab production with Pichia pastoris using the constitutive GAP promoter, Biochem. Eng. J. 79 (2013) 172–181. https://doi.org/10.1016/j.bej.2013.07.013.

[97] M. Pfeffer, M. Maurer, J. Stadlmann, J. Grass, M. Delic, F. Altmann, D. Mattanovich, Intracellular interactome of secreted antibody Fab fragment in Pichia pastoris reveals its routes of secretion and degradation, Appl. Microbiol. Biotechnol. 93 (2012) 2503–2512. https://doi.org/10.1007/s00253-012-3933-3.

[98] M. Dragosits, G. Frascotti, L. Bernard-Granger, F. Vázquez, M. Giuliani, K. Baumann, E. Rodríguez-Carmona, J. Tokkanen, E. Parrilli, M.G. Wiebe, R. Kunert, M. Maurer, B. Gasser, M. Sauer, P. Branduardi, T. Pakula, M. Saloheimo, M. Penttilä, P. Ferrer, M. Luisa Tutino, A. Villaverde, D. Porro, D. Mattanovich, Influence of growth temperature on the production of antibody Fab fragments in different microbes: a host comparative analysis, Biotechnol. Prog. 27 (2011) 38–46. https://doi.org/10.1002/btpr.524.

[99] S. Lin, N.R. Houston-Cummings, B. Prinz, R. Moore, B. Bobrowicz, R.C. Davidson, S. Wildt, T.A. Stadheim, D. Zha, A novel fragment of antigen binding (Fab) surface display platform using glycoengineered Pichia pastoris, J. Immunol. Methods. 375 (2012) 159–165. https://doi.org/10.1016/j.jim.2011.10.003.

[100] C. Sivelle, R. Sierocki, K. Ferreira-Pinto, S. Simon, B. Maillere, H. Nozach, Fab is the most efficient format to express functional antibodies by yeast surface display, MAbs. 0 (2018) 01–34. https://doi.org/10.1080/19420862.2018.1468952.

[101] J. Hou, K. Tyo, Z. Liu, D. Petranovic, J. Nielsen, Engineering of vesicle trafficking improves heterologous protein secretion in Saccharomyces cerevisiae, Metab. Eng. 14 (2012) 120–127. https://doi.org/10.1016/j.ymben.2012.01.002.

[102] P. Xu, D. Raden, F.J. Doyle, A.S. Robinson, Analysis of unfolded protein response during single-chain antibody expression in Saccaromyces cerevisiae reveals different roles for BiP and PDI in folding, Metab. Eng. 7 (2005) 269–279. https://doi.org/10.1016/j.ymben.2005.04.002.

[103] A.H. Horwitz, C.P. Chang, M. Better, K.E. Hellstrom, R.R. Robinson, Secretion of functional antibody and Fab fragment from yeast cells, Proc. Natl. Acad. Sci. U. S. A. 85 (1988) 8678–8682.

[104] S.R. Hamilton, T.U. Gerngross, Glycosylation engineering in yeast: the advent of fully humanized yeast, Curr. Opin. Biotechnol. 18 (2007) 387–392. https://doi.org/10.1016/j.copbio.2007.09.001.

[105] M. Mayer, U. Kies, R. Kammermeier, J. Buchner, BiP and PDI cooperate in the oxidative folding of antibodies in vitro, J. Biol. Chem. 275 (2000) 29421–29425. https://doi.org/10.1074/jbc.M002655200.

[106] O. Spadiut, S. Capone, F. Krainer, A. Glieder, C. Herwig, Microbials for the production of monoclonal antibodies and antibody fragments, Trends Biotechnol. 32 (2014) 54–60. https://doi.org/10.1016/j.tibtech.2013.10.002.

[107] R.R. Porter, The hydrolysis of rabbit y-globulin and antibodies with crystalline papain, Biochem. J. 73 (1959) 119–126.

[108] R.G.A. Jones, J. Landon, A protocol for "enhanced pepsin digestion": a step by step method for obtaining pure antibody fragments in high yield from serum, J. Immunol. Methods. 275 (2003) 239–250.

[109] K. Inouye, S. Ohnaka, Pepsin digestion of a mouse monoclonal antibody of IgG1 class formed F(ab')(2) fragments in which the light chains as well as the heavy chains were truncated, J. Biochem. Biophys. Methods. 48 (2001) 23–32.

[110] M. Adamczyk, J.C. Gebler, J. Wu, Papain digestion of different mouse IgG subclasses as studied by electrospray mass spectrometry, J. Immunol. Methods. 237 (2000) 95–104.

[111] A.C. Wang, I.Y. Wang, Cleavage sites of human IgGl immunoglobulin by papain, Immunochemistry. 14 (1977) 197–200. https://doi.org/10.1016/0019-2791(77)90194-X.

[112] S.M. Andrew, J.A. Titus, Fragmentation of immunoglobulin G, Curr. Protoc. Cell Biol. Editor. Board Juan Bonifacino Al. Chapter 16 (2003) Unit 16.4. https://doi.org/10.1002/0471143030.cb1604s17.

[113] A. Nascimento, I.F. Pinto, V. Chu, M.R. Aires-Barros, J.P. Conde, A.M. Azevedo, Studies on the purification of antibody fragments, Sep. Purif. Technol. 195 (2018) 388–397. https://doi.org/10.1016/j.seppur.2017.12.033.

[114] M. Spitali, Downstream Processing of Monoclonal Antibody Fragments, in: Process Scale Purif. Antibodies, Wiley-Blackwell, 2017: pp. 537–558. https://doi.org/10.1002/9781119126942.ch25.

[115] T.L. Kirley, A.B. Norman, Characterization of a recombinant humanized anti-cocaine monoclonal antibody and its Fab fragment, Hum. Vaccines Immunother. 11 (2015) 458–467. https://doi.org/10.4161/21645515.2014.990856.

[116] D. Ren, G. Pipes, G. Xiao, G.R. Kleemann, P.V. Bondarenko, M.J. Treuheit, H.S. Gadgil, Reversed-phase liquid chromatography–mass spectrometry of site-specific chemical modifications in intact immunoglobulin molecules and their fragments, J. Chromatogr. A. 1179 (2008) 198–204. https://doi.org/10.1016/j.chroma.2007.11.088.

[117] J.E. Nettleship, J. Ren, N. Rahman, N.S. Berrow, D. Hatherley, A.N. Barclay, R.J. Owens, A pipeline for the production of antibody fragments for structural studies using transient expression in HEK 293T cells, Protein Expr. Purif. 62 (2008) 83–89. https://doi.org/10.1016/j.pep.2008.06.017.

[118] N. Camper, T. Byrne, R.E. Burden, J. Lowry, B. Gray, J.A. Johnston, M.E. Migaud, S.A. Olwill, R.J. Buick, C.J. Scott, Stable expression and purification of a functional processed Fab′ fragment from a single nascent polypeptide in CHO cells expressing the mCAT-1 retroviral receptor, J. Immunol. Methods. 372 (2011) 30–41. https://doi.org/10.1016/j.jim.2011.06.029.

[119] S. Hober, K. Nord, M. Linhult, Protein A chromatography for antibody purification, J. Chromatogr. B. 848 (2007) 40–47. https://doi.org/10.1016/j.jchromb.2006.09.030.

[120] B. Kelley, Industrialization of mAb production technology The bioprocessing industry at a crossroads, MAbs. 1 (2009) 443–452.

[121] L. Jendeberg, P. Nilsson, A. Larsson, P. Denker, M. Uhlén, B. Nilsson, P.A. Nygren, Engineering of Fc(1) and Fc(3) from human immunoglobulin G to analyse subclass specificity for staphylococcal protein A, J. Immunol. Methods. 201 (1997) 25–34.

[122] A. Surolia, D. Pain, M. Islam Khan, Protein A: nature's universal anti-antibody, Trends Biochem. Sci. 7 (1982) 74–76. https://doi.org/10.1016/0968-0004(82)90082-2.

[123] B. Jansson, M. Uhlén, P.A. Nygren, All individual domains of staphylococcal protein A show Fab binding, FEMS Immunol. Med. Microbiol. 20 (1998) 69–78.

[124] B. Akerström, T. Brodin, K. Reis, L. Björck, Protein G: a powerful tool for binding and detection of monoclonal and polyclonal antibodies, J. Immunol. Baltim. Md 1950. 135 (1985) 2589–2592.

[125] L.-Y. Lian, I.L. Barsukov, J.P. Derrick, G.C.K. Roberts, Mapping the interactions between streptococcal protein G and the Fab fragment of IgG in solution, Nat. Struct. Mol. Biol. 1 (1994) 355–357. https://doi.org/10.1038/nsb0694-355.

[126] L. Björck, G. Kronvall, Purification and some properties of streptococcal protein G, a novel IgG-binding reagent, J. Immunol. Baltim. Md 1950. 133 (1984) 969–974.

[127] L.J. Bailey, K.M. Sheehy, R.J. Hoey, Z.P. Schaefer, M. Ura, A.A. Kossiakoff, Applications for an engineered Protein-G variant with a pH controllable affinity to antibody fragments, J. Immunol. Methods. 415 (2014) 24–30. https://doi.org/10.1016/j.jim.2014.10.003.

[128] W. Kastern, E. Holst, E. Nielsen, U. Sjöbring, L. Björck, Protein L, a bacterial immunoglobulin-binding protein and possible virulence determinant., Infect. Immun. 58 (1990) 1217–1222.

[129] W. Choe, T.A. Durgannavar, S.J. Chung, Fc-Binding Ligands of Immunoglobulin G: An Overview of High Affinity Proteins and Peptides, Materials. 9 (2016). https://doi.org/10.3390/ma9120994.

[130] G. Rodrigo, M. Gruvegård, J. M. Van Alstine, Antibody Fragments and Their Purification by Protein L Affinity Chromatography, Antibodies. 4 (2015) 259–277. https://doi.org/10.3390/antib4030259.

[131] B.H. Nilson, L. Lögdberg, W. Kastern, L. Björck, B. Akerström, Purification of antibodies using protein L-binding framework structures in the light chain variable domain, J. Immunol. Methods. 164 (1993) 33–40.

[132] M.D. Château, B.H.K. Nilson, M. Erntell, E. Myhre, C.G.M. Magnusson, B. Åkerström, L. Björck, On the Interaction between Protein L and Immunoglobulins of Various Mammalian Species, Scand. J. Immunol. 37 (1993) 399–405. https://doi.org/10.1111/j.1365-3083.1993.tb03310.x.

[133] W. Kastern, U. Sjöbring, L. Björck, Structure of peptostreptococcal protein L and identification of a repeated immunoglobulin light chain-binding domain., J. Biol. Chem. 267 (1992) 12820–12825.

[134] J.P. Murphy, C.J. Duggleby, M.A. Atkinson, A.R. Trowern, T. Atkinson, C.R. Goward, The functional units of a peptostreptococcal protein L, Mol. Microbiol. 12 (1994) 911–920. https://doi.org/10.1111/j.1365-2958.1994.tb01079.x.

[135] M. Wikström, T. Drakenberg, S. Forsén, U. Sjöbring, L. Björck, Three-dimensional solution structure of an immunoglobulin light chain-binding domain of protein L. Comparison with the IgG-binding domains of protein G, Biochemistry. 33 (1994) 14011–14017.

[136] M. Wikström, U. Sjöbring, T. Drakenberg, S. Forsén, L. Björck, Mapping of the immunoglobulin light chain-binding site of protein L, J. Mol. Biol. 250 (1995) 128–133. https://doi.org/10.1006/jmbi.1995.0364.

[137] N. Kruljec, T. Bratkovič, Alternative Affinity Ligands for Immunoglobulins, Bioconjug. Chem. 28 (2017) 2009–2030. https://doi.org/10.1021/acs.bioconjchem.7b00335.

[138] M. Graille, E.A. Stura, N.G. Housden, J.A. Beckingham, S.P. Bottomley, D. Beale, M.J. Taussig, B.J. Sutton, M.G. Gore, J.-B. Charbonnier, Complex between Peptostreptococcus magnus Protein L and a Human Antibody Reveals Structural Convergence in the Interaction Modes of Fab Binding Proteins, Structure. 9 (2001) 679–687. https://doi.org/10.1016/S0969-2126(01)00630-X.

[139] Y. Wei, J. Xu, L. Zhang, Y. Fu, X. Xu, Development of novel small peptide ligands for antibody purification, RSC Adv. 5 (2015) 67093–67101. https://doi.org/10.1039/C5RA07829F.

[140] Menegatti, Naik, Carbonell, The hidden potential of small synthetic molecules and peptides as affinity ligands for bioseparations, Pharm. Bioprocess. 1 (2013) 467–485.

[141] B.H. Nilson, A. Solomon, L. Björck, B. Akerström, Protein L from Peptostreptococcus magnus binds to the kappa light chain variable domain, J. Biol. Chem. 267 (1992) 2234–2239.

[142] A.C.A. Roque, M.Â. Taipa, C.R. Lowe, An artificial protein L for the purification of immunoglobulins and Fab fragments by affinity chromatography, J. Chromatogr. A. 1064 (2005) 157–167. https://doi.org/10.1016/j.chroma.2004.11.102.

[143] G. Hassanzadeh-Ghassabeh, N. Devoogdt, P. De Pauw, C. Vincke, S. Muyldermans, Nanobodies and their potential applications, Nanomed. 8 (2013) 1013–1026. https://doi.org/10.2217/nnm.13.86.

[144] S. Muyldermans, Single domain camel antibodies: current status, Rev. Mol. Biotechnol. 74 (2001) 277–302. https://doi.org/10.1016/S1389-0352(01)00021-6.

[145] T. De Meyer, S. Muyldermans, A. Depicker, Nanobody-based products as research and diagnostic tools, Trends Biotechnol. 32 (2014) 263–270. https://doi.org/10.1016/j.tibtech.2014.03.001.

[146] N. Eifler, G. Medaglia, O. Anderka, L. Laurin, P. Hermans, Development of a novel affinity chromatography resin for platform purification of lambda fabs, Biotechnol. Prog. 30 (2014) 1311–1318. https://doi.org/10.1002/btpr.1958.

[147] L. Esser, S. Shukla, F. Zhou, S.V. Ambudkar, D. Xia, Crystal structure of the antigen-binding fragment of a monoclonal antibody specific for the multidrug-resistance-linked ABC transporter human P-glycoprotein, Acta Crystallogr. Sect. F Struct. Biol. Commun. 72 (2016) 636–641. https://doi.org/10.1107/S2053230X16009778.

[148] H.-N. Song, D.-H. Kim, S.-G. Park, M.K. Lee, S.-H. Paek, E.-J. Woo, Purification and characterization of Fab fragments with rapid reaction kinetics against myoglobin, Biosci. Biotechnol. Biochem. 79 (2015) 718–724. https://doi.org/10.1080/09168451.2014.993354.

[149] J. Rousseaux, R. Rousseaux-Prévost, H. Bazin, Optimal conditions for the preparation of Fab and F(ab′)2 fragments from monoclonal IgG of different rat IgG subclasses, J. Immunol. Methods. 64 (1983) 141–146. https://doi.org/10.1016/0022-1759(83)90392-7.

[150] A. Ljunglöf, K.M. Lacki, J. Mueller, C. Harinarayan, R. van Reis, R. Fahrner, J.M. Van Alstine, Ion exchange chromatography of antibody fragments, Biotechnol. Bioeng. 96 (2007) 515–524. https://doi.org/10.1002/bit.21124.

[151] R. Mhatre, W. Nashabeh, D. Schmalzing, X. Yao, M. Fuchs, D. Whitney, F. Regnier, Purification of antibody Fab fragments by cation-exchange chromatography and pH gradient elution, J. Chromatogr. A. 707 (1995) 225–231. https://doi.org/10.1016/0021-9673(95)00319-I.

[152] T. Gundinger, A. Pansy, O. Spadiut, A sensitive and robust HPLC method to quantify recombinant antibody fragments in E. coli crude cell lysate, J. Chromatogr. B. 1083 (2018) 242–248. https://doi.org/10.1016/j.jchromb.2018.02.044.

[153] J.M. Donaldson, C. Zer, K.N. Avery, K.P. Bzymek, D.A. Horne, J.C. Williams, Identification and grafting of a unique peptide-binding site in the Fab framework of monoclonal antibodies, Proc. Natl. Acad. Sci. 110 (2013) 17456–17461. https://doi.org/10.1073/pnas.1307309110.

[154] Y. Zhao, L. Gutshall, H. Jiang, A. Baker, E. Beil, G. Obmolova, J. Carton, S. Taudte, B. Amegadzie, Two routes for production and purification of Fab fragments in biopharmaceutical discovery research: Papain digestion of mAb and transient expression in mammalian cells, Protein Expr. Purif. 67 (2009) 182–189. https://doi.org/10.1016/j.pep.2009.04.012.

[155] H.S. Karkov, B.O. Krogh, J. Woo, S. Parimal, H. Ahmadian, S.M. Cramer, Investigation of protein selectivity in multimodal chromatography using in silico designed Fab fragment variants, Biotechnol. Bioeng. 112 (2015) 2305–2315. https://doi.org/10.1002/bit.25642.

[156] J.R. Robinson, H.S. Karkov, J.A. Woo, B.O. Krogh, S.M. Cramer, QSAR models for prediction of chromatographic behavior of homologous Fab variants, Biotechnol. Bioeng. 114 (2017) 1231–1240. https://doi.org/10.1002/bit.26236.

[157] M.A. Mascelli, E.T. Lance, L. Damaraju, C.L. Wagner, H.F. Weisman, R.E. Jordan, Pharmacodynamic profile of short-term abciximab treatment demonstrates prolonged platelet inhibition with gradual recovery from GP IIb/IIIa receptor blockade, Circulation. 97 (1998) 1680–1688.

[158] D.M. Knight, C. Wagner, R. Jordan, M.F. McAleer, R. DeRita, D.N. Fass, B.S. Coller, H.F. Weisman, J. Ghrayeb, The immunogenicity of the 7E3 murine monoclonal Fab antibody fragment variable region is dramatically reduced in humans by substitution of human for murine constant regions, Mol. Immunol. 32 (1995) 1271–1281. https://doi.org/10.1016/0161-5890(95)00085-2.

[159] R.J. Brezski, R.E. Jordan, Cleavage of IgGs by proteases associated with invasive diseases, MAbs. 2 (2010) 212–220.

[160] S. Kaku, K. Umemura, S. Yano, K. Suzuki, T. Kawasaki, M. Nakashima, YM337, A platelet glycoprotein IIb/IIIa antagonist, lessens photochemically-induced ischemic brain damage in monkeys, Drug Dev. Res. 47 (1999) 162–169. https://doi.org/10.1002/(SICI)1098-2299(199908)47:4<162::AID-DDR2>3.0.CO;2-9.

[161] C.H. Meyer, F.G. Holz, Preclinical aspects of anti-VEGF agents for the treatment of wet AMD: ranibizumab and bevacizumab, Eye. 25 (2011) 661–672. https://doi.org/10.1038/eye.2011.66.

[162] N. Ferrara, L. Damico, N. Shams, H. Lowman, R. Kim, Development of ranibizumab, an anti-vascular endothelial growth factor antigen binding fragment, as therapy for neovascular age-related macular degeneration, Retina Phila. Pa. 26 (2006) 859–870. https://doi.org/10.1097/01.iae.0000242842.14624.e7.

[163] Y. Chen, C. Wiesmann, G. Fuh, B. Li, H.W. Christinger, P. McKay, A.M. de Vos, H.B. Lowman, Selection and analysis of an optimized anti-VEGF antibody: crystal structure of an affinity-matured fab in complex with antigen11Edited by I. A. Wilson, J. Mol. Biol. 293 (1999) 865–881. https://doi.org/10.1006/jmbi.1999.3192.

[164] T.A. Moreno, S.J. Kim, Ranibizumab (Lucentis) versus Bevacizumab (Avastin) for the Treatment of Age-Related Macular Degeneration: An Economic Disparity of Eye Health, Semin. Ophthalmol. 31 (2016) 378–384. https://doi.org/10.3109/08820538.2016.1154174.

[165] L. Zou, H. Lai, Q. Zhou, F. Xiao, Lasting controversy on ranibizumab and bevacizumab, Theranostics. 1 (2011) 395–402.

[166] N. Goel, S. Stephens, Certolizumab pegol, MAbs. 2 (2010) 137–147.

[167] T. Bourne, G. Fossati, A. Nesbitt, A PEGylated Fab' fragment against tumor necrosis factor for the treatment of Crohn disease: exploring a new mechanism of action, BioDrugs Clin. Immunother. Biopharm. Gene Ther. 22 (2008) 331–337.

[168] G. Pasut, Pegylation of biological molecules and potential benefits: pharmacological properties of certolizumab pegol, BioDrugs Clin. Immunother. Biopharm. Gene Ther. 28 Suppl 1 (2014) S15-23. https://doi.org/10.1007/s40259-013-0064-z.

[169] J.U. Lee, W. Shin, J.Y. Son, K.-Y. Yoo, Y.-S. Heo, Molecular Basis for the Neutralization of Tumor Necrosis Factor α by Certolizumab Pegol in the Treatment of Inflammatory Autoimmune Diseases, Int. J. Mol. Sci. 18 (2017). https://doi.org/10.3390/ijms18010228.

[170] Y.Y. Syed, Idarucizumab: A Review as a Reversal Agent for Dabigatran, Am. J. Cardiovasc. Drugs Drugs Devices Interv. 16 (2016) 297–304. https://doi.org/10.1007/s40256-016-0181-4.

[171] T.C. Hutcherson, N.E. Cieri-Hutcherson, R. Bhatt, Evidence for Idarucizumab (Praxbind) in the Reversal Of the Direct Thrombin Inhibitor Dabigatran: Review Following the RE-VERSE AD Full Cohort Analysis, Pharm. Ther. 42 (2017) 692–698.

[172] P.A. Reilly, J. van Ryn, O. Grottke, S. Glund, J. Stangier, Idarucizumab, a Specific Reversal Agent for Dabigatran: Mode of Action, Pharmacokinetics and Pharmacodynamics, and Safety and Efficacy in Phase 1 Subjects, Am. J. Med. 129 (2016) S64–S72. https://doi.org/10.1016/j.amjmed.2016.06.007.

[173] P. Sié, Spotlight on idarucizumab and its potential for the reversal of anticoagulant effects of dabigatran, Drug Des. Devel. Ther. 10 (2016) 1683–1689. https://doi.org/10.2147/DDDT.S94167.

[174] J. Entwistle, J.G. Brown, S. Chooniedass, J. Cizeau, G.C. MacDonald, Preclinical evaluation of VB6-845: an anti-EpCAM immunotoxin with reduced immunogenic potential, Cancer Biother. Radiopharm. 27 (2012) 582–592. https://doi.org/10.1089/cbr.2012.1200.271.

[175] T. Eisen, G. Hedlund, G. Forsberg, R. Hawkins, Naptumomab estafenatox: targeted immunotherapy with a novel immunotoxin, Curr. Oncol. Rep. 16 (2014) 370. https://doi.org/10.1007/s11912-013-0370-0.

[176] L.G. Presta, Engineering antibodies for therapy, Curr. Pharm. Biotechnol. 3 (2002) 237–256.

[177] J. Cizeau, D.M. Grenkow, J.G. Brown, J. Entwistle, G.C. MacDonald, Engineering and biological characterization of VB6-845, an anti-EpCAM immunotoxin containing a T-cell epitope-depleted variant of the plant toxin bouganin, J. Immunother. Hagerstown Md 1997. 32 (2009) 574–584. https://doi.org/10.1097/CJI.0b013e3181a6981c.

[178] D.M. Shaw, N.B. Connolly, P.M. Patel, S. Kilany, G. Hedlund, O. Nordle, G. Forsberg, J. Zweit, P.L. Stern, R.E. Hawkins, A phase II study of a 5T4 oncofoetal antigen tumour-targeted superantigen (ABR-214936) therapy in patients with advanced renal cell carcinoma, Br. J. Cancer. 96 (2007) 567–574. https://doi.org/10.1038/sj.bjc.6603567.

[179] G. Forsberg, N.-J. Skartved, M. Wallén-Ohman, H.C. Nyhlén, K. Behm, G. Hedlund, T. Nederman, Naptumomab estafenatox, an engineered antibody-superantigen fusion protein with low toxicity and reduced antigenicity, J. Immunother. Hagerstown Md 1997. 33 (2010) 492–499. https://doi.org/10.1097/CJI.0b013e3181d75820.

[180] M.K. Robinson, R.K. Alpaugh, H. Borghaei, Naptumomab estafenatox: a new immunoconjugate, Expert Opin. Biol. Ther. 10 (2010) 273–279. https://doi.org/10.1517/14712590903575620.

[181] I. Colombo, M. Overchuk, J. Chen, R.M. Reilly, G. Zheng, S. Lheureux, Molecular imaging in drug development: Update and challenges for radiolabeled antibodies and nanotechnology, Methods San Diego Calif. (2017). https://doi.org/10.1016/j.ymeth.2017.07.018.

[182] R. Weissleder, U. Mahmood, Molecular Imaging, Radiology. 219 (2001) 316–333. https://doi.org/10.1148/radiology.219.2.r01ma19316.

[183] P.J. Kennedy, C. Oliveira, P.L. Granja, B. Sarmento, Antibodies and associates: Partners in targeted drug delivery, Pharmacol. Ther. 177 (2017) 129–145. https://doi.org/10.1016/j.pharmthera.2017.03.004.

[184] A.M. Wu, P.D. Senter, Arming antibodies: prospects and challenges for immunoconjugates, Nat. Biotechnol. 23 (2005) 1137–1146. https://doi.org/10.1038/nbt1141.

[185] C. Souriau, P.J. Hudson, Recombinant antibodies for cancer diagnosis and therapy, Expert Opin. Biol. Ther. 3 (2003) 305–318. https://doi.org/10.1517/14712598.3.2.305.

[186] H. Hong, J. Sun, W. Cai, Radionuclide-Based Cancer Imaging Targeting the Carcinoembryonic Antigen, Biomark. Insights. 3 (2008) 435–451.

[187] S. Kaur, G. Venktaraman, M. Jain, S. Senapati, P.K. Garg, S.K. Batra, Recent trends in antibody-based oncologic imaging, Cancer Lett. 315 (2012) 97–111. https://doi.org/10.1016/j.canlet.2011.10.017.

[188] G.J. Kelloff, K.A. Krohn, S.M. Larson, R. Weissleder, D.A. Mankoff, J.M. Hoffman, J.M. Link, K.Z. Guyton, W.C. Eckelman, H.I. Scher, J. O'Shaughnessy, B.D. Cheson, C.C. Sigman, J.L. Tatum, G.Q. Mills, D.C. Sullivan, J. Woodcock, The progress and promise of molecular imaging probes in oncologic drug development, Clin. Cancer Res. Off. J. Am. Assoc. Cancer Res. 11 (2005) 7967–7985. https://doi.org/10.1158/1078-0432.CCR-05-1302.

[189] D. Lamonica, M. Czuczman, H. Nabi, D. Klippenstein, Z. Grossman, Radioimmunoscintigraphy (RIS) with bectumomab (Tc99m labeled IMMU-LL2, Lymphoscan) in the assessment of recurrent non-Hodgkin's lymphoma (NHL), Cancer Biother. Radiopharm. 17 (2002) 689–697. https://doi.org/10.1089/108497802320970307.

[190] M.J. Blend, H. Hyun, M. Kozloff, H. Levi, G.Q. Mills, M. Gasparini, G. Buraggi, L. Hughes, C.M. Pinsky, D.M. Goldenberg, Improved staging of B-cell non-Hodgkin's lymphoma patients with 99mTc-labeled LL2 monoclonal antibody fragment, Cancer Res. 55 (1995) 5764s–5770s.

[191] C.A. Boswell, M.W. Brechbiel, Development of radioimmunotherapeutic and diagnostic antibodies: an inside-out view, Nucl. Med. Biol. 34 (2007) 757–778. https://doi.org/10.1016/j.nucmedbio.2007.04.001.

[192] R.J. Flanagan, A.L. Jones, Fab antibody fragments: some applications in clinical toxicology, Drug Saf. 27 (2004) 1115–1133.

[193] J.M. Scherrmann, Antibody treatment of toxin poisoning--recent advances, J. Toxicol. Clin. Toxicol. 32 (1994) 363–375.

[194] C. Maillaud, Y. Barguil, M. Mikulski, M. Cheze, C. Pivert, M. Deveaux, F. Lapostolle, First successful curative use of digoxin-specific Fab antibody fragments in a life-threatening coconut crab (Birgus latro L.) poisoning, Toxicon Off. J. Int. Soc. Toxinology. 60 (2012) 1013–1017. https://doi.org/10.1016/j.toxicon.2012.06.017.

[195] M. Eddleston, N. Fabresse, A. Thompson, I. Al Abdulla, R. Gregson, T. King, A. Astier, F.J. Baud, R.E. Clutton, J.-C. Alvarez, Anti-colchicine Fab fragments prevent lethal colchicine toxicity in a porcine model: a pharmacokinetic and clinical study, Clin. Toxicol. Phila. Pa. (2018) 1–9. https://doi.org/10.1080/15563650.2017.1422510.

[196] G. Spraggon, X-Ray Crystallography for Biotherapeutics, in: Biophys. Methods Biotherapeutics, Wiley-Blackwell, 2014: pp. 25–64. https://doi.org/10.1002/9781118354698.ch2.

[197] L. Griffin, A. Lawson, Antibody fragments as tools in crystallography, Clin. Exp. Immunol. 165 (2011) 285–291. https://doi.org/10.1111/j.1365-2249.2011.04427.x.

[198] C. Hunte, H. Michel, Crystallisation of membrane proteins mediated by antibody fragments, Curr. Opin. Struct. Biol. 12 (2002) 503–508.

[199] A. Gardulf, Clinical experiences in primary and secondary immunodeficiencies and immune-mediated conditions using Gammanorm®, Immunotherapy. 8 (2016) 633–647. https://doi.org/10.2217/imt-2015-0013.

[200] I. Campos-Pinto, E. Espitia-Saloma, S.A.S.L. Rosa, M. Rito-Palomares, O. Aguilar, M. Arévalo-Rodríguez, M.R. Aires-Barros, A.M. Azevedo, Integration of cell harvest with affinity-enhanced purification of monoclonal antibodies using aqueous two-phase systems with a dual tag ligand, Sep. Purif. Technol. 173 (2017) 129–134. https://doi.org/10.1016/j.seppur.2016.09.017.

[201] A. Nascimento, S.A.S.L. Rosa, M. Mateus, A.M. Azevedo, Polishing of monoclonal antibodies streams through convective flow devices, Sep. Purif. Technol. 132 (2014) 593–600. https://doi.org/10.1016/j.seppur.2014.06.005.

[202] E. Harlow, D. Lane, Antibodies: A Laboratory Manual, CSHL Press, 1988.

[203] L. Coleman, S.M. Mahler, Purification of Fab fragments from a monoclonal antibody papain digest by Gradiflow electrophoresis, Protein Expr. Purif. 32 (2003) 246–251. https://doi.org/10.1016/j.pep.2003.07.005.

[204] A.A. Homaei, R.H. Sajedi, R. Sariri, S. Seyfzadeh, R. Stevanato, Cysteine enhances activity and stability of immobilized papain, Amino Acids. 38 (2009) 937–942. https://doi.org/10.1007/s00726-009-0302-3.

[205] Z. Lakhrif, M. Pugnière, C. Henriquet, A. di Tommaso, I. Dimier-Poisson, P. Billiald, M.O. Juste, N. Aubrey, A method to confer Protein L binding ability to any antibody fragment, MAbs. 8 (2015) 379–388. https://doi.org/10.1080/19420862.2015.1116657.

[206] S.A. Camperi, M.M. Marani, M. Ceron, M. Camila, F. Albericio, O. Cascone, Protein purification by affinity chromatography with peptide ligands selected from the screening of combinatorial libraries, (2010). http://ri.conicet.gov.ar/handle/11336/14495 (accessed December 5, 2017).

[207] W.-W. Zhao, F.-F. Liu, Q.-H. Shi, X.-Y. Dong, Y. Sun, Biomimetic design of affinity peptide ligands for human IgG based on protein A-IgG complex, Biochem. Eng. J. 88 (2014) 1–11. https://doi.org/10.1016/j.bej.2014.03.015.

[208] R.-Z. Wang, D.-Q. Lin, W.-N. Chu, Q.-L. Zhang, S.-J. Yao, New tetrapeptide ligands designed for antibody purification with biomimetic chromatography: Molecular simulation and experimental validation, Biochem. Eng. J. 114 (2016) 191–201. https://doi.org/10.1016/j.bej.2016.06.030.

[209] B. Bakhshinejad, H.M. Zade, H.S.Z. Shekarabi, S. Neman, Phage display biopanning and isolation of target-unrelated peptides: in search of nonspecific binders hidden in a combinatorial library, Amino Acids. 48 (2016) 2699–2716. https://doi.org/10.1007/s00726-016-2329-6.

[210] K. Fukunaga, M. Taki, Practical Tips for Construction of Custom Peptide Libraries and Affinity Selection by Using Commercially Available Phage Display Cloning Systems, J. Nucleic Acids. (2012). https://doi.org/10.1155/2012/295719.

[211] J. Beech, L. Saleh, J. Frentzel, H. Figler, I.R. Corrêa, B. Baker, C. Ramspacher, M. Marshall, S. Dasa, J. Linden, C.J. Noren, K.A. Kelly, Multivalent site-specific phage modification enhances the binding affinity of receptor ligands, Bioconjug. Chem. 26 (2015) 529–536. https://doi.org/10.1021/acs.bioconjchem.5b00011.

[212] P.D. Skottrup, G. Sørensen, M. Ksiazek, J. Potempa, E. Riise, A Phage Display Selected 7-mer Peptide Inhibitor of the Tannerella forsythia Metalloprotease-Like Enzyme Karilysin can be Truncated to Ser-Trp-Phe-Pro, PLOS ONE. 7 (2012) e48537. https://doi.org/10.1371/journal.pone.0048537.

[213] J. Ling, H. Liao, R. Clark, M.S.M. Wong, D.D. Lo, Structural Constraints for the Binding of Short Peptides to Claudin-4 Revealed by Surface Plasmon Resonance, J. Biol. Chem. 283 (2008) 30585–30595. https://doi.org/10.1074/jbc.M803548200.

[214] R. Derda, S.K.Y. Tang, S.C. Li, S. Ng, W. Matochko, M.R. Jafari, Diversity of phage-displayed libraries of peptides during panning and amplification, Mol. Basel Switz. 16 (2011) 1776–1803. https://doi.org/10.3390/molecules16021776.

[215] J. Pande, M.M. Szewczyk, A.K. Grover, Phage display: concept, innovations, applications and future, Biotechnol. Adv. 28 (2010) 849–858. https://doi.org/10.1016/j.biotechadv.2010.07.004.

[216] D.J.H. Gaskin, K. Starck, N.A. Turner, E.N. Vulfson, Phage display combinatorial libraries of short peptides: ligand selection for protein purification, Enzyme Microb. Technol. 28 (2001) 766–772. https://doi.org/10.1016/S0141-0229(01)00330-1.

[217] A. Nascimento, A. Mullerpatan, A.M. Azevedo, P. Karande, S. Cramer, Development of phage biopanning strategies to identify affinity peptide ligands for kappa light chain Fab fragments, Biotechnol. Prog. n/a (n.d.) e2884. https://doi.org/10.1002/btpr.2884.

[218] D. Chandra, S. Timmick, C. Goodwine, N. Vecchiarello, D.G. Shastry, A. Mullerpatan, J.P. Trasatti, S. Cramer, P. Karande, Design of peptide ligands for affinity purification of human growth hormone, J. Chem. Technol. Biotechnol. 0 (n.d.). https://doi.org/10.1002/jctb.6029.

[219] H. Prinz, Hill coefficients, dose–response curves and allosteric mechanisms, J. Chem. Biol. 3 (2010) 37–44. https://doi.org/10.1007/s12154-009-0029-3.

[220] H.S. Karkov, Investigations into multimodal chromatographic selectivity using in silico designed Fab fragment variants, Rensselaer Polytechnic Institute, n.d. https://search.proquest.com/docview/1694581571?pq-origsite=gscholar.

[221] New England Biolabs: Ph.D.™ Phage Display Libraries. Instruction Manual, Version 2.1 Access online https://www.neb.com/-/media/catalog/datacards-or-manuals/manuale8110.pdf, (n.d.).

[222] D.J. Rodi, R.W. Janes, H.J. Sanganee, R.A. Holton, B.A. Wallace, L. Makowski, Screening of a library of phage-displayed peptides identifies human Bcl-2 as a taxol-binding protein11Edited by I. A. Wilson, J. Mol. Biol. 285 (1999) 197–203. https://doi.org/10.1006/jmbi.1998.2303.

[223] S.J. McConnell, T. Dinh, M.-H. Le, D.G. Spinella, Biopanning Phage Display Libraries Using Magnetic Beads Vs. Polystyrene Plates, BioTechniques. 26 (1999) 208–214. https://doi.org/10.2144/99262bm06.

[224] T. Hatanaka, S. Ohzono, M. Park, K. Sakamoto, S. Tsukamoto, R. Sugita, H. Ishitobi, T. Mori, O. Ito, K. Sorajo, K. Sugimura, S. Ham, Y. Ito, Human IgA-binding peptides selected from random peptide libraries: affinity maturation and application in IgA purification, J. Biol. Chem. 287 (2012) 43126–43136. https://doi.org/10.1074/jbc.M112.389742.

[225] H.S. Karkov, B.O. Krogh, J. Woo, S. Parimal, H. Ahmadian, S.M. Cramer, Investigation of protein selectivity in multimodal chromatography using in silico designed Fab fragment variants, Biotechnol. Bioeng. 112 (2015) 2305–2315. https://doi.org/10.1002/bit.25642.

[226] H.-M. Chu, J. Wright, Y.-H. Chan, C.-J. Lin, T.W. Chang, C. Lim, Two potential therapeutic antibodies bind to a peptide segment of membrane-bound IgE in different conformations, Nat. Commun. 5 (2014) 3139. https://doi.org/10.1038/ncomms4139.

[227] M. Paloni, C. Cavallotti, Molecular Modeling of the Interaction of Protein L with Antibodies, ACS Omega. 2 (2017) 6464–6472. https://doi.org/10.1021/acsomega.7b01123.

[228] S. Yun, S. Lee, J.P. Park, J. Choo, E.K. Lee, Modification of phage display technique for improved screening of high-affinity binding peptides, J. Biotechnol. 289 (2019) 88–92. https://doi.org/10.1016/j.jbiotec.2018.11.020.

[229] E.O. Saphire, R.L. Stanfield, M.D. Max Crispin, P.W.H.I. Parren, P.M. Rudd, R.A. Dwek, D.R. Burton, I.A. Wilson, Contrasting IgG Structures Reveal Extreme Asymmetry and Flexibility, J. Mol. Biol. 319 (2002) 9–18. https://doi.org/10.1016/S0022-2836(02)00244-9.

[230] K.L. Morrison, G.A. Weiss, Combinatorial alanine-scanning, Curr. Opin. Chem. Biol. 5 (2001) 302–307.

[231] G.A. Weiss, C.K. Watanabe, A. Zhong, A. Goddard, S.S. Sidhu, Rapid mapping of protein functional epitopes by combinatorial alanine scanning, Proc. Natl. Acad. Sci. 97 (2000) 8950–8954. https://doi.org/10.1073/pnas.160252097.

[232] S.D. Mahan, G.C. Ireton, B.L. Stoddard, M.E. Black, Alanine-Scanning Mutagenesis Reveals a Cytosine Deaminase Mutant with Altered Substrate Preference, Biochemistry. 43 (2004) 8957–8964. https://doi.org/10.1021/bi049720z.

[233] E. Davidson, B.J. Doranz, A high-throughput shotgun mutagenesis approach to mapping B-cell antibody epitopes, Immunology. 143 (2014) 13–20. https://doi.org/10.1111/imm.12323.

[234] J. Pons, A. Rajpal, J.F. Kirsch, Energetic analysis of an antigen/antibody interface: alanine scanning mutagenesis and double mutant cycles on the HyHEL-10/lysozyme interaction, Protein Sci. Publ. Protein Soc. 8 (1999) 958–968. https://doi.org/10.1110/ps.8.5.958.

[235] D.J. Sloan, H.W. Hellinga, Dissection of the protein G B1 domain binding site for human IgG Fc fragment, Protein Sci. Publ. Protein Soc. 8 (1999) 1643–1648. https://doi.org/10.1110/ps.8.8.1643.

[236] D.M. Krüger, H. Gohlke, DrugScorePPI webserver: fast and accurate in silico alanine scanning for scoring protein-protein interactions, Nucleic Acids Res. 38 (2010) W480-486. https://doi.org/10.1093/nar/gkq471.

[237] L. Serrano, J.L. Neira, J. Sancho, A.R. Fersht, Effect of alanine versus glycine in alpha-helices on protein stability, Nature. 356 (1992) 453–455. https://doi.org/10.1038/356453a0.

[238] L. Raguine, M. Ali, V. Bender, E. Diefenbach, M.R. Doddareddy, D. Hibbs, N. Manolios, Alanine scan of an immunosuppressive peptide (CP): analysis of structure-function relationships, Chem. Biol. Drug Des. 81 (2013) 167–174. https://doi.org/10.1111/cbdd.12080.

[239] D. Hu, S. Hu, W. Wan, M. Xu, R. Du, W. Zhao, X. Gao, J. Liu, H. Liu, J. Hong, Effective Optimization of Antibody Affinity by Phage Display Integrated with High-Throughput DNA Synthesis and Sequencing Technologies, PLoS ONE. 10 (2015). https://doi.org/10.1371/journal.pone.0129125.

[240] K. Kallberg, H.-O. Johansson, L. Bulow, Multimodal chromatography: An efficient tool in downstream processing of proteins, Biotechnol. J. 7 (2012) 1485–1495. https://doi.org/10.1002/biot.201200074.

[241] V. Halan, S. Maity, R.B. and A.S. Rathore*, Multimodal Chromatography for Purification of Biotherapeutics – A Review, Curr. Protein Pept. Sci. (2018). http://www.eurekaselect.com/156487/article (accessed October 14, 2019).

[242] K. Zhao, F. Yang, H. Xia, F. Wang, Q. Song, Q. Bai, Preparation of a weak anion exchange/hydrophobic interaction dual-function mixed-mode chromatography stationary phase for protein separation using click chemistry, J. Sep. Sci. 38 (2015) 703–710. https://doi.org/10.1002/jssc.201401020.

[243] G. Zhao, X.-Y. Dong, Y. Sun, Ligands for mixed-mode protein chromatography: Principles, characteristics and design, J. Biotechnol. 144 (2009) 3–11. https://doi.org/10.1016/j.jbiotec.2009.04.009.

[244] Q.-C. Wu, D.-Q. Lin, W. Shi, Q.-L. Zhang, S.-J. Yao, A mixed-mode resin with tryptamine ligand for human serum albumin separation, J. Chromatogr. A. 1431 (2016) 145–153. https://doi.org/10.1016/j.chroma.2015.12.066.

[245] H.-F. Tong, D.-Q. Lin, W.-N. Chu, Q.-L. Zhang, D. Gao, R.-Z. Wang, S.-J. Yao, Multimodal charge-induction chromatography for antibody purification, J. Chromatogr. A. 1429 (2016) 258–264. https://doi.org/10.1016/j.chroma.2015.12.047.

[246] S.J. Mountford, R. Daly, A.J. Robinson, M.T.W. Hearn, Design, synthesis and evaluation of pyridine-based chromatographic adsorbents for antibody purification, J. Chromatogr. A. 1355 (2014) 15–25. https://doi.org/10.1016/j.chroma.2014.06.006.

[247] K.A. Kaleas, M. Tripodi, S. Revelli, V. Sharma, S.A. Pizarro, Evaluation of a multimodal resin for selective capture of CHO-derived monoclonal antibodies directly from harvested cell culture fluid, J. Chromatogr. B Analyt. Technol. Biomed. Life. Sci. 969 (2014) 256–263. https://doi.org/10.1016/j.jchromb.2014.08.026.

[248] J. Wang, J. Zhou, Y.K. Gowtham, S.W. Harcum, S.M. Husson, Antibody purification from CHO cell supernatant using new multimodal membranes, Biotechnol. Prog. 33 (2017) 658–665. https://doi.org/10.1002/btpr.2454.

[249] I.F. Pinto, M.R. Aires-Barros, A.M. Azevedo, Multimodal chromatography: debottlenecking the downstream processing of monoclonal antibodies, Pharm. Bioprocess. 3 (2015) 263–279. https://doi.org/10.4155/pbp.15.7.

[250] I. Arora, Chromatographic Methods for the Purification of Monoclonal Antibodies and their Alternatives:A Review, in: 2013.

[251] R. Bhambure, D. Gupta, A.S. Rathore, A novel multimodal chromatography based single step purification process for efficient manufacturing of an E. coli based biotherapeutic protein product, J. Chromatogr. A. 1314 (2013) 188–198. https://doi.org/10.1016/j.chroma.2013.09.026.

[252] J.P. Welsh, M.G. Petroff, P. Rowicki, H. Bao, T. Linden, D.J. Roush, J.M. Pollard, A practical strategy for using miniature chromatography columns in a standardized high-throughput workflow for purification development of monoclonal antibodies, Biotechnol. Prog. 30 (2014) 626–635. https://doi.org/10.1002/btpr.1905.

[253] K.M. Lacki, E. Brekkan, High throughput screening techniques in protein purification, Methods Biochem. Anal. 54 (2011) 489–506.

[254] J. Pollard, P. McDonald, A. Hesslein, Lessons learned in building high-throughput process development capabilities, Eng. Life Sci. 16 (2016) 93–98. https://doi.org/10.1002/elsc.201400254.

[255] J.L. Coffman, J.F. Kramarczyk, B.D. Kelley, High-throughput screening of chromatographic separations: I. Method development and column modeling, Biotechnol. Bioeng. 100 (2008) 605–618. https://doi.org/10.1002/bit.21904.

[256] B. Çetin, M.B. Özer, M.E. Solmaz, Microfluidic bio-particle manipulation for biotechnology, Biochem. Eng. J. 92 (2014) 63–82. https://doi.org/10.1016/j.bej.2014.07.013.

[257] F.A. Gomez, Microfluidics in Protein Chromatography, in: D. Walls, S.T. Loughran (Eds.), Protein Chromatogr. Methods Protoc., Humana Press, Totowa, NJ, 2011: pp. 137–150. https://doi.org/10.1007/978-1-60761-913-0_8.

[258] J. Huft, C.A. Haynes, C.L. Hansen, Fabrication of High-Quality Microfluidic Solid-Phase Chromatography Columns, Anal. Chem. 85 (2013) 1797–1802. https://doi.org/10.1021/ac303153a.

[259] S. Choi, J.-K. Park, Two-step photolithography to fabricate multilevel microchannels, Biomicrofluidics. 4 (2010). https://doi.org/10.1063/1.3517230.

[260] D. Qin, Y. Xia, G.M. Whitesides, Soft lithography for micro- and nanoscale patterning, Nat. Protoc. 5 (2010) 491–502. https://doi.org/10.1038/nprot.2009.234.

[261] S.K. Sia, G.M. Whitesides, Microfluidic devices fabricated in poly(dimethylsiloxane) for biological studies, Electrophoresis. 24 (2003) 3563–3576. https://doi.org/10.1002/elps.200305584.

[262] I.F. Pinto, C.R.F. Caneira, R.R.G. Soares, N. Madaboosi, M.R. Aires-Barros, J.P. Conde, A.M. Azevedo, V. Chu, The application of microbeads to microfluidic systems for enhanced detection and purification of biomolecules, Methods. 116 (2017) 112–124. https://doi.org/10.1016/j.ymeth.2016.12.005.

[263] I.F. Pinto, R.R.G. Soares, S.A.S.L. Rosa, M.R. Aires-Barros, V. Chu, J.P. Conde, A.M. Azevedo, High-Throughput Nanoliter-Scale Analysis and Optimization of Multimodal Chromatography for the Capture of Monoclonal Antibodies, Anal. Chem. 88 (2016) 7959–7967. https://doi.org/10.1021/acs.analchem.6b00781.

[264] M.S. Shapiro, S.J. Haswell, G.J. Lye, D.G. Bracewell, Design and characterization of a microfluidic packed bed system for protein breakthrough and dynamic binding capacity determination, Biotechnol. Prog. 25 (2009) 277–285. https://doi.org/10.1002/btpr.99.

[265] M.S. Shapiro, S.J. Haswell, G.J. Lye, D.G. Bracewell, Microfluidic Chromatography for Early Stage Evaluation of Biopharmaceutical Binding and Separation Conditions, Sep. Sci. Technol. 46 (2010) 185–194. https://doi.org/10.1080/01496395.2010.511641.

[266] I.F. Pinto, D.R. Santos, R.R.G. Soares, M.R. Aires-Barros, V. Chu, A.M. Azevedo, J.P. Conde, A regenerable microfluidic device with integrated valves and thin-film photodiodes for rapid optimization of chromatography conditions, Sens. Actuators B Chem. 255 (2018) 3636–3646. https://doi.org/10.1016/j.snb.2017.09.167.

[267] H.S. Rho, A.T. Hanke, M. Ottens, H. Gardeniers, A microfluidic device for the batch adsorption of a protein on adsorbent particles, Analyst. 142 (2017) 3656–3665. https://doi.org/10.1039/C7AN00917H.

[268] M.N.S. Pedro, A.M. Azevedo, M.R. Aires-Barros, R.R.G. Soares, Minimizing the Influence of Fluorescent Tags on IgG Partition in PEG–Salt Aqueous Two-Phase Systems for Rapid Screening Applications, Biotechnol. J. 14 (2019). https://doi.org/10.1002/biot.201800640.

[269] M.J. Jacinto, R.R.G. Soares, A.M. Azevedo, V. Chu, A. Tover, J.P. Conde, M.R. Aires-Barros, Optimization and miniaturization of aqueous two phase systems for the purification of recombinant human immunodeficiency virus-like particles from a CHO cell supernatant, Sep. Purif. Technol. 154 (2015) 27–35. https://doi.org/10.1016/j.seppur.2015.09.006.

[270] I. Olsson, U.-B. Axiö-Fredriksson, M. Degerman, B. Olsson, Fast horizontal electrophoresis. I. Isoelectric focusing and polyacrylamide gel electrophoresis using PhastSystem™, ELECTROPHORESIS. 9 (1988) 16–22. https://doi.org/10.1002/elps.1150090104.

[271] R. Fradique, A.M. Azevedo, V. Chu, J.P. Conde, M.R. Aires-Barros, Microfluidic platform for rapid screening of bacterial cell lysis, J. Chromatogr. A. (2019) 460539. https://doi.org/10.1016/j.chroma.2019.460539.

[272] A.R. Silva-Santos, C.P.A. Alves, D.M.F. Prazeres, A.M. Azevedo, A process for supercoiled plasmid DNA purification based on multimodal chromatography, Sep. Purif. Technol. 182 (2017) 94–100. https://doi.org/10.1016/j.seppur.2017.03.042.

[273] S. Xiong, L. Zhang, Q.-Y. He, Fractionation of proteins by heparin chromatography, Methods Mol. Biol. Clifton NJ. 424 (2008) 213–221. https://doi.org/10.1007/978-1-60327-064-9_18.

[274] S. Fekete, A. Beck, D. Guillarme, Characterization of cation exchanger stationary phases applied for the separations of therapeutic monoclonal antibodies, J. Pharm. Biomed. Anal. 111 (2015) 169–176. https://doi.org/10.1016/j.jpba.2015.03.041.

[275] A. Staby, J.H. Jacobsen, R.G. Hansen, U.K. Bruus, I.H. Jensen, Comparison of chromatographic ion-exchange resins V. Strong and weak cation-exchange resins, J. Chromatogr. A. 1118 (2006) 168–179. https://doi.org/10.1016/j.chroma.2006.03.116.

[276] A. Staby, M.-B. Sand, R.G. Hansen, J.H. Jacobsen, L.A. Andersen, M. Gerstenberg, U.K. Bruus, I.H. Jensen, Comparison of chromatographic ion-exchange resins IV. Strong and weak cation-exchange resins and heparin resins, J. Chromatogr. A. 1069 (2005) 65–77.

[277] G. Joucla, C. Le Sénéchal, M. Bégorre, B. Garbay, X. Santarelli, C. Cabanne, Cation exchange versus multimodal cation exchange resins for antibody capture from CHO supernatants: identification of contaminating host cell proteins by mass spectrometry, J. Chromatogr. B Analyt. Technol. Biomed. Life. Sci. 942–943 (2013) 126–133. https://doi.org/10.1016/j.jchromb.2013.10.033.

[278] M. Zhu, G. Carta, Protein adsorption equilibrium and kinetics in multimodal cation exchange resins, Adsorption. 22 (2016) 165–179. https://doi.org/10.1007/s10450-015-9735-z.

[279] D. Gonze, W. Abou-Jaoudé, The Goodwin Model: Behind the Hill Function, PLOS ONE. 8 (2013) e69573. https://doi.org/10.1371/journal.pone.0069573.

[280] R. Gesztelyi, J. Zsuga, A. Kemeny-Beke, B. Varga, B. Juhasz, A. Tosaki, The Hill equation and the origin of quantitative pharmacology, Arch. Hist. Exact Sci. 66 (2012) 427–438. https://doi.org/10.1007/s00407-012-0098-5.

[281] X.M. He, C. Voß, J. Li, Exploring the Unique Selectivity of Hydrophobic Cation Exchanger Nuvia cPrime for the Removal of a Major Process Impurity: A Case Study with IgM, Curr. Protein Pept. Sci. 20 (2019) 65–74. https://doi.org/10.2174/1389203718666171017130506.

[282] J.A. Woo, H. Chen, M.A. Snyder, Y. Chai, R.G. Frost, S.M. Cramer, Defining the property space for chromatographic ligands from a homologous series of mixed-mode ligands, J. Chromatogr. A. 1407 (2015) 58–68. https://doi.org/10.1016/j.chroma.2015.06.017.

[283] S.M. Timmick, N. Vecchiarello, C. Goodwine, L.E. Crowell, K.R. Love, J.C. Love, S.M. Cramer, An impurity characterization based approach for the rapid development of integrated downstream purification processes, Biotechnol. Bioeng. 115 (2018) 2048–2060. https://doi.org/10.1002/bit.26718.

[284] C. J. Welch, High throughput analysis enables high throughput experimentation in pharmaceutical process research, React. Chem. Eng. (2019). https://doi.org/10.1039/C9RE00234K.

[285] S. Parimal, S. Garde, S.M. Cramer, Interactions of Multimodal Ligands with Proteins: Insights into Selectivity Using Molecular Dynamics Simulations, Langmuir ACS J. Surf. Colloids. 31 (2015) 7512–7523. https://doi.org/10.1021/acs.langmuir.5b00236.

[286] J. Vajda, E. Mueller, E. Bahret, Dual salt mixtures in mixed mode chromatography with an immobilized tryptophan ligand influence the removal of aggregated monoclonal antibodies, Biotechnol. J. 9 (2014) 555–565. https://doi.org/10.1002/biot.201300230.

[287] A. Tiselius, S. Hjertén, Ö. Levin, Protein chromatography on calcium phosphate columns, Arch. Biochem. Biophys. 65 (1956) 132–155. https://doi.org/10.1016/0003-9861(56)90183-7.

[288] M. Niimi, T. Masuda, K. Kaihatsu, N. Kato, S. Nakamura, T. Nakaya, F. Arai, Virus purification and enrichment by hydroxyapatite chromatography on a chip, Sens. Actuators B Chem. 201 (2014) 185–190. https://doi.org/10.1016/j.snb.2014.04.011.

[289] D.L. Wensel, B.D. Kelley, J.L. Coffman, High-throughput screening of chromatographic separations: III. Monoclonal antibodies on ceramic hydroxyapatite, Biotechnol. Bioeng. 100 (2008) 839–854. https://doi.org/10.1002/bit.21906.

[290] B.V. Ayyar, S. Arora, C. Murphy, R. O'Kennedy, Affinity chromatography as a tool for antibody purification, Methods San Diego Calif. 56 (2012) 116–129. https://doi.org/10.1016/j.ymeth.2011.10.007.

[291] P. Gagnon, Improved antibody aggregate removal by hydroxyapatite chromatography in the presence of polyethylene glycol, J. Immunol. Methods. 336 (2008) 222–228. https://doi.org/10.1016/j.jim.2008.05.002.

[292] A. Hirano, T. Arakawa, T. Kameda, Effects of arginine on multimodal anion exchange chromatography, Protein Expr. Purif. 116 (2015) 105–112. https://doi.org/10.1016/j.pep.2015.07.013.

[293] Y.L. Jeyachandran, E. Mielczarski, B. Rai, J.A. Mielczarski, Quantitative and qualitative evaluation of adsorption/desorption of bovine serum albumin on hydrophilic and hydrophobic surfaces, Langmuir ACS J. Surf. Colloids. 25 (2009) 11614–11620. https://doi.org/10.1021/la901453a.

[294] J. Robinson, M.A. Snyder, C. Belisle, J. Liao, H. Chen, X. He, Y. Xu, S.M. Cramer, Investigating the impact of aromatic ring substitutions on selectivity for a multimodal anion exchange prototype library, J. Chromatogr. A. 1569 (2018) 101–109. https://doi.org/10.1016/j.chroma.2018.07.049.

[295] J. Pezzini, G. Joucla, R. Gantier, M. Toueille, A.-M. Lomenech, C. Le Sénéchal, B. Garbay, X. Santarelli, C. Cabanne, Antibody capture by mixed-mode chromatography: A comprehensive study from determination of optimal purification conditions to identification of contaminating host cell proteins, J. Chromatogr. A. 1218 (2011) 8197–8208. https://doi.org/10.1016/j.chroma.2011.09.036.

[296] J. Pezzini, C. Cabanne, R. Gantier, V.N. Janakiraman, X. Santarelli, A comprehensive evaluation of mixed mode interactions of HEA and PPA HyperCel™ chromatographic media, J. Chromatogr. B. 976–977 (2015) 68–77. https://doi.org/10.1016/j.jchromb.2014.11.020.

[297] J. Pezzini, C. Cabanne, J.-W. Dupuy, R. Gantier, X. Santarelli, A study on the nature of interactions of mixed-mode ligands HEA and PPA HyperCel using phenylglyoxal modified lysozyme, J. Chromatogr. B. 960 (2014) 209–213. https://doi.org/10.1016/j.jchromb.2014.04.046.

[298] V. Brenac Brochier, A. Schapman, P. Santambien, L. Britsch, Fast purification process optimization using mixed-mode chromatography sorbents in pre-packed mini-columns, J. Chromatogr. A. 1177 (2008) 226–233. https://doi.org/10.1016/j.chroma.2007.08.086.

[299] T. Arakawa, M. Futatsumori-Sugai, K. Tsumoto, Y. Kita, H. Sato, D. Ejima, MEP HyperCel chromatography II: Binding, washing and elution, Protein Expr. Purif. 71 (2010) 168–173. https://doi.org/10.1016/j.pep.2009.11.004.

[300] J. Chen, J. Tetrault, Y. Zhang, A. Wasserman, G. Conley, M. DiLeo, E. Haimes, A.E. Nixon, A. Ley, The distinctive separation attributes of mixed-mode resins and their application in monoclonal antibody downstream purification process, J. Chromatogr. A. 1217 (2010) 216–224. https://doi.org/10.1016/j.chroma.2009.09.047.

[301] R. Ravichandran, V. Padmanabhan, M.A. Vijayalakhsmi, N.S. Jayaprakash, Studies on recovery of lactoferrin from bovine colostrum whey using mercapto ethyl pyridine and phenyl propyl amine HyperCel™ mixed mode sorbents, Biotechnol. Bioprocess Eng. 20 (2015) 148–156. https://doi.org/10.1007/s12257-014-0408-7.

[302] J.P. Welsh, H. Bao, K. Barlow, J.M. Pollard, E. Brekkan, K.M. Lacki, T.O. Linden, D.J. Roush, High-throughput techniques to evaluate the effect of ligand density for impurity separations with multimodal cation exchange resins, Eng. Life Sci. 16 (2016) 160–168. https://doi.org/10.1002/elsc.201400251.

[303] B.K. Nfor, M. Noverraz, S. Chilamkurthi, P.D.E.M. Verhaert, L.A.M. van der Wielen, M. Ottens, High-throughput isotherm determination and thermodynamic modeling of protein adsorption on mixed mode adsorbents, J. Chromatogr. A. 1217 (2010) 6829–6850. https://doi.org/10.1016/j.chroma.2010.07.069.

[304] D.R. Santos, R.R.G. Soares, I.F. Pinto, C.R.F. Caneira, R.M.R. Pinto, V. Chu, J.P. Conde, Label-Free Detection of Biomolecules in Microfluidic Systems Using On-Chip UV and Impedimetric Sensors, IEEE Sens. J. 19 (2019) 7803–7812. https://doi.org/10.1109/JSEN.2019.2917305.

[305] X.-C. Liu, W.H. Scouten, Boronate Affinity Chromatography, in: P. Bailon, G.K. Ehrlich, W.-J. Fung, W. Berthold (Eds.), Affin. Chromatogr. Methods Protoc., Humana Press, Totowa, NJ, 2000: pp. 119–128. https://doi.org/10.1007/978-1-60327-261-2_12.

[306] A.M. Azevedo, A.G. Gomes, L. Borlido, I.F.S. Santos, D.M.F. Prazeres, M.R. Aires-Barros, Capture of human monoclonal antibodies from a clarified cell culture supernatant by phenyl boronate chromatography, J. Mol. Recognit. JMR. 23 (2010) 569–576. https://doi.org/10.1002/jmr.1068.

[307] A.L. Grilo, M. Mateus, M.R. Aires-Barros, A.M. Azevedo, Monoclonal Antibodies Production Platforms: An Opportunity Study of a Non-Protein-A Chromatographic Platform Based on Process Economics, Biotechnol. J. 12 (2017). https://doi.org/10.1002/biot.201700260.

[308] R.J. Carvalho, J. Woo, M.R. Aires-Barros, S.M. Cramer, A.M. Azevedo, Phenylboronate chromatography selectively separates glycoproteins through the manipulation of electrostatic, charge transfer, and cis-diol interactions, Biotechnol. J. 9 (2014) 1250–1258. https://doi.org/10.1002/biot.201400170.

[309] B. Zhang, S. Mathewson, H. Chen, Two-dimensional liquid chromatographic methods to examine phenylboronate interactions with recombinant antibodies, J. Chromatogr. A. 1216 (2009) 5676–5686. https://doi.org/10.1016/j.chroma.2009.05.084.

[310] D. Li, Y. Chen, Z. Liu, Boronate affinity materials for separation and molecular recognition: structure, properties and applications, Chem. Soc. Rev. 44 (2015) 8097–8123. https://doi.org/10.1039/C5CS00013K.

[311] S.A.S.L. Rosa, C.L. da Silva, M.R. Aires-Barros, A.C. Dias-Cabral, A.M. Azevedo, Thermodynamics of the adsorption of monoclonal antibodies in phenylboronate chromatography: Affinity versus multimodal interactions, J. Chromatogr. A. 1569 (2018) 118–127. https://doi.org/10.1016/j.chroma.2018.07.050.

[312] A.G. Gomes, A.M. Azevedo, M.R. Aires-Barros, D.M.F. Prazeres, Studies on the adsorption of cell impurities from plasmid-containing lysates to phenyl boronic acid chromatographic beads, J. Chromatogr. A. 1218 (2011) 8629–8637. https://doi.org/10.1016/j.chroma.2011.10.004.

[313] S.A.S.L. Rosa, R. dos Santos, M.R. Aires-Barros, A.M. Azevedo, Phenylboronic acid chromatography provides a rapid, reproducible and easy scalable multimodal process for the capture of monoclonal antibodies, Sep. Purif. Technol. 160 (2016) 43–50. https://doi.org/10.1016/j.seppur.2016.01.002.

[314] J. Qian, T. Liu, L. Yang, A. Daus, R. Crowley, Q. Zhou, Structural characterization of N-linked oligosaccharides on monoclonal antibody cetuximab by the combination of orthogonal matrix-assisted laser desorption/ionization hybrid quadrupole-quadrupole time-of-flight tandem mass spectrometry and sequential enzymatic digestion, Anal. Biochem. 364 (2007) 8–18. https://doi.org/10.1016/j.ab.2007.01.023.

[315] P. Muhammad, D. Li, Z. Liu, Boronate Affinity Chromatography, in: Encycl. Anal. Chem., John Wiley & Sons, Ltd, 2006. https://doi.org/10.1002/9780470027318.a9414.

[316] L.I. Bosch, T.M. Fyles, T.D. James, Binary and ternary phenylboronic acid complexes with saccharides and Lewis bases, Tetrahedron. 60 (2004) 11175–11190. https://doi.org/10.1016/j.tet.2004.08.046.

[317] R. dos Santos, S.A.S.L. Rosa, M.R. Aires-Barros, A. Tover, A.M. Azevedo, Phenylboronic acid as a multi-modal ligand for the capture of monoclonal antibodies: development and optimization of a washing step, J. Chromatogr. A. 1355 (2014) 115–124. https://doi.org/10.1016/j.chroma.2014.06.001.

[318] T.S. Raju, B. Scallon, Fc Glycans Terminated with N-Acetylglucosamine Residues Increase Antibody Resistance to Papain, Biotechnol. Prog. 23 (2007) 964–971. https://doi.org/10.1021/bp070118k.

[319] D. Shukla, B.L. Trout, Understanding the Role of Arginine and Citrate as Eluents in Affinity Chromatography, in: Dev. Biotechnol. Bioprocess., American Chemical Society, 2013: pp. 67–86. https://doi.org/10.1021/bk-2013-1125.ch005.

[320] X.-C. Liu, Boronic Acids as Ligands for Affinity Chromatography, Chin. J. Chromatogr. 24 (2006) 73–80. https://doi.org/10.1016/S1872-2059(06)60004-7.

[321] J.W. Poulsen, C.T. Madsen, C. Young, F.M. Poulsen, M.L. Nielsen, Using Guanidine-Hydrochloride for Fast and Efficient Protein Digestion and Single-step Affinity-purification Mass Spectrometry, J. Proteome Res. 12 (2013) 1020–1030. https://doi.org/10.1021/pr300883y.

[322] L.O. Narhi, D.J. Caughey, T. Horan, Y. Kita, D. Chang, T. Arakawa, Effect of Three Elution Buffers on the Recovery and Structure of Monoclonal Antibodies, Anal. Biochem. 253 (1997) 236–245. https://doi.org/10.1006/abio.1997.2375.

Curriculum vitae

André Nascimento

Biotechnology and Biosciences PhD Student

+351 919135549 a.n.nascimento@gmail.com

Portuguese Lisbon, Portugal

pt.linkedin.com/in/andrennascimento

researchgate.net/profile/Andre_Nascimento5

Key skills

- Downstream Processing
- Chromatography
- ÄKTA systems
- Antibodies and derivatives
- Phage display
- Peptide chromatography
- HPLC
- Microfluidics
- Virus and VLPS
- Upstream

Key competences

- English
- Experimental planning
- Thesis orientation

Education

PhD in Biotechnology and Biosciences

Instituto Superior Técnico (IST)/ Rensselaer Polytechnic Institute (RPI)
Sep 2015 – Present

PhD Project: Development of a novel purification platform for fab antibody fragments based on affinity peptides and multimodal ligands

Advisors: Prof. Ana Azevedo (iBB-IST), and Prof. Steven Cramer (RPI, Troy, NY)

Co-Advisors: Prof. Pankaj Karande (RPI, Troy, NY)

Masters in Biotechnology

Instituto Superior Técnico (IST)
Sep 2011 – Dec 2013

Master thesis: Polishing of Monoclonal Antibodies Stream through Convective Flow Devices (Bioseparation Engineering Laboratory (BEL) - BioEngineering Research Group (BERG)).

Classification of 17 (0-20 scale)

Bachelor in Biochemistry

Faculdade de Ciências e Tecnologia (FCT-UNL)
Sep 2007– May 2011

Erasmus student at Pharmacy School of London
(Feb 2010 – Jul 2010)

Classification of 14 (0-20 scale)

Professional Research Experience

Research Assistant

Institute for Bioengineering and Biosciences (iBB/IST)
Sep 2019 – Present

Project: Highthrouput screen of chromatographic conditions using microfluidics.

Junior Research Fellow

Instituto de Biologia Experimental e Tecnológica (iBET)
Dec 2014 – Aug 2015

Project: Downstream process of virus and virus-like particle.

Research Assistant

Laboratório Nacional de Energia e Geologia (LNEG)
Apr 2014 – Nov 2014

Project: BioBlocks - Design of bio-based products as precursors for the bio-industry of chemical synthesis and biomaterials.

Publications

A. Nascimento, A. Mullerpatan, P. Karande, A.M. Azevedo, S.M. Cramer, *Development of Phage Biopanning Strategies to Identify Affinity Peptide Ligands for Kappa Light Chain Fab Fragments*. Biotechnol. Prog. (2019).

C. Pinto, G. Silva, A.S. Ribeiro, M. Oliveira, M. Garrido, V.S. Bandeira, **A. Nascimento**, A.S. Coroadinha, C. Peixoto, A. Barbas, J. Paredes, C. Brito, P.M. Alves, *Evaluation of AAV-mediated delivery of shRNA to target basal-like breast cancer genetic vulnerabilities*. J. Biotechnol. 300 (2019) 70–77.

A. Nascimento, I.F. Pinto, V. Chu, M.R. Aires-Barros, J.P. Conde, A.M. Azevedo, *Studies on the purification of antibody fragments*. Sep. Purif. Technol. 195 (2018) 388–397.

A. Nascimento, S.A.S.L. Rosa, M. Mateus, A.M. Azevedo, *Polishing of monoclonal antibodies streams through convective flow devices*. Sep. Purif. Technol. 132 (2014) 593–600.

Oral Communications

A. Nascimento, M.N. São Pedro, I.F. Pinto, A.M. Azevedo. *A Microfluidic high-throughput platform to debottleneck downstream process development.*. 5th HTDP, Porto, Portugal, 4-7 November 2019.

A. Nascimento, M.N. São Pedro, I.F. Pinto, A.M. Azevedo. *Debottlenecking process development using a microfluidic high-throughput platform*. Affinity 2019, Stockolm, Sweden, 26-28 June 2019.

A. Nascimento, A. Mullerpatan, A.M. Azevedo, M.R. Aires-Barros, P. Karande, S.M. Cramer. *Phage display-aided identification of affinity peptide ligands against Kappa Fab fragments*. 12th European Symposium on Biochemical Engineering Sciences – ESBES 2018, Lisbon, Portugal, 9-12 September 2018.

A. Mullerpatan, **A. Nascimento**, R.Ghosh, E. Kane, P. Karande, S. M. Cramer. *Single-step purification of small non-mAb biologics by peptide-ELP based affinity precipitation*. Division of Biochemical Technology (BIOT), 255th ACS National Meeting, New Orleans Louisiana, 18-22 March 2018.

Poster Communications

A. Nascimento, A. Mullerpatan, A.M. Azevedo, P. Karande, S.M. Cramer. *Development of phage biopanning strategies for the discovery of Fab-binding peptide affinity ligands: an evolutionary approach to universality.* Affinity 2019, Stockolm, Sweden, 26-28 June 2019.

Miguel Ambrósio, A.M. Azevedo, M.R. Aires-Barros, **A. Nascimento**. *Phenylboronate: a pseudo-universal ligand for Fab fragments*. Affinity 2019, Stockolm, Sweden, 26-28 June 2019.

A. Nascimento, A. Mullerpatan, A.M. Azevedo, M.R. Aires-Barros, P. Karande, S.M. Cramer. *Phage display-aided identification of affinity peptide ligands against Kappa Fab fragments*. Division of Biochemical Technology (BIOT), 255th ACS National Meeting, New Orleans Louisiana, 18-22 March 2018.

R. Ghosh, A. Mullerpatan, T. Baltazar, C. Catarino, **A. Nascimento**, P. Karande, S.M. Cramer. *Identifying peptide affinity ligands to demonstrate selectivity between dermal fibroblasts and endothelial cells*. Division of Biochemical Technology (BIOT), 255th ACS National Meeting, New Orleans Louisiana, 18-22 March 2018.

A. Nascimento , S.A.S.L. Rosa, M. Mateus, A.M. Azevedo. *Convection Flow Devices for the Polishing of Monoclonal Antibodies*. XVI Latin-American Congress on Chromatography (XVI COLACRO), Lisboa, Portugal, 5-9 January 2016.

Experience in orientation

Co-supervision of MSc student **Rachid Santos** in Bioseparations Laboratory at Institute for Bioengineering and Biosciences (iBB), Instituto Superior Técnico, September 2019 – Present. **Project title**: Multimodal strategies for the purification of antibody Fab fragments.

Co-supervision of MSc student **Miguel Ambrósio** in Bioseparations Laboratory at Institute for Bioengineering and Biosciences (iBB), Instituto Superior Técnico, September 2018 – November 2019. **Project title**: Purification of antibody fragments by phenylboronate chromatography using a microfluidic device.

Co-supervision of MSc student **Jovana Delic** (Erasmus student form University of Novi Sad, Novi Sad, Serbia) in Bioseparations Laboratory at Institute for Bioengineering and Biosciences (IBB), Instituto Superior Técnico, January 2016 – July 2016. **Project title**: Novel strategies for the purification of Fab fragments based on aqueous two-phase systems.